CRANFIELD UNIVERSITY

NASIRU TUKUR

TECHNO-ECONOMICS OF NATURAL GAS PIPELINE COMPRESSION SYSTEM

SCHOOL OF AEROSPACE, TRANSPORT AND MANUFACTURING (SATM)
Centre for Propulsion Engineering

DOCTOR OF PHIILOSOPHY
Academic Year: 2017 - 2018

Supervisor: Professor Pericles Pilidis and Dr Uyioghosa Igie
April 2018

CRANFIELD UNIVERSITY

SCHOOL OF AEROSPACE, TRANSPORT AND
MANUFACTURING (SATM)
Centre for Propulsion Engineering

DOCTOR OF PHIILOSOPHY

Academic Year 2017 - 2018

NASIRU TUKUR

TECHNO-ECONOMICS OF NATURAL GAS PIPELINE COMPRESSION SYSTEM

Supervisor: Professor Pericles Pilidis and Dr Uyioghosa Ige
January 2018

ABSTRACT

The demand for the natural gas is on the increase as a result of industrialization and urbanization. There is need of transporting this natural gas from production fields to consumer market through long distances pipelines. Transporting natural gas through a long distance requires constructing of compressor station driven by a gas turbine at a suitable distance along the pipeline. Pipeline construction is capital expensive that requires important data such as the pipe diameter, pipe thickness, pipeline length, proper gas compressor and gas turbine sizes, flow rate and required operating pressure. The technical and economic success of a pipeline compressor station depends on the operation of gas compressor and gas turbine involved. Therefore, to techno-economic tool to assess the pipeline project becomes imperatives.

The objective of this research is the application of TERA on gas turbine compressor station in natural gas pipeline taking into account the station location, equipment selection, power matching based on ambient temperature variation while optimizing for the project lifecycle lowest cost. The model and methodology developed to provide useful decision-making guide for Nigerian government on investment of Trans-Sharan gas pipeline. This research was divided into two aspects, the performance aspect, and the economic aspect. The performance presents a model for booster station definition along the gas pipeline. The model was developed using thermodynamic gas properties, HYSYS and Weymouth gas flow equation. The model also accounts for the variation in the elevation and ambient temperature at each of the compressor stations located along the pipeline network. For each of the stations gas compressor and gas turbine model was selected. The model has been verified using pressure ratio and a number of booster station spacing of a pilot project, Trans-Sahara gas pipeline (TSGP). The project was aimed at exporting natural gas from Niger Delta, Nigeria to the consumer market in Europe via Niger and Algeria. The project is expected to transport 30bcm/year of natural gas through 56-inch pipe diameter and a total distance of 4180km with 18 compression stations.

For the power matching, the daily three hourly temperature measurements for winter, hot, and dry seasons were recorded for each of the compressor stations along the gas pipeline. The power requirement for the centrifugal compressors was calculated based on the three hourly intervals. The gas turbines were simulated in Turbomatch based on these ambient temperatures. The result shows that both the centrifugal compressor polytropic head and the gas turbine output power are strongly influenced by the ambient temperature with gas turbine power output dropping by average 0.95% for every $10^{o}C$ rise in ambient temperature and the centrifugal compressor polytropic head increasing by average of.1% for every $10^{o}C$ rise in ambient temperature vis-viz increase in the centrifugal shaft power.

The major costs associated with the natural gas pipeline is the capital cost and operating cost. At baseline case, the project capital cost is USD 15.7 billion and the project lifecycle cost is USD 27.6 billion. The project life cycle cost is made of the following 33% fuel cost,10% maintenance cost, 26% pipeline cost, 6% gas turbine cost, 12% gas compressor cost, and 13% auxiliary cost. For this baseline, The NPV at 15% discount rate negative.

For the optimised case, the studies considered two gas turbines of 43.3MW and 100MW capacities. For the first case, optimisation study was done for two 43.3MW gas turbine driving two gas compressors while for case 2, one 100MW gas turbine was used to drive one gas compressor. The result shows 10 number of compressor stations along the pipeline. The optimized result also shows a reduction in the lifecycle cost from USD 20.1 billion in 43.3MW to USD 18.8 billion in 100MW. The NPV at 15% discount rate for both engines is seen to be positive.

Keywords:

Gas compressor, gas turbine, booster station, power matching, lifecycle cost, ambient temperature, gas temperature

ACKNOWLEDGMENTS

All thanks are to Allah for the uncountable bounties. He is most beneficial and the most merciful.

I wish to thank the management Petroleum Technology Development Fund for giving me the overseas scholarship.

Special thanks go to my supervisor the erudite Professor Pericles Pilidis for his patience, help, encouragement, and comments. Prof, it is privileged to have you supervise my PhD. I would like to thank Dr. Uyi and Dr. Waleed Al-busaidi for their assistance. I would also like to thank Gillian Hargreaves and Nicola Datt for their help and understanding.

My sincere love and appreciation go to darling wife Maryam Muhammed Tukur and my daughter Fadimatu for their unwavering support and understanding throughout this difficult time. My appreciation also goes to my brother and sisters for their support and encouragement.

My sincere thanks go to my friends in Cranfield; Gali, Dahiru, Emma, Didy and all my colleagues in the office especially Silas, Saleh, and Ezedeen. It is a pleasure meeting you all.

TABLE OF CONTENTS

LIST OF ABBREVIATIONS

CNG	Compressed Natural Gas	
CO_2	Carbon dioxide	
C_O	Capital Cost	
C_t	Net Cash Flow	
D	Diameter	mm
DP	Design Point	
E	Pipeline Efficiency	%
f_d	Darcy Friction Factor	
f_f	Fanning Friction Factor	
ɣ	Specific Ratio	
G	Gas gravity	
GA	Genetic Algorithm	
GT	Gas Turbine	
GTL	Gas to Liquid	
GTS	Gas to Solids	
GTW	Gas to Wire	
H	Actual Head	KJ/kg
Hp	Polytropic Head	KJ/kg
HPC	High Pressure Compressor	
HPT	High Pressure Turbine	
H*	Isentropic Head	
k_{ref}	Reference Specific Heat Ratio (1.4)	
L	Length	Km
LCC	Lifecycle Cost	
LPT	Low Pressure Turbine	
n	Polytropic Factor	
ɳm	Mechanical Efficiency	%
ɳp	Polytropic Efficiency	%
NPV	Net Present Value	
$\dot{m}_c$	Corrected Mass Flow rate	kg/s
MOP	Maximum Operating Pressure	Bar

MW	Molecular Weight	
ODP	Off Design Point	
P	Pressure	Bar
P1	Inlet Pressure	Bar
P2	Outlet Pressure	Bar
Pb	Pressure at Base	Bar
Pc	Critical Pressure	Bar
Pg	Gas power	kW
PMC	Pipe Material Cost	
Pr	Reduced Pressure	Bar
P_{ref}	Reference Inlet Pressure (101.325kpa)	
Q	Volume flow rate	m^3/day
r	Discount rate	
R	Gas Constant	
ROW	Right of Way	
R_{ref}	Reference Gas Constant (287.058J/Kg.K)	
SCADA	Supervisory Control and Data Acquisition	
t	Pipeline thickness	mm
T	Absolute Temperature	K
T1	Inlet Temperature	K
T2	Outlet Temperature	K
Tb	Temperature at Base	K
Tc	Critical Temperature	K
TERA	Techno-economic and Environmental Risk Assessment	
TET	Turbine Entry Temperatures	K
T_f	Gas Temperature	K
Tr	Reduced Temperature	K
T_{ref}	Reference inlet temperature (288.15^{o}K)	
TSGP	Trans Saharan Gas pipeline	
V	Specific Volume	
VA	Flow Velocity at Point A	m/s
VB	Flow Velocity at Point B	m/s

W	Standard Flow	m^3/d
Z	Compressibility Factor	

1 INTRODUCTION

1.1 Research Background

By the year 2050, the global population is projected to reach 9 billion, which represents a 28% increase from its present position. This increase, coupled with industrialization and the projected increase in standards of living have been forecasted to have a significant effect on world's energy demand. Part of this energy demand will be met using natural gas. Natural gas is regarded as a clean and cost-effective fossil fuel; hence, several countries meet their increasing energy demand by burning natural gas to reduce CO_2 emission. This is so because the CO2 emissions have a serious impact on climate change and global warming. This made natural gas a valued resource for the world energy market. Therefore, its importance cannot be overemphasized. Natural gas supplied more than 24% of the total primary energy demand in 2008 [1]. Figure 1-1 shows the projected European countries natural gas demand and supply between 2005 and 2030. The difference between the demand and supply of natural gas within Europe is likely to reach up 36 to 113 Bcm by the year 2020 if no medium projects are put in place [2]. However, there are some ongoing planned gas supply projects which aimed at filling this future demand such as Trans-Sharan gas pipeline (TSGP).

The Trans-Saharan gas pipeline project has been classified as the medium term project probability project in Nigeria. The aimed of this project is to transport natural gas from the Niger Delta, Nigeria to the consumer market in Europe via Niger and Algeria. Nigeria has proven reserves of unexploited natural gas of about 5.153Tcm. The country has planned for gas to power developmental projects especially in the Northern part of the country. If these projects are completed cities such as Abuja is expected by the year 2030 to consume about 1.3Bcm/y of natural gas, Kaduna and Kano are expected to consume 3.7Bcm/y and 1.3Bcm/y respectively. It is expected the planned TSGP will help boost the gas shortfall in northern Nigeria [2].

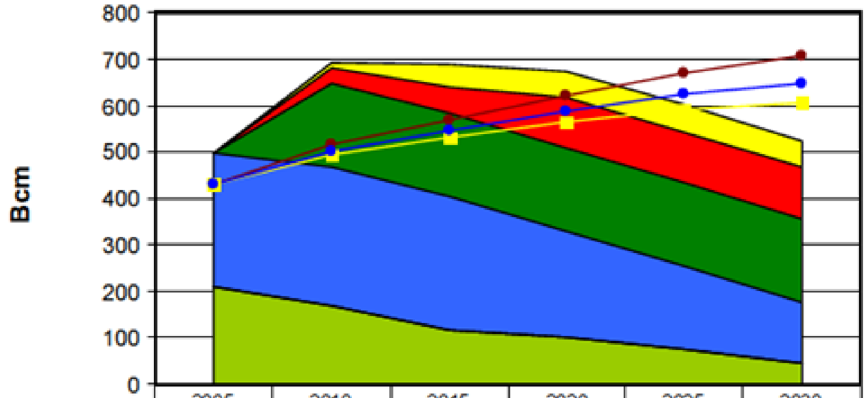

	2005	2010	2015	2020	2025	2030
Low Probability Projects	0	8	49	57	57	57
Medium Probability Projects	0	35	55	109	109	109
High Probability Projects	0	179	179	179	179	179
Contracted Supplies	289	299	288	229	179	131
Indigenous Production	207.49	168	117	99	76	46
Gas Demand, Medium	428	501	547	586	623	647
Gas Demand Low	428	493	532	563	591	606
Gas Demand, High	428	514	568	620	669	708

Figure 1-1 Natural Gas Demand and Supply for EU [2]

The oil and gas proven reserves are not equally distributed around the world; thus huge quantities of these reserves are found in remote locations which are a distance away from consuming market. Rajnauth et al [3], said the methods of transporting natural gas includes; Gas to Liquid (GTL), Compressed Natural Gas (CNG), Gas to Solids (GTS), Gas to Wire (GTW) and pipelines.

A large quantity of natural gas is being transported via pipeline network systems across long distances. A typical gas transmission network is composed of large numbers of pipes, valves, and regulators, with injection and delivery points and compressor stations [4]. Gas pipeline networks are associated with pressure loss as a result of friction between the gas flow and the pipe inner wall. To ensure the steady flow of natural gas through pipelines, compressor stations are placed at suitable intervals along the pipeline. These compression systems must be carefully monitored in order to ensure a high level of operational reliability. The majority of the gas compression systems employ centrifugal compressors, driven by either gas turbines or electric motors with/without gearboxes [5]. Figure 1-2 shows pipeline and compressor stations.

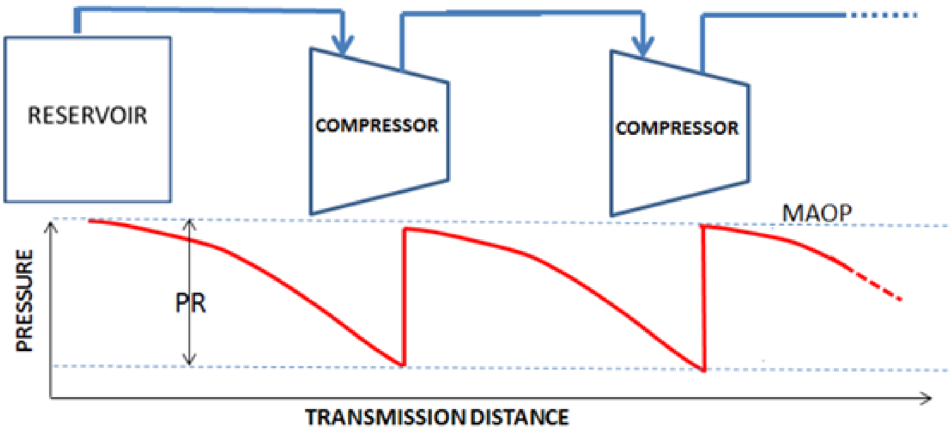

Figure 1-2 Pipeline layout and compressor stations [6]

Generally, gas compressors and gas turbines are capital expensive and operate under different local conditions. The operation of these machines involves the interaction of several components which lead degradation of the compressor and gas turbines as a result of wear and tear. In the compression stations, emission does occur as a result of leakages throughout the chain of activities resulting from leaky seals, pipe joints, and valves. Technical and economic achievement of any compression station operation depends to a large extent on the operation of the compressor involved [7].

The focus of this research is the application of Techno-economic assessment of the natural gas pipeline compression system; considering the optimization of compressor station location and equipment. The TERA concept was established at Cranfield University, UK. According to Ogaji et al [8], TERA has been successfully applied to the aviation, power generation and marine fields. Khan et al [9] described TERA as the multidisciplinary tool for modeling of gas turbines and engine asset management. The center of TERA is the performance module which explained the thermodynamics of the component parameters and simulating the design point, off-design point, and performance degradation of the gas turbine engines. The other modules include the risk; environmental and economic are all built from the performance module.

The only known work on TERA application on natural gas pipeline transportation was done by Nasir [10] in Cranfield University, UK. He looked at the techno-economic assessment of using a gas turbine or electric motor as a prime mover on a natural gas pipeline under a given operating condition. The study concluded that electric motor may at first seem better in terms of environmental pollution, but from the electricity generation today and in the near future, the use of electric motor contributes more to environmental pollution than the gas turbine. Also, for the interstate pipeline, the electric motor drive may not be a feasible option in areas where electricity supply is not available. The study also suggested that the compression cost reduces with increase in pipe size due to pressure increase and reduction in compression power required. More so, as the throughput increases the compression power requirement also increase. Hence, the fuel cost also increases.

El- Suleiman [11] Investigated TERA on CO_2 compression power requirement for gas turbine driven (pumps and compressor). The author developed and implemented Variflow to an existing GT simulation tool so as to enhance the off-design performance. Variflow is a gas turbine performance simulation code developed in Cranfield University. This code was used for the implementation of variable stators. The economic model was developed based on net present value. The maximum and minimum GT power used are 33.9 MW and 9.4 MW capacities. The study shows NPV for using the 33.9 MW GT was about £13.9 million while that of 9.4 MW is about £1.2 million. The equivalent payback periods were 3 and 7 years respectively for the project duration of 25 years.

The two studies did not look at the effect of gas temperature on the operation of gas compressor and gas turbine. Also, the power matching between the gas compressor and gas turbine at the different ambient temperatures were not considered. Hence, a gap in knowledge exists which this study tries to cover.

1.2 Research Aim

The aim of this research is to develop a techno-economic assessment of the natural gas pipeline compression system, with a major focus on optimization of compressor station location and equipment.

1.3 Research Objectives

- Perform simulation of design and off-design performance of selected gas turbine as mechanical drive for natural gas pipeline application
- Evaluate the effects of ambient temperature, altitude, turbine entry temperature on the operation of gas turbines used in the gas pipeline (for the specific case of TSGP).
- Analyse technical requirement for booster station spacing and equipment selection.
- Estimate the centrifugal compressor power requirement based on different gas temperature and match it with gas turbine power output.
- Estimate the centrifugal compressor power requirement based on single gas temperature (isothermal flow) and match it with gas turbine power output.
- Optimize the turbine power output for pipeline compression based on lowest lifecycle cost.

1.4 Statement of Problem

A pipeline project was proposed to transport natural gas from Nigeria to Europe via Niger, Algeria to Spain. This pipeline forms the basis of this research. The economic performance of natural gas pipeline transmission depends strongly on how the booster stations were arranged and the type of compressor used. For Natural gas supply to be effective the following criteria are to be considered.

- ➢ Adequate proven reserves to meet the demand
- ➢ Reasonable capital and operating costs
- ➢ Efficient of the gas transmission equipment such as the compressors and it drivers

To meet the last two criteria mentioned above it is important to answer the following questions:

- ✓ What is the appropriate pipeline arrangement to be used?

- ✓ What sizes of gas compressor and gas turbine engines required at each station based on the ambient temperatures of every location?
- ✓ How many booster stations are to be constructed along the pipeline?
- ✓ Which arrangement has the lowest lifecycle cost?

1.5 Contribution to Knowledge

The trans-Saharan gas pipeline project was conceived by Nigerian Government, aimed at exporting natural gas from the Niger Delta region in Nigeria to consumer market in Europe via Niger and Algeria.

The project is expected to transport 30bcm/year of natural gas through 56-inch pipe diameter and total pipeline distance of 4180km with 18 number of compression stations at suitable intervals along the pipeline network. In Nigeria, TSGP is regarded as a strategic project because when constructed will generate revenues and open opportunities for the Nigerian gas sector [2]. A feasibility report on this project was conducted in 2006 [2]. It is worthy to note that, the report only mentions the number of compressor stations along the pipeline without providing the exact location where there are to be constructed [2]. Also, from the report, no equipment selection was made. In this research, the compressor station locations were identified, the locations ambient temperatures were segmented based on the hourly difference. The gas compressor powers were calculated and the gas turbines were simulated based on the gas compressor power output and the ambient temperature of each of the station locations. Hence, the research contributions to knowledge are:

- TERA application on gas compressor station taking into account the ambient temperature, gas temperature, power matching, and equipment selection while optimizing for the lowest lifecycle cost.
- Model and methodology developed will provide useful decision-making for Nigerian government on investment of Trans-Saharan gas pipeline.

1.6 Thesis Structure

Chapter one presents the research background. The chapter also discussed aim, objectives, statement of the problem, contribution to knowledge, and thesis structure.

Chapter two presents an extensive literature of related studies. Natural gas pipeline components are reviewed. Gas compressor types, performance, configuration are reviewed. Gas turbine performance and configuration were also reviewed. The economic aspect of compressor station was also considered.

In chapter three, detailed TERA methodology for the gas compression system. The TERA framework is made up of different modules and each module focuses on different problems and the results obtained from the modules were integrated into TERA framework. The modules include performance, economic and lifing. The chapter also gives a general overview of Turbomatch.

Chapter four presents the research baseline case is developed. The booster station location and equipment were identified, the ambient temperature was segmented. Economic decisions were made in Excel based on the necessary data received from the compressors, gas turbines and pipeline. Baseline economic calculation considers the capital and operating costs based on the lifecycle cost (LCC) and Net Present Value (NPV) approach. The module considered the ambient temperature variation for the three season’s winter, dry and hot. The power variation and the corresponding TET for each of the compressor station which would affect the GT fuel consumption are also considered. The module was based on lifecycle cost approach.

Chapter five presents the model development for gas temperature variation. The ambient temperature along the pipeline was segmented based on hourly variation and seasons of the year, winter, dry and hot. The performance simulation of the selected gas turbine for both the design and off-design points was done in Turbomatch. The gas compressor power requirement was also calculated based on the gas temperature variation and time interval. The gas compressor performance curve was developed. The chapter also presents the effects of gas temperature on both the gas compressor and gas turbine power requirements. It further presents the power matching for both the gas compressor and gas turbine at different ambient temperatures.

Chapter Six presents a model for booster station spacing along the pipeline. The model also accounts for the variation in elevation and ambient temperature at each of the compressor station locations along the pipeline network. In this chapter centrifugal compressors and gas turbines were selected, booster stations arrangements were made. The temperature, pressure, and pressure losses along the pipeline were obtained within a reasonable accuracy. The model has been verified using pressure ratio and a number of booster station spacing of a pilot project, Trans-Sahara gas pipeline (TSGP).

Chapter Seven; in chapter seven TERA optimization code was developed using Genetic Algorithm (GA). The objective function, variable, and constraint are identified. The results are presented and discussed.

Chapter Eight presents a summary of the conducted research and finally lists areas for further model improvements and research.

2 NATURAL GAS PIPELINE COMPONENTS

2.1 Pipeline Network

A Pipeline network is an integrated transmission, distribution and gathering grid that used in natural gas transport to and from nearly any location for many years. Pipeline transport is regarded as a convenient means of transporting natural gas from the production site to the end users [3]. Generally, pipelines are constructed above the ground, underground or subsea in the case of offshore arrangement and are constructed in a manner that natural gas reaches its final destination in the fast and effective way [12]. The gas pipeline size ranges from 6 inches to 56-inch diameters depending on the purpose and throughput. The natural gas pipeline is classified into the three categories as shown in Figure 2-1.

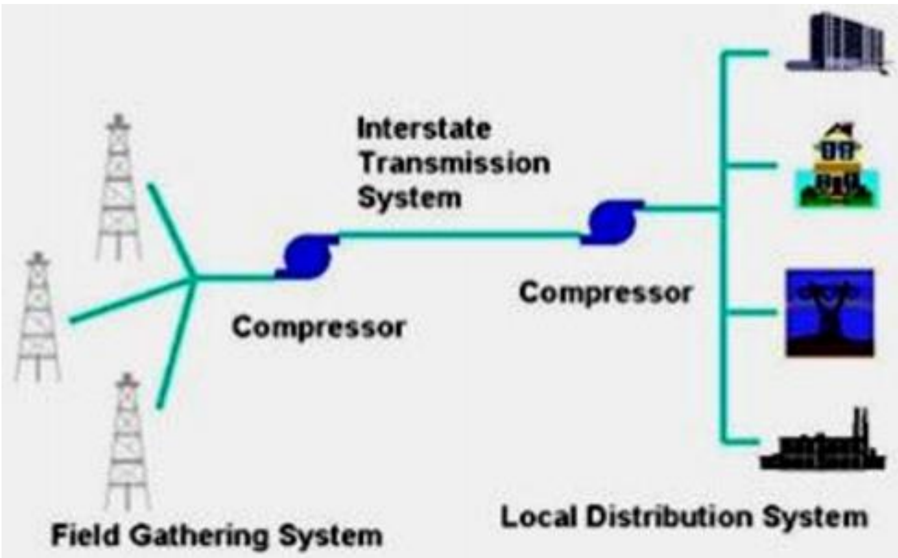

Figure 2-1 Pipeline layout [12]

- ✓ Gas gathering pipelines- these are pipelines used in transporting natural gas away from the production well to another facility for further refinement or send to the transmission line. These categories of pipelines are usually used for a short distance with a small diameter.
- ✓ Gas transmission pipelines- these types of pipelines are used for long distance with large diameters transporting gas around the country or intercontinental. In these categories of the pipeline, compressor stations

are incorporated at a suitable distance along the pipeline to avoid pressure drop along the pipeline.

- ✓ Gas distribution pipeline- these are pipelines used for delivering natural gas to consumers at low pressure. The distribution pipeline differs from the transmission line due to its small pipes diameter, its simplicity as there are no valves, compressors or nozzles, and its operation at low and medium pressures [12]. They are typically used in terminals for gas distribution to tanks and storage facilities for onward distribution to residential and other end users.

2.2 Design of Pipeline

Designing a natural gas pipeline network requires detailed knowledge of the head loss caused by fluid friction; it is also vital to considered variables such as the length, diameter, elevation and the quantity of the gas being transported. Nasir [10], concluded that if the pipe distance is huge the changes in pressure are important, it is necessary to approach the problem using the concepts of compressible fluid flow.

The pipeline flow rate is dependent on the natural gas properties, pipe length and diameter, initial gas temperature and pressure and the pressure drop due to friction. The construction of a new pipeline or the expansion of the existing one requires the optimization of its operational condition, size, and topology to reduce its capital and operating cost [10]. Montoya-O [13], suggested that the acceptable convergence of these approaches depend on the first value given by the designer.

2.2.1 Gas Flow Analysis

As the gas flows through a pipeline, The total energy of the gas at different points consists of energy due to pressure, energy due to velocity and the energy due to an elevation above the established datum [14]. These components of the flowing fluid are connected by Bernoulli’s equation to form an energy conservation equation. Bernoulli's equation is expressed as follows, considering two points as shown in Equation **(2-1)**.

$$Z_A + \frac{P_A}{\gamma} + \frac{V_A^2}{2g} + H_P = Z_B + \frac{P_B}{\gamma} + \frac{V_B^2}{2g} + h_f \quad \textbf{(2-1)}$$

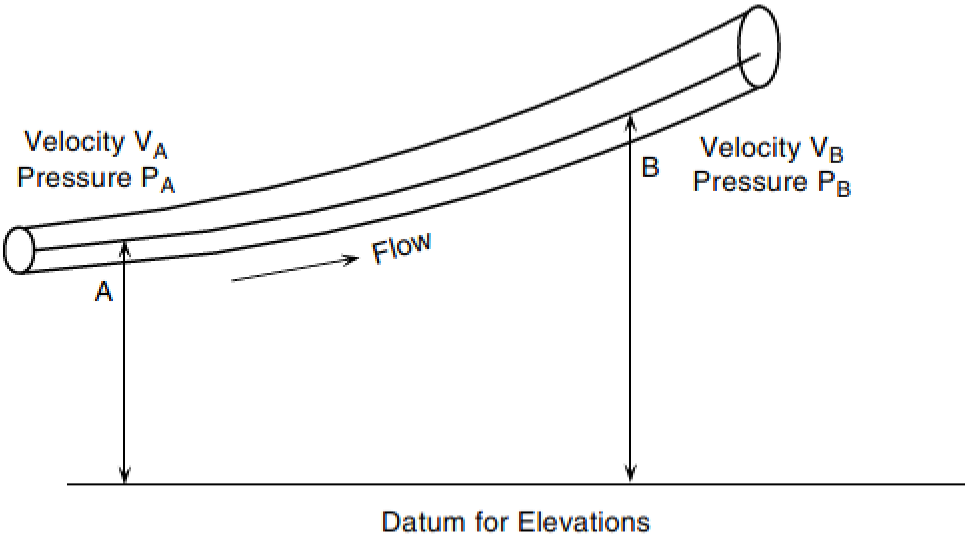

Figure 2-2 Energy flow of a fluid [14]

Where H_P is the equivalent head added to the fluid by a compressor at A and h_f represents the total frictional pressure loss between points A and B.

Over the years several formulas were developed to predict the performance of pipeline transporting gas starting with the basic energy Equation **(2-1)**. These equations are aimed at providing the relationship between gas properties, such as compressibility factor and gravity, with the flow rate, pipeline length, and diameter and the pressure fluctuation along the pipeline[15]. Therefore, for a given pipe length and size, it is possible to predict the flow rate passing through the pipeline based upon inlet and outlet pressure of a pipe segment. Flow Equations

The isothermal pressure drop calculation approach for single dry gas pipelines are widely used and are the basic link in the gas delivery system [16]. Various equations are available that relate gas flow rate with gas properties, pipe diameter and length, and upstream and downstream pressures [14]. These equations are mention below:

1. General flow equation

2. Weymouth equation
3. Colebrook-white equation
4. Modified Colebrook-White equation
5. AGA equation

The general flow equation, also called the fundamental flow equation, for the steady-state isothermal flow in a gas pipeline. This equation provides the relationship between pressure drop and flow rate. The S.I form of this equation is shown in Equation **(2-2)** and is widely used. The equation is expressed in terms of temperatures, pressures, gas properties, pipe diameter and flow rate [17].

$$Q = 1.1494 \times 10^{-2} \left(\frac{T_b}{P_b}\right) \left(\frac{P_1^2 - P_2^2}{G T_f L_e Z}\right)^{0.5} D^{2.5} \tag{2-2}$$

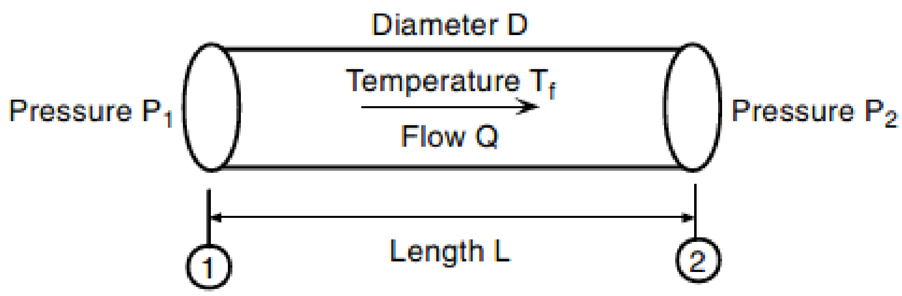

Figure 2-3 Steady flow in gas pipeline [14]

Upon examining the equation 2-2 it can be seen for a pipe segment of length L and diameter D, the gas flow rate Q at standard condition depends on many factors. The Q is dependent on the gas compressibility Z and the gas gravity G. When the gas gravity is increased the flow rate will reduce. Also, as the compressibility factor Z increases, the throughput will reduce. Furthermore, as the gas temperature T_f increases, the flow rate will reduce. The pipe lenth and its inner wall also affect the pressure of the flowing gas. If the pipe segment length increases at a given pressures P_1 and P_2 the throughput will decrese.

The term $P_1^2 - P_2^2$ is the force that causes the flow rate from upstream end to the downstream end.

Weymouth flow equation is used for high pressure, high flow rate, and large diameter gas transmission systems. The S.I units for this was adopted in this research and is shown in Equation **(2-3)**.

$$Q = 3.7435 \times 10^{-3} E \left(\frac{T_b}{P_b}\right)\left(\frac{P_1^2 - e^s P_2^2}{G T_f L_e Z}\right)^{0.5} D^{2.667} \tag{2-3}$$

This equation determines the flow rate via a pipeline for a given value of inlet and outlet pressures, gas gravity, compressibility pipe length, and diameter. The summary of flow equations is shown in Table 1

Table 1 Summary of Flow Equations [10]

Equation	Application
General Flow	Fundamental flow equation using friction or transmission factor; used with Colebrook-White friction factor or AGA transmission factor or AGA transmission factor
Colebrook-White	Friction factor calculated for pipe roughness and Reynolds number; popular equation for general gas transmission
Modified Colebrook-White	Modified equation based on U. S. Bureau of Mines experiments; gives higher pressure drop compared to original Colebrook equation
AGA	Transmission factor calculated for partially turbulent and fully turbulent flow considering roughness, bend index, and Reynolds number
Panhandle A Panhandle B	Panhandle equations do not consider pipe roughness; instead, an efficiency factor is used; less conservative than Colebrook or AGA
Weymouth	Does not consider pipe roughness; uses an efficiency factor, used for high-pressure gas flow

2.2.2 Gas Velocity in a Pipeline

The velocity of a flowing gas in a pipeline represents the speed at which the gas molecules travel from one point to another. This gas velocity is dependent on the pressure and, hence it varies along the pipeline even if the pipe diameter is constant. Very high velocity is achieved at the downstream end, where the pressure is the lowest. Accordingly, the lowest velocity is achieved at the upstream end, where the pressure is higher [18]. From Figure 2-3 consider a gas flowing from point 1 to point 2 with no gas addition or deliveries within these points, the mass flow rate for this gas can express as follows.

$$M = Q_1\rho_1 = Q_2\rho_1 = Q_b\rho_b \tag{2-4}$$

Where Q_b is the gas flow rate and ρ_b is the gas density all at standard conditions. Therefore, Equation **(2-4)** can be simplify into

$$Q_1 = Q_b\frac{\rho_b}{\rho_1} \tag{2-5}$$

Applying the gas law equation, we get

$$\rho_1 = \frac{P_1}{Z_1RT_1} \tag{2-6}$$

Where P_1 and T_1 are the pressure and temperature at section 1 of the pipe. Also, at standard conditions,

$$\rho_b = \frac{P_b}{Z_bRT_b} \tag{2-7}$$

Adding Equations **(2-5), (2-6), and (2-7),** we get

$$Q_1 = Q_b\left(\frac{P_b}{T_b}\right)\left(\frac{T_1}{P_1}\right)\left(\frac{Z_1}{Z_b}\right) \tag{2-8}$$

Since Z_b = 1, Equation 2-8 can be simplify into

$$Q_1 = Q_b\left(\frac{P_b}{T_b}\right)\left(\frac{T_1}{P_1}\right)Z_1 \tag{2-9}$$

Therefore, the velocity can be obtained from

$$u_1 = \frac{Q_1}{A} \tag{2-10}$$

Where A is the cross-sectional area

2.3 Components of Pipeline

2.3.1 Mainline Valve Stations

Valves are a mechanical device that controls the flow of natural gas through a pipeline. These valves are often open to permit the flow of gas and they can be closed as well to stop the flow of the gas to a certain section of the pipeline [19]. Valves are installed along the pipeline for safety, maintenance and repairs motives. In the event of a pipeline rupture, the segment of the damaged pipeline can be isolated by closing off the main valves on either side of the rupture location. Valves can be placed at intervals of 5 to 20 miles along the pipeline, and are subjected to regulation by the safety codes [19]. The cost of the mainline valves equipment can be specified as a lump sum figure that includes mainline valve and operator, blowdown valves and piping [14].

2.3.2 Meter Stations and Regulators

The gas flow rates are to be measured at a certain number of locations for the purpose of monitoring the pipeline system performance and more importantly at places where the transfer of custody take place. The metering techniques used may vary according to the accuracy required, whether for gas sales or for performance monitoring [14]. The metering and regulatory stations are constructed adjacent to the pipeline right of way (ROW), so as to reduce the pressure for delivery to a customer or to protect a section of a pipeline with lower maximum operating pressure (MOP). The metering stations consist of valves, meters, fitting, and instrumentation. The cost of the meter stations are usually estimated as a fixed price including the material and labor and the lump sum of the cost is added to the pipeline cost [14].

2.3.3 SCADA and Telecommunication System

Supervisory Control and Data Acquisition (SCADA) system control the pressure and flow by monitoring and controlling the pump operation and valves position.

The systems also perform series of additional function including leak detection, alarm processing, throughput analysis, hydraulic analysis and other functions considered critical to the safe operation of the pipeline. Usually, the starting and stopping of compressor units are done remotely using SCADA. According to Menon [14], the cost of SCADA equipment ranges from $2 million to $5 million or more depending on the pipeline length, number of compressor stations, mainline valves and metering stations. Sometimes SCADA equipment is estimated as a percentage of the total project cost.

2.3.4 Compression Stations

The movement of natural gas through a pipeline is under pressure. As natural gas flows through a pipeline, it loses pressure due to friction between the gas and the inside wall of the pipe. In other to keep the natural gas moving at the desired rate, the pressure must be increased. This is achieved with compressor stations located along a pipeline at suitable intervals.

Compression stations are built at an interval of 40 to 100 miles along the gas pipeline and consume approximately 3 to 5% of the total natural gas transported [20]. Its operation and location are dependent on the allowable pressure, flow rate and topography and usually; its facilities require about 15 to 22 acres of land [21].

The basic components of natural gas compression stations include compressor units, emergency shutdown systems, scrubber/filters, cooling facilities, and onsite computerized flow control and dispatch system and Supervisory Control and Data Acquisition (SCADA) that maintain the operational integrity of the stations [22]. Other components of compression station include mufflers fuel; lube oil system, backup generators, and gas system.

As shown in Figure 2-4 the natural gas streamline entering the compression station at point C is passed through scrubbers and filters at point D. the scrubbers and filters removed liquid and solid impurities and allow clean gas to enter through the smaller piping assigned to individual compressors at point E. the compressor units re-pressurize the gas volume to gas cooling facilities at point H. when the natural gas is compressed its temperature and pressure increase. The gas is cooled at the coolers before returning to the main pipeline so as to protect the inner coating of the pipeline and increase its transmission efficiency.

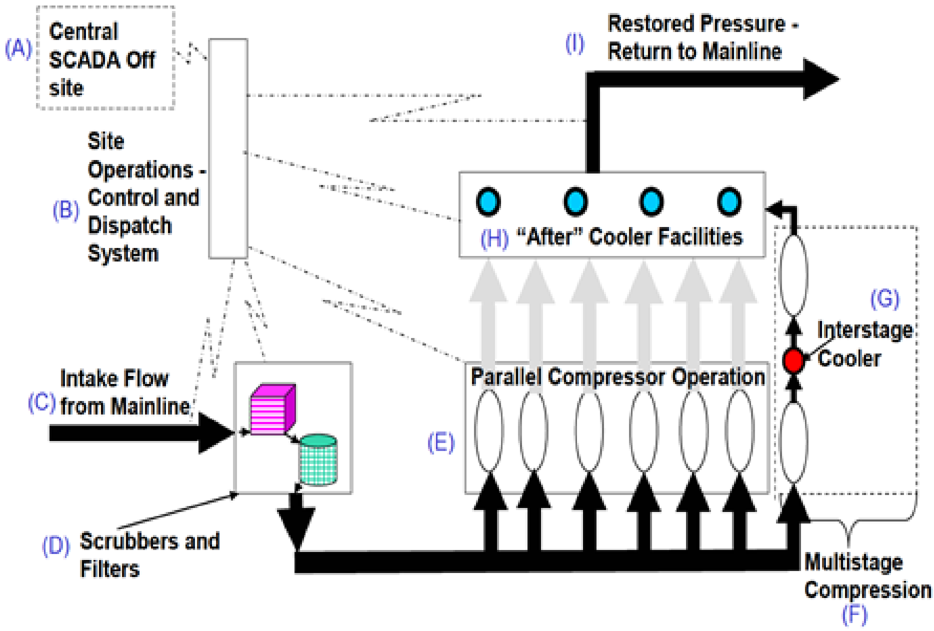

Figure 2-4 Generalized compressor station schematic [22]

2.3.4.1 Thermodynamics of Gas Compression

The natural gas compression task is to carry a gas from a suction pressure to a higher discharge pressure by means of mechanical work. The real process of compression is often related to one of the three ideal processes: Isothermal, Isentropic and Polytropic compressions [23]. The process is said to be isothermal compression when the temperature is kept constant during the compression process. The process is said to isentropic or adiabatic reversible if no heat is added or removed from the system while the polytropic compression process is like the isentropic cycle reversible but is not adiabatic [24].

For isothermal compression, the temperature remains constant, but the pressure and volume of the compressed gas vary from inlet to outlet. As seen from the ideal gas law.

$$P_1V_1 = P_2V_2 \qquad \textbf{(2-11)}$$

Where $P_1 and\ P_2$ are the inlet and outlet pressure conditions and $V_1 and\ V_2$are the inlet and outlet volumes.

For isentropic compression the discharge temperature is determined by pressure ratio shown in the equation below:

$$\frac{T_2}{T_1} = \left(\frac{P_2}{P_1}\right)^{\frac{\Upsilon-1}{\gamma}} \quad \textbf{(2-12)}$$

Where $T_1 and\ T_2\ are$ the inlet and outlet temperature conditions and γ is the ration of specific heats $\frac{C_P}{C_V}$.

For polytropic compression is similar to adiabatic compression of the discharge temperature is determined by the following equation:

$$\frac{T_2}{T_1} = \left(\frac{P_2}{P_1}\right)^{\frac{n-1}{n}} \quad \textbf{(2-13)}$$

Where n is polytropic factor

A polytropic process is a process which occurs with an interchange of both heat and work between the system and its surrounding while isentropic process is process during which the entropy of working fluid remains constant.

2.3.4.2 Compressor Configurations

Generally, compressors are arranged in series or parallel and this arrangement is usually made based on economics and simulation of failure analysis [25]. Figure 2-5 is compressor stations with three compressors in parallel Arrangement

Figure 2-5 Three compressors in parallel arrangement [26]

It has been frequently assume that parallel compressors arrangement yield very good flow compression if one unit fails. In 2000 Ohanian and Kurz [27] have shown identical compressors in series arrangement yield better flow compression than in the parallel arrangement. This is so because the relationship between flow in pipeline and pressure ratio at the compressor station is dictated by pipeline hydraulics.

In parallel compressors arrangement, the failure of one compressor forces the remaining compressors operates at or near choke with very low-efficiency due flow limitation range [27]. Figure 2-6 shows the Operating point of parallel arrangement.

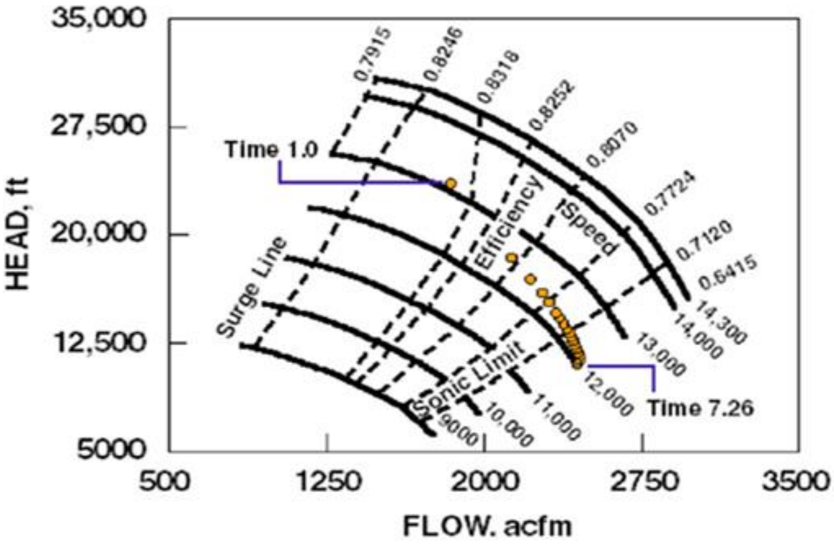

Figure 2-6 Operating points of parallel arrangement[27]

For the compressors in series arrangements, the operation is normally away from the choke region hence with higher efficiencies. The failure of one compressor could lead to the remaining compressors operate with good compression and efficiency to complement the failure than in the parallel arrangements as shown in Figure 2-7

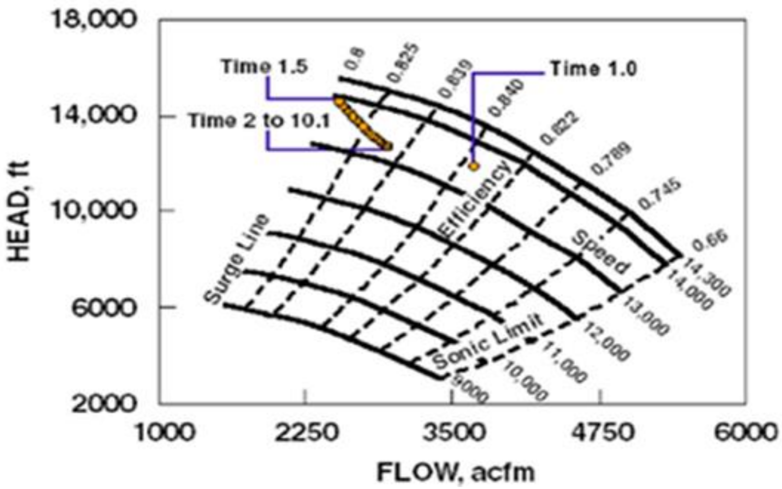

Figure 2-7 Operating points of series arrangement[27]

The proportion of power consumption and fuel emission also varies from one compressor arrangement to the other. Figure 2-8 shows data collected from an operating compression station over a six months period. From Figure 2-8, it evidently shows that parallel arrangements impacts covering a huge power operating range also it depicts available power limitation at 75^{O} F [18].

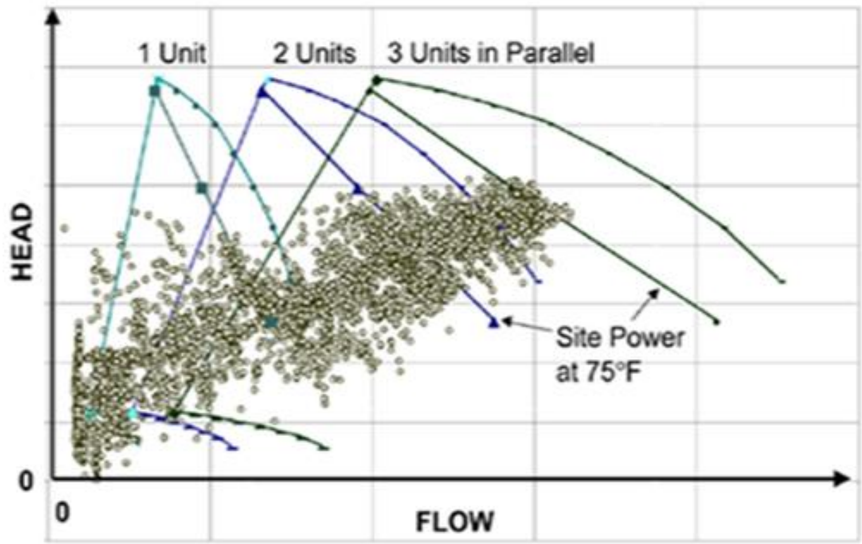

Figure 2-8 Six months data of gas compression station [28]

The gas compressor arrangement and its frequency along the pipeline is always a source of concern during the early stage of the pipeline design [29]. It is believed that the high-pressure natural gas transmission system obviously consists of large compressors and drivers which have simple control system compare to others. The performance of a pipeline is centered on its loading requirement in terms of the station frequencies taking into account the performance of their layout arrangement. The number of compressors installed in each compressor station along a pipeline network has a significant impact on availability, fuel consumption and capacity of the network [29].

2.3.4.3 Economic Aspects of Compressor Station

The important criteria for economic evaluation of gas compression station include capital cost, operating cost, lifecycle cost, and emissions. In addition, Ohanian and Kurz [27] confirmed that the types of compressor and the driver also have an impact on the cost and fuel consumption.

Efficiency and operating range of the compressor and its driver are regarded as the important performance parameters for the economic evaluation of any gas compression station [30]. The efficiency is related to the amount of fuel consumed to bring a certain amount of gas from a suction pressure to discharge pressure while the operating range deals with the range of possible operating conditions in terms of flow and head at an acceptable efficiency within the power capability of the driver [26]. The higher the operating range with higher efficiency will lead to higher revenue from gas sales and lower fuel consumption on the compressor stations.

The cost of emission penalty of methane from the compression stations and exhaust of the turbine driver also form part of economics and environmental aspect of the compressor station. Typically, methane is considered about 20 times potent greenhouse gas as CO2. Therefore, 1Kg of methane is equivalent to 20Kg of CO2 [26].

The availability of the station to operate the actual hours it required to operate per year also play an important role in the economics of compressor station operation [26]. The cost related to availability is the inability of the compressor station to perform its duty for a certain amount of time, thus not earning money[26]. The income loss can be due to transportation tariffs, reduction in pipeline throughput or penalties because contractual agreements are not met.

2.4 Compressors

Compressors are a mechanical device used in the industrial process to provide air for combustion or other purposes, to recirculate fluids through a process and convey gas through a pipeline. The inlet pressure level can be any value from a deep vacuum to high positive pressure while the discharge pressure can range from sub-atmospheric levels to high values in the tens of thousands of pounds per square inch [31].The pressures at the inlet and outlet are related. The compressible fluid can either be vapor or gas and can have a wide molecular range. The application of compressed gas varies from consumer products, such as domestic refrigerators, power plants and to large petrochemical plants installations. There are different types of compressors these include; reciprocating, rotary, centrifugal and axial but the majority of the compression systems employ centrifugal compressors, driven by either gas turbines or electric motors with/without gearboxes [30]. The choice of the type of compressor depends mainly on the flow required to be compressed, the density of the gas in conjunction with the total head and the duty which has to be performed [32]. The Figure 2-9 below shows compressor accepting mass flow.

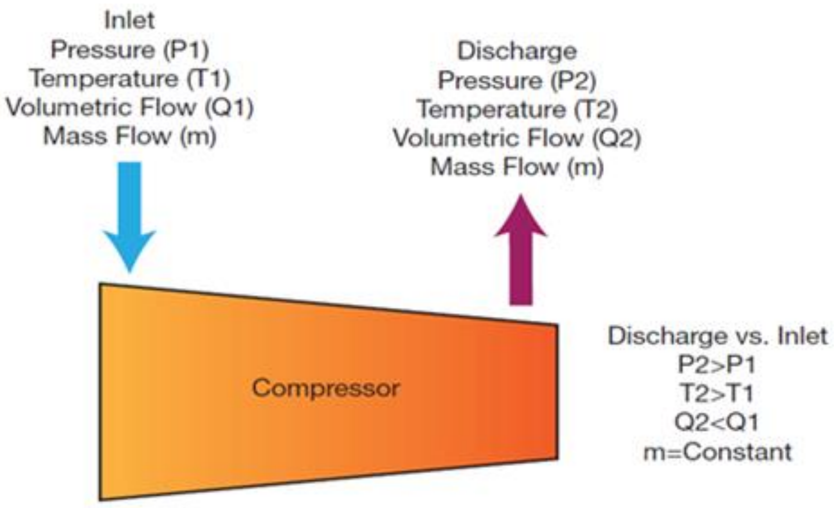

Figure 2-9 Compressor accepting mass flow [33]

2.4.1 Rotary Compressor

This is the type of compressor belongs to a positive displacement type of compressor that has spinning rotor and number of vanes. Rotary compressor develops its pressuring ability from spinning components. In this type of compressor, the gas pressures are increased by trapping it between vanes and make it reduce in volume as the impeller rotates around an axis eccentric to the casing as shown in Figure 2-10

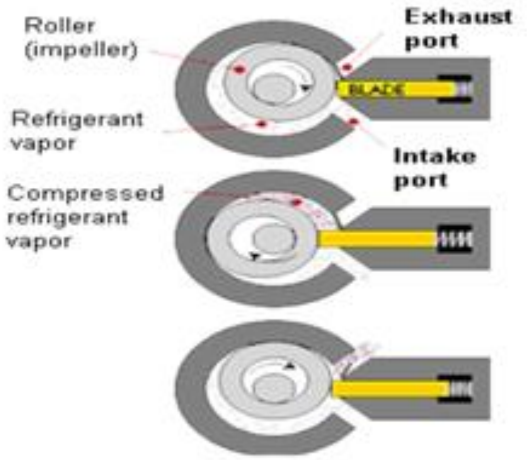

Figure 2-10 Rotary compressors [34]

According to Kolmetz [34], rotary compressors are simple to design, easy to install due to its few rotating parts, its two stages design provide good efficiency and its low to medium initial and maintenance cost is added to its advantages. Generally, rotary compressors are classified as follows:

1. Vane type compressor
2. Screw type compressor
3. Lop and Scroll type compressor

The major difference between these types of compressors is their rotating device.

2.4.2 Reciprocating Compressor

The reciprocating compressor is a positive displacement type of compressor that uses piston movement within the cylindrical housing to compress the gas from one pressure level to another higher pressure level by reducing the gas volume. The compression cycle of this type of a compressor consist of two strokes; the suction stroke and the compression stroke [34]. In a reciprocating compressor, the maximum permissible discharge gas temperature defines the maximum compression ratio [34]. These types of compressors are mainly used when the high-pressure head is needed at a low flow. Reciprocating compressors are widely used in petrochemicals industries, gas storage, and gas transport. The reliability and efficiency of a reciprocating compressor depend strongly on the performance of its suction and discharge valves respectively [35]. Reciprocating compressors are supplied either in a single stage or multistage type. The major components of a reciprocating compressor are pistons, cylinders crankshaft, piston rod packing, crossheads, suction valves and discharge valves. The advantages of reciprocating compressors include; lower initial cost, large range of horsepower, simple design and easy to install

2.4.3 Axial Compressor

An axial compressor is one in which the flow enters the compressor in an axial direction that is parallel to the axis of rotation and it is made of a drum, to which blades of specific geometry are attached. The axial compressor compresses its working fluid by accelerating the fluid and then diffusing it to convert the kinetic energy obtain into pressure increase. This fluid is accelerated by rotating blades called rotor and then diffused in stationary blades called stator. This process is repeated many times until the desired pressure ratio is obtained. Axial flow compressors are normally used in applications with low differential pressure (head) and high flow rates requirements. Axial compressors are used in air-compressors of the gas turbine, mix refrigerant applications and natural gas services [31]. The axial compressors are available in different sizes producing pressure in excess of 100psi at intake volumes between 23,500 to 588,500 [34]. This device can be deriving from either steams turbines or electric motors.

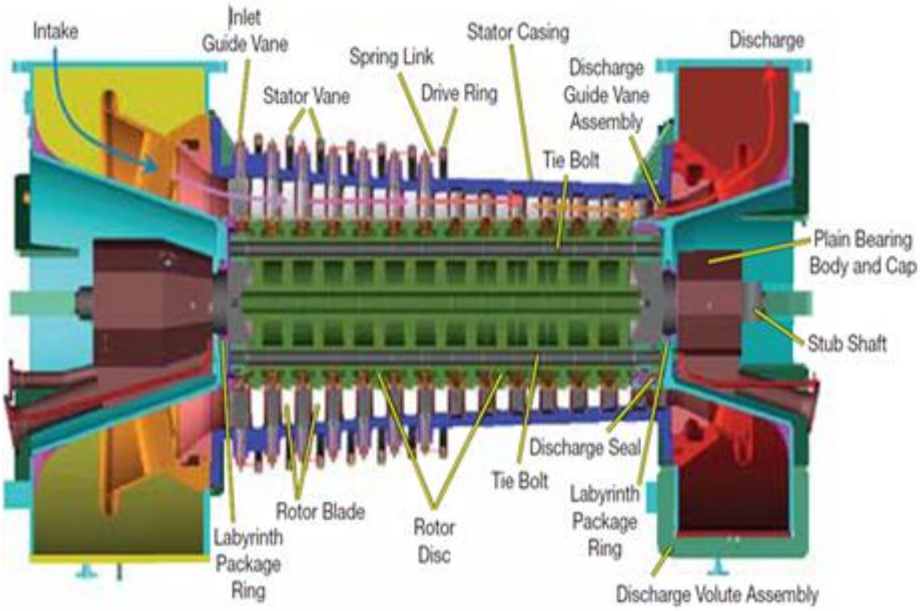

Figure 2-11 Axial compressor [33]

2.4.4 Centrifugal Compressor

Centrifugal compressors compress gases in accordance with the principle of dynamic. The rotating impellers apply initial force to the flow thereby transfer the mechanical shaft energy into enthalpy. Accordingly, the pressure, temperature, and velocity of the gas leaving the impeller are higher than that of the inlet [36]. In centrifugal compressors, the maximum pressure rise depends on the rotation speed of the impeller and impeller diameter.

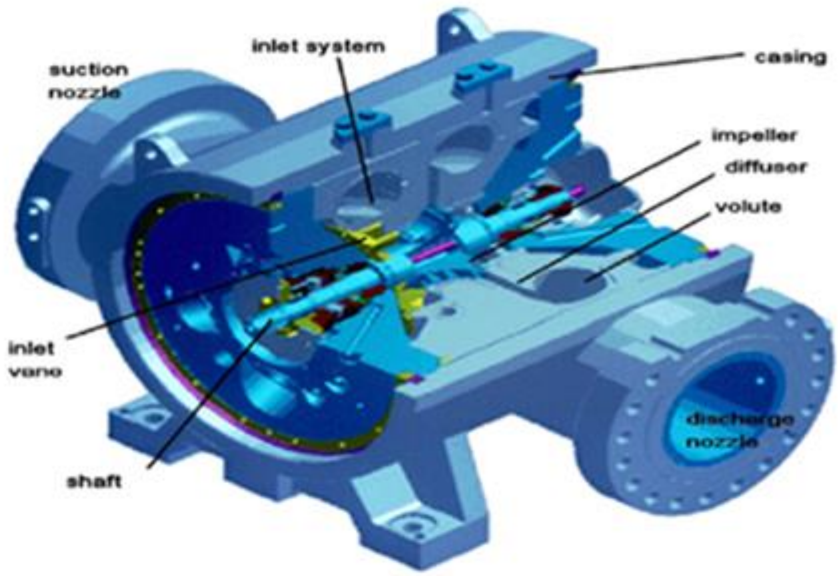

Figure 2-12 Typical centrifugal compressor [37]

Centrifugal can either be single stage or multi-stage. The single-stage centrifugal has an intake volume between 100 to 150,000acfm while the multi-stage has an intake volume between 500-200,000acfm [34]. The discharge pressure of the centrifugal compressor is up to 2,352 with impeller speed from 3000rpm and above.

The power requirement of Centrifugal compressor can range from as low as 400 kW to more than 40 MW. Centrifugal compressors can be driven by the gas turbine, a steam turbine or electric motor. Kolmetz [34] concluded that the configurations of centrifugal compressors depend on its application requirement as listed below:

I. Horizontal split casing for operations below 60 bars
II. Vertical split compressors it is a multistage type and used for high pressure up to 700 kg/cm2
III. Bell casing barrel with rings instead of bolts used for high pressures
IV. Bell shape casings with single vertical end cover used for natural gas transportation
V. SR type used for relatively low pressures

2.4.5 Centrifugal Compressor Configurations

The arrangements of multistage centrifugal compressors are usually based on the flow route and it contains 1 to 10 impellers. The number of impellers required is dependent on the head required as suggested by the rule of thumb 30KJ/Kg head per impeller; although in some cases the head can be greater than this. Centrifugal compressors are said to be in a straight arrangement in one casing when the intercooling is not required as shown in Figure 2-13. The impeller arrangements are separated into two casings when the intercooler is needed. The casings arrangement can either be compound as shown in Figure 2-14 or back to back arrangement as shown in Figure 2-15. Centrifugal compressor has different arrangement when it requires operating at a high volumetric flow rate. In this arrangement, the compressor will have two inlets each at the two ends of the casing while the exit of this arrangement is at the center of the casing. This arrangement is called a dual flow as shown in Figure 2-16.

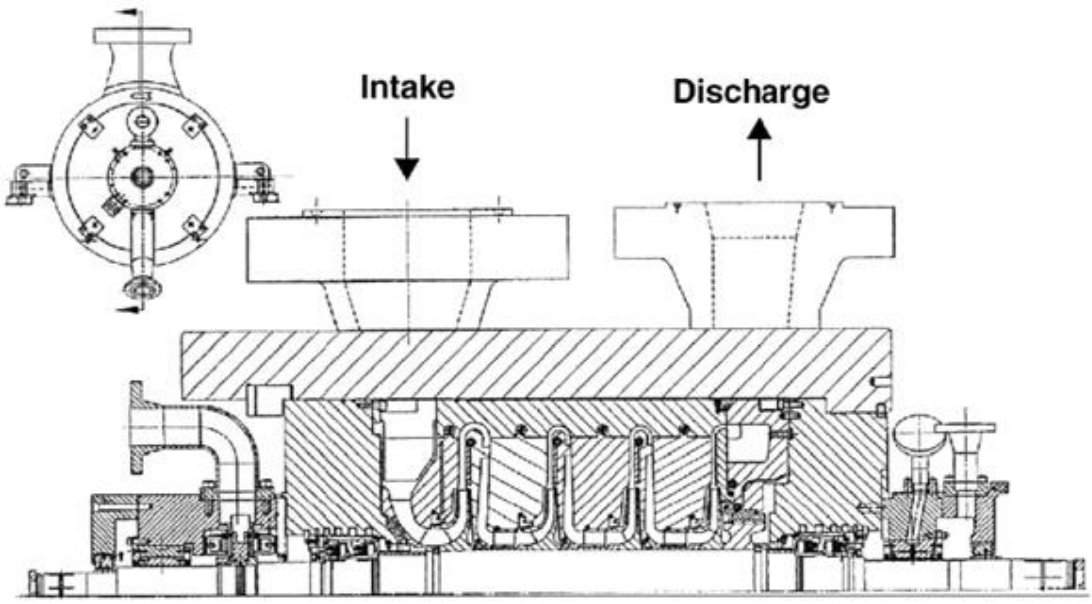

Figure 2-13 Straight multistage compressor arrangement when cooling is not required [38]**.**

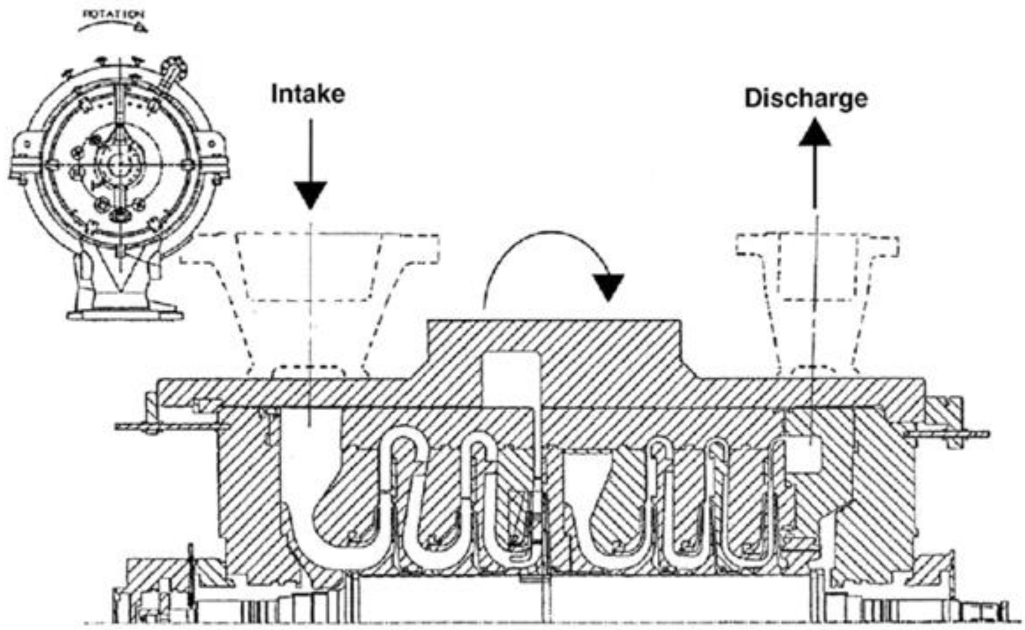

Figure 2-14 Compound centrifugal compressor arrangement with intercooling [38]

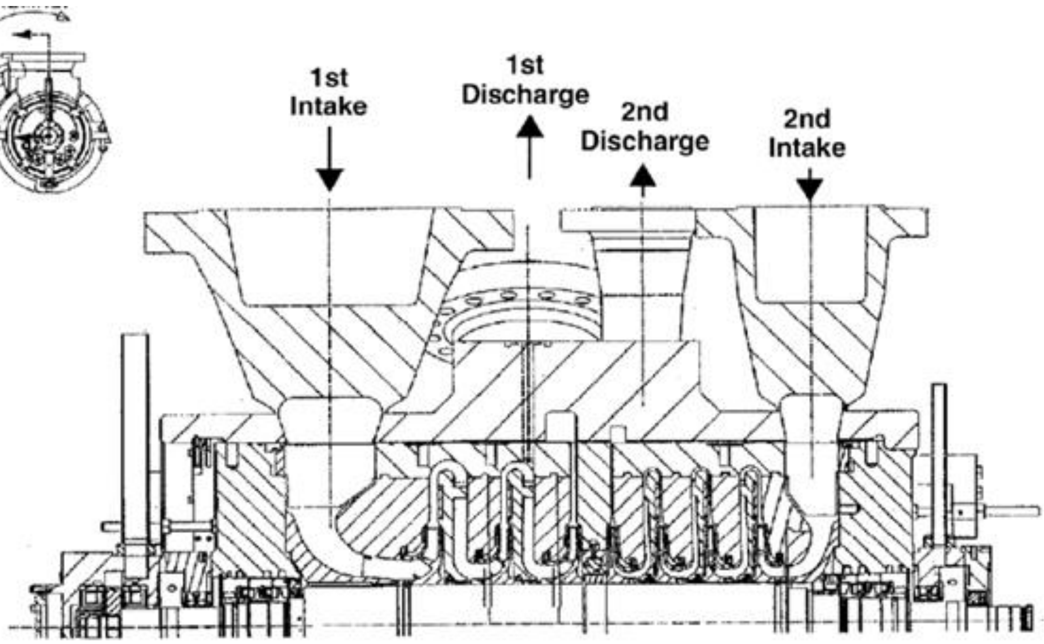

Figure 2-15 Multistage centrifugal compressor back-to-back arrangement with intercooler [38]**.**

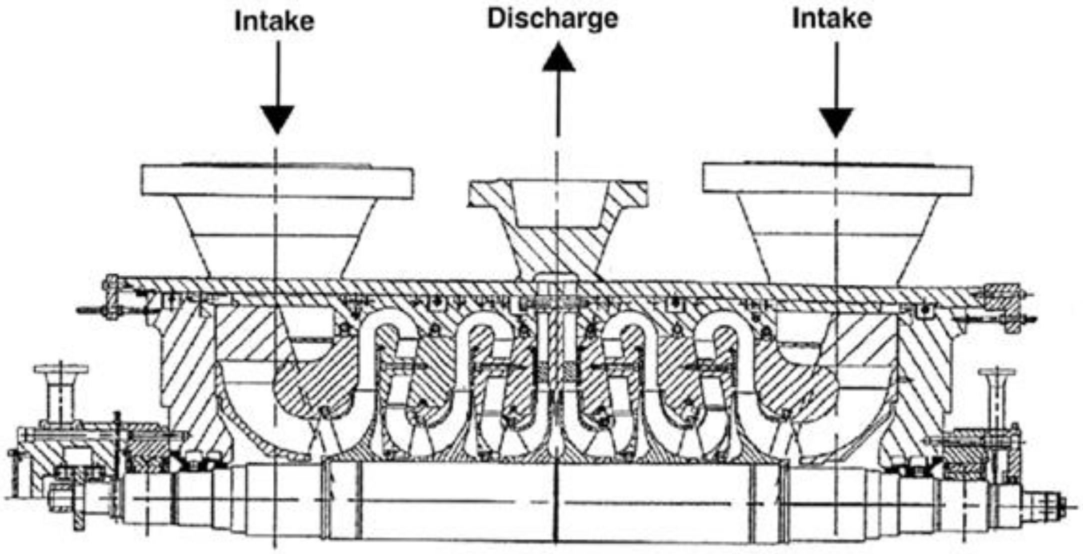

Figure 2-16 Double flow multistage centrifugal compressor used for large flow rate [38]**.**

The above explanations of the different compressor arrangements are known as the beam types in which the impellers are mounted between the radial bearings inside each of the casings. For a single stage compressor, it's configurations is regarded as a beam or overhang type of arrangements. The beam arrangement involves mounting a sole impeller on the fixed end of the transmission shaft.

2.4.6 Centrifugal Compressor System

The general method of energy transfer in the centrifugal compressor is governed by the principle of thermodynamic equations which include the equation of state, conservation of mass, conservation of energy and conservation of momentum [39]. Stagnation properties are used to examine the thermodynamics of centrifugal compressor. The stagnation properties consider the kinetic energy of the following gas through the compressor because of the gases encountered very high velocities within the centrifugal compressors [39]. The centrifugal compressor *T-S* diagram is shown (a**)** **(b)**

Figure 2-17 (a). The gas enters the casing with the suction temperature and pressure of $\boldsymbol{T_{OO}\ and\ P_{00}}$ respectively. As a result of the pressure loss at the inlet nozzle, the kinetic energy increases in the form of velocity rise due the static pressure drop which reaches to $\boldsymbol{P_1}$ at the exit of the nozzle. At the inlet of the nozzle the pressure drop is denoted by $\boldsymbol{P_{01} - P_1}$ for the isentropic process while $\boldsymbol{P_{00} - P_1}$ for the polytropic process. Though, for both polytropic and isentropic processes the stagnation temperature is the same [39]. At stage 1 the gas then enters into the impeller zone with an absolute velocity of $\boldsymbol{V_1}$ and both the isentropic and polytropic processes in the impeller are specified by (1-2) and (1-2') respectively. The velocity of the gas increases at the exit of the impeller which reaches $\boldsymbol{V_2}$ as shown in Figure 2-17 (b). Apart from the impeller, the remaining pressure rise is achieved in diffuser at stage 2.

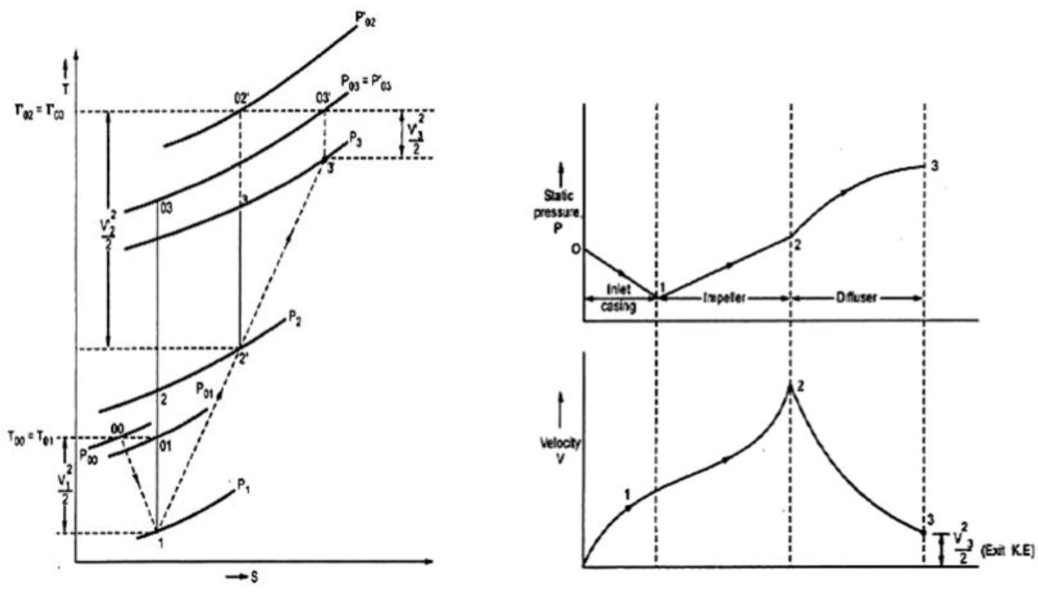

(a) **(b)**

Figure 2-17 Variation in Aerodynamic and Thermodynamic Parameters (a) Centrifugal compressor T-S diagram (b) Compressor stage static Pressure and velocity [39]

2.4.6.1 Selection of Centrifugal Compressor

According to Akhtar [40], the selection of a compressor depends on the process design parameters such as gas composition, flow rate, inlet pressure, inlet temperature and outlet pressure as the train arrangement series, parallel, multiple bodies, multiple sections, intercooling, and others.

If the compressor process design requires various ranges of operating conditions; then selection will be made based on the principle of the rated point. The operating conditions to consider are defined by API 617, wish include highest volumetric flow rate; lowest molecular weight; very high-pressure ratio and very high inlet temperature [24]. Compressors are also selected on the basis of the low capital cost and maintenance cost.

Centrifugal compressors are selected based on the number of impellers, a number of casings, operating speed and impeller diameter, type of drive, control method, sealing type and bearing type as well as the philosophy of having high efficiency over wide range of operating conditions [37].

Centrifugal compressor has a wider operating range and reasonable operating pressure ratio when compared to other types of compressors. According to Boyce [41], centrifugal compressors are appropriate for users in gas pipeline transportation and process plant because of their wide operating range and reasonable pressure ratio. The Figure 2-18 shows a comparison of operating range and pressure ratio of different types of compressors.

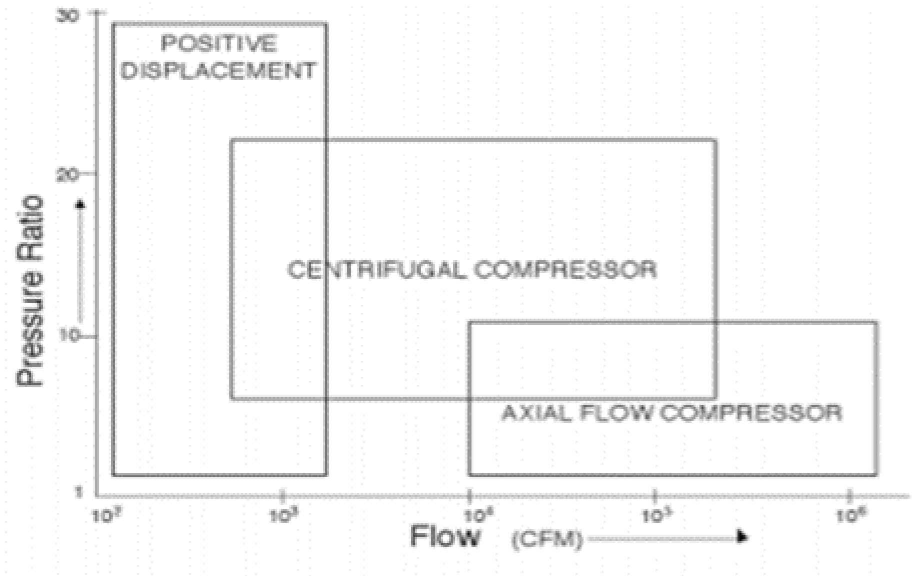

Figure 2-18 Comparison in operating range and pressure ratio of different types of compressors [41]

2.4.6.2 Centrifugal Compressor Applications

Generally, centrifugal compressors because of their simplicity, high efficiency, reliable operation, and easy maintenance when working in a wide range of conditions, have been widely used in many diverse economy branches [42]. Centrifugal compressors are used in metallurgy, power generation, chemical industries, cement factories and wastewater treatment, as well as armored vehicles. Centrifugal compressors are also used in upstream and midstream sector of oil and gas such as gas gathering, gas lift and compression for injection, compression for a gas pipeline, air compression and LNG compression [37].

2.4.6.3 Centrifugal Compressor Performance

Centrifugal compressors play a major role in gas production from offshore fields, gas transportation, gas receiving, gas recompression and other similar activities. The deterioration of compressor performance from its actual design either by wear, fouling or excessive internal leakages can have a direct impact on revenue and profitability of gas production and transportation. The precise real-time performance gas compressors data is required by the operators for monitoring as well as maintenance scheduling work where necessary [40]. Centrifugal compressors performance is guaranteed by manufacturers at the tender stage in accordance with the provision of American Petroleum Institute (API) standard 617[43]. In general, the compressor performance loss will cause an increase in engine power or higher fuel consumption. Brun and Nored [44] described the following as performance parameters of centrifugal compressors:

- Flow/flow coefficient
- Head/head coefficient
- Efficiency
- Power absorbed

The two parameters that directly affect the performance of centrifugal compressors are head and capacity. All the other parameters such as temperature, pressure, molecular weight and standard volumetric flow rates affect the performance indirectly [45].

The centrifugal gas compressor performance can be described by the relationships of actual flow (Q), Isentropic head (H*), Isentropic efficiency (ɳ), with the operating speed (N) as parameters [27]. If the gas composition is known the compressor head (H) can be obtained from suction and discharge pressure and temperature. Therefore, the isentropic head (H*) can be expressed as follows:

$$H^* = h\big(P_d, S(P_s, T_s)\big) - h(P_s, T_s) \tag{2-14}$$

While the isentropic efficiency can be obtained as follows:

$$\eta_s = \frac{H^*}{H} \tag{2-15}$$

The actual head (H), which defines the power as well as discharge temperature, can be obtained from the relationship between isentropic head and isentropic efficiency.

$$H = \frac{H^*}{\eta} = h(P_s, T_s) - h(P_s, T_s) \tag{2-16}$$

The operation of centrifugal compressor is defined by a map with pressure ratio and non- dimensional mass flow as coordinates as shown in Figure 2-19. However, the usable portion of the map is limited by the surge, choke and maximum permissible speed lines [46].

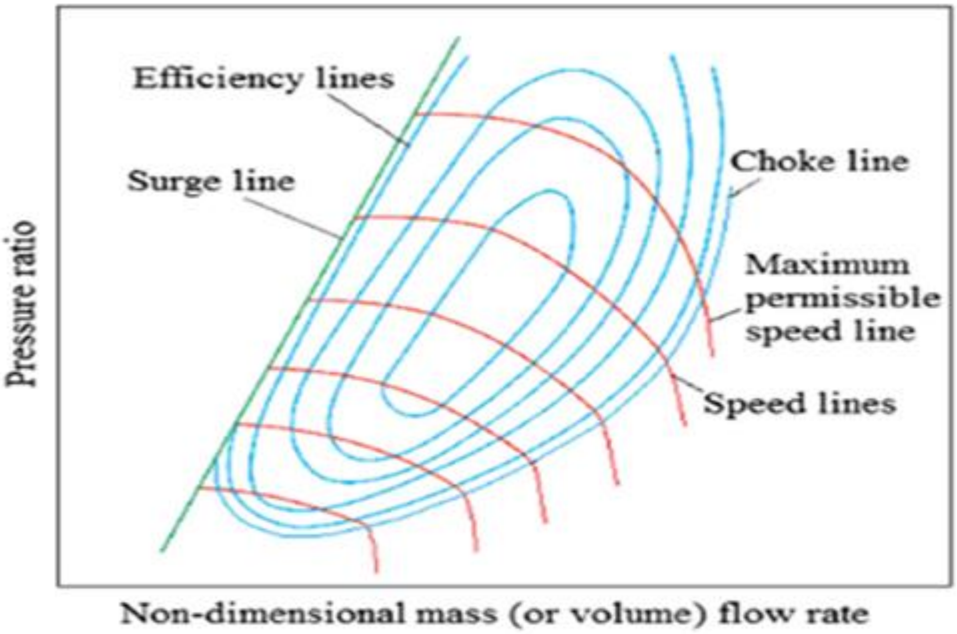

Figure 2-19 Compressor Performance Map [46]

2.4.6.4 Surge

Surge is defined as the operating point at which the compressor peak head capability and flow limit are reached [47]. Once surge occurs the compressor losses its ability to main the peak head and the whole system becomes unstable which leads to increase in temperature, high vibration, and change in axial thrust.

2.4.6.5 Choke

Choke or stone wall is defined as the flow in which the gas velocity at one of the impellers approaches the sound velocity. From an aerodynamic point of view, choke refers to a situation where flow passages become blocked either due to the occurrence of compression shocks or due to massive flow separation [48].

2.4.6.6 Minimum Permissible Speed

It is the minimum speed acceptable for compressor operation. Speeds beyond this point may control the compressor to stop or go into an idle condition.

2.4.7 Compressor Power

Compressor gas power is defined as the amount of power required to compress a certain quantity of gas through a specified pressure ration. A compression process typically follows the pressure-volume relation known as a polytropic process also dynamic compressor generally follows the polytropic cycle. The polytropic head requires the knowledge of either discharge temperature or polytropic efficiency [49]. The general thermodynamic equation for polytropic head is given

$$H_p = ZRT_1 \frac{n}{n-1} (\Upsilon_p^{\frac{n-1}{n}} - 1) \quad \textbf{(2-17)}$$

While polytropic efficiency can be written as follows:

$$\eta_p = \frac{H_P}{H} \quad \textbf{(2-18)}$$

If the density is known, the actual flow (Q) can be calculated from standard flow

$$Q(P,T) = \frac{P_S}{\rho(P,T)} Q_{std} = \frac{W}{\rho(P,T)} \quad \textbf{(2-19)}$$

Therefore, the aerodynamic or gas power of the compressor is determined by this formula:

$$P_g = \rho_1 Q_1 H = \frac{P_1}{Z_1 R T_1} Q_1 H \quad \textbf{(2-20)}$$

After the gas power (GP) has been determined, mechanical losses such as friction in bearings and seals are usually approximateld as 1 to 2% of the absorbed power [37]. Therefore, the expected absorbed power of compressor should include all the mechanical losses by introducing the mechanical efficiency (η_m), the compressor absorbed power turn into

$$P = \frac{P_g}{\eta_m} \quad \textbf{(2-21)}$$

2.4.8 Compressor Driver

Centrifugal compressors are regarded as high-speed machine and ideally should have high-speed drivers. The drivers used in pipeline application include; electric motor, gas turbine, steam turbine and reciprocating engine [50]. The selections of these drivers are based on the consideration of life cycle cost, fuel or energy cost, reliability, and availability, low weight, good thermal efficiency and realistic part power torque [51].

Gas engine driver is not competitive in terms of installed cost at the power level demanded by large diameter and high-pressure pipeline transmission network [28]. In gas pipeline transmission gas turbines are widely used since they are appropriate for driving centrifugal compressors [52]. The gas turbine operating range match that of the centrifugal compressor which is between 50 -105% of the compressor rated speed [53]. Gas turbine has a wide operating range as compared to other drivers which make it suitable to drive centrifugal compressors. The operating comparison of different drives is shown in Figure 2-20.

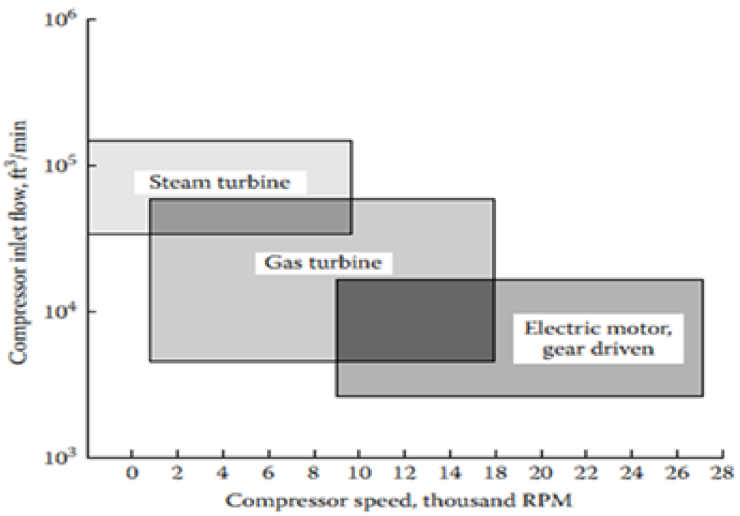

Figure 2-20 Comparison of different drives [54]

2.5 Gas Turbine

The gas turbine is a device that converts heat into work and the ideal cycle used by gas turbines is the Brayton, Froude or constant pressure cycle [55]. The gas turbine is regarded as one of the versatile equipment of turbo-machinery today; because it is used in several accept of civil aviation and industries such as power generation, process plants, oil and gas and other domestic smaller related industries. Also, gas turbines are used to drive compressors.

2.5.1 Gas Turbine Improvement and Performance

Nowadays, simple cycle model has an efficiency of about 40% with an inlet temperature of 1500^{O}C and outlet temperature up to 630^{O}C [56]. Due to the development of gas turbine technology in 1992, the combined cycle plant at Killingholme, UK achieved efficiency of 52%. The thermal efficiencies of the simple cycle gas turbine are in the range of 40% while in combined cycle arrangement the thermal efficiencies of 60% are achieved presently [57]. Also, the recent fleets of the gas turbine have features like advanced combustion systems, multi-fuel capabilities and reduced maintenance [58].

The gas turbine power output is affected by turbine inlet temperature, pressure ratio, and component inefficiencies. In an effort to increase the performance of gas turbine, simple cycles gas turbine were improved by introducing other components known as advanced cycle gas turbine [59,60]. Gas turbine cycles have been integrated with systems such as intercooler, recuperator and reheat so as to improve the cycle's efficiency and its overall performance. The combined cycle gas turbine is widely used in power generation replacing the older generating plant due to its substantial reduction in fuel consumption and overall improvement in cycle efficiency [61].

In a gas turbine, the high-pressure air is generated by an air compressor and fed into the combustor, where the fuel is burnt. The excess air and the combustion products leave the combustor at very high pressure and temperature. This gas is expanded in the gas generator turbine, which has the sole responsibility of providing power to turn the air compressor. This gas leaves the gas generator turbine with high pressure and temperature and thereby further expands in the power turbine. The power turbine is connected to the driven equipment. At this point, the driver and the driven can run at a speed that is autonomous of the speed of the gas generator portion of the gas turbine [49].

The increase in speed and temperature of gas generator provides the power turbine with higher temperature, higher pressure, and higher mass flow which allows the power turbine to produce more power. If the power supplied by the power turbine is greater than the power absorbed by the load, both the driven compressor and power turbine will accelerate together until equilibrium is reached [49].

2.5.2 Industrial Gas Turbine Configuration

Gas turbines are configured in a single shaft, double shafts or triple shafts designs. Many of the recent gas turbines are of the triple aero-derivative shaft design. In a single shaft gas turbine as shown in Figure 2-21 both the generator and power turbine are mounted on the same shaft. This type of turbine is commonly limited to generator derive applications, due to the fact that the turbine starting load is considerably lower for a generator application because generator load is started under zero and are mostly used for power generation [28].

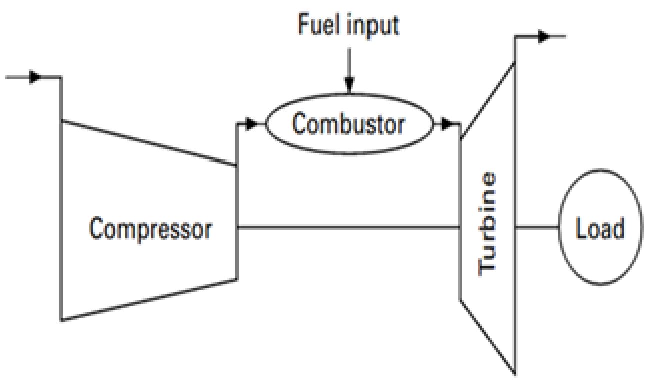

Figure 2-21 Single shaft gas turbine [62]

As shown in Figure 2-22 dual shaft gas turbines are available with a free turbine, in which the speed of the gas generator is autonomous of the speed of power turbine. The speed of the output shaft has no effect on the gas generator performance because there is no mechanical coupling between the gas generator and power turine [49]. The Dual shaft turbine engines have better efficiency than the single shaft engine since the gas generator is allowed to run at a lower speed during a part load operation. Dual shafts engine are used for mechanical drive, pump and compressor applications

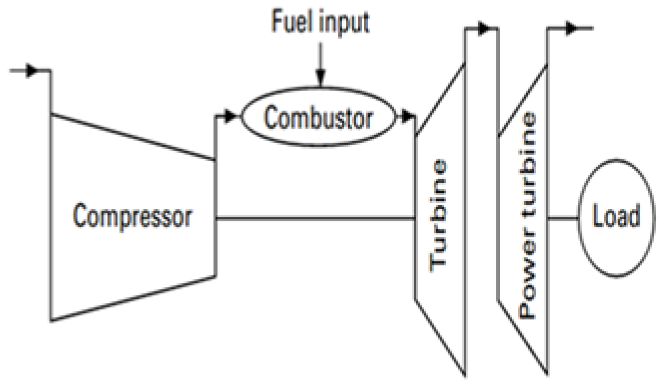

Figure 2-22 Double shaft gas turbine [62]

Figure 2-23 shows an aero derivative three shafts gas turbine engine, based on the advance aircraft engine technologies and materials; they are significantly lighter and flexible as compared to heave duty gas turbine..

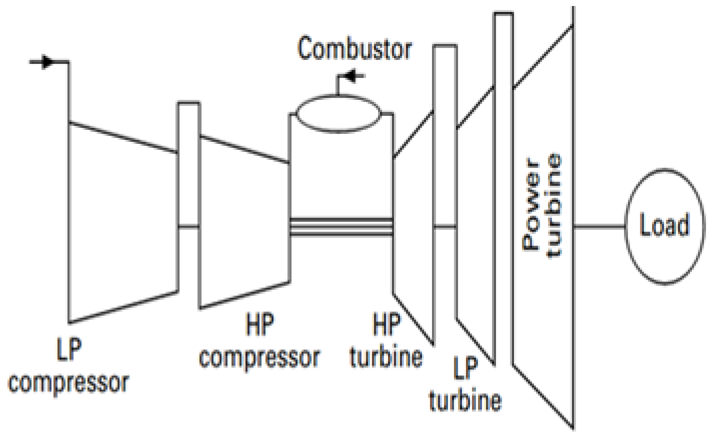

Figure 2-23 Triple shaft gas turbine [62]

2.5.3 Gas Turbine Application

Gas turbine was first developed for power generation but it was not successful because of the low performance [11]. Gas turbine achieved its major breakthrough during the World War II when is used in the military jet engine [60,63]. Generally, gas turbine application was broadly divided in two; these are industrial gas turbine and aero gas turbine. The aero engines are used for aircraft propulsion; these types of engines operate at the high-pressure ratio, high turbine inlet temperature, and high power to weight ratio [11]. The aero engines are manufactured to be very efficient and reliable depending on the application either civil or military.

industrial gas turbine is also grouped into two namely, heavy-duty gas turbines and aero-derivative gas turbine [64]. These gas turbines are manufactured based on the power requirement, reliability, availability, and ease of maintenance [62]. The gas turbine designed based on the aero application requirement are regarded as aero-derivatives; thus, maintain the features stated above. Many of the civil aircraft engines have medium component life, reasonable fuel consumption and have a thermal efficiency of up to 42% [65].

The heavy duty gas turbines have low power to weight ratio and bulky because they are not originally designed to fly [11]. They have a moderate pressure ratio of order 10-18, thermal efficiency ranges from 30-38%. They are designed is based on the durability of components. In the early 1960s, there is technological gap exists between heavy duty gas turbines and aero-derivative gas turbines but lately is gap has been reduced reasonably. Currently, these gas turbines have the same technological development thereby closing the gap [66]. The current applications of gas turbines include the following:

1. Power generation.
2. Marine Propulsion.
3. Combine heat and power.
4. Pipeline transmission.

The gas turbines are rated based on application. When used for power generation, they are measured in (kW) or (MW) and when used as mechanical drives, they are measured in (hp) ([11].

2.5.4 Gas Turbine Power

According to Brun and Nored [44], the following four methods are used for determining gas turbine power:

- Direct torque coupling measurements
- Direct generator power measurements
- Indirect driven centrifugal compressor shaft power measurement
- Indirect gas turbine heat balance measurement

The direct measurements methods involve the use of either an input power from the generator or the torque measuring coupling and are usually associated with the lowest uncertainty. However, determining the shaft power output of a gas turbine using the centrifugal compressor shaft power usually yield uncertainties but is widely used and acceptable [44].

Kurz et al [49] said that the amount of power at the power turbine shaft is affected by the following factors:

- Ambient temperature
- Ambient pressure
- Power turbine speed
- Inlet fuel
- Accessory loads
- Relative humidity and altitude

2.5.5 Effects of Ambient Condition on Gas Turbine Performance

The power output and efficiency of industrial gas turbine differ according to the ambient temperature conditions. The amount of these variations affects the fuel consumption and power output of the engine greatly. The power output of a gas turbine decreases with reduction in air mass flow rate; the density of the air reduces as the ambient temperature increases. Also, the efficiency of the engine decreases because the compressor requires more power to compress air at high temperature [55].

Kakaras et al [67], concluded that ambient air temperature is a strong function of efficiency and power output of the gas turbine. Depending on the type of gas turbine, power output is reduced by a percentage between 5 to 10 percent of the ISO –rated power output (15^{O}C) for every 10 K increase in the air temperature. Also, the specific heat consumption increase between 1.5 and 4 percent at the same time [67].

Lubomirsky et al [29], suggested that gas turbine drivers are selected based on the maximum power requirement at the maximum ambient temperature during the project preliminary stage; a margin in then applied to cater for the whole pipeline operation and fluctuations as depicted in Figure 2-24. Usually, gas turbine drivers are selected based on the site conditions. This is because its power output, efficiency, and fuel consumption can be quite different than its performance at design conditions. Therefore, is imperative to ensure the gas turbine selected will provide the power required by the gas compressor.

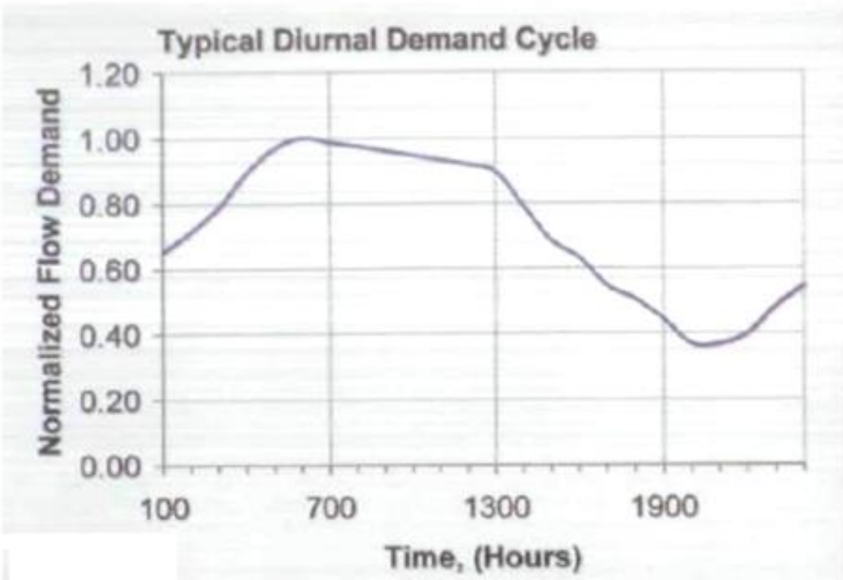

Figure 2-24 Compressor station flow variations [29]

The capital and operating costs of the different gas turbine engine configurations vary. The industrial gas engines are mostly heavier with operating life cycle of about 35 years. The aero-derivative engines are lighter and have a shorter operating life cycle. The reliability and availability of these engines are different due to different number of rotating equipment and bearings used. The selection of engine requires details analysis of its various components.

2.5.6 Effect of Operating Conditions on Gas Turbine Components Performance

Connors [68] concluded that the critical component of the gas turbine is the high-pressure turbine (HPT) because it operates at high temperature and high shaft speed. This causes an increase in stress acting on the turbine blades and disc. The hot section components can suffer creep deformation, thermal and mechanical fatigue when operated at high temperatures [69]. These deformations can lead to the hot section component to losing its ability to function as it was initially designed for, reduce its life expectancy rate and causes the component to fail prematurely [70]. According to Naeem [71], the failure in service of gas turbine blades can cause damage to other components of the engine, hence will lead to complete failure of the engine is care is not taken. Therefore, careful operation and appropriate evaluation of engine life can help reduce unsafely incidents in gas turbine operations.

3 METHODOLOGY

3.1 Abstract

The focus of this chapter is the application of Techno-Economics Environmental Risk Assessment (TERA) on compression system used on the natural gas pipeline. In this context, compression system means the use of centrifugal compressors and industrial gas turbine engines for compression of natural gas along the pipeline. The TERA framework is made of the different modules; the module considered in research is the performance module, economic module, and Lifting module. Also, the considerations for pipeline study and the GT optimization based on the compressor station location and equipment selection are considered. Subsequently, a structured framework for this assessment was incorporated in the adapted TERA framework for natural gas pipeline compression system.

3.2 Pipeline and Compressor Module

This module evaluates the design and off-design conditions of centrifugal compressors using the available thermodynamic gas equations. The equations involve the use of available gas compressor inlet parameter and gas property calculation for the estimation of power requirement by the centrifugal compressor. This module defines the centrifugal compressor power requirement for both the design point and off-design conditions and also defines the driver power requirement. The synergy between the gas compressor and the driver is to ensure maximum supply of pressure along the gas pipeline. The baseline case study has the compressor inlet pressure of 67.85 bar and outlet pressure of 95 bar respectively for the first booster station.

To ensure the continuous flow of natural gas through the pipeline the data obtained from the preliminary report on Trans Saharan Gas pipeline is adopted and pressure drop analysis using Weymouth equation was developed in Excel for the pipeline simulation. Figure 3-1 shows the proposed pipeline elevation adopted for this research.

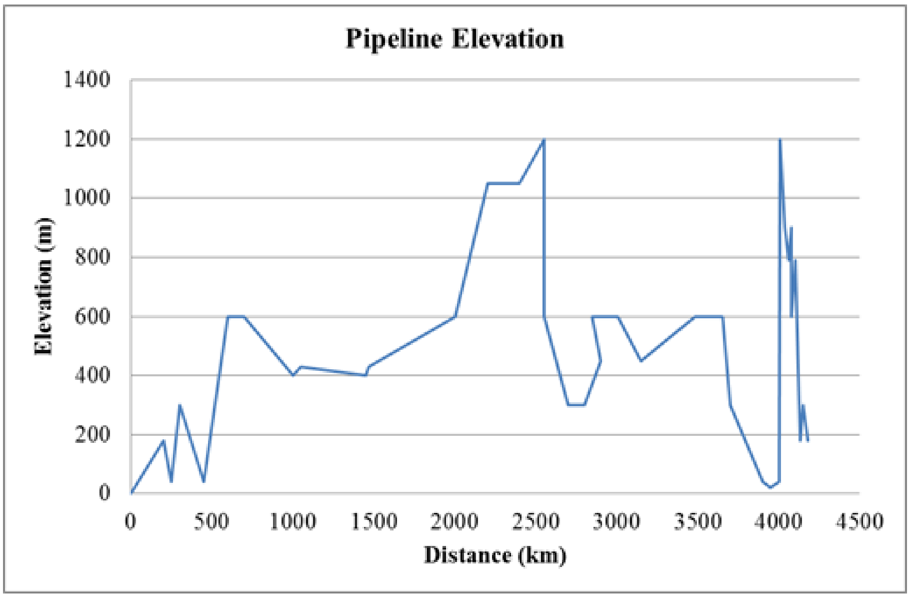

Figure 3-1 Pipeline elevation and distance

3.3 TERA Framework

The Idea of TERA framework was developed in Cranfield University, based on the research work conducted in the areas of aviation and power generation and has been proven to be effective [8]. This framework has multi-discipline modules for performance modeling of costs, noise, the environmental impact of gas turbine and aircraft weight. According to Orgaji et al [8], the TERA framework consists of several modules which include, performance module, economics module, environmental module, emission module, weight module, noise and lifing modules. Each of these modules focuses on different problems and the results obtained from these different modules will be integrated into the TERA framework. In this research performance, economic and lifing modules are considered.

TERA framework is an investment decision tool that encompasses investigating the excellent available option for engine performance, environmental impact from engine emission, costs reduction during the engine lifespan, engine availability and reliability [72]. According to Ogaji et al. [8] TERA framework is used as an avenue for ranking and selecting the excellent option for investment by identifying the risk involves and efficiently manage resources allocation.

The TERA framework has been applied to both aero and power generation technologies and now gas compression system. The framework is shown in Figure 3-2 also different TERA framework modules were explained below.

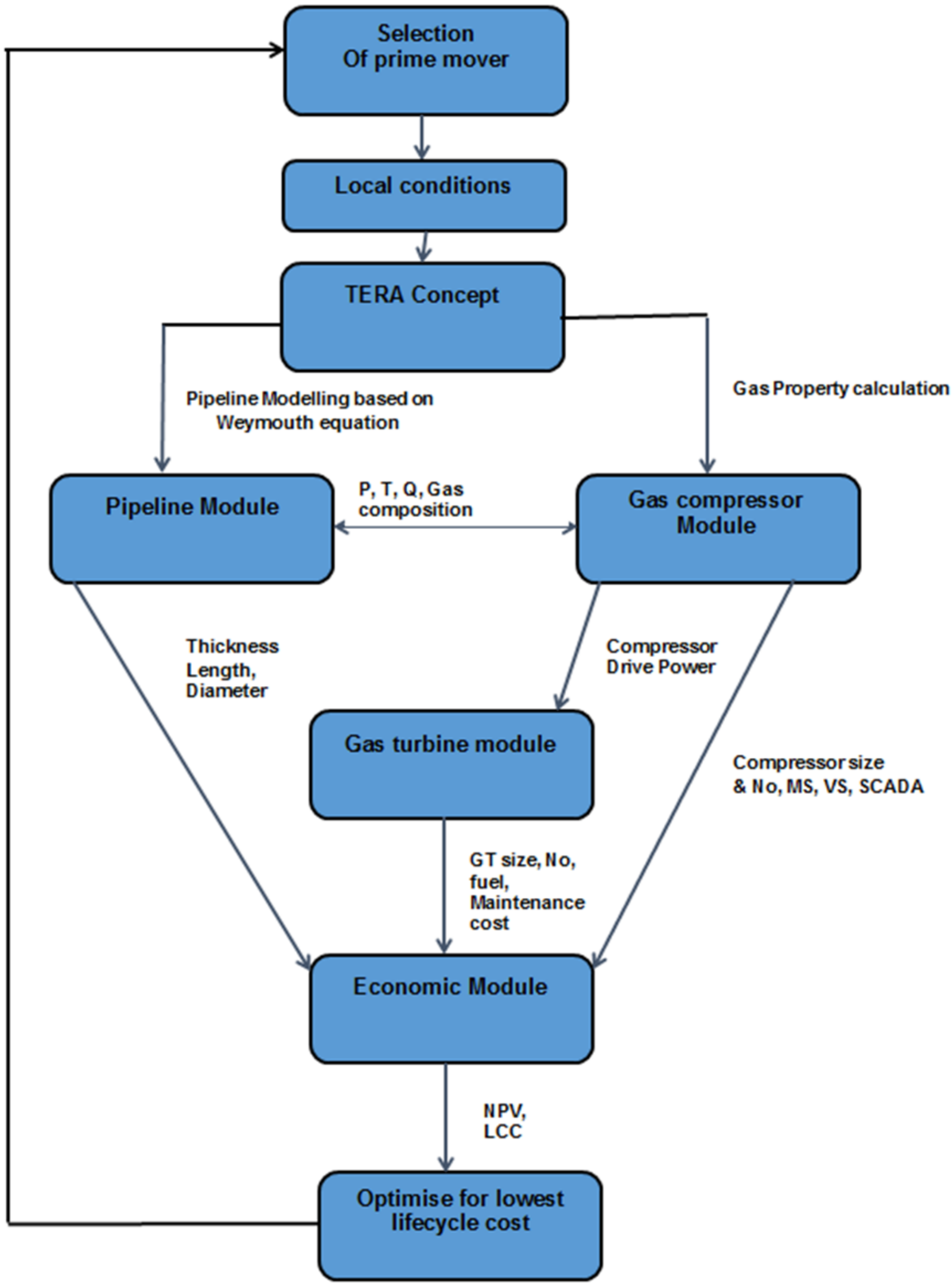

Figure 3-2 TERA framework for natural gas pipeline compression system

3.3.1 Performance Module

The performance model is the core of TERA framework. Turbomatch code which is developed at Cranfield University was used for modeling the performance of the selected industrial gas turbine engines both at the design point (DP) and off-design point (ODP). Usually, the performance modeling provides information about the industrial gas turbine engines under consideration. During engines simulation, Turbomatch scales the compressor and turbine maps of the input file to locate the design point on the map while the off-design point is calculated based on the input operating conditions. The parameters considered for the off-design operation are:

- ✓ Ambient temperature
- ✓ Turbine entry temperature
- ✓ Altitude

3.3.2 Economic Module

The economic module is one of the core modules of TERA framework that deals with the estimation of the project lifecycle cost from the knowledge of capital cost and operating cost, which is derived as a function of fuel cost and maintenance cost. The aim of this module is to calculate the project profit by considering the capital cost and operating cost

3.3.3 Lifing Module

Lifing is regarded as the entire operating cycle of an engine, through the analysis of creep and fatigue. The lifing module is responsible for the estimation of high-pressure turbine disk through a full working cycle of the engine. The disks and high-pressure turbines are regarded as very vital parameters when considering the lifing of an engine. The disks and high-pressure turbine are described as the factors that limit the working cycle of an engine which is influenced by the operating TET. To this end, as the operating TET varies, the stress on the turbine blade and disk are impacted [73]. Hence, calculating the remaining life of the turbine blade will be dependent on the operating TET. As suggested by Gad-Griggs [74], for every 20^{O} (K) increase in

TET the HPT blades lifetime reduces by half. This will Increase the maintenance cost of the GT. However, in this research, $30 per KW (Pa) was assumed and used in the maintenance costing. The output of the lifing module is the time between overhaul.

3.3.4 Overview of Turbomatch

TURBOMATCH is a code developed at Cranfield University by the department of power and propulsion engineering and it is used for design, off-design and transient performance simulation of engines configurations. FORTRAN programming language was used in developing the Turbomatch code. Currently, the code has been improved from Turbomatch 1.0 to 2.0 so as to accommodate the demand for new challenges. The Turbomatch 2.0 uses both kerosene and natural gas as fuel.

The Turbomatch code consists of many pre-programmed modules known as Bricks. The Bricks correspond to individual gas turbine components such as a compressor, turbine burners etc. The bricks name are coded using six capital letters name, which suggest its purpose, for example, TURBIN (turbine), COMPRE (compressor), BURNER (combustor) and NOZCON (convergent nozzle). These bricks are interlinked using an interface so as to provide the ability to simulate different engine components since the bricks calculate the thermodynamic processes occurring within a component.

The bricks operate with the gas state at the inlet to the component to generate the gas state at the outlet. The gas state is described by a number of quantities known collectively as station vector of that station and is corded with word Vector. Data such as efficiencies, pressure ratios and loss factors which did not form part station vectors. These items are collectively called Brick Data and usually, the outputs of brick are thrust and power. The Turbomatch performance results are presented in “txt” files, and also it has the capacity of extracting various components parameters into excel for easy analysis by the user. Figure 3-3 shows the bricks data and engine vector.

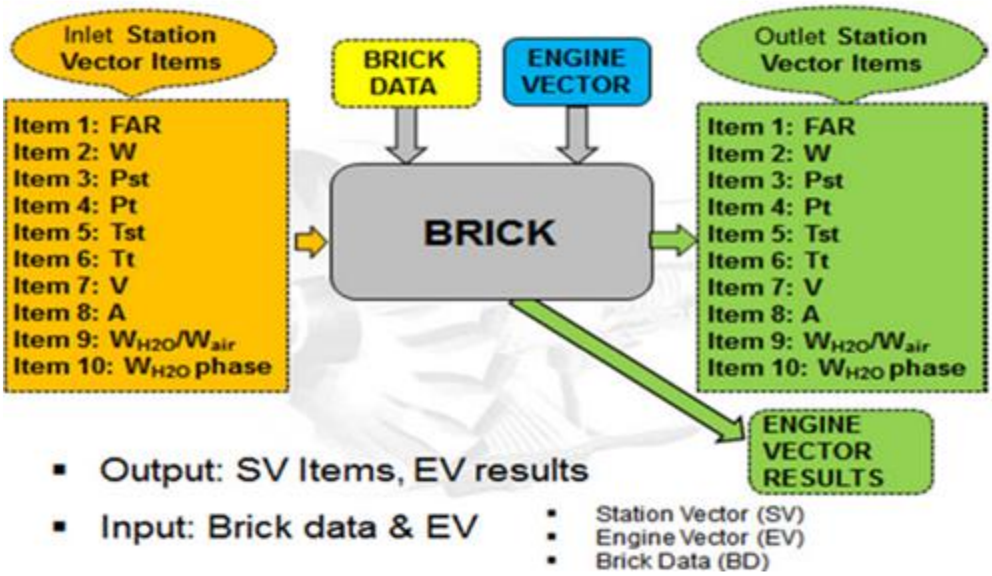

Figure 3-3 Turbomach bricks and engine vector data [75]

3.4 Conclusion

The methodology as presented explained the various modules of TERA framework. The applications of these different modules are in subsequent chapters so as to carry out required analysis that will give the detail explanation of the modules. Chapter 5 explained the performance module of the selected GT at both design and off-design conditions. The pipeline module was presented in chapter 6 while the optimization aspect was presented in chapter 7.

4 Techno-Economics- Baseline Case

4.1 Abstract

The major cost associated with the natural gas pipeline is the capital cost and operating cost. The operating cost is the cost related to operation and maintenance of the pipeline system. This research develops a techno-economic model to determine the economics of fuel consumption and maintenance cost of

gas pipeline operation based on ambient temperature variations for 18 compressor station for a distance of 4180km based on previously selected gas compressors and gas turbines.

The model estimated a project capital cost of USD 15.7 billion and the project lifecycle cost of USD 27.6billion. The project lifecycle cost consist of the following components fuel cost 33%, maintenance cost 10%, pipeline cost 26%, auxiliaries equipment cost 13%, gas compressor cost 12% and gas turbine cost 6%. The annual revenue from the gas sale is projected at USD 5.1 billion. The operating cost varies depending on the gas turbine used and the ambient temperature of the location. The result shows that the fuel cost increases with increase in ambient temperature.

From annual fuel consumption in station 2, the result shows that for 1% rise in the ambient temperature for each operational season, there is a corresponding 3.5% increase in the fuel cost per year. This increase is due to the GT power required to drive the gas compressor. As such, to meet the demand, the governor supplies additional fuel flow to raise the TET. This increase in fuel flow is reflected in additional fuel cost per year.

4.2 INTRODUCTION

Generally, the price of natural gas consists of the actual price of the gas commodity and the cost of transmitting and distributing the gas. The main cost associated with natural gas transmission and distribution is the capital costs and operating costs. A competitively designed pipeline could minimize the combination of the annual costs of compression and initial fixed charges for the pipeline. Figure 4-1 shows how to achieve an optimum pipeline construction and operation [76].

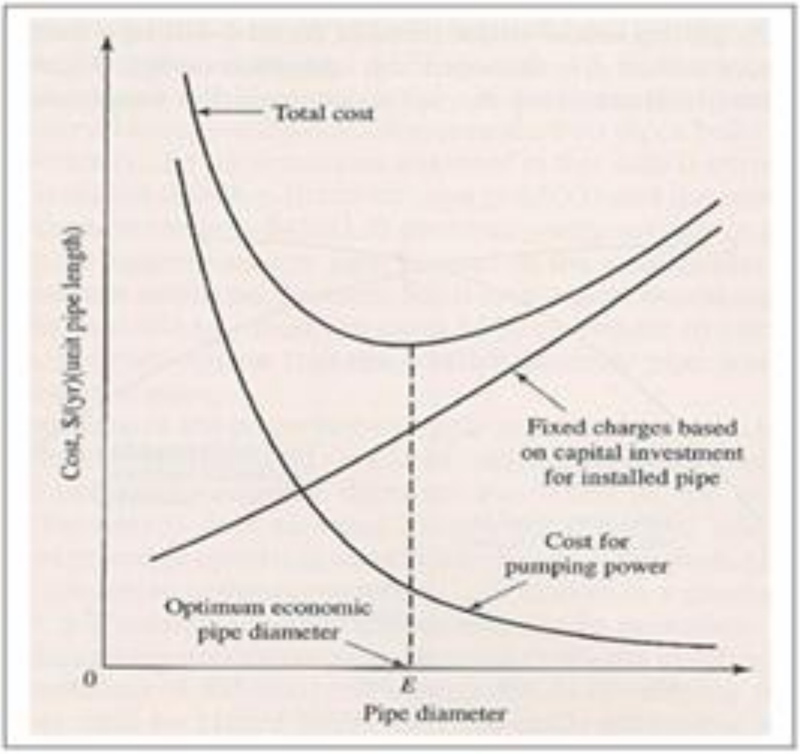

Figure 4-1 Gas pipeline optimum cost [76]

The gas compressor operating costs combined with the fixed charges associated with the pipeline will create the function representing the total cost of the pipeline. In gas pipeline transportation, the major initial capital costs of the pipeline are dominated by the cost of the pipe and compressor stations. According to Menon [14], the gas compressors and pipe take up to 96% of the construction materials. Also, the major operating cost for a gas pipeline is the cost of fuel consumed by the compressors stationed along the gas pipeline.

Generally, the major cost associated with the natural gas pipeline is the capital cost and operating cost. The operating cost is the cost related to operation and maintenance of the pipeline system. This paper develops a techno-economic model to determine the economics of fuel consumption and maintenance cost of gas pipeline operation based on ambient temperature variations for each of the compressor station along the trans-Saharan gas pipeline.

The TSGP route and pipeline data are shown in Figure 4-2 and Table 2 respectively.

Figure 4-2 Trans-Sahara gas pipeline route [2]

Table 2 Pipeline data [2]

Parameters	Values
Gas flow	(30 bcmy)
Nominal Diameter	56"
Outer Diameter	56" (1422.4mm)
Inner Diameter	54.38" (1381.2mm)
Wall Thickness	0.812" (20.62mm)
Design Pressure	100 barg
MAOP	95 barg
Pipe Grade	API 5L X70
Design Code	0.72
Design Factor	ASME B31.8
Roughness	0.0003" (7.62 μm)

The study inspired by selecting four gas turbines of 13.4MW, 15.2MW, 17MW, and 19.3MW. These gas turbines were selected based on the gas compressor power requirement and site conditions. Each compressor station consists of four identical gas compressors driven by four identical gas turbines. The ambient temperature of each of the station locations was segmented on an hourly basis as shown in Appendix A. Gas turbines performance simulation was carried out based on their location ambient temperature. Pressure drop along the pipeline was evaluated using the Weymouth equation; elevation difference is also considered in selecting the gas turbine. The gas compressor power was calculated based on the varying gas temperatures at a certain time interval. Gas compressor power and gas turbine power matching were executed to ensure that the driver provides the power required by driven at all time. The TET and its corresponding fuel flow were obtained from Turbomatch and it forms the basis for fuel cost and maintenance cost.

The operation and maintenance cost of a gas turbine comprises variable and fixed charges. This cost to a large extent depends on the decision taken during the design and manufacturing stage of the equipment. Among the variable cost, the fuel cost is usually calculated separately because it contributes the largest cost. In this research, the operation and maintenance cost was based on the 2014 cost estimates and the fuel price assumed to be fixed [11].

The project capital cost was in line with the gas pipeline hydraulics analysis and gas turbine world estimates. The revenue is the quantity of natural gas to be sold. This study considered the gas price for Spain as published in 2016 quarterly Europe Energy Portal. The project economic performance based on the lifecycle cost and the net present value was developed in Excel. Table 3 shows the assumptions made for the economic analysis. In this case also, the following major assumptions in the operation of the GT are considered:

- Gas temperature is equivalent to ambient temperature at the entry of compressor station or at the delivery point as suggested by Menon [14].
- gas composition is constant throughout the study
- The pipeline is cleaned (has no degradation).

- Smaller GT are used as mechanical drivers and operates throughout the year
- Project life time of 30 years
- The GT operations is based on the ambient temperature variations winter, dry and hot seasons

Table 3 Assumptions for the economic analysis

Parameter	Value
Plant life (years)	30
Fuel cost ($/kg)	0.16
Discount rate (%)	15
Natural gas price ($/MMbtu)	4.04
Auxiliaries (%)	3.5
Material cost ($)	1110
Coating & wrapping ($/feet)	5
Installation cost ($/ mile)	846594.2312
Pipe thickness (inch)	0.812
Pipe grade	X70

4.3 Method of Approach

The economic module was developed in Excel based on the necessary data received from the gas compressors, gas turbines, and pipeline. The calculation for the economic module considers the capital and operating costs for the entire project duration. The module considered the ambient temperature variation for the three seasons'; winter, dry and hot. The power variation and the corresponding TET for each of the compressor station which would affect the fuel consumption and maintenance cost were also considered. The module was based on lifecycle cost and NPV approach as shown in Figure 4-3. The ambient temperatures for the entire 18 booster station locations are segmented based on the different time of the day and seasons of the year. The gas compressors powers were calculated based on the constant flow rate and varying gas temperatures. The selected gas turbines were simulated based on the location ambient temperature and gas compressor power requirement. The lifecycle cost and NPV were computed from the established economic model with costs associated with the project over its useful life.

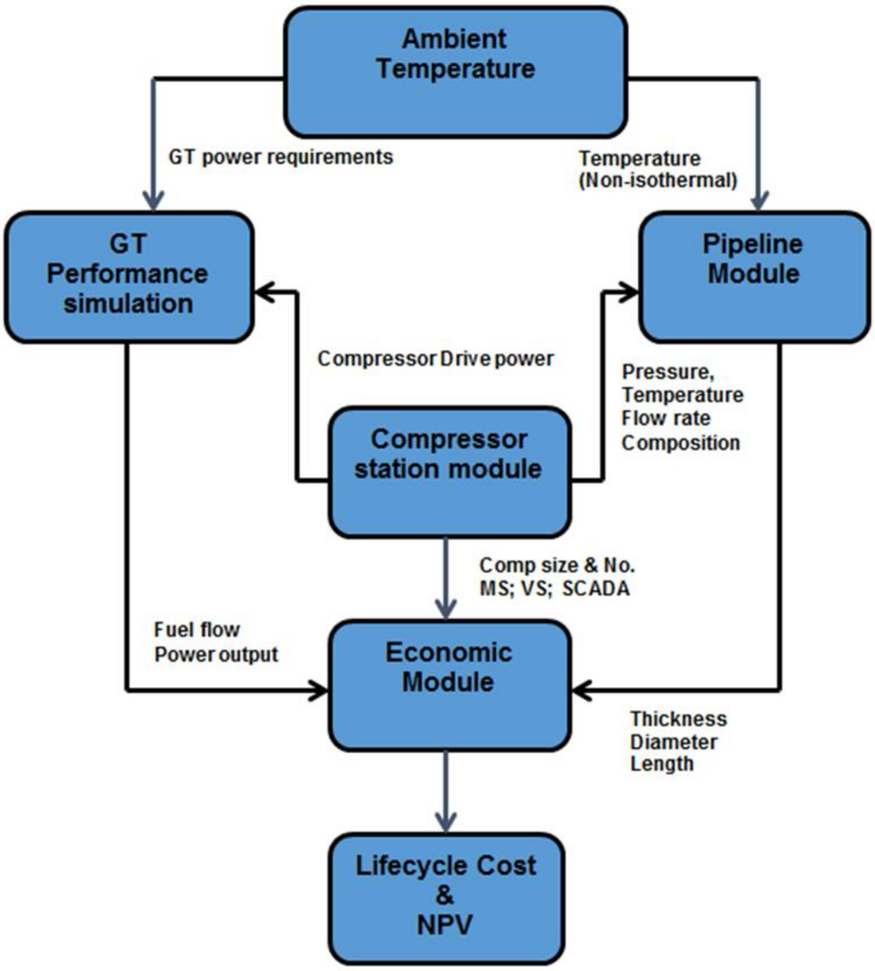

Figure 4-3 Model developed scheme

4.4 Component Cost

For a constructed natural gas pipeline there would be a capital and operating costs of the pipe. Factors that affect the pipeline costing include the pipe diameter, operating pressure, distance and terrain through which the pipeline passes [77].

According to Menon [16], the major components that form the basis for the initial capital cost for the natural gas pipeline is as follows:

- Pipeline
- Compressor stations
- Mainline valve
- Metering station
- Supervisory control and data acquisition (SCADA).

4.4.1 Pipeline Cost

In natural gas transmission system the cost related to the pipeline includes; the material cost, installation cost, coating, and wrapping cost. Generally, the pipe costing is a function of material use, pipe diameter, wall thickness, and length. For a given length, diameter and thickness the material cost would be calculated using the below equation:

$$PMC = \frac{10.68(D - t)tLC\ X\ 5280}{2000} \qquad \textbf{(4-1)}$$

Where C is the cost of material in ($/ton), t, L, and D, are the thickness, length and the diameter of the pipe respectively. American Petroleum Institute (API) categories welded and seamless pipeline used for natural gas and petroleum industries. API 5l which is suitable for transporting natural gas and X70 steel grade is used in this work. The cost of the steel material was obtained from the pipeline manufacturers' website.

To obtain the pipe wall thickness for a given diameter and operating pressure, this research adopted the ASME B31.8 design equation which is usually used as a standard for natural gas transmission system stated below.

$$t = \frac{Pd_o}{2FETS_y} \qquad \textbf{(4-2)}$$

Where P is the internal pressure, d_o is the outer diameter, S_y is the minimum yield stress, F is the design factor, E is the longitudinal weld-joint factor and T is temperature derating factor.

The pipeline installation cost is a function of the terrain, diameter, and length. Generally, the installation cost increases with the increase in the length of pipe.

To come up with the installation cost of the pipeline, the equation for estimating the installation cost of the pipeline for a given diameter and length was obtained from a wealth of historical data available for construction of various pipe sizes from the Institute of transportation studies stated below:

$$Y = 343.21X^2 + 2073.9X + 170013 \quad \textbf{(4-3)}$$

Where Y, is the cost in ($/mile) and X, is the (diameter/inches). The cost for coating and wrapping is estimated in ($/feet). Therefore, the total capital cost for pipeline is given as

$$P_c = P_{mc} + P_{intc} + C_{CW} \quad \textbf{(4-4)}$$

Where P_c, is the pipe is cost, P_{mc} is pipe material cost, P_{intc} is the pipe installation cost and C_{CW} is the cost of coating and wrapping.

4.4.2 Compressor Stations

To transport natural gas through a pipeline, one or more compressor stations are to be installed along the pipeline to provide the necessary gas pressure. The performance of centrifugal compressor and gas turbine to some extent influence the economic success of a compression. The capital cost for compressor station includes the first cost and installation cost [26]. The compressor station first cost includes the cost of the compressor, driver and other equipment needed for the successful operation of the compressor and its driver.

The compressor provides the required discharge pressure based on the Maximum Allowable Operating Pressure (MAOP) of the pipeline and the driver will provide the power required by the gas compressor irrespective of the site elevation and ambient temperature. The compressor cost is given in dollars per KW installed as stated below.

$$C_c = cost\ per\ \left(\frac{\$}{kW}\right) * Number\ of\ (KW)\ installed \quad \textbf{(4-5)}$$

The gas turbine capital cost varies base on the capacity as provided by the Gas Turbine World Handbook show in Figure 4-4 the cost decreases as the size of compressor capacity (KW) increases.

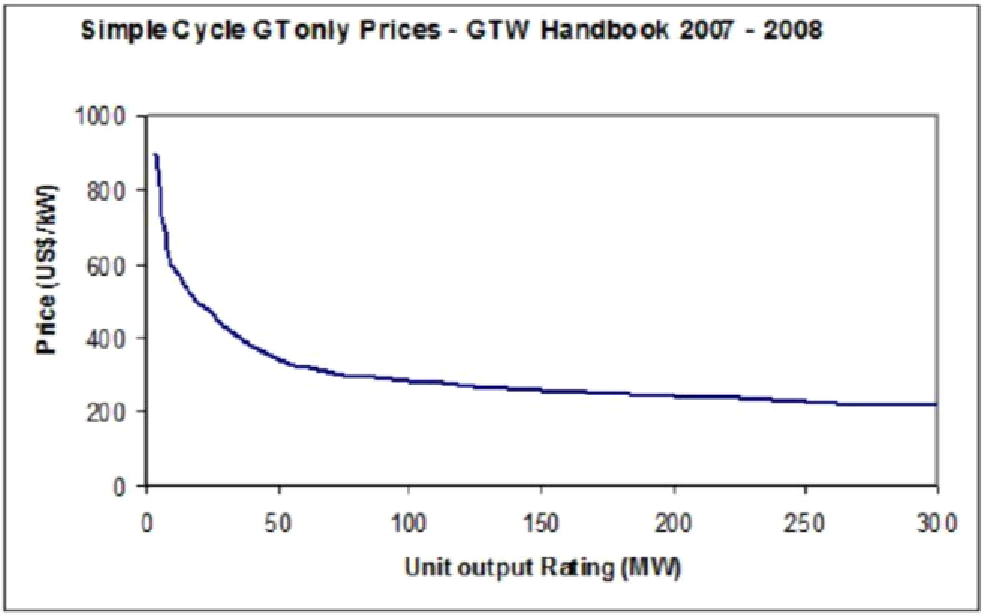

Figure 4-4 Gas turbine price [78]

The gas turbine capital cost was calculated based on the following assumptions [79].

- Increase the cost of gas turbine per KW by multiplying by 2 to cater for installation cost
- A factor of 1.38 has been adopted for shipping cost

4.4.3 Valve Stations

Valve stations are also an important component of pipeline transmission system. They are installed to separate segments of the pipeline for maintenance repair and safety reason. The valves can be open to allow free flow of natural gas or close to stop the flow of the gas and for the easy access during pipeline repair. These valves are installed at every 5 to 20 miles which are subject to regulation by safety codes [14]. This research adopted 20 miles along the gas pipeline and estimated to cost between 5% of the total project cost [14].

4.4.4 Metering Station

Metering stations are constructed at certain intervals along the gas pipeline. The aim of these stations is to allow pipeline companies to track the amount of gas flowing along the pipeline and also allows for performance monitoring of the pipeline transmission especially at the location where the ownership handover will take place. Generally, metering stations are regarded as a cash register. The metering stations are assessed as fixed price, including material and labor for a particular site [14].

4.4.5 Supervisory Control and Data Acquisition (SCADA)

These are equipment responsible for taking a measurement and collecting data along the pipeline. They are designed to gather information along the pipeline and transfer this information to a central computer facility. The information collected will display to the operators in form of text or graphic. The SCADA system consists of both hardware and software equipment and the cost of SCADA equipment range from $2 million to $5 million or even more [14]. The cost of the SCADA facilities is the function of the pipe length, a number of compressor stations along the pipeline. SCADA is also estimated as a percentage of the total project cost.

4.5 Operating Cost

After the constructed pipeline, compressor stations, and other equipment along the pipeline are put into use there going to be operating cost over the useful years of the pipeline, which is 30 years adopted for this study. The cost of operation and maintenance considered include the following:

- fuel cost
- maintenance cost

4.5.1 Fuel Cost

Fuel cost is the dominant factor in operating cost. The important performance parameters for economic evaluation in compressor station operation are the efficiency and operating range. The efficiency is relative to the quantity of fuel consumed in order to deliver a certain amount of gas from a suction pressure to discharge pressure. High thermal efficiency gas turbine drivers and high isentropic efficiency gas compressor are good packages for the cost-effective system. Operating range defines the range of likely operating conditions in terms of flow and head at an acceptable efficiency, within the power capability of the driver.

To understand the quantity of fuel consumed by the selected gas turbines, daily ambient temperature fluctuations for each station were segmented into three seasons and hours of the day with an emphasis on large variation in ambient temperature at 3:00hrs, 9:00hrs, 15:00hrs. TURBOMATCH code was used for the design and off-design simulation of these gas turbines with varying ambient temperatures for each of the compressor stations along the gas pipeline. Table 4 shows the annual fuel cost for station 2

From Table 4 below, the result shows that for 1% rise in the ambient temperature for each operational season, there is corresponding 3.5% increase in the fuel cost per year. This increase is due to the GT power required to drive the gas compressor. As such, to meet the demand, the governor supplies additional fuel flow to raise the TET. This increase fuel flow is reflected in additional fuel cost per year.

Table 4 Annual fuel consumption cost for station 2

	TET(K)	Tamb(K)	Shaft Power(MW)	Fuel Flow(kg/s)	Hours of operations in a day	Number of Hours in seasons	Fraction Hours of operations in a day	Total Hours of operations in a season	Fuel cost ($/kg)	Conversion	Cost ($/y)
Winter											
03:00	1460	304.35	10.165	0.63723	4	2952	0.166667	492	0.16	3600	180585.88
09:00	1500	310.35	10.898	0.67888	15	2952	0.625	1845	0.16	3600	721459.35
15:00	1550	317.1	11.94	0.73947	5	2952	0.208333	615	0.16	3600	261949.85
Dry									0.16		
03:00	1490	308.1	10.784	0.67112	4	2928	0.166667	488	0.16	3600	188643.78
09:00	1520	312.35	11.365	0.70466	15	2928	0.625	1830	0.16	3600	742768.01
15:00	1560	318.1	12.193	0.75376	5	2928	0.208333	610	0.16	3600	264841.11
Hot									0.16		
03:00	1510	310.6	11.202	0.69454	4	2880	0.166667	480	0.16	3600	192026.42
09:00	1520	311.85	11.411	0.70644	15	2880	0.625	1800	0.16	3600	732436.99
15:00	1600	323.85	13.907	0.80942	5	2880	0.208333	600	0.16	3600	279735.55

4.5.2 Maintenance Cost

Maintenance cost is referred as the cost incurred in order to keep the gas pipeline network in good operating condition so as to meet the constant supply obligation. Maintenance cost is one of the important parameter used in economic analysis of natural gas pipeline projects. It is an important factor that contributes to the determination of the project lifecycle cost. Maintenance costs consist of labor and parts required in keeping the machines running at the desired power setting. The regular maintenance includes a change of oil seal, lube oil, plugs. Maintenance is classified as scheduled or unscheduled. The unscheduled Maintenance usually affects the economy of the pipeline project since it requires total shut down of the station plants. Many of the scheduled maintenance does not require plant shut down. Generally, observing regular maintenance as suggested by equipment manufacturers help to keep the maintenance cost low. Poor maintenance schedule greatly affects performance and availability of the equipment. In this research, the maintenance cost of $30 per kW (Pa) is assumed [10].

4.6 Lifecycle Cost for Baseline Case

This study considers the life cycle cost analysis for Trans-Saharan Gas Pipeline. The gas pipeline is a 56-inch pipe diameter and 4180 km distance spanning from Brass in Nigeria to Beni Saf in Algeria. This pipeline will transport 30 billion cubic meters per year of natural gas with 18 compressor station along the pipeline. The gas compressor and gas turbine for each station were selected in chapter four of this thesis. The performance results of the gas turbines based on ambient temperature variations, gas compressor, and turbine power matching were presented in the previous chapter. The incorporation of the modules which have the economic module as the key is depicted here. The economic evaluation is based on lifecycle cost to analyze the capital cost, operating cost, and maintenance cost.

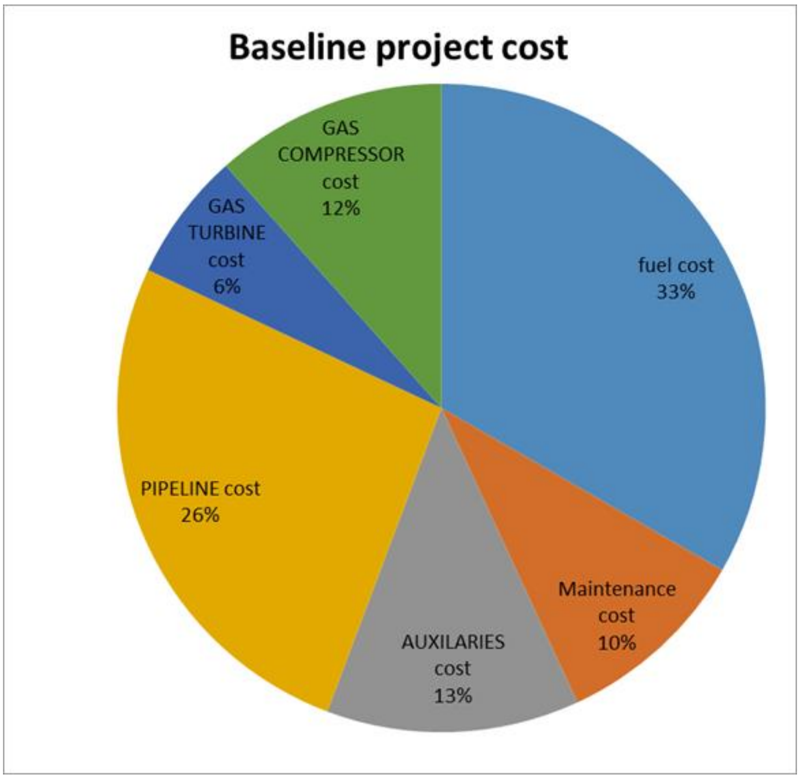

Figure 4-5 Baseline project cost

Figure 4-5 shows the breakdown cost for the baseline case. The fuel cost dominates the project cost. The pipeline cost is the second dominant while the gas compressor cost is double the gas turbine cost. The total lifecycle cost for the baseline case is $ 27.6 billion.

4.7 Lifing in Gas Turbine (HPT) Blades

Gas turbine components are exposed to increasingly challenging operating conditions, especially the High-Pressure Turbine (HPT) blades. The design lifetime for the gas turbine blades used in this research was assumed to be 25000 equivalent hours. The other assumptions made was for every 20^{O}(K) increase in TET the HPT blades lifetime reduces by half and for every 20^{O}(K) reduction in TET, the HPT blades lifetime increase by half [74]. Also the maximum HPT blades lifing hours is set at 50000 hours. The operating hours of the HTP blade reduce due to the following factors increased temperature during operations, start-up, shutdowns, and strips. However, the operating hours also increases when the engine is operating under ISO conditions or reduced temperatures [80].

This research focused on temperature effect on blade life. In natural gas pipeline transportation, the gas turbine is expected to provide the power required by the gas compressor. The gas compressor power changes as the gas temperature change since the gas temperature is one of the functions used to compute the value of gas compressor polytropic head. As the gas temperature increases, the gas compressor power requirement increases and vice versa. Therefore, to provide the power needed by the gas compressor, turbine entry temperature of the gas turbine changes as a result of the power requirement. Maximum gas compressor power demand is achieved by increasing the turbine operating temperatures

The continuous operations of the gas turbine at high temperature will result in high stresses, which will impact on the mechanical integrity of turbine blades and components. This will have an effect on the maintenance cost as a result of replacing the HPT blades. Figure 4-6 below shows the impact of ambient temperature on gas turbine TET and lifting.

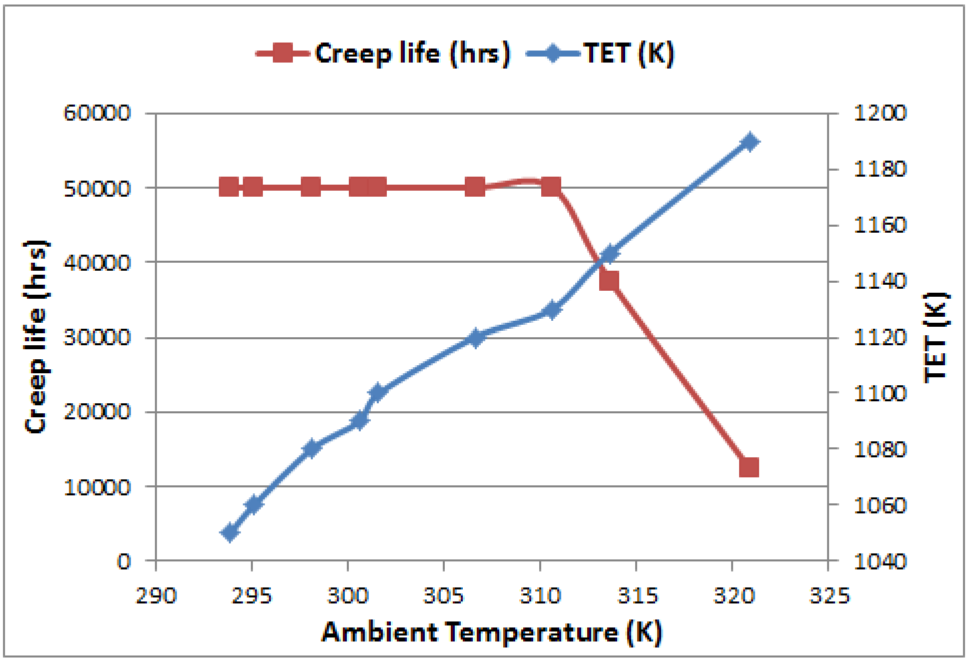

Figure 4-6 Effect of ambient temperature on TET and lifing

4.8 Conclusion

The model is a continuation of the gas compressor station spacing and power matching based on ambient temperature variation. Having previously obtained 18 compressor stations for the base case of TSGP and power matching for both the gas compressor and gas turbine for the stations at a different ambient temperature a techno-economic model was developed to calculate the capital cost and the operating cost based on ambient temperature variations. The compressor station locations ambient temperatures for the year was divided into winter, dry and hot seasons. The following were investigated: effect of ambient temperature on fuel cost and the project lifecycle cost.

From annual fuel consumption in station 2, the result shows that for 1% rise in the ambient temperature for each operational season, there is corresponding 3.5% increase in the fuel cost per year. This increase is due to the GT power required to drive the gas compressor. As such, to meet the demand, the governor supplies additional fuel flow to raise the TET. This increase fuel flow is reflected in additional fuel cost per year.

5 Matching Of Gas Turbine and Gas Compressor Power at Different Ambient Conditions

5.1 Abstract

It is worthy to note that the reports on Trans-Saharan gas pipeline project mention the number of compressor station without providing the exact location where there are to be constructed. This research presents the compressor station locations along the gas pipeline and power matching for centrifugal compressor and gas turbines based on ambient temperature variation. In this chapter compressor stations at station 2 is considered as the reference point. Station 2 daily temperature fluctuations were segmented into hours of the day with an emphasis on large variation in ambient temperature at 3:00hrs, 9:00hrs, 15:00hrs. The results show that for every 1% increase in ambient temperature, there was 3.5% increase in power required to drive the gas compressor and 1% decrease in gas turbine output power.

5.2 Theory of Analysis

In this, the ambient temperature along the pipeline was segmented based on hourly variation and seasons of the year, winter, dry and hot. The performance simulations of the gas turbines for both the design and off-design points were done in Turbomatch. Turbomatch is FORTRAN code developed at Cranfield University. The model approach can be divided as follows:

- Define the ambient temperature based on time interval at each of the compressor station locations
- Calculate the gas compressor power requirement at each station based on the ambient temperature and time interval.
- Using Turbomatch to simulate the gas turbine power based on the ambient temperature and time interval of each station locations.
- Find the gas turbine TET that will drive the gas compressor based on the compressor power requirement.

The calculation of gas temperature at any point along the pipeline is complicated since the gas temperature varies as the ambient temperature changes along the pipeline. Thus, this research made the following assumptions:

- Gas temperature is equivalent to ambient temperature at the entry of compressor station or at the delivery point as suggested by Menon [14].
- gas composition is constant throughout the study
- The pipeline is cleaned (has no degradation).

These assumptions were made to ensure that the pressure drop and gas compressor power are calculated reasonably.

5.3 Gas Turbine Performance Characteristics

Gas turbines are versatile machines that have been used in aerospace and industrial applications for many years. Gas turbines are used successfully to power aircraft, generate electricity as well as mechanical drive in pipeline compression, storage, and offshore applications. Kurz and Ohanian [81] confirmed that in gas pipeline transportation, the ideal means of compression is the combination of centrifugal compressor and industrial gas turbine. A gas turbine for industrial application consists of either a compressor driven by a gas generator turbine with a separate power turbine known as two-shaft engine or air compressor and gas turbine on one shaft, where the turbine provides both powers for the compressor and the load known as single shafft engine [27]. The two shafts industrial gas turbine configuration is regarded as excellent for pipeline compression [26].

Industrial gas turbine consists of various components such as air compressor, combustor, generator turbine and power turbine. Bryton cycle described the physical processes that occur in a gas turbine. For a gas turbine, the working fluid travels without an interruption. The compressor draws in air and increases its pressure and passed the increased pressure into the combustion chamber where the fuel is burned. The high temperature and high-pressure gasses from the combustion chamber are then expanded in a gas turbine generator to extract useful power. The compressor absorbed part of the turbine power out to provide power for the compression process through the shaft connecting the compressor and turbine. The remaining power out from the turbine is used to drive the pipeline centrifugal compressor. The pipeline compressor and the power turbine run at the same speed, independent of the gas turbine generator.

Gas turbine generator is controlled by the quantity of fuel that is supplied to the combustor and its operating constraints are maximum speed and turbine entry temperature. Generally, the turbine entry temperature and gas turbine speed increase with an increase in fuel flow, till one of this parameters reach its operating limit. Accordingly, this will provide the power turbine with gas at higher temperature, pressure and mass flow and this help the power turbine to produce more power. However, if the power supplied by the power turbine is bigger than the power absorbed by the load, both the power turbine and the load will accelerate until equilibrium is attained.

5.3.1 Operating Ambient Temperatures

The techno-economics of this project is directly or indirectly affected by the performance of gas turbine parameters including power, efficiency, capacity, fuel flow and operating ambient condition. Generally, the performances of gas turbines are greatly affected by the ambient condition. For gas turbines are designed based on ISA conditions.

It is necessary to obtain the ambient temperature condition and altitude variation for the geographical site where the engine installations take place. This is because gas turbine engine is an air-breathing engine and any effect on the density and mass flow of air will certainly affect the performance parameters of the gas turbine like power output and efficiency. According to Pilidis [55], the performance of gas turbine engine is better in cold regions as compared to hotter regions. Therefore, the difference in ambient temperature conditions must be considered.

Figure 5-1 shows the daily ambient temperature for booster station 2. The ambient temperature segment for the winter, dry, and hot seasons.

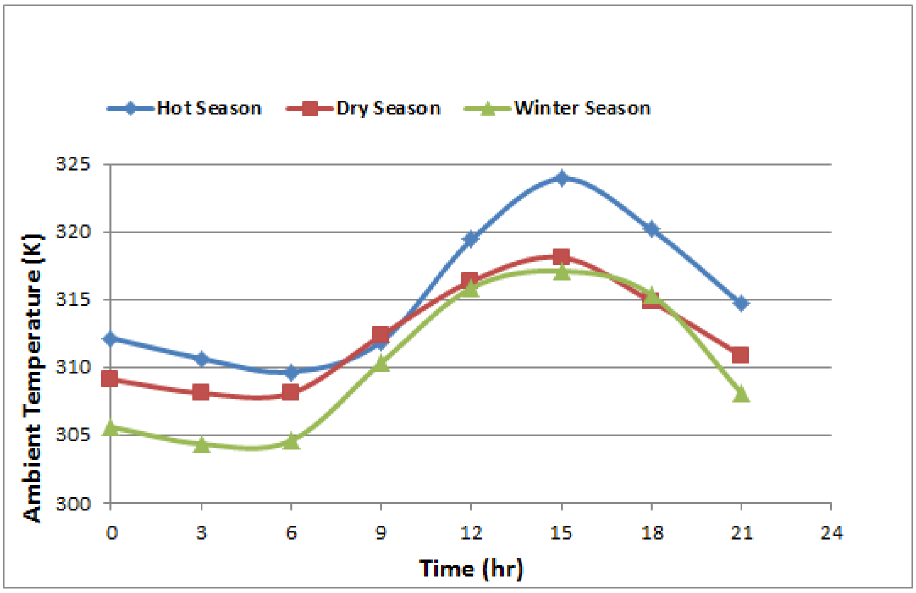

Figure 5-1 Station 2 ambient temperature

As shown from the above figure, for this proposed project the industrial gas turbine to be employed will operate at different operating conditions and this will affect fuel consumption and thermal efficiency of the turbine thereby increasing the operating cost of the project in hotter regions. Therefore, a close coupling between the drive and driven is required so as to achieve a reasonable efficiency and fuel consumption.

5.3.2 Performance Modelling

Turbomatch was used to simulate the thermodynamic models of the gas engines under investigation. The engine design points were achieved by varying the component efficiencies, Turbine Entry Temperatures (TET) and bleeds so as to attain at values similar to those in public domain. The off-design performance is regarded as any deviation from the original design point due to internal alteration of engine components or external alteration such as changes in ambient temperature conditions and altitude. In order to meet the power required to drive the pipeline centrifugal compressor, the study inspired by engines of different configuration, power output and with good thermal efficiencies were considered for simulation, these are 13.4MW, 15.2MW, 17MW, and 19.3MW. The engine's design point input files from Turbomatch are shown in Appendix B.

5.3.2.1 Study Inspired by LM1600 Industrial Gas Turbine

LM1600 is small size gas turbine associated with lightweight and low fuel consumption over a wide operating range. Apart from its marine propulsion used, the LM1600 gas turbines are used in power generation, offshore platform power, and pipeline compression. The engine can operate in the simple cycle or in steam injected configuration. LM1600 gas turbine consists of a double rotor generator and aerodynamically coupled power turbine. The engine configuration consists of three-stage low-pressure compressor, seven stage high-pressure compressor, a combustor, single stage high and low-pressure turbines and a power turbine. The power turbine is connected to the gas generator through a transmitting duct while the double concentric gas generator shafts connect the low and high-pressure compressor and turbine rotors. If power turbine is designed for frequent thermal cycling and can operate at a constant speed for generator drive applications, and over a cubic load curve for mechanical drive applications. A pressure ratio of 22:1 is achieved in ten compression stages and a single stage each is required for the high and low-pressure turbines. Figure 5-2 shows a schematic diagram of LM1600

The design point simulation of the industrial gas turbine was carried out using in-house Turbomatch code developed in Cranfield University as mentioned earlier in the methodology with the engine parameters obtained from GE website so as to meet the required power out. A reasonable result is obtained from the simulation as shown in Table 5 below.

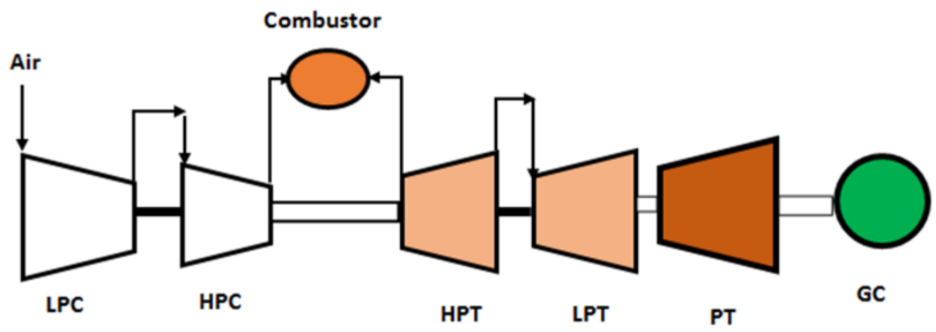

Figure 5-2 Schematic Diagram of LM1600 Gas Turbine

Table 5 Engine model verification at design point

S/No	Properties	GE Website	Turbomatch	Difference
1	Efficiency (%)	38	38.1	-0.1
2	Power output (MW)	15.2	15.2	0
3	Pressure ratio	22	22.2	-0.2
4	Fuel flow (kg/s)	0.8401	0.8751	-0.035
5	Inlet mass Flow (kg/s)	45.86	46	-0.14
6	TET (K)	-	1550	-
7	Comp turbine efficiency	-	0.88	-
8	Power turbine efficiency	-	0.89	-

At the design point, the compressor map was drawn using the variation in mass flow, efficiency and pressure ratio along with constant rotational speed. The data obtained from Turbomatch simulation is shown in Figure 5-3 and Figure 5-4. A compressor running line is obtained when its rotational speed, pressure ratio, and mass flow match with each other.

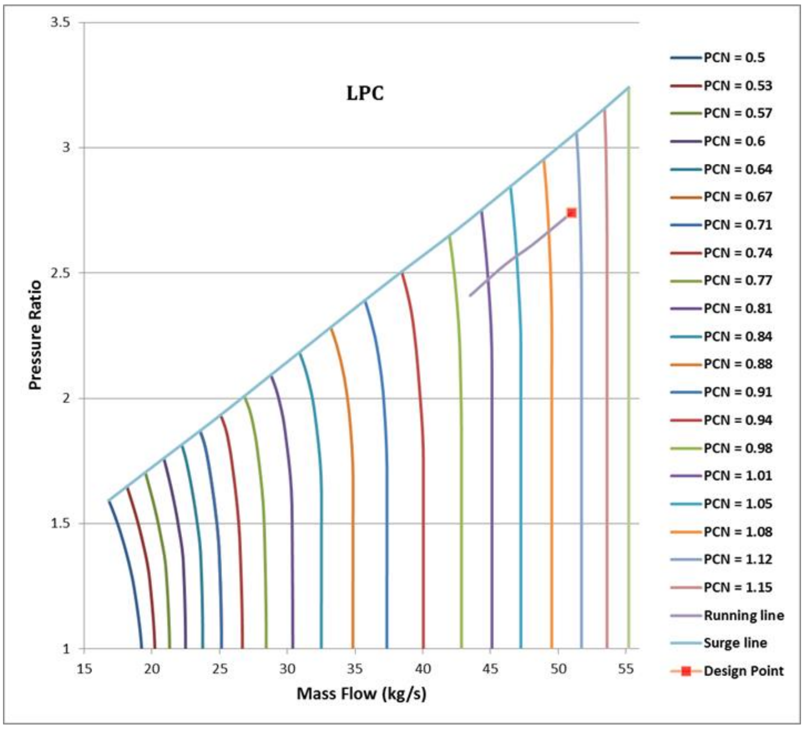

Figure 5-3 LM1600 Low-pressure compressor map

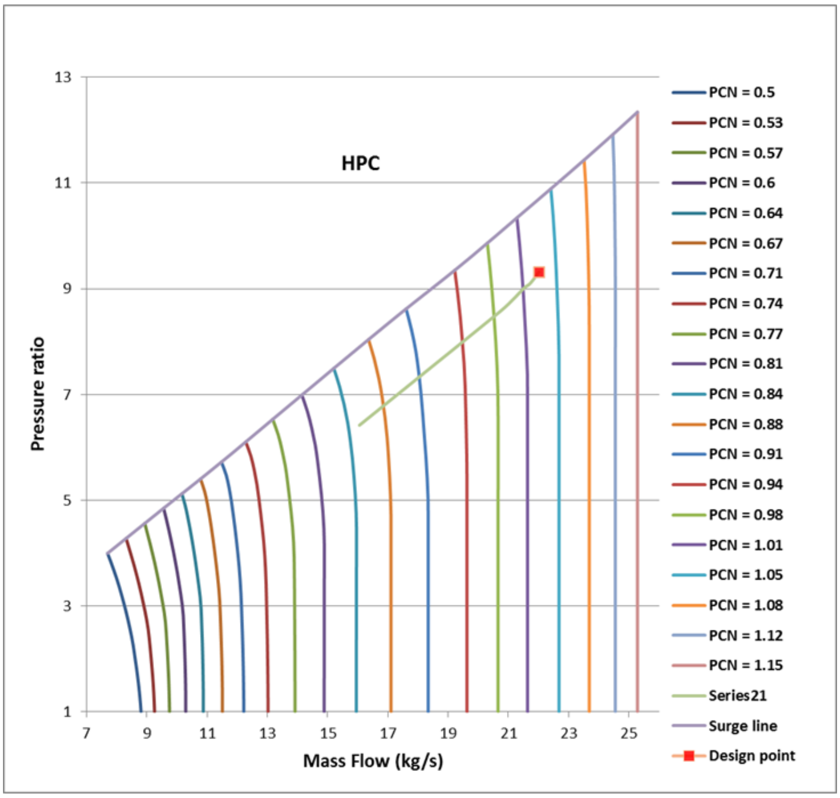

Figure 5-4 LM1600 High-pressure compressor map

5.3.2.2 Study Inspired by SGT-500 Industrial Gas Turbine

The study inspired by SGT-500, the engine is a three-shaft Industrial Gas Turbine which contains double shaft compressor, low-pressure compressor, and high-pressure compressor. The compressor has the total number of 18 stages. The three-stage power turbine speed is 3600 rpm for power generation and 3450 rpm for a mechanical drive. SGT-500 is a lightweight with high efficiency. Figure 5-5 shows a schematic diagram of SGT-500

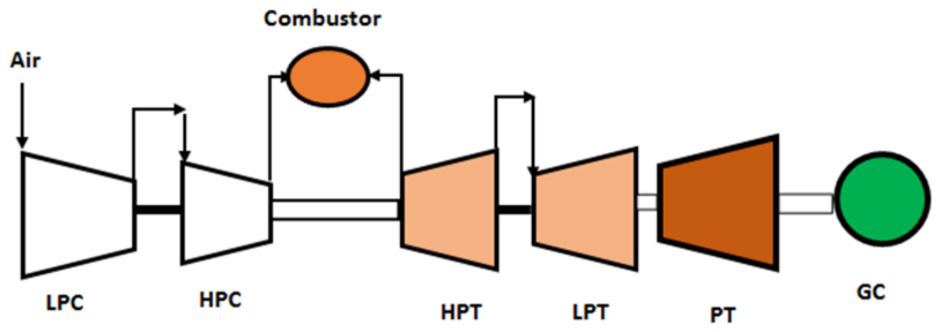

Figure 5-5 Schematic Diagram of SGT-500 Gas Turbine

The design point simulation and verification of the engine were also carried out by Turbomatch reasonable result is obtained from the simulation as shown in Table 6.

Table 6 SGT-500 Engine model verification at design point

S/No	Properties	Siemens Website	Turbomatch	Difference
	Efficiency (%)	34.2	34.3	-0.1
2	Power output (MW)	19.3	19.3	0
3	Pressure ratio	13	13	0
4	Fuel flow (kg/s)	1.1521	1.1345	0.02
5	Inlet mass Flow (kg/s)	96.75	96.75	0
6	TET (K)	-	1300	-
7	Comp turbine efficiency	-	0.88	-
8	Power turbine efficiency	-	0.88	-

At the design point, the compressor map was drawn using the variation in mass flow, efficiency and pressure ratio along with constant rotational speed. The data obtained from Turbomatch simulation is shown in Figure 5-6 and Figure 5-7. A compressor running line is obtained when its rotational speed, pressure ratio, and mass flow match with each other.

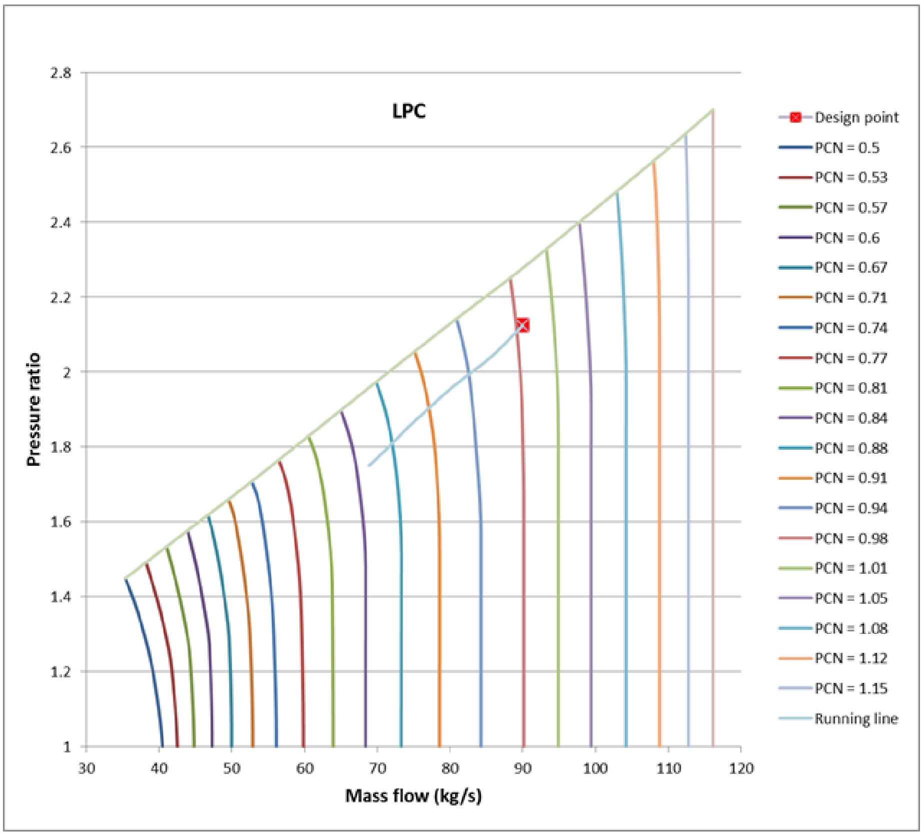

Figure 5-6 SGT-500 Low-pressure compressor map

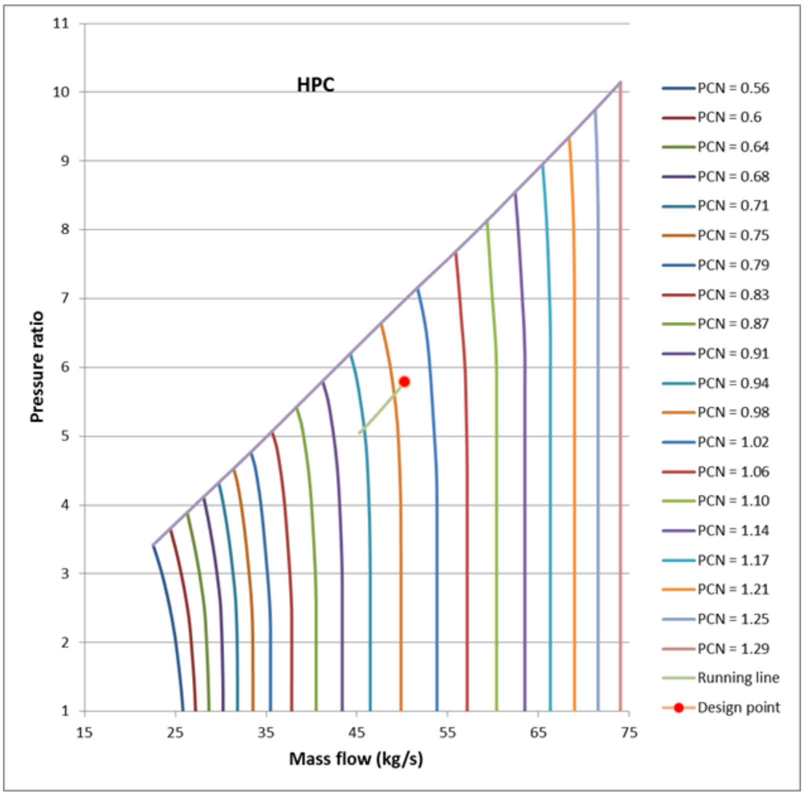

Figure 5-7 SGT-500 High-pressure compressor map

5.3.2.3 SGT-400 Industrial Gas Turbine Inspired

The SGT-400 is a double shaft gas turbine available in two different power ratings for both power generation and mechanical drive applications. The SGT-400 free power turbine has two stages. When used as a mechanical drive its drive the compressor directly. There is no need for gearbox connection since the turbine speed ranges from 4800 rpm to 10000 rpm. Figure 5-8 shows a schematic diagram of SGT-400 gas turbine.

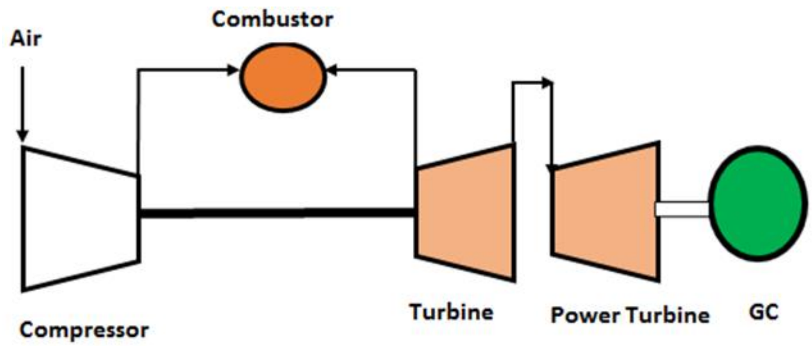

Figure 5-8 Schematic Diagram of SGT-400 Gas Turbine

The design point simulation and verification of the engine were also carried out by Turbomatch reasonable result is obtained from the simulation as shown in Table 7.

Table 7 SGT-400 Engine model verification at design point

S/No	Properties	Siemens Website	Turbomatch	Difference
1	Efficiency (%)	36.2	37	-0.8
2	Power output (MW)	13.4	13.4	0
3	Pressure ratio	16.8	16.8	0
4	Fuel flow (kg/s)	0.7553	0.7941	-0.038
5	Inlet mass Flow (kg/s)	38.645	38.64	0.005
6	TET (K)	-	1440	-
7	Comp turbine efficiency	-	0.88	-
8	Power turbine efficiency	-	0.88	-

5.3.3 Gas Turbine off Design Conditions

The off-design performance of this engine was conducted based on inlet air temperature and altitude variation of the areas where these gas turbines and gas compressors are to be installed. The purpose of this simulation is to ensure that the turbine provides the required power needed by the gas compressor despite the changes in ambient temperature condition. The daily ambient temperature of each compressor locations is used for the off-design simulation condition of a gas turbine used in that station.

5.3.3.1 Influence of inlet air temperature on triple shafts gas turbine

The inlet air temperature is a strong function for efficiency and power output of the gas turbine. As the ambient air temperature increases, the density of inlet air decreases. Therefore, at constant volume flow rate, the mass flow rate into the gas turbine decreases and this has an equivalent influence on its performance. The reduction in the inlet air density means a decrease of mass flow into the turbine.

As the inlet air temperature raises the work done per unit mass of compression increases because more work is required to compress hot air but the expansion work done by the turbine remains the same. Hence, the useful work reduces as a result but the thermal efficiency and fuel flow decrease.

The effect of turbine entry temperature and air ambient condition on power output is shown in Figure 5-9 below. As the turbine entry temperature increases the power output increase and the power output decreases with increase in ambient condition.

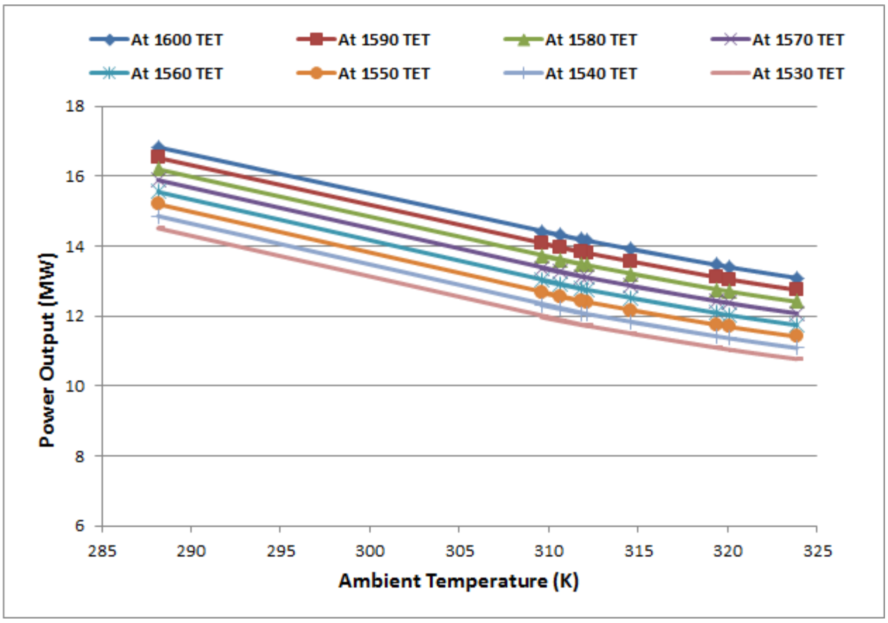

Figure 5-9 Power output against ambient temperatures at different turbine entry temperature

Increase in power output is achieved by increasing the TET. This process is permitted within reasonable limits, although TET increase is highly harmful to the gas turbine blade creep. Appendix C shows Turbomatch off-design results for power requirement of the compressor stations along the pipeline.

The effect of turbine entry temperature and air ambient condition on fuel flow consumption is shown in Figure 5-10 below. As the turbine entry temperature increases the fuel flow increases and the fuel flow decreases with increase in ambient condition. Usually, the increase in power output of the gas turbine is achieved by the fuel flow control to the combustor. Therefore, as the power output increases the fuel consumption also increases.

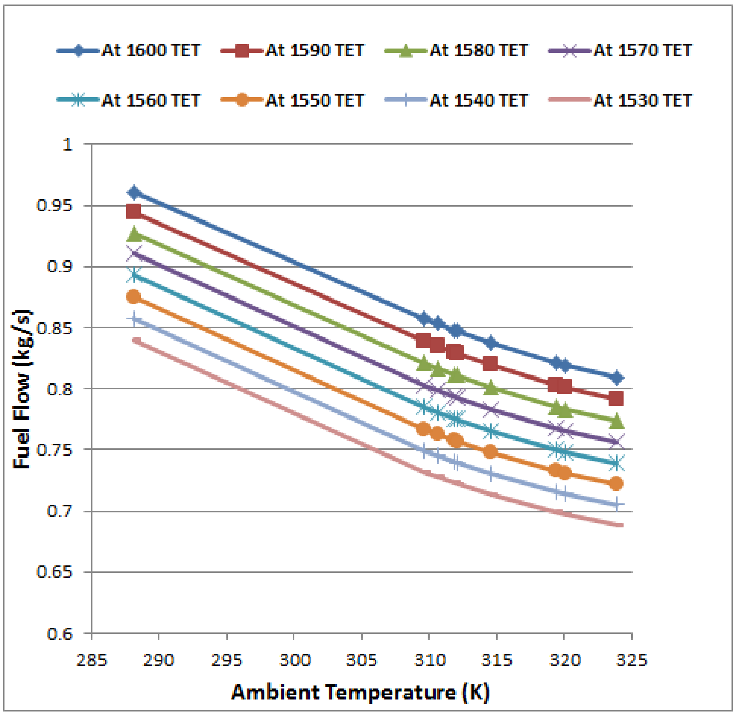

Figure 5-10 Fuel flow against ambient temperature at different turbine entry temperature

The effect of turbine entry temperature and air ambient condition on thermal efficiency is shown in Figure 5-11 below. As the turbine entry temperature increases the thermal efficiency increases. The thermal efficiency decreases as ambient temperature increases. At the higher ambient condition, the thermal efficiency decreases because more work is required by the gas compressor as a result of an increase in inlet air temperature, therefore low conversion of combustion energy into useful work. Lower TET has less effect on efficiency.

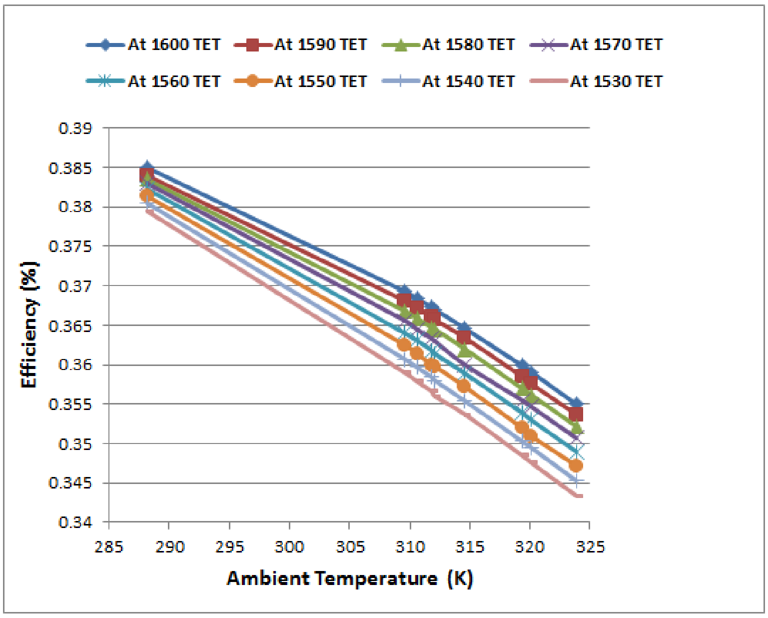

Figure 5-11 Efficiency against ambient temperature at different turbine entry temperature

The effect of ambient condition on power output and fuel flow is shown in Figure 5-12 below. As the ambient condition increases the power output and fuel flow decreases. The power output and fuel flow increase as the ambient condition decrease. The fuel consumed formed the basis for operating cost in this research.

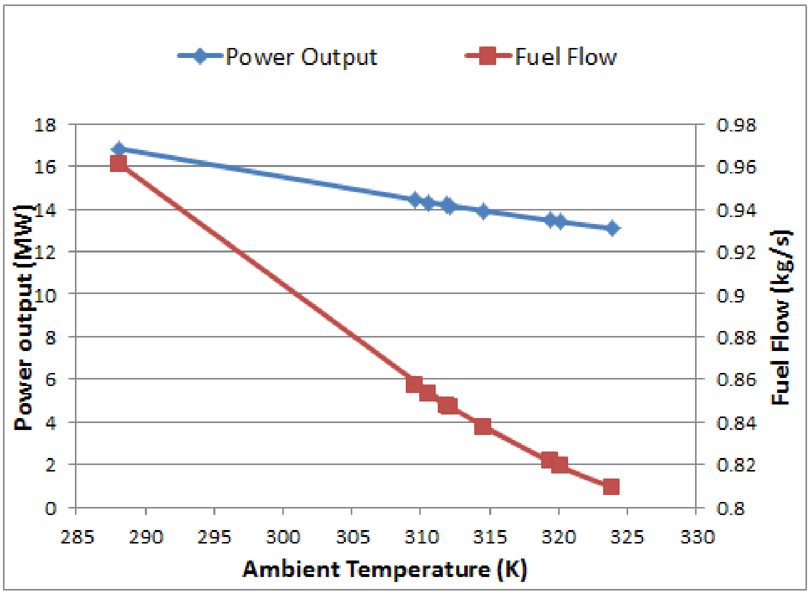

Figure 5-12 Variation of power output and fuel flow against ambient temperature

5.4 GAS COMPRESSOR

5.4.1 Ideal gas law

Ideal gas law is the fundamental thermodynamic law of understanding the operation of compressor, which is expressed in equation shown below [82]

$$Pv = RT \tag{5-1}$$

Where:
P = pressure
v = specific volume
T= absolute temperature
R = gas constant, and is a function of gas molecular weight

Gas does not conform to this law. Therefore, the deviation from the ideal gas is a function of the gas temperature, and pressure at which it operates. The ideal gas law can be converted to a real gas law by introducing a deviance parameter known as compressibility factor Z [34]. According to Savidge (2000), [83], compressibility factor is defined as the ratio between actual gas volume and ideal gas volume.

$$Pv = ZRT \tag{5-2}$$

Equation **(5-2)** has shown the exact relationship between real gasses since there is always a relationship between the pressure, volume, and temperature of the gas. This equation is the frequently used method for estimating the performance of a compressor. In order to calculate the value of the other gas properties, there is a need to obtain the value of the compressibility factor.

The compressibility factors Z of different gasses are determined from the generalized Nelson-Obert chart, in which compressibility factor is plotted as a function of reduced temperature T_r and reduced pressure P_r [36]. The reduced temperature is obtained by dividing the actual temperature of the gas by critical temperature:

$$T_r = \frac{T}{T_c} \; ; \; P_r = \frac{P}{P_c} \tag{5-3}$$

The specific volume of different gas at the same temperature and pressure are different. Though, experimental data has been established that at the reduced temperature and reduced pressure, the reduced volumes of different gasses are the same [84].

Nelson-Obert developed a compressibility chart of several gasses based on the experimental data and it gives satisfactory values of many of the gasses and mixture of gasses [36].

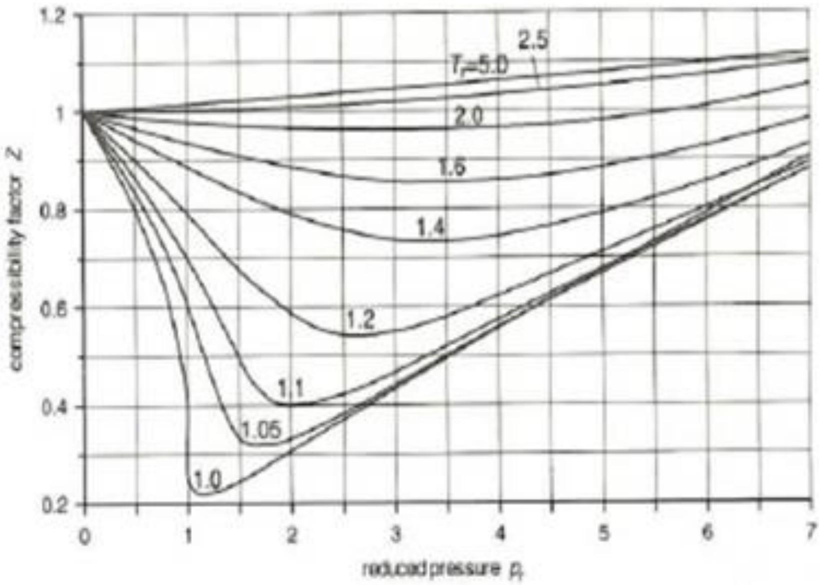

Figure 5-13 Nelson-Obert compressibility chart [36]

HYSYS has also used for the calculation of gas compressor polytropic efficiency. HYSYS software presently deals with enhanced Peng-Robinson (PR) and Soave-Redlich- Kwong (SRK) equations of state to estimate thermodynamic properties of the gas in operation. PR equation of state supports the broadest array of operating conditions also has the greatest variety of systems. Over the years PR and SKR are some of the equations developed to calculate the constants in Vander Waals equation [26]. The constants A and B are shown in the equation below:

$$a = 0.4278R^2 \frac{T_c^{2.5}}{P_c} \quad \textbf{(5-4)}$$

$$b = 0.08664\ \frac{RT_c}{P_C} \quad \textbf{(5-5)}$$

SRK (1972), modified the equation by introducing the acentric factor. This acentric factor is responsible for measuring the defect of the molecule. The SRK equation is given as

$$a(T) = 0.4274(\frac{R^2T_c^2}{P_C})\{1 + m[1 - (\frac{T}{T_C})^{0.5}]\}^2 \quad \textbf{(5-6)}$$

Where,

$$m = 0.480 + 1.57\boldsymbol{\omega} - \mathbf{0.17}\boldsymbol{\omega}^{\mathbf{2}} \quad \textbf{(5-7)}$$

Peng-Robinson equation is expressed as follows

$$a = \frac{0.457247R^2T_c^2}{P_c} \quad \textbf{(5-8)}$$

$$b = \frac{0.07780RT_c}{P_C} \quad \textbf{(5-9)}$$

5.4.1.1 Natural Gas Composition

Natural gas is a mixture of hydrocarbon and non-hydrocarbon components. The hydrocarbon components consist of methane, ethane, propane butane and Pentane. The non-hydrocarbon constituents include nitrogen, carbon dioxide, and water. The composition of this natural gas highly depends on the resources of the location. In some locations, gases such as carbon dioxide or hydrogen sulfide are available in large proportion and are usually regarded as sour gases. Generally, exploitation of sour gases is associated with difficulties and high cost [85].

Gas composition data is one of the important considerations for compressor selection as it helps to determine the average molecular weight, compressibility factor and specific heat ratio required for compression. Gas composition is critical for determining of specific heat ratio and compressibility [36][.

5.4.1.2 Gas Compressor Power Estimation

In ideal conditions, the gas compressor work is performed at constant entropy as shown in Figure 5-14. The isentropic efficiency is regarded as the ratio between the isentropic work to actual work. The adiabatic process assumes that there is no heat pass in and out of the system.

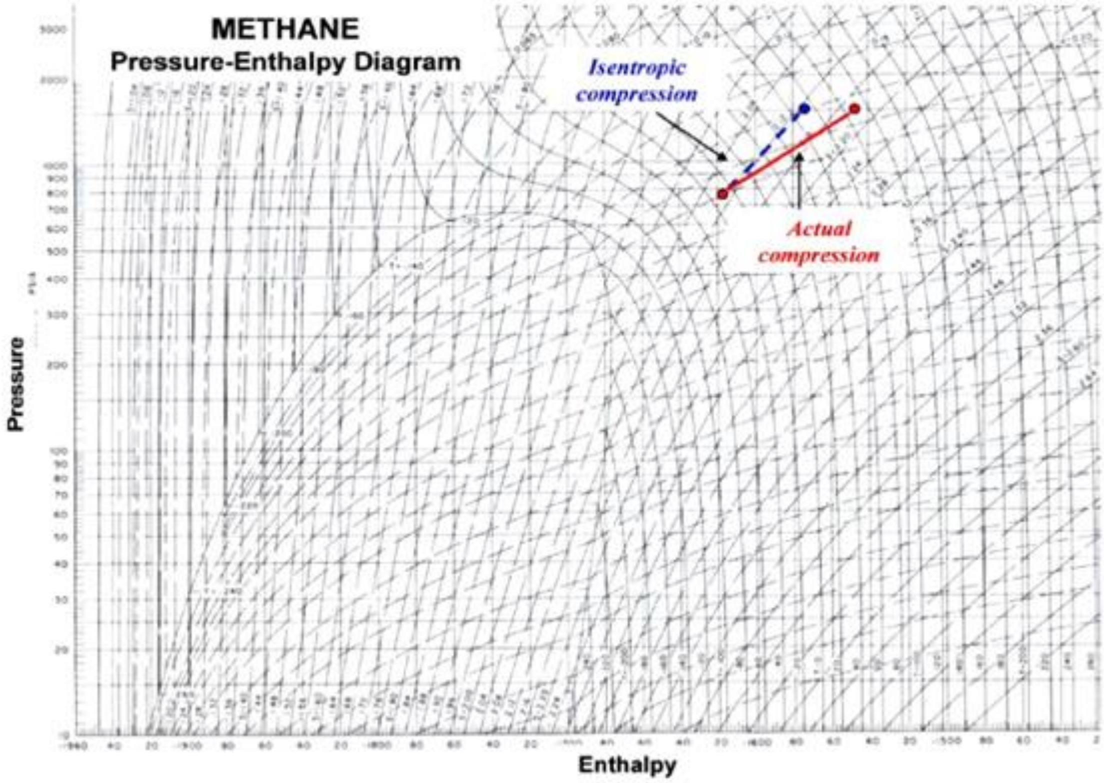

Figure 5-14 Mollier Diagram compression Process for Methane [86]

Generally, Isentropic, adiabatic, and polytropic processes are regarded as the important process use in thermo-system. Estimating the centrifugal compressor power requirement, the n-value approach was adopted in this research. Also, the polytropic calculation was considered based on the fact that polytropic efficiency is independent of the thermodynamic state of gas undergoing compression while the adiabatic efficiency is a function of the compression pressure ratio as expressed by the equations below.

$$\eta_{poly} = \frac{\frac{n}{n-1}}{\frac{k}{k-1}} \quad \textbf{(5-10)}$$

$$\eta_{ad} = \frac{PR^{\frac{(k-1)}{k}} - 1}{PR^{\frac{(n-1)}{n}} - 1} \quad \textbf{(5-11)}$$

The gas compressor discharge temperature is one of the factors that limit the stage compression ratio. Therefore, it should be kept within the reasonable value. The discharge temperature is the function of inlet temperature, pressure ratio, and process exponent

$$T_2 = T_1 r_{p^{(n-1)/n}} = \frac{T_{1rp^{(n-1)/n}}}{\eta_{ad}} + T_1 \quad \textbf{(5-12)}$$

The isentropic head constitutes the required input energy to achieve the reversible compression process while the polytropic head is the function of compressibility factor, process exponent, molecular weight, inlet temperature and pressure ratio express as follows:

$$H_{ad} = \frac{Z_a}{1{,}000} \frac{8{,}314}{MW} T_1 \frac{k}{k-1} [r_p^{\frac{k-1}{k}} - 1] \quad \textbf{(5-13)}$$

$$H_p = \frac{Z_a}{1{,}000} \frac{8{,}314}{MW} T_1 \frac{n}{n-1} [r_p^{\frac{n-1}{n}} - 1] \quad \textbf{(5-14)}$$

$$Power_g = \frac{mH_p}{3{,}600\ \eta_p} \quad \textbf{(5-15)}$$

The compressor horsepower is calculated using equation **(5-15)** while to determine the compressor break horsepower mechanical losses need to be accounted for as shown in the expression below:

$$Ps = Power_g + Lm \quad \textbf{(5-16)}$$

Compressor inlet gas volumetric flow is calculated as

$$Q = \frac{m}{p} \quad \textbf{(5-17)}$$

Where Q is inlet volumetric flowrate in (m^3/h), m is the mass flow rate in (kg/h) and p is the density of the gas at inlet condition in (kg/m^3).

$$p = \frac{P_S}{Z_s R T_s} \tag{5-18}$$

Where p is gas density in (kg/m^3), P_s is the suction pressure in (bara), Z_s is the compressibility factor, R is the gas constant, T_s is the suction temperature (K) and molecular weight of the gas. Using the above equations the gas compressor configuration was obtained.

Based on the power requirement for the centrifugal compressor at compression station 2, Dresser-Rand Datum C centrifugal compressor was selected Table 8 summarizes the characteristics of the centrifugal compressor.

Table 8 Gas compressor parameters

Compressor station 2 Configuration	
Actual Volume flow (m^3/h)	10510
Inlet temperature (^{O}C)	22.22
Discharge Temperature (^{O}C)	56.11
Inlet pressure (bar)	65.39
Discharge Pressure (bar)	95
Polytropic head (kJ/kg)	47.32
Power (kw)	10904
Efficiency (%)	0.761

5.4.1.3 Centrifugal Compressor Map

The compressor performance curves comprise of a graph showing the variation of the polytropic head, efficiency, pressure ratio, and power at several constant speed and at a different flow rate as shown in Figure 5-15, Figure 5-16, Figure 5-17, Figure 5-18, and Figure 5-19. A new compressor performance curve for compressor station 2 was obtained from the scaling of the existing OEM curve see Appendix D. To obtain a new compressor map there is to need to correct the mass flow rate.

Berdanier et al, [87], suggested that the effect of humidity factor should be ignored because it has an insignificant impact on this correction. The following equation for corrected mass flow is applied since there is no change in diameter.

$$\dot{m}_c = \dot{m}_{act} \frac{P_{ref}}{P_{act}} \sqrt{\frac{k_{ref}}{k_{act}}} \sqrt{\frac{Z_{act}}{Z_{ref}}} \sqrt{\frac{R_{act}}{R_{ref}}} \sqrt{\frac{T_{act}}{T_{ref}}} \qquad \textbf{(5-19)}$$

Where:

N_c; corrected rotational speed
$\dot{m}_c$; corrected mass flow rate
P_{ref}; Reference inlet pressure (101.325kpa)
T_{ref}; Reference inlet temperature (288.15^{o}K)
Z_{ref}; Reference compressibility factor (1.0)
k_{ref}; Reference specific heat ratio (1.4)
R_{ref}; Reference gas constant (287.058J/(kg.K)

New compressor maps were obtained by scaling the corrected values using the factors defined below [87].

$$S_f\ PR = (PR_{DP} - 1)/(PR_{DP\ Map} - 1) \qquad \textbf{(5-20)}$$

$$S_f\ NDW = \left(\frac{W\sqrt{\theta}}{\delta}\right)_{DP} / \left(\frac{W\sqrt{\theta}}{\delta}\right)_{DP\ Map} \qquad \textbf{(5-21)}$$

$$S_f\ EFF = \eta_{DP}/\eta_{DP\ Map} \qquad \textbf{(5-22)}$$

$S_f\ PR$ = scaling factor for pressure ratio
$S_f\ NDW$= scaling factor for non-dimensional mass flow
$S_f\ EFF$ = scaling factor for efficiency

The subscript DP is a design point parameter of the new map and the subscript DP Map is the design point parameters of the existing map. Figure 5-15 shows the pressure ratio performance curve, the inlet volume flow is plotted along the x-axis and the pressure ratio is plotted along the y-axis. The red colour-mark represents the operating point of the centrifugal compressor. As the inlet volume to compressor increases its rotational speed and pressure ratio also increases. The low-pressure ratio causes the operating envelope to shift towards lower flow rate. Additionally, the surge margin is decreasing propositionally with the reduction of inlet pressure.

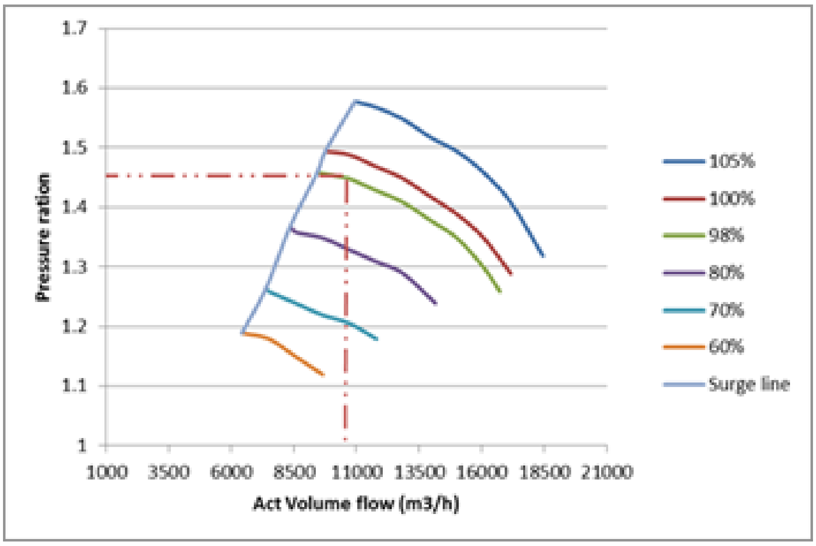

Figure 5-15 Pressure ration curve

Figure 5-16 is the compressor polytropic head curve, the inlet volume flow is plotted along the x-axis and the polytropic head is plotted along the y-axis. The corresponding flow is called the operating flow. As the inlet volume to compressor increases its rotational speed and polytropic head also increase. The compressor surge line defines the minimum flow necessary during the operation to avoid damage of the compressor due vibration

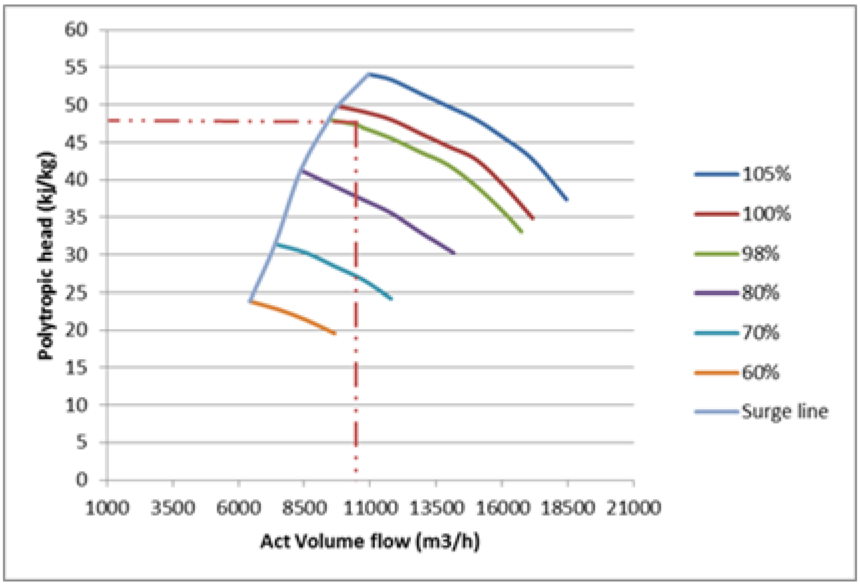

Figure 5-16 Polytropic head curve

Figure 5-17 is the compressor discharge temperature curve, the inlet volume flow is plotted along the x-axis and the temperature is plotted along the y-axis. From the map, it shows that at constant rotational speed and suction flow, the surge margin is reduced due to drop in temperature. As the inlet volume to the compressor increases its rotational speed and temperature also increased and the surge margin reduced.

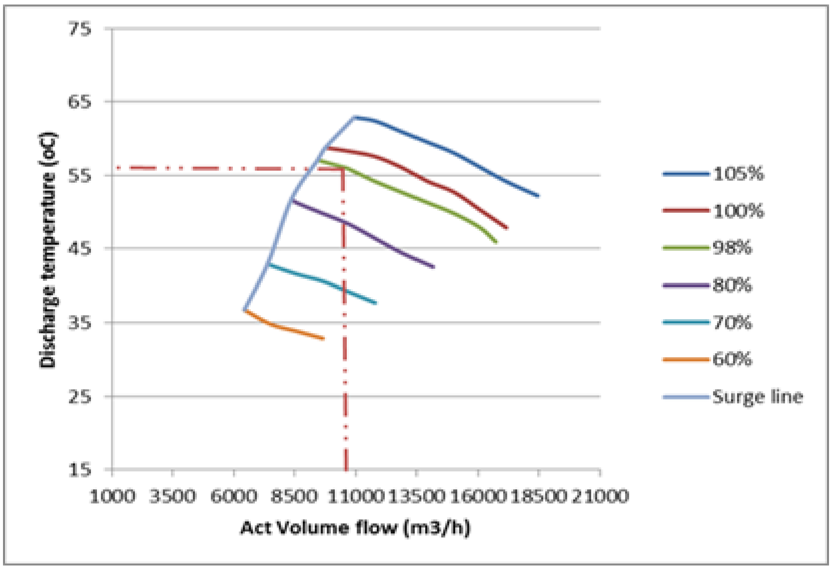

Figure 5-17 Discharge temperature curve

Figure 5-18 represents the off-design power performance of the centrifugal compressor. The inlet volume flow is plotted along the x-axis and the power is plotted along the y-axis. The power varies with the inlet volume flow and the rotational speed. Power increased with increase in rotational speed and inlet volume flow

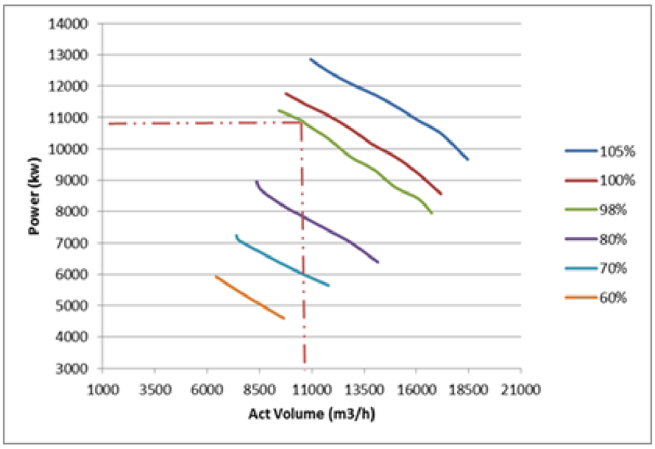

Figure 5-18 Gas power curve

Figure 5-19 represents the off-design power performance of the centrifugal compressor. The inlet volume flow is plotted along the x-axis and the efficiency is plotted along the y-axis. As we see from the performance curve, the efficiency curve is raising as the flow rate increase. Then the curve reaches the maximum point and starts decreasing. The maximum point is called Best Efficiency Point (BEP).

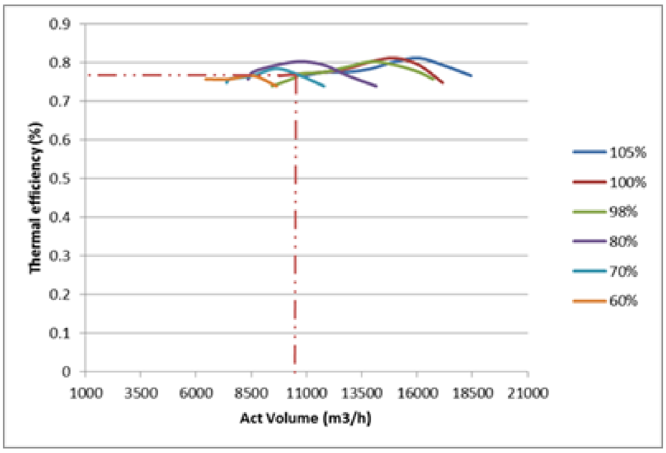

Figure 5-19 Thermal efficiency curve

5.4.2 Effect of Gas Temperature on Compressor Performance

Using constant volume flow rate and same gas composition, the gas compressor polytropic head and gas power trend demonstrate an increase with an increase in suction temperature, as shown Figure 5-20 and Figure 5-21 below. Gas compressor head increases proportionally with the increase in inlet temperature and vise versa. The compressor power also increases proportionally with the increase in polytropic head, since the power is a function of mass flow rate, polytropic head, and efficiency.

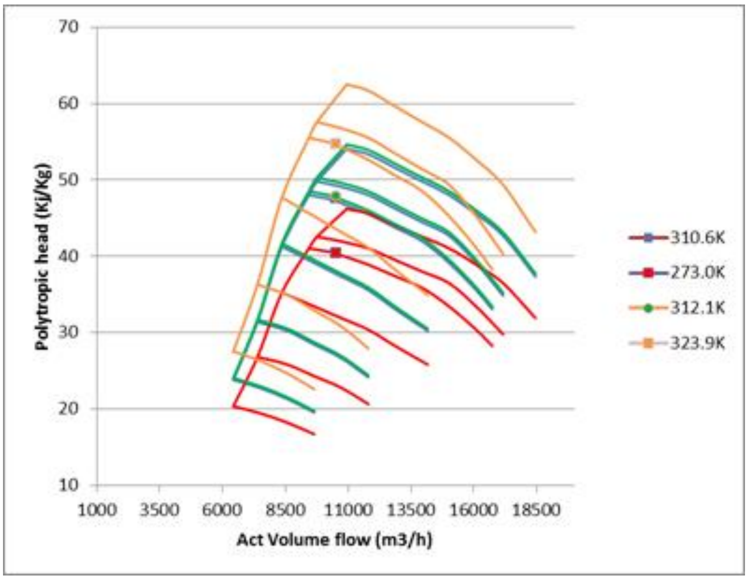

Figure 5-20 Effect of gas inlet temperature on polytropic head

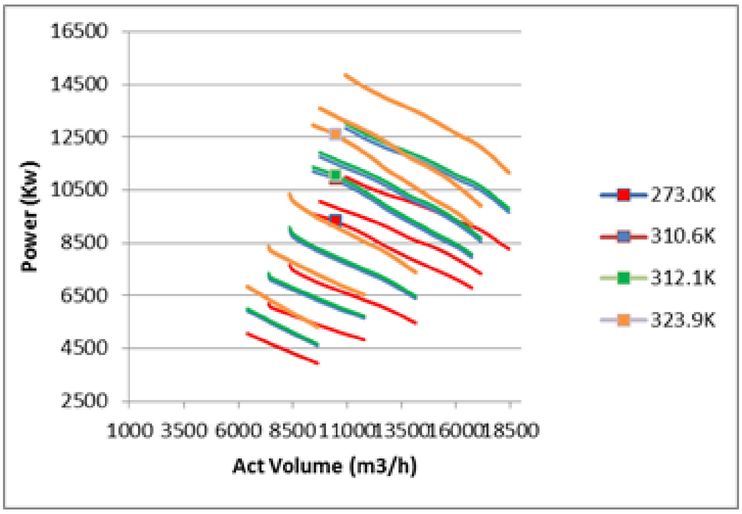

Figure 5-21 Effect of gas temperature on gas compressor power

The gas temperature factor is of great importance for mechanical drive applications. Both the centrifugal compressor polytropic head and the gas turbine output power are strongly influenced by the gas temperature. For every 1% increase in gas temperature, there was 3.5% increase in power required to drive the gas compressor and 1% decrease in gas turbine output power.

This variation in power for both the equipment has to be compensated for, in order to maintain a steady flow of the natural gas across the trans-Saharan gas pipeline route. Unless an inlet cooling technique is used, there is little that can be done regarding the ambient temperature. This implied that the gas turbine will require more fuel to compensate for the reduction in the gas turbine shaft power and increase in the centrifugal compressor power in order to maintain the steady flow rate of the natural gas across the pipeline network.

5.5 Power matching for gas compressor and gas turbine

The calculation of gas temperature at any point along the pipeline is complicated. Thus, this research assumed that the gas temperature is equivalent to ambient temperature at the entry of compressor station or at the delivery point as suggested by Menon [14] also shown in Equation 6-25. The assumption was made so that the pressure drop and gas compressor power would be calculated reasonably. Figure 5-22 below shows the power matching for gas compressor and gas turbine at different TET, as the ambient temperature fluctuates daily in winter, dry and hot seasons across Trans-Sahara pipeline stations. An increase in ambient condition from ISO increases the polytropic head of the centrifugal compressor, and as such increases, the gas compressor power demand, whereas the same effect on the gas turbine resulting in a decrease in gas turbine output power for the three seasons. For every 1% increase in gas temperature, there was 3.5% increase in power required to drive the gas compressor and 1% decrease in gas turbine output power. The gas compressor power demand was matched to the gas turbine shaft output power at the time of day when the ambient temperature was minimum, mid and maximum (3:00hrs, 9:00hrs, 15:00hrs) respectively for the three seasons under consideration. The graph shows that both equipment power matches at the point of the intercession of gas turbine shaft output power with the centrifugal gas compressor power at different TET. In the hot season, at 3:00 hrs, the gas compressor power requirement was 10.904(MW), and the gas turbine TET of 1510(K) will provide the power matching for the centrifugal gas compressor. Table 4 summarizes the matching point of the gas turbine and gas compressors at 3:00. 9:00, 15:00, and at the hot season. Some of the station's power matchings are shown in Appendix E.

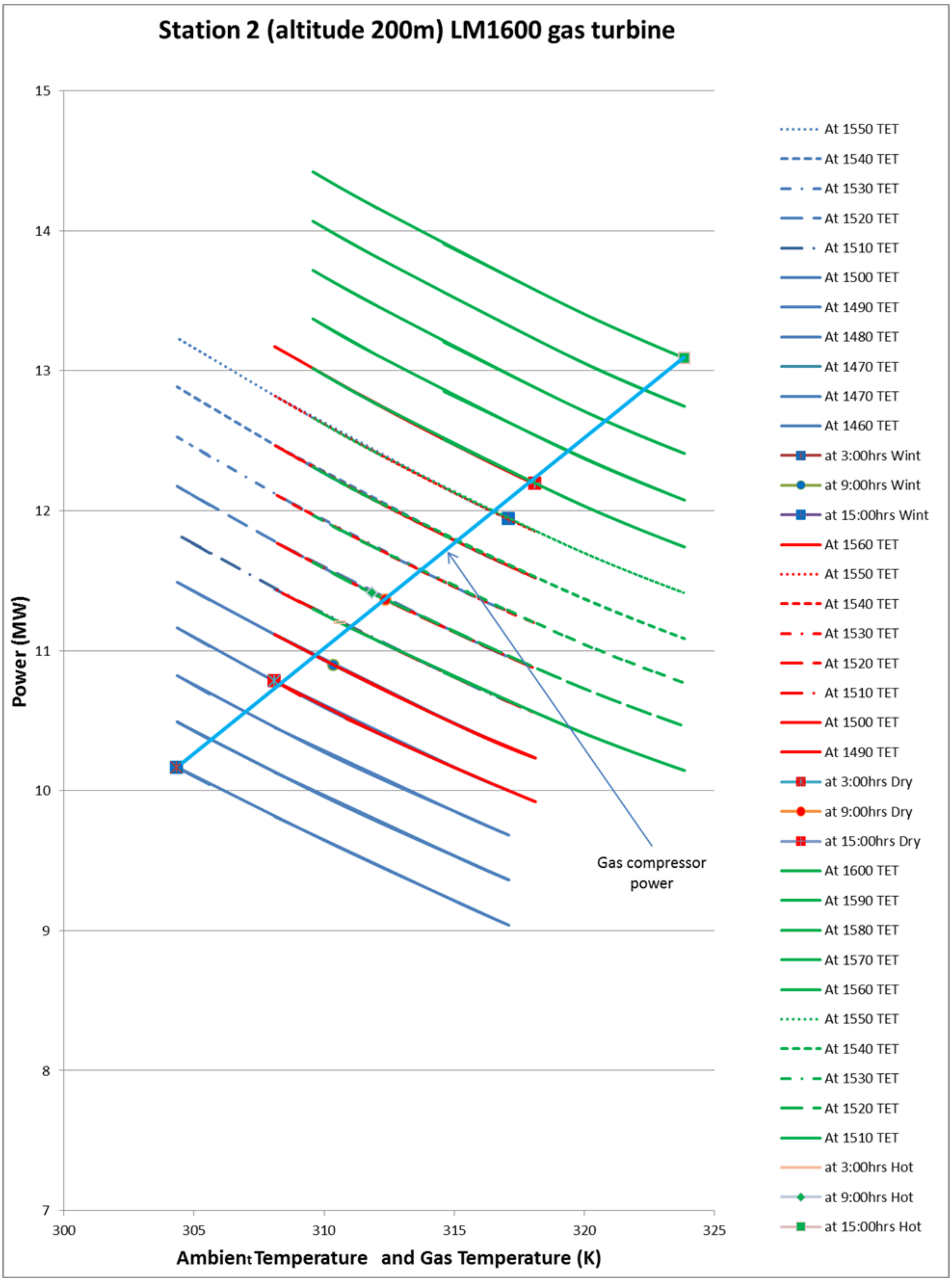

Figure 5-22 Gas compressor and gas turbine power matching

5.6 Conclusion

Centrifugal compressors used in oil and gas industry operate within a specified envelope which consists of many operating points. The variation in the operating point is as a result of a change in process conditions. One of the process conditions is the ambient temperature. Therefore, the ambient temperature along this gas pipeline was segmented based on hourly variation, the gas compressor and gas turbine power matching was done based on this ambient temperature variation. The result shows that for centrifugal compressors power increases with increase in ambient temperatures while the gas turbine the power decreases with increase in ambient temperatures. For every 1% increase in ambient temperature, there was 3.5% increase in power required to drive the gas compressor and 1% decrease in gas turbine output power. A very significant part of this matching is reflected in the life cost of the gas turbine driven a centrifugal compressor in terms of fuel cost which translated to increase in the gas turbine TET to compensate for the variations in power.

6 Booster Station Spacing and equipment selection

6.1 Abstract

The economic performance of a gas pipeline system depends on how compressor stations are constructed, the type of compressor employed, selection of driver, and appropriate spacing of booster stations along the gas pipeline. The suitable spacing of booster station along the pipeline can minimize its operating cost by reducing the cost of booster station fuel consumption. The aim is to introduce a new model for booster station definition along the gas pipeline. The model also accounts for the variation in the elevation and ambient temperature at each of the compressor station located along the pipeline network. In this part centrifugal compressors and gas turbines were selected, booster stations arrangements were made. The temperature, pressure, and pressure losses along the pipeline were obtained within a reasonable accuracy. The model has been verified using pressure ratio and a number of booster station spacing of a pilot project, Trans-Sahara gas pipeline (TSGP). The project was initiated for exporting natural gas from Niger Delta, Nigeria to the consumer market in Europe via Niger and Algeria.

6.2 Method of Analysis

The model was developed using thermodynamic gas properties, Weymouth gas flow equation and HYSYS. The performance of a gas compressor is based on the inlet parameters, gas composition, and allowable operating pressure of the pipeline. The pipeline is determined based on the volume flow rate, operating pressure, distance, pipe diameter, and thickness. The model approach can be divided into four main groups as demonstrated in Figure 6-1

1. Identify the gas composition, volume flow, distance, pipeline operating pressure, pipe thickness and diameter
2. Specify the compressor inlet parameters at the design point based on the pipeline operating pressure. Obtain the compressor efficiency from the HYSYS, calculate the polytropic head and compressor gas power

3. Using Weymouth flow equation calculate the pressure drop along the gas pipeline putting into consideration the pipe segment distance, ambient temperature, and elevation.
4. Select the compressor model based on the volume flow and gas power requirement, also select the gas turbine model based on the gas compressor power requirement.

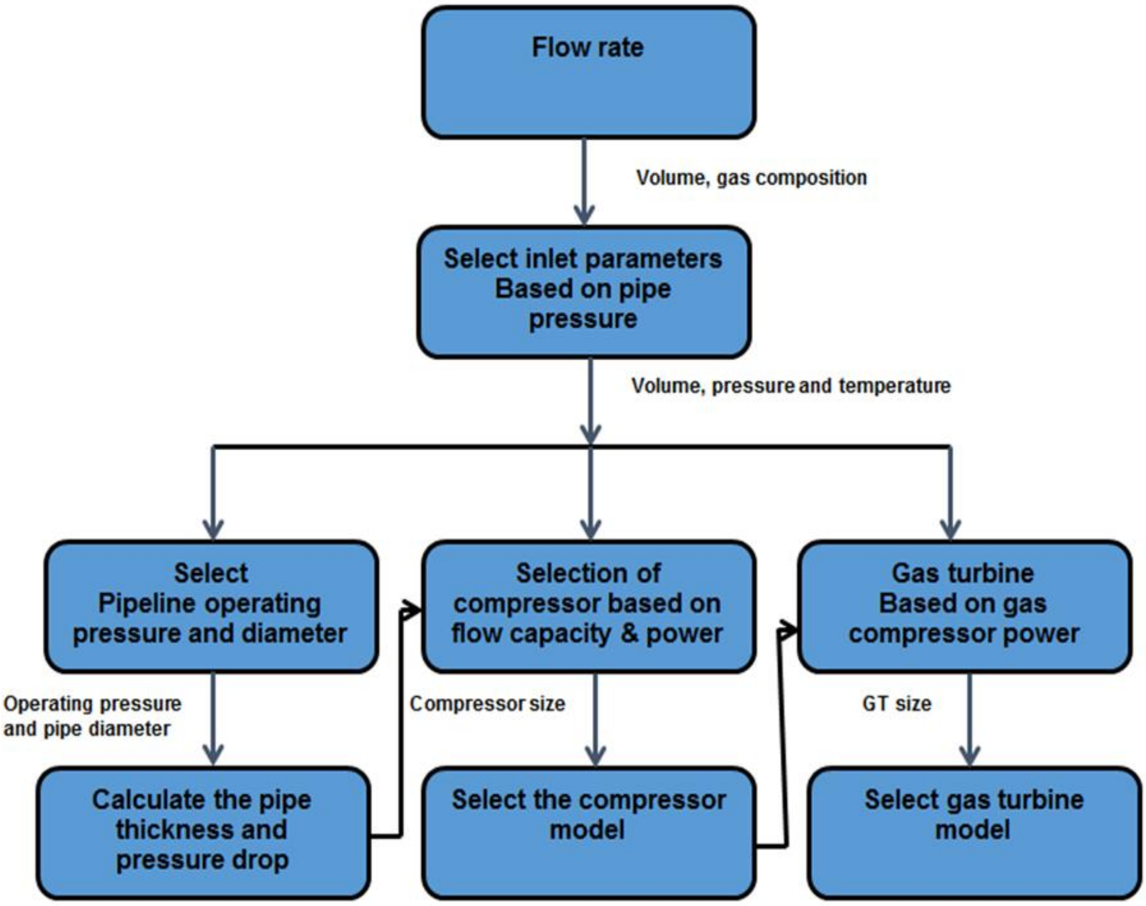

Figure 6-1 Model developed scheme

6.2.1 Assumptions

For this booster station spacing the following assumptions were made:

- Gas temperature is equivalent to ambient temperature at the entry of compressor station or at the delivery point as suggested by Menon [14].
- gas composition is constant throughout the study

- Constant pipe diameter
- Gas compressor pressure ratio between 1.4 and 1.65 for pipeline compression
- No degradation
- 18 compressor stations are used.

6.3 Gas turbines

Natural gas-fired gas turbines have been selected as the main driver for the gas compressors in this pipeline project because this system does not require additional infrastructure since fuel is tapped from the transported gas [88]. The system also has a less balancing problem since there are no reciprocating and rubbing components. It also has low lubricating oil consumption and is very reliable [60]. The selected gas turbine design and off-design performance simulation were carried out using Turbomatch. The parameters that affect the gas turbine performance such as the ambient temperature, mass flow, turbine inlet temperature and fuel flow were investigated. See chapter 5 for the design and off-design performance of the selected gas turbines.

6.4 Natural gas flow

There are many equations used to calculate pressure drop in natural gas pipeline transportation these include: General flow equation, Weymouth equation, Colebrook-white equation, modified Colebrook-white, AGA equation etc. [14]. The Weymouth equation is right flow equation when dealing with high pressure, high flow rate, and large diameter gas transmission system as described in [16]. This research used Weymouth equation determines the discharge pressure via a pipeline for a given mass flow rate, gas gravity, compressibility, inlet pressures, pipe length and pipe diameter. The competitive pipeline should maintain a pressure drop in the range between 3.50 and 5.83 psi/mile as suggested by [24].

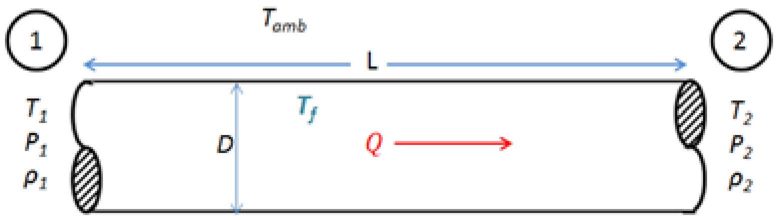

Figure 6-2 Gas pipeline segment [6]

As shown in Figure 6-2 above, the gas flow through a pipeline segment of constant diameter was assumed to satisfy the continuity of mass-energy and momentum. The Weymouth SI unit equation is stated as follows:

$$Q = 3.7435 \times 10^{-3} E \left(\frac{T_b}{P_b}\right) \left(\frac{P_1^2 - e^s P_2^2}{G T_f L_e Z}\right)^{0.5} D^{2.667} \tag{6-1}$$

Where L_e is the equivalent length, s is the elevation adjustment parameter and E is the pipeline efficiency, a decimal value less than or equal to 1. The Q is the gas volumetric flow rate while T_b and P_b are the reference temperature and pressure. The equation provides the relationship between gas throughput in a pipe segment of length L, based on the upstream and downstream pressures P_1 and P_2 putting into consideration of elevation difference.

6.4.1 Pipeline Friction Factor

To calculate the pressure drop in a pipeline, there is a need to understand the concept of friction factor. The two related friction factors used by engineers are the Darcy and Fanning friction factors expressed below:

$$f_f = \frac{f_d}{4} \tag{6-2}$$

Where

f_f = fanning Friction factor

f_d = Darcy friction factor

This research adopts the Darcy friction factor because is widely used and is expressed as:

$$f_f = \frac{f_d}{4} \tag{6-3}$$

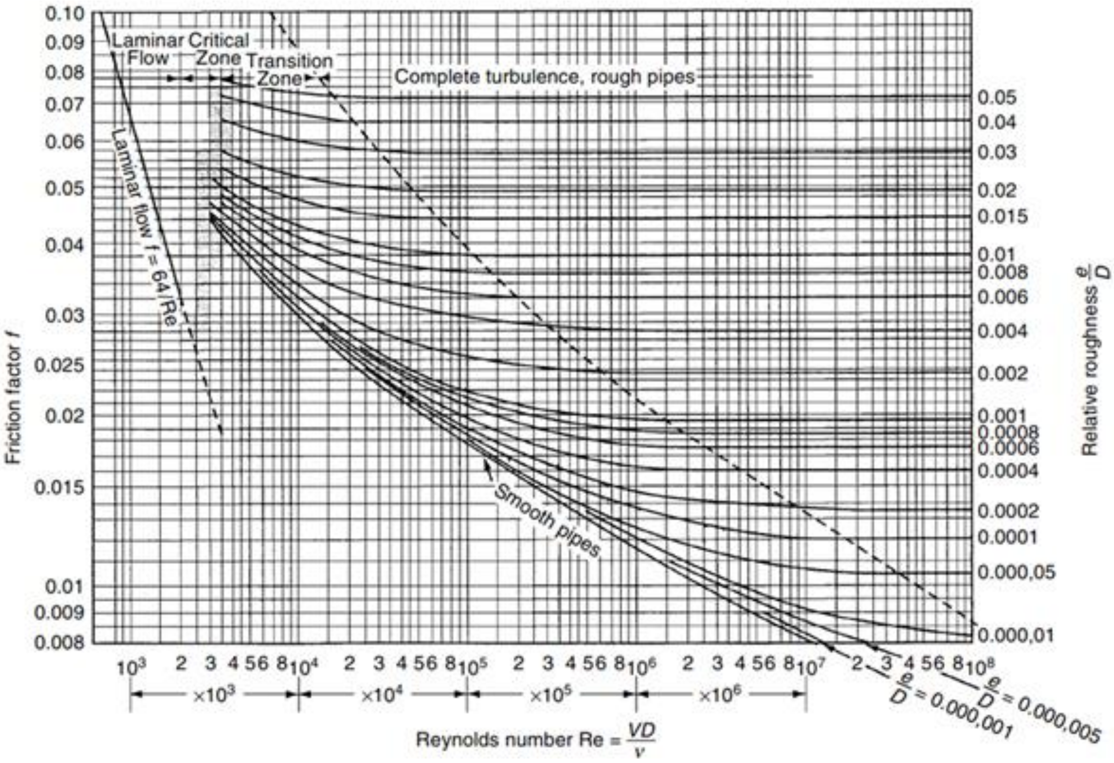

Figure 6-3 Moody chart

The friction factor for the base flow rate is calculated iteratively using Colebrook-White equation by the initial assumption of 0.1 friction factor [14].

$$\frac{1}{\sqrt{f}} = -2log_{10}\left(\frac{e}{3.7D} + \frac{2.51}{R_e\sqrt{f}}\right) \tag{6-4}$$

$$R_e = 0.5134\left(\frac{P_b}{T_b}\right)\left(\frac{GQ}{\mu D}\right) \tag{6-5}$$

The procedure includes calculating the Reynolds number in Equation **(6-5)** and pipeline roughness (e/D). The friction factor is then calculated by an equation using trial and error approach until convergence is reached. The value of friction factor is obtained when an error of less than 0.1% is achieved by comparison of the left and right-hand side of the equation.

The exit pressure at the end of the pipeline segment can be calculated by rearranging the Equation **(6-1)**.

$$P_1^2 - e^s P_2^2 = \frac{Q^2 G T_f L_e Z}{(3.7435 \times 10^{-3})^2 (E)^2 \left(\frac{T_b}{P_b}\right)^2 (D^{2.667})^2} \tag{6-6}$$

$$e^s P_2^2 = P_1^2 - \frac{Q^2 G T_f L_e Z}{(3.7435 \times 10^{-3})^2 (E)^2 \left(\frac{T_b}{P_b}\right)^2 (D^{2.667})^2} \tag{6-7}$$

$$P_2 = \frac{\left(\sqrt{P_1^2 - \frac{Q^2 G T_f L_e Z}{(3.7435 \times 10^{-3})^2 (E)^2 \left(\frac{T_b}{P_b}\right)^2 (D^{2.667})^2}}\right)}{e^s} \tag{6-8}$$

As shown in Equation **(6-8)**, the calculation for exit pressure of the pipe segment is not a direct substitution since the equivalent length, elevation adjustment parameter, and gas compressibility are unknown. In order to get the actual value for pipeline discharge pressure, this involves using a sequence of iterations. To obtain the discharge pressure of pipe for the initial iteration the flow compressibility factor of 0.95 was assumed. The calculated discharge pressure value and the known value of inlet pressure can be substituted in the equation calculating the pipeline average pressure as express in Equation **(6-9)**.

$$P_{avg} = \frac{2}{3}\left(P_1 + P_2 - \frac{P_1 * P_2}{P_1 + P_2}\right) \tag{6-9}$$

Menon [14], concluded that Equation **(6-9)** is found to be the more precise equation for calculating the average gas pressure in a pipeline segment. Having obtained the value of average pressure, a new gas compressibility factor is the then calculated. Generally, compressibility factor is a function of gas gravity, temperature, and pressure and is obtained using the following correlation.

$$Z = \frac{1}{\left[1 + \left(\frac{P_{avg\ 344,400(10)^{1.785G}}}{T_f^{3.825}}\right)\right]} \tag{6-10}$$

Where G is the gas gravity and is express as follows

$$G = \frac{M_g}{29} \quad \textbf{(6-11)}$$

As the process continues, the values of compressibility factor are calculated and compared with its initial value obtained. The iteration will continue until convergence of two values of compressibility factor is achieved. At the convergence level, the discharge pressure estimate will attain its definite value. Therefore, the pressure drop along the pipe segment is the difference between the inlet and outlet pressure express as follows:

$$\Delta P = P_2 - P_1 \quad \textbf{(6-12)}$$

6.4.2 Elevation Difference

The equivalent length, L_e, and the elevation adjustment parameter, e^s, take into consideration the difference in elevation between the inlet and the exit of the gas pipe segment as explained in Equation **(6-13)** where e is the logarithms base (e = 2.718) [14].

$$L_e = \frac{L(e^s - 1)}{S} \quad \textbf{(6-13)}$$

The s parameter is dependent on the gas gravity, the difference in elevation between the inlet and exit of the pipe segment, gas temperature, and gas compressibility factor is expressed in the equation below. Where $H_2\, and\, H_1$ are the elevation at exist and inlet of the pipe segment.

$$S = 0.0684G\left(\frac{H_2 - H_1}{T_f Z}\right) \quad \textbf{(6-14)}$$

By considering the elevation effect along the whole gas transmission network that involves many segments. Therefore, the pipeline equivalent length can be obtained by taking the slope variations of the various segments.

$$L_e = j_1 L_1 + j_2 L_e S^{s1} + j_3 L_3 e^{s2} + \ldots\ldots \quad \textbf{(6-15)}$$

Where

$$j = \frac{e^s - 1}{S} \quad \textbf{(6-16)}$$

And J is the parameter that represents the slope of each pipe sub-segment

6.5 Ambient Temperature and Gas Temperature

The gas temperature at the exit of a long-distance gas pipeline is usually in equilibrium with the ambient temperature of the exit location as shown in Figure 6-4.

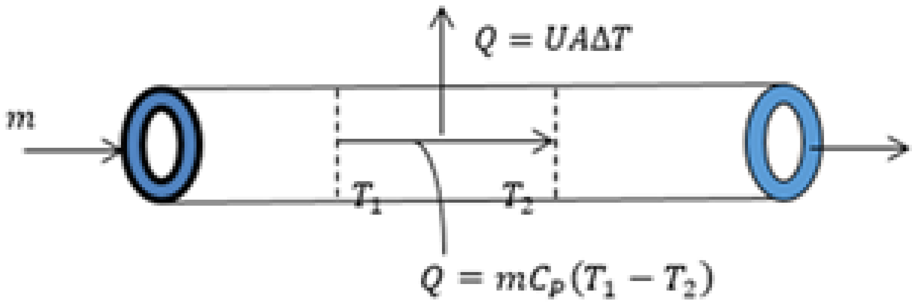

Figure 6-4 Relation between gas temperature and ambient temperature

Usually, heat transfer coefficient in gas pipeline transport is calculated using the following equation.

$$Q = UA\Delta T \quad \textbf{(6-17)}$$

Where Q is heat flow (W), A is area (m^2), ΔT is temperature difference (K) and U is the overall heat transfer coefficient of insulated pipe (W/m^2K) which is determined using the following equation.

$$U = \frac{1}{\frac{D_3}{D_1 + h_{in}} + \frac{D_3 * In\left(\frac{D_2}{D_1}\right)}{2 * k_{pipe}} + \frac{D_3 \ * In\left(\frac{D_3}{D_2}\right)}{2 * k_{insulation}} + \frac{1}{h_{out}}} \quad \textbf{(6-18)}$$

Where k_{pipe} and $k_{insulation}$ are the thermal conductivities of the pipe and insulation while $h_{in}$is heat transfer coefficient in the pipe and h_{out} is heat transfer coefficient at the outside insulation surface. The temperature difference ΔT is also expressed as follows:

$$\Delta T = \frac{T_1 - T_2}{In\frac{T_1 - T_a}{T_2 - T_a}} \quad \textbf{(6-19)}$$

Where $T_1$is the inlet temperature, T_2 is the gas temperature, and T_a is the ambient temperature. Therefore, the heat flow (Q) is determined using the following expression:

$$Q = U\pi dL\frac{T_1 - T_2}{In\frac{T_1 - T_a}{T_2 - T_a}} \quad \textbf{(6-20)}$$

To obtain the gas discharge temperature, there is need to equate gas flow equation and heat flow equation as shown in the equation below:

$$mC_p(T_1 - T_2) = U\pi dL\frac{T_1 - T_2}{In\frac{T_1 - T_a}{T_2 - T_a}} \quad \textbf{(6-21)}$$

$$T_2 = T_a + (T_1 - T_a)exp^{\frac{-U\pi d}{mC_p}L} \quad \textbf{(6-22)}$$

$$\theta = \frac{-U\pi d}{mC_p} \quad \textbf{(6-23)}$$

$$e^{\theta} = 0 \quad \textbf{(6-24)}$$

$$Therefore, T_2 = T_a \quad \textbf{(6-25)}$$

It is proved that Gas temperature is equivalent to ambient temperature.

6.6 Components Interaction

A typical gas pipeline transmission system requires a compromise between the maximum operating pressure, pipe diameter, flow rate, compressor spacing and the gas turbine drivers. Each of these mentioned parameters can have an impact on the capital and operating cost of the gas pipeline project to some extent. Pipeline design optimization increases the economics of the capital and operating competitiveness of the project. During the pipeline operations, the pressure ratio varies with a change in ambient temperature. Hence, the gas compressor has to react to satisfy the new changes while still maintain the maximum allowable operating pressure of the pipeline. This is possible since compressor rotational speed changes directly with the available flow rate. In this research, both the gas composition and volumetric flow is assumed to be constant as mentioned earlier. The change in ambient temperature or the gas temperature affects the volumetric gas flow rate since the compressor suction flow rate is the function of ambient temperature and inlet pressure.

$$Q_2 = Q \left(\frac{P_b}{P_2}\right)\left(\frac{T_{amb}}{T_b}\right)\left(\frac{Z_2}{1.0}\right) \quad \textbf{(6-26)}$$

The actual mass flows rate is defined as the actual volumetric flow rate multiply by compressor gas inlet density as express below:

$$W_2 = Q_2 * \rho_2 \quad \textbf{(6-27)}$$

From open source booster stations spacing along the pipeline are between 40-100 miles away from each other, in some cases, this distance can be more depending on the type of compressor and gas turbine employed.

6.7 Result

In this research the total distance considered is 4180km and the distance from one compressor station to another varies depending on the gas compressor and gas turbine used. Figure 6-5 & Figure 6-6 below shows the distance between one compressor to another and the pipe route elevation.

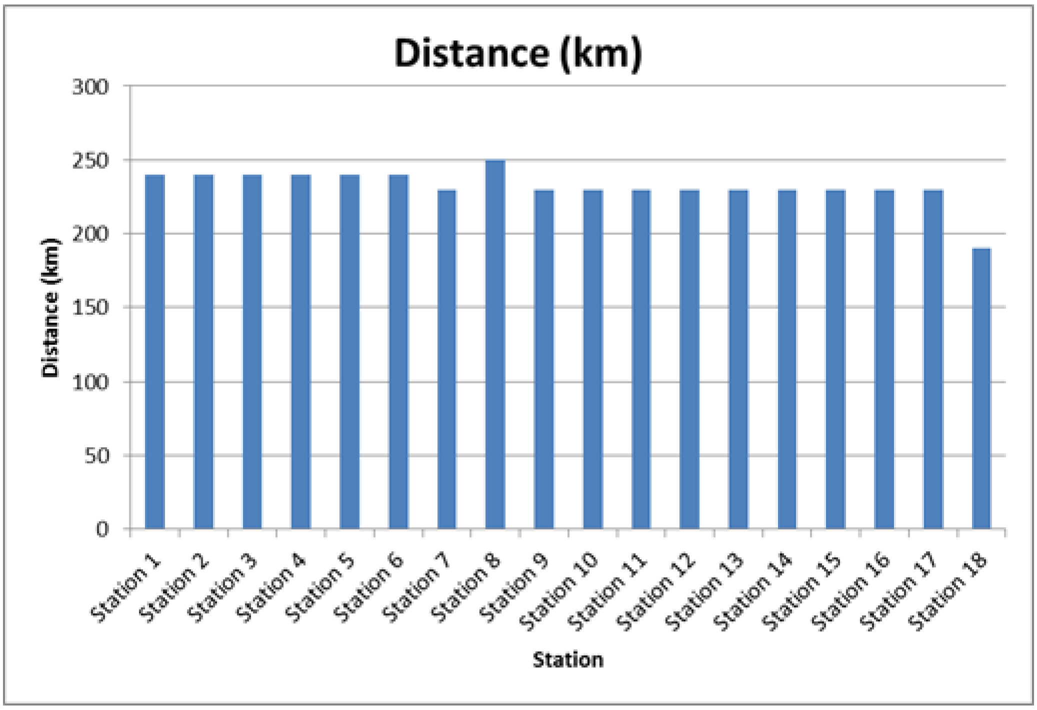

Figure 6-5 Pipeline segment distance

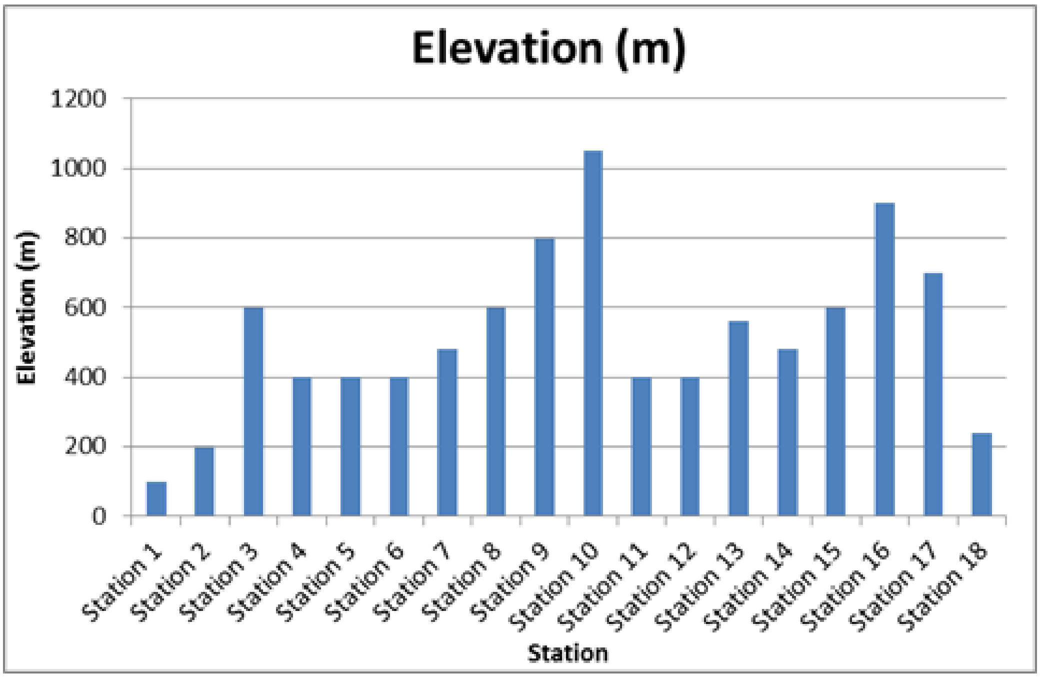

Figure 6-6 Pipeline elevation

To verify the method of analysis mentioned above a pipe data is adopted from Trans-Saharan gas pipeline report. The pipeline data is shown in Table 9

Generally, onshore gas transmission network is designed and built to operate in the pressure range of 40-90 bar. However, an institute of gas Engineers and Managers (IGEM) report on Transmission and Distribution (TD1 Edition 5) allows for maximum operating up to 100 bar.

For this base case, an MAOP of 95 bar was used. Using the TSGP report that suggested a ratio of 1.4 for the first compressor station, the maximum pressure ratio of 1.65 is maintained. Therefore, the inlet pressure for the first compressor station can be calculated using the following equation:

$$P_1 = \frac{MAOP}{Pressure\ ratio} \quad \textbf{(6-28)}$$

$$P_1 = 67.85\ bar$$

Using the base temperature, the pipe segment for the data for the first station at the design point is obtained as shown in Table 9.

Table 9 Parameters for the first pipe segment

Parameters	Values
Mass flow Q (m3/day)	82000000
Pipe inlet pressure P1 (bar)	95
Pipe exit pressure P2 (bar)	67.85
Pressure ratio PR	1.4
Base temperature (K)	288.15
Gas temperature Tf (K)	288.15
Base pressure Pb (bar)	101
Gas gravity (G)	0.6048
Compressibility factor Z	0.8273
Pipe internal diameter (mm)	1381.2
Elevation (m)	100
Equivalent length Le (km)	242.1
Efficiency E (%)	0.918

Using the gas flow reference point of 15°C for temperature and 101 bar for pressure, the friction factor can be calculated as follows:

$$R_e = 0.5134\left(\frac{P_b}{T_b}\right)\left(\frac{GQ}{\mu D}\right) \quad \textbf{(6-29)}$$

From pipe data

Pipe roughness = (0.0003”) 7.62μm

Pipe nominal diameter = (54.38”) 1381.2mm

Relative roughness ε = $\frac{e}{D}$

ε = 5.5167* 10^{-6}

μ = 1.069* 10^{-4}

G = 0.60497

Reynolds Number Re = 1.5286 * 10^{7}

The pipeline friction factor is obtained from the Moody chart as

f = 0.013

To verify pipe exit pressure for station one Equations **(2-8)**, **(2-12)** and **(2-13)** were used.

$$S = 0.0684 * 0.6048 \left(\frac{200}{308.7 * 0.892}\right)$$

$$S = 0.03$$

$$L_e = \frac{L(e^S - 1)}{S}$$

Where e = 2.718

$$e^S = 1.0305$$

Therefore,

$$L_e = \frac{240(1.0305 - 1)}{0.03}$$

$$L_e = 244km$$

$$P_2 = \frac{\left(\sqrt{902500 - \frac{(82 * 10\text{^}6)^2 * 0.6048 * 308.71 * 244 * 0.892}{(3.7435 \times 10^{-3})^2 (0.918)^2 \left(\frac{288.15}{101}\right)^2 (1381.2^{2.667})^2}}\right)}{1.0305}$$

$$P_2 = 63\ bar$$

6.7.1 Stations Inlet and Outlet Pressures

As the natural gas flows through a pipeline, its pressure decreases due to friction between gas and inner walls of the pipe. Compressor stations are located along the pipeline to provide the needed pressure so that the gas flows at the desired rate. The maximum operating pressure for this research is 95 kpa. This means that the outlet pressure of each gas compressor is 95 kpa and the inlet of each new pipe segment is 95 kpa. The pressure drop within each of pipe segment depends largely on the pipe length; elevation and temperature since the pipe diameter and gas composition are constant. The pressure drop with the pipeline was calculated using equation **(2-8)**. The Figure 6-7 & Figure 6-8 below shows the pipe outlet pressure and the compressor pressure ratio.

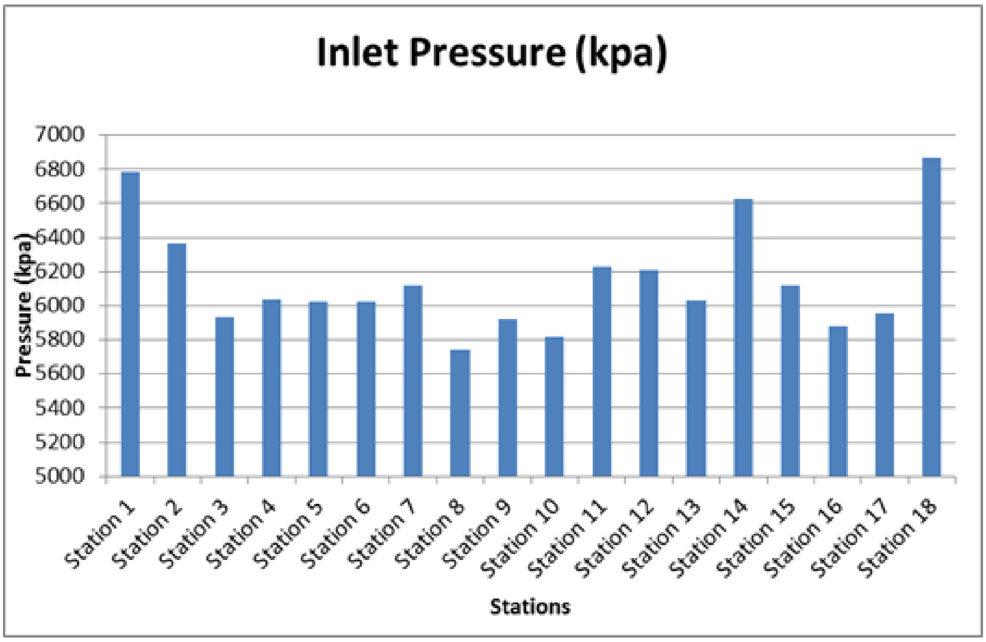

Figure 6-7 Pipe segment exit pressures

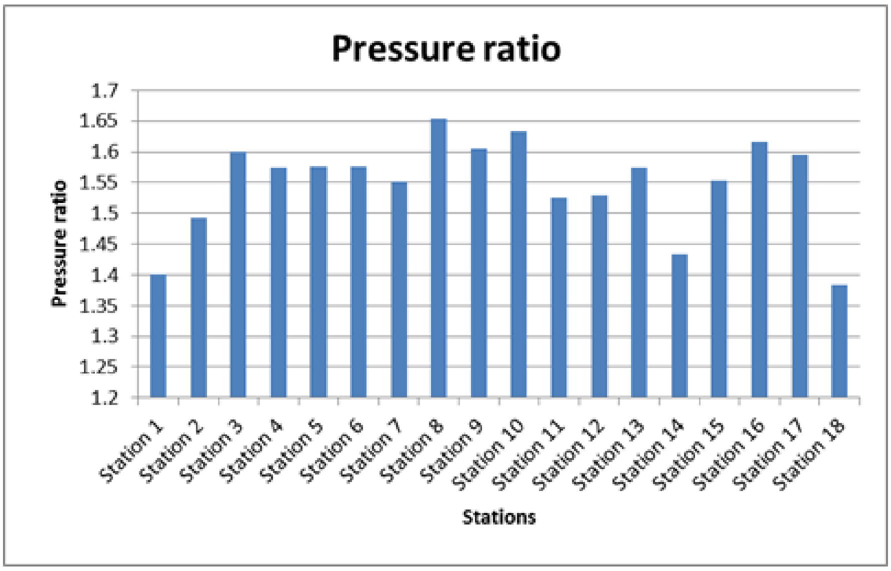

Figure 6-8 Gas compressor pressure ratio

6.7.2 Stations Inlet and Outlet Temperatures

As the pressure of the gas increases by the gas compressor, the gas temperature also rises. The exit of a compressor is the inlet of a pipeline. Thus, the gas temperature reduces as it continues to move within the pipeline due to the pressure decrease until it reaches equilibrium with the ambient temperature. The Figure 6-9 below shows gas temperature inlet temperature which is the pipeline exit temperature as well as the very high ambient temperature for each of the compressor station locations.

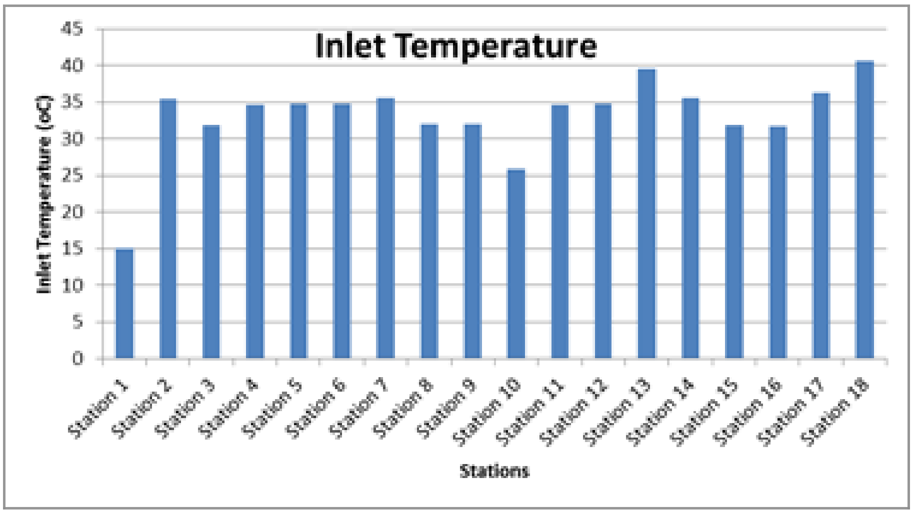

Figure 6-9 Compressors inlet temperature

The gas compressor exit temperatures for the whole compressor stations were obtained using the following equation:

$$T_2 = T_1 + \Delta T_{atual} \quad \textbf{(6-30)}$$

Where

$$\Delta T_{atual} = T_1 \frac{[\left(\frac{P_2}{P_1}\right)^{\frac{n-1}{n}} - 1]}{\eta_P} \quad \textbf{(6-31)}$$

The gas compressor outlet temperatures for all the stations were shown in Figure 6-10.

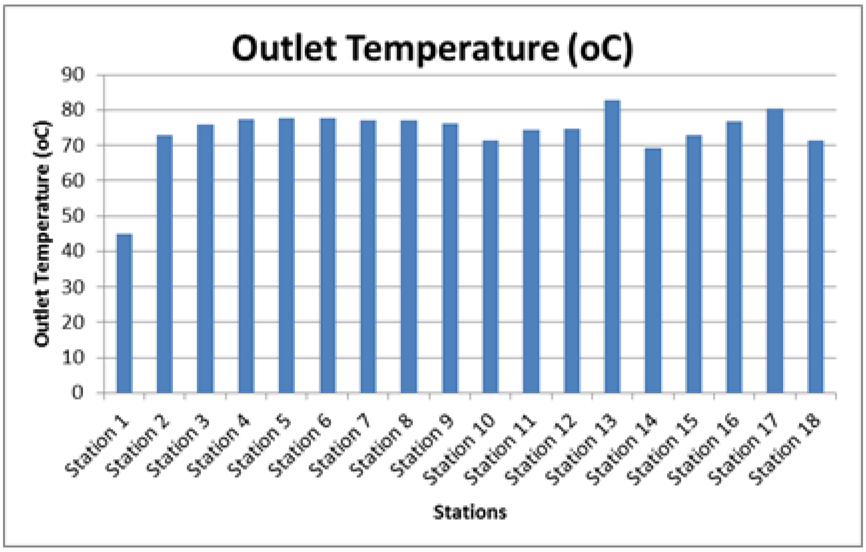

Figure 6-10 Gas compressor outlet temperature

6.7.3 Compressor Selection

The centrifugal compressors are usually selected based on the rated principle of rated point as mentioned above. In this research, the selection was based on very high temperature, pressure, and power. Since the flow rate and gas composition are constant. Parallel compressor station arrangement was considered for this base case study as shown in Figure 6-11.

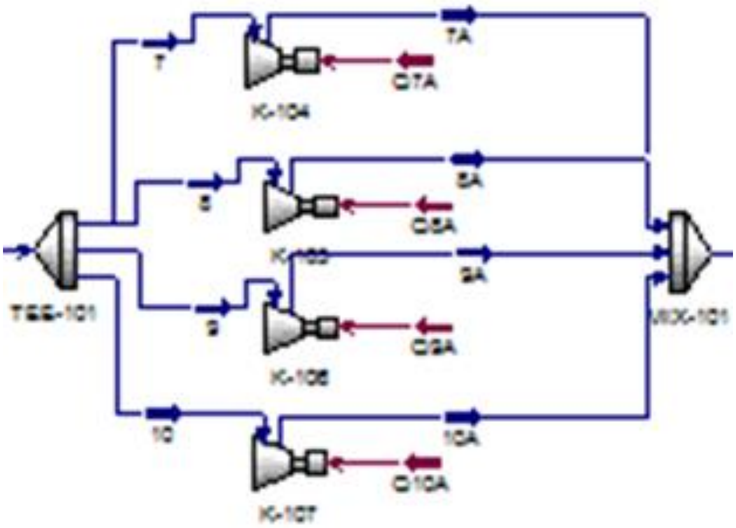

Figure 6-11 Compressor station configuration

Four identical gas compressors each driven by gas turbine arranged in parallel, the flow rate from the pipeline divided into four equal part as passes through the compressors. The compressors have the same pressure ratio and power. The gas compressor power for all the stations is shown in Figure 6-12 below.

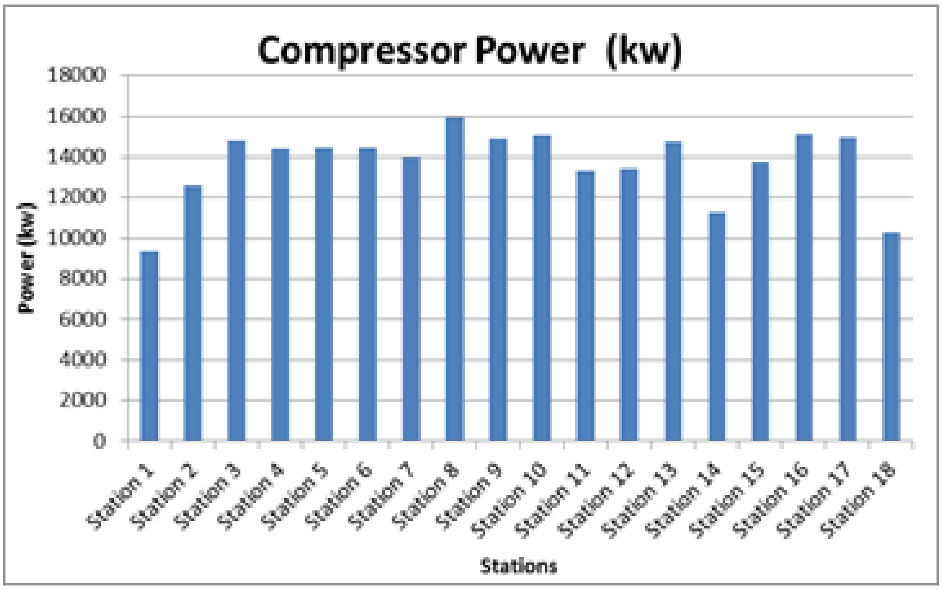

Figure 6-12 Compressor power requirement

The gas compressor power is calculated using the following equation:

$$P_g = \frac{mH_P}{3600\eta_P} \tag{6-32}$$

Where $H_P$the polytropic head and it is function of compressibility factor, process exponent, molecular weight, inlet temperature and pressure ratio as express below:

$$H_p = \frac{Z_a}{1000} \frac{8314}{MW} T_1 \frac{n}{n-1} \left[r_p^{\frac{n-1}{n}} - 1 \right] \quad \textbf{(6-33)}$$

The variation of gas compressor power along the pipeline is a result of change in inlet temperature and pressure since in T_1 and r_p will change the value of polytropic head as well as the power. Based on the compressor power requirement and the mass flow rate three different types of gas compressors and three gas turbines were selected for the 18 compressor stations as shown in the Table 10 below.

Table 10 Selected compressor and gas turbine

Stations No	Power (kw)	Gas Compressor	Gas Turbines
1	9323	Dresser-Rand Datum C (16964 HP)	Twin shafts (13.4MW) Industrial
2	12606	Dresser-Rand Datum C (16964 HP)	Triple shafts (15.2 MW) aero derivative
3	14802	Dresser-Rand Datum C (20120 HP)	Triple shafts (17 MW) aero derivative
4	14411	Dresser-Rand Datum C (20120 HP)	Triple shafts (17 MW) aero derivative
5	14461	Dresser-Rand Datum C (20120 HP)	Triple shafts (17 MW) aero derivative
6	14467	Dresser-Rand Datum C (20120 HP)	Triple shafts (17 MW) aero derivative
7	13966	Dresser-Rand Datum C (20120 HP)	Triple shafts (17 MW) aero derivative
8	15968	Dresser-Rand Datum C (20120 HP)	Triple shafts (19.3 MW) Industrial
9	14897	GE HE-S (22000 HP)	Triple shafts (19.3 MW) Industrial
10	15046	GE HE-S (22000 HP)	Triple shafts (19.3 MW) Industrial
11	13311	Dresser-Rand Datum C (20120 HP)	Triple shafts (17 MW) aero derivative
12	13412	Dresser-Rand Datum C (20120 HP)	Triple shafts (17 MW) aero derivative
13	14763	Dresser-Rand Datum C (20120 HP)	Triple shafts (17 MW) aero derivative
14	11252	Dresser-Rand Datum C (16964 HP)	Triple shafts (15.2 MW) aero derivative
15	13739	Dresser-Rand Datum C (20120 HP)	Triple shafts (17 MW) aero derivative
16	15118	GE HE-S (22000 HP)	Triple shafts (19.3 MW) Industrial
17	14975	GE HE-S (22000 HP)	Triple shafts (19.3 MW) Industrial
18	10292	Dresser-Rand Datum C (16964 HP)	Twin shafts (13.4MW) Industrial

6.8 Discussion

This research maintained a constant pipe diameter and gas composition. The study shows that ambient temperature, distance, and elevation are the important requirements to consider when spacing compressor stations.

Station 8 in Figure 6-12, has the very high gas compressor power requirement of 15968 kW this is because the pipeline segment that precedes the station is the longest with a distance of 250 km, elevation 600m and compressor inlet temperature of 31.97^{O}C. Long distance pipeline is associated with high-pressure losses. The compressor inlet pressure is 57.4 bar. Therefore it requires more work by the gas compressor to raise this pressure to 95 bar at the exit of the gas compressor. The station also has the highest gas compressor pressure ratio of 1.65 which also increased the value of polytropic head as well as the power since the pressure ratio and inlet temperature are parameters that affect the value polytropic head.

Station 16, has the second highest value of the gas compressor power of 15118 kW. The pipe segment that precedes this station has a distance of 230 km, elevation 900m and the compressor inlet temperature of 31.72^{O}C. The elevation and distance are important parameters that cause the pressure loss along the gas pipeline. The compressor inlet pressure is 58.9 bar and a pressure ratio of 1.61 so as to raise this pressure to 95 bar at the exit gas compressor.

Station 10, has the third highest value of gas compressor power of 15046 kW. The pipe segment that precedes this station has a distance of 230 km, station elevation 1050m, and the compressor inlet temperature of 25.8^{O}C. The compressor inlet pressure is 58.2 bar and a pressure ratio of 1.63 so as to raise this pressure to 95 bar at the exit gas compressor.

6.9 Validation of the Result with HYSYS

Aspen HYSYS is a proven and comprehensive process-modeling tool used by the leading global oil and gas companies, universities and engineering companies for optimization process and process simulation in design and operations [89]. Aspen HYSYS is broadly used to model several facets of the oil and gas production fields, including separation systems, pipe segment, compressors, and gas dehydration. It is also regarded as an instrument of choice for determining of performance, separation, heat and material balance [90].

Aspen HYSYS uses fluid package concept to accommodate the required information for carrying both physical property and flash calculations. This path will allow the user to define the necessary information like the components, package property and interaction parameters within a single entity. The HYSYS inbuilt property packages allow the user to select the properties of mixture ranges from light hydrocarbon, complex oil mixture and non-electrolyte chemical systems. Peng-Robinson and Peng-Robinson Stryjek-Vera enhanced equations of state are provided by HYSYS for proper calculation of hydrocarbon systems [91]. Though, Peng-Robinson property package is the recommended for oil, gas, and petrochemical related applications.

However, the numerous components that made up of HYSYS present a remarkable approach for steady-state flow modeling. These components are to form the basis of flowsheets, by connecting the right components and streams you can simulate a wide range of oil, gas, chemical, and petrochemical process. Simple and complex oil and gas pipelines are model in Aspen HYSYS pipeline segment model and Aspen HYSYS upstream hydraulics. The HYSYS components adopted in this research include:

1. Pipe segment
2. Mixer
3. Tee
4. Compressor

Generally, HYSYS operates with a degree of freedom concept, which boosts the flexibility of obtaining results. As information is provided by the user, HYSYS will calculate the unknown base on the input information provided.

6.9.1 Aspen HYSYS Pipeline Segment Model

The Aspen HYSYS pipeline segment is the suggested solution for simulating a single and multiple pipelines. Generally, these types of segments are defined by terrain or environmental changes along the pipeline route. In order to provide precise simulation with pipe segment, there is a need to divide the whole pipeline into smaller units depending on the characteristics of each segment. To use the pipe segment model, the user must specify any two of the following parameters: mass/molar flow rate or inlet pressure, discharge pressure. The third parameter will be obtained once two of the parameters are specified. Other input parameters for the pipe segment model include:

- ✓ Length of the pipe
- ✓ Outer diameter
- ✓ Inner diameter
- ✓ Elevation change
- ✓ Number of increments
- ✓ Pipe material

6.9.2 Mixer

The mixer is the HYSYS operation components that merge two or more inlet streams so as to provide a single outlet stream. Within the mixer component, the material and heat balance is achieved; this is because the unidentified temperature between the inlet and outlet streams is always calculated. However, if the mixer inlet properties are provided the outlet stream properties is calculated automatically since the pressure, enthalpy and gas composition of that stream is known. Mostly, temperature and pressure are the unknown parameters to be determined. If the inlet parameters are identified, no further information needs to be stated for the outlet stream. Therefore, the problem is totally defined; no degrees of freedom remain.

6.9.3 Tee

Tee is the HYSYS operation components that divide single feed stream into several product streams with similar composition and condition as the feed stream. The required numbers of the product streams are specified from the feed stream; the TEE component generates automatically and allocates the composition and conditions of the feed stream to the product streams. The difference obtainable on the product streams is the flow rate which is pending on the ratio specified by the user.

6.9.4 Centrifugal Compressor

The centrifugal compressor component is used to raise the inlet pressure of the gas stream so as to obtain a higher outlet pressure of the gas stream. Subject to the information provided, the centrifugal compressor calculates either the pressure, temperature and compression efficiency of the stream. The centrifugal compressor also calculates the power required to achieve the compression. Generally, HYSYS uses the equation of state, thermodynamic and proportionality laws for proper design and operation of centrifugal compressors.

There are several ways to solve centrifugal compressors in HYSYS depending on the information provided. These methods involve using compressor curves or without compressor curves as shown in Table 11 below.

Table 11 Solving centrifugal compressor in HYSYS [92]**.**

Without Curves	With Curves
1. Flow rate and inlet pressure are known. Then: A) Specify outlet pressure. And, B) Specify either Adiabatic or Polytropic efficiency. HYSYS calculates the required energy, outlet temperature, and other efficiency.	Flow rate and inlet pressure are known. Then: A) Specify operating speed. B)HYSYS uses curves to determine efficiency and head. HYSYS calculates outlet pressure, temperature, and applied duty.
2. Flow rate and inlet pressure are known. Then: A) Specify efficiency and duty. HYSYS calculates outlet pressure, temperature, and other efficiency.	Flow rate, inlet pressure, and efficiency are known. Then: A)HYSYS interpolates curves to determine operating speed and head. HYSYS calculates outlet pressure, temperature, and applied duty.

Generally, there is flexibility in using the centrifugal compressor component with respect to which information to be provided and what can be calculated by HYSYS.

To validate the developed model results, HYSYS was used to simulate the data in Table 9 using the same elevation, distance, and operating conditions. For example, the station 2 pipe segment has an elevation of 200m and distance of 240km as shown in Figure 6-13.

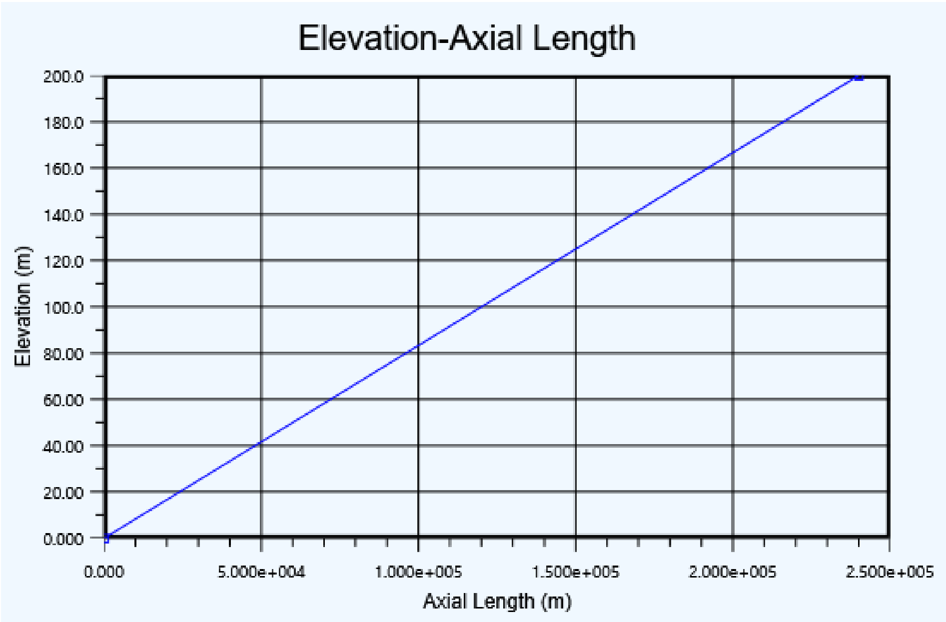

Figure 6-13 HYSYS elevation and distance

The pipe segment exit pressure result is shown in Figure 6-14 The 9500kpa from the y-axis is the operating pressure at the exit of a compressor while the distance of 240000m from x-axis represents the pipe distance. The pressure from the exit of this pipe segment is 6300 kpa which confirmed the pressure drop calculation made above and the result for station 2 in Figure 6-7.

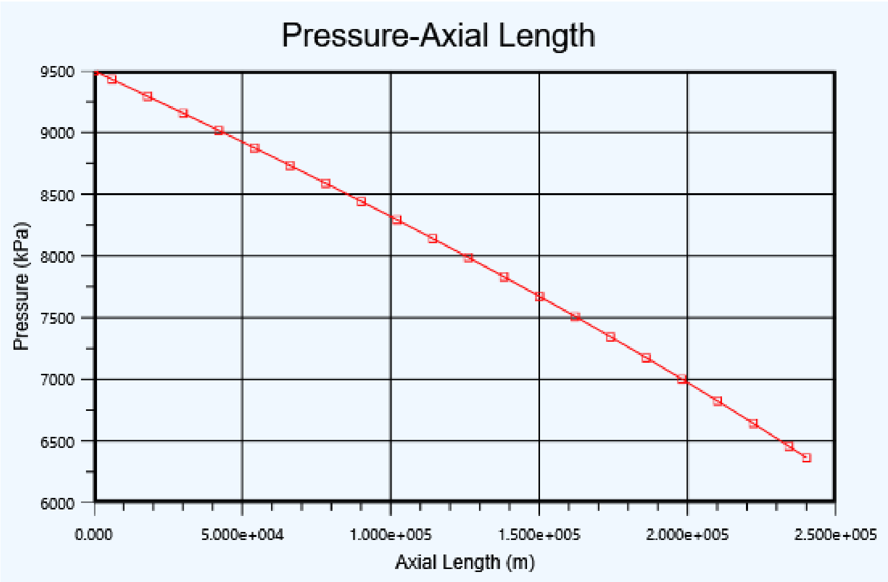

Figure 6-14 HYSYS pressure drop for station two

Temperature-axial length results shown in Figure 6-15, the y-axis is the gas compressor exit temperature which confirmed the result of station 1 in Figure 6-10 obtained using Equation **(6-31)**. The x-axis is the pipe distance of 240000m, the temperature at the exit of this pipe segment is 35^{O}C which is the inlet of the compressor at station 2 as confirmed in Figure 6-9 and equation **(6-25)**.

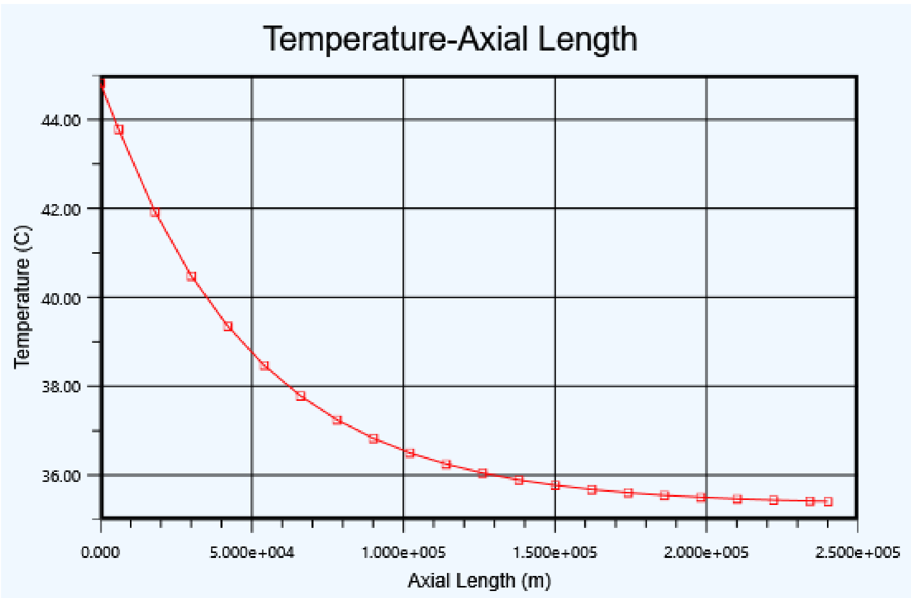

Figure 6-15 HYSYS Temperature result

6.10 Conclusion

Compressor station spacing along the natural gas pipeline is affected by gas composition, inlet conditions, pipeline parameters and the terrain. This research focused on inlet conditions, pipe segment distance, and elevation. Station 8 in Figure 6-12, shows that gas compressor with high-pressure ratio and inlet temperature require more head and power to transport natural gas. From station 8 and station 10 it shows that the pipe segment distance has more effect on the gas pressure loss along the pipeline than the elevation. Station 16 and station 10 have the same pipe distance but different elevation. Their pressure ratio difference is not significant but station 16 has more power requirement than the station 10 due to its high inlet temperature. The result shows pressure ratio has more effect on polytropic head and power than the inlet temperature. It is shown that increasing the ambient temperature by 0.25^{O}C and pressure ratio by 0.04 the power will increase with 850 kW.

7 TERA Optimization

7.1 Abstract

The optimization design of the natural gas transmission network, which is expected to convey natural gas from the production field in Niger Delta Nigeria to delivery point in Algeria through Niger, is presented in this research. The sum of the pipeline cost, gas compressor cost, gas turbine cost, fuel cost and staffing constitute the objective function of this research while the distance between compressor stations is the variable and the operating pressure of 100 bar is the constraint. The pipeline design parameters including pipe diameter, pressure delivery, ambient temperature and location of compressor station on each of the pipeline are considered in this optimization study. The studies considered two gas turbines of 43.3MW and 100MW capacities. The 43.3MW station has two compressors driven by two gas turbines at each of the compression stations while the 100MW plant has one gas compressor driven by one gas turbine. The result shows 10 compressor stations along the pipeline. The optimized result also shows a reduction in the lifecycle cost from USD 20.1 billion in 43.3MW to USD 18.8 billion in 100MW. The NPV at 15% discount rate for both engines is seen to be positive.

7.2 Optimization

The existence of several objectives in a problem, in principle gives rise to a set of optimal solutions. Optimization refers to a process of making system decision. Optimization function allows comparison of the various choices for determining which might be good in terms of maximal profit and minimal cost. The optimization input consists of variables, the process, or function is known as the cost function, fitness function or objective function and the output is the cost or fitness[93]. The optimization process is shown

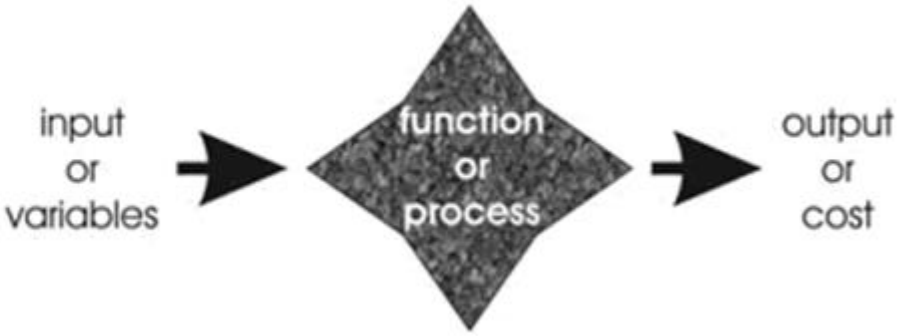

Figure 7-1 Optimisation process [93]

7.3 Overview of Genetic Algorithms

A genetic algorithm (GA) is an optimization and search technique based on the principles of genetics and natural selection [93]. With GA a population composed of many individuals evolves under specified selection rules to a state that maximizes the fitness which minimizes the cost function.

The idea of genetic algorithm was started by H.J. Holland in 1960 [94]. A genetic algorithm is a non-linear type of optimization and it has been successfully used in solving several engineering problems. A genetic algorithm is based on the phenomena of chromosome gene code interchange, a procedure totally based on random selection of data modification [10].

Khouja et al [95] explained that it is generally accepted that any genetic algorithm to solve the problem must have the following basic components:

- Genetic representation for potential solution
- A way to create an initial population of solutions
- An evaluation function
- Genetic operators that alter the genetic composition of parents during reproduction
- Values for the parameters

The basic steps followed by GA include the random creation of an initial population from the data supplied, which constitute the population of individual solutions covering the whole range of possible solutions. The population data is selected by a random method and mathematical method is used in encoding the search space of the entire individual [96]. Genetic algorithm generally tries to find the very good solution to a problem by genetically breeding the individuals in the population over a number of generations.

The second stage of the GA involves evaluating the data and see whether the stopping criteria are achieved. The iteration process will stop and results presented if a positive response is achieved [97]. However, negative response will give rise to the chance of parent selection. When parents are selected randomly then, the crossover is performed based on crossover probability. The selection of both the parents and crossover points are done randomly. The mutation is performed after this stage. The probability of mutation determines the number of points of mutation. The data is then evaluated using the developed equations. The best-fitted data is obtained from the data that gives the excellent result be it cost, operational time or any other conditions.

7.4 GA Operators

These are operators used in the genetic algorithm in order to maintain genetic diversity. In the evolution processes, genetic variations are a necessity and are in analogous to those occurring in the natural world. In this research, GA Toolbox in MATLAB was used and MATLAB code was also developed for the optimization. Discussed below are the major GA operators which include crossover, mutation, and selection.

7.4.1 Crossover

Crossover is the key genetic operator. It operates on two chromosomes at a time and generates offspring by combining both chromosomes. The easiest way of executing crossover is to select arbitrarily some crossover point copy everything before this point from the first parent and also copy all after the crossover point from the other parent [98]. Performing crossover can be complex and depends mainly on the encoding of chromosomes [99]. There are several ways in which crossover can be performed, these include: one point crossover, two-point crossover, and uniform crossover

7.4.2 Mutation

Mutation is a background operator that creates spontaneous arbitrary changes in various chromosomes. Mutation is simply achieved by altering one or more genes. It serves either of the following in GA application [100].

1. Replacing the lost genes from the population during the selection process.
2. Providing the genes that were not present in the initial population.

The total number of percentage genes in the population is called mutation probability. The mutation probability controls the likelihood at which genes are introduced into the population for trial.

Mutation process is archived by altering one parent while crossover process involved two parents. Mutation process introduces traits which are not part of the original population and prevents the GA from converging very fast, before sampling the entire search surface [93].

7.4.3 Elitism

Elitism is the process of copying the fitness chromosomes into the new population so as to ensure that the best fitness chromosomes are not lost I the crossover and mutation to form new population (n). Generally, elitism increases the performance of generic algorithms because it averts a loss of the best found solution.

7.5 Why Optimization

Using constant volume flow rate and same gas composition, the gas compressor polytropic head and gas power increased with an increase in gas temperature. In this research, the gas temperature is assumed to be equivalent to ambient temperature at the entry of compressor station or at the delivery point as mentioned in chapter 5. The ambient temperature fluctuates daily in winter, dry and hot seasons across Trans-Sahara pipeline stations, these temperature fluctuations have an impact on the compressor power and pressure drop along the pipeline. Figure 7-2 below shows different gas temperature and pressure drops for one station.

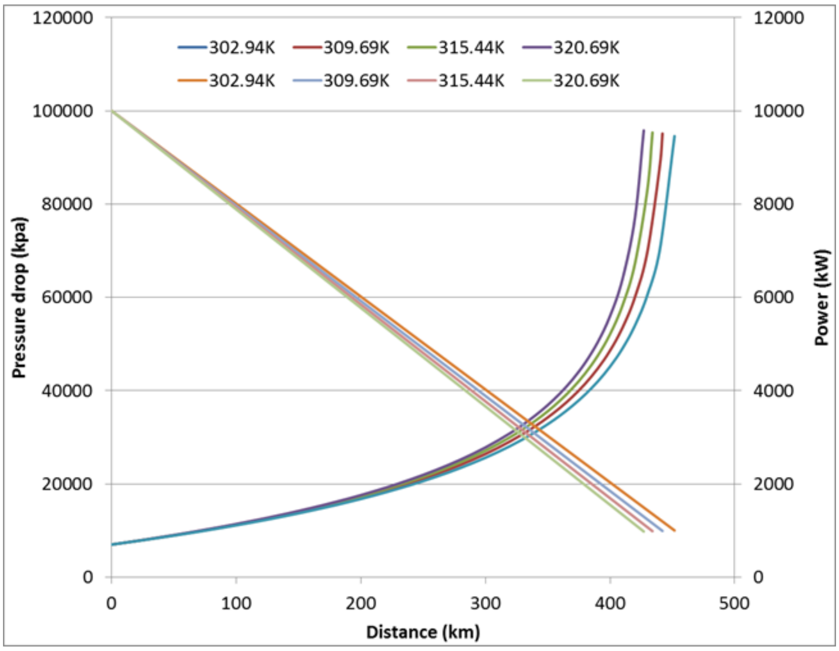

Figure 7-2 Impact of gas temperature on compressor power and pipeline pressure drop

Figure 7-2 shows that at a high gas temperature of 320.69K, the maximum allowable pressure drop coincide at a pipe distance of 427km while at a low gas temperature of 302.94K the maximum allowable pressure drop is achieved at a little further distance of 451km. This implies that, high gas temperature is associated with increased in specific volume of the gas in the pipe, resulting in the increase of the gas velocity and the pressure drop in the pipeline. As the gas temperature increases, throughput will decrease. Thus, the hotter the gas the lower the flow rate. As the flow rate decreases the pressure drop will increase. Also, the decrease in pressure drop causes the inlet pressure to the next compressor goes higher. Accordingly, at lower gas temperature the flow rate increases while the pressure drop reduces. The increase in pressure drop along the pipeline causes the inlet pressure to the compressors to reduce. The influence of the gas temperature on gas compressor power requirement has become more pronounced as the pipeline distance increases.

The compressor power is one of the key parameters for calculating fuel consumption of the compressor drivers. Also, the operational cost of running the compressor is usually assumed to be equal to the cost of the fuel consumed by the driver. Consequently, the temperature of the gas at the inlet of the compressor has a significant effect on the operational cost of running the compressors.

Different gas temperatures provide different power requirement, distances and pressure drop along the pipeline. Given the variations direct analytical solution is not available; hence, the need for optimization, the aim of optimization in this chapter is to provide the lowest lifecycle cost based on the optimal distance and power requirement of different compressor stations along the pipeline. Genetic algorithms from MATLAB toolbox was used to carry out the optimization. Two gas turbines of different size and configuration were selected for the optimization 100MW and 43.3MW capacities. For the 100MW scenario one gas turbine was used per station while for the 43.3MW two gas turbines are used per station. The optimization procedure and results are presented below.

7.5.1 Optimization Conditions

The aim of this section is to optimize gas turbine engines for mechanical drive, based on the different gas temperature, power demand, and distance between compressor stations. GA was used in this research because it is easy to learn, widely used in research and more importantly, is suitable for optimizing gas turbine power as it would usually define the properties of the most cost-effective equipment to guide investment decisions; and help determine the minimum lifecycle costs. The engines selected for the optimization is made of simple cycle two shafts engine with 43.3MW and an intercooled gas turbine with a capacity of 100MW.

During the optimization process, the baseline case of 18 compressor stations discussed in chapter 3 was used as a reference point. The gas compressor station 1 was assumed to be fixed, and the maximum allowable operating pressure was set at 100bar. The pipe diameter and thickness was also assumed to be the 56-inch and 0.875-inch diameter of API 5L X80 standard.

The model integrated both the performance and economic module. The performance module calculates the required gas compressor power and gas turbine matching power based on TET and fuel consumed. The economic module calculates the cost associated with this matching requirement. As the optimization variable (in this case distance) changes, the values corresponding to the ambient conditions (temperature) at different time intervals is utilized by the model to obtain the required gas compressor and gas turbine matching based on the set limit.

In order to solve a GA problem, the numbers of variables, objective function, boundaries, and assumptions have to be specified. The optimization design space is specified by the domain boundaries. This was achieved by considering the minimum and maximum distances between the compressor stations and possible gas turbine power requirement to compress the pressure along the pipeline. The optimization boundaries for station 2, were set between the minimum and maximum as [200, 448], [200, 443] for the 100MW and 43.3MW respectively. The minimum boundary is always 200 while the maximum varies from one location to another depending on the ambient temperature and the site elevation.

Also, a relationship between a function and a variable has to be identified. In this research, power and distance are identified as the function and variable respectively. From the Weymouth flow equation and gas compressor polytropic head equation, a relationship between the power and distance was developed. Therefore, any change in a variable (distance) will affect the function (power) and vise versa. Using the GA optimization tool, the objective function, constraints, and initial condition were specified. The population search consists of two different engines with different configurations; the purpose of this search is to get the cost-effective project. For this optimization, the following assumptions were made:

- Compressor station one is fixed
- Project lifespan of 30 years

- NPV of 13%, 14%, and 15% are considered.
- The best engine is the most cost-effective engine.
- One gas turbine per station for 100MW capacities and two gas turbines per station for 43.3MW capacities.
- In the economic analysis, the capital cost, fuel cost, and maintenance are considered.
- Pipeline distance of 4180km

Figure 7-3 shows an overview of the optimization process implemented in this research. From the flow chart, the first step is to set the baseline condition, which comprises of 18 station gas compressors. Next is to obtain the ambient condition of each station location at a different time interval of the day. The model then calculates the gas compressor power requirement at the specified temperature of different intervals and obtains the gas turbine TET required to meet gas compressor power demand. If the variation between the power demanded by the gas compressor and power provided by the gas turbine is less than or equal to 10%, the process is repeated to get the exact matching TET. Otherwise, the model converges and calculates the corresponding cost. As the distance between the compressor stations is varied, the process is repeated to obtain an optimal distance for which the result is reasonable with the selected number of the gas turbine.

After the objective function, constraints and initial conditions were specified, using the MATLAB code developed for this optimization as shown in Appendix G, the code will read from the developed model and interpolate where necessary so as to present the required cost-effective fitness value results. See Appendix H for part of the model developed.

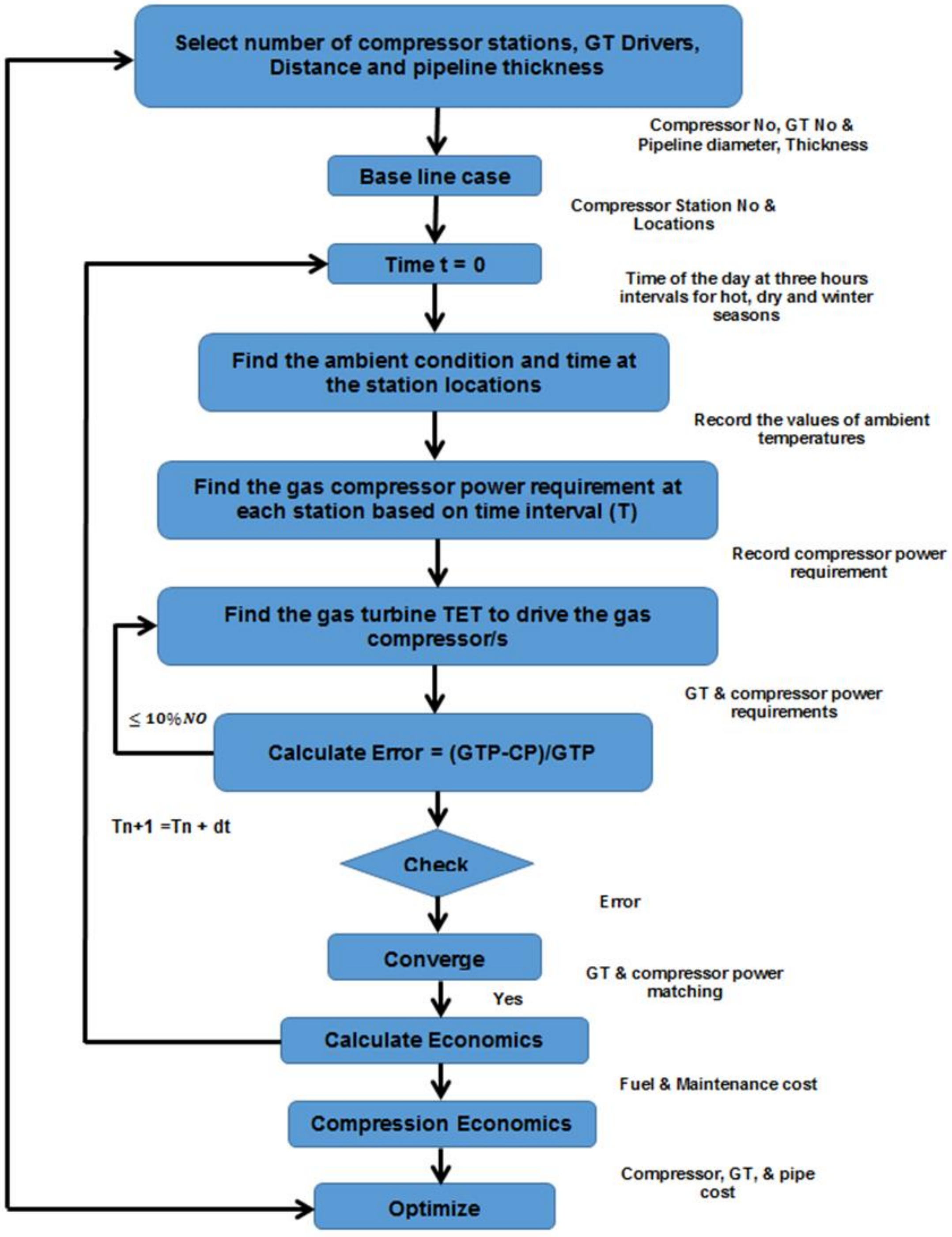

Figure 7-3 Optimization Process

7.6 Details of the Selected Gas Turbines

The optimization study was inspired by two gas turbines, these are LM6000 and LMS100.

I. LM6000 gas turbine

LM6000 gas turbine is a stationary engine variant of the CF6 engines family. The LM6000 PC is rated to provide a power output of more than 43 MW at ISO conditions. More than 1000 units of LM6000 gas turbine engine has been produced, and have had over 21 million hours of operations [67]. The LM6000 is a simple cycle, two shafts, and high-performance gas turbine. The engine consists of 5 stage low-pressure compressor, 14 stage high-pressure compressors, an annular combustor, 2 stage high-pressure turbines and 5 stage low-pressure turbines. The air is compressed into the low pressure and high-pressure compressors by the ratios of about 2.3 and 12.5, which among to the total compression ratio of approximately 30 relative to ambient temperature. The air is then sent into combustor where it mixes with the fuel from the nozzles. The hot gas from the combustor is then passed into the high-pressure turbine that drives the high-pressure compressor. The gas will further expand through the low-pressure turbine which drives the low-pressure compressor and the output load.

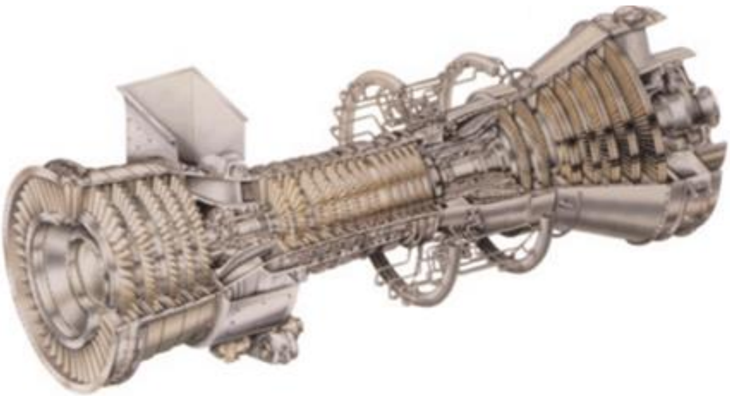

Figure 7-4 LM6000 Industrial gas turbine

The design point simulation of LM6000 industrial gas turbine was carried out in Turbomatch as mentioned earlier in the methodology with the engine parameters obtained from GE website so as to meet the required power out by the gas compressor. A good result is obtained from the simulation as shown in table

Table 12 Engine model verification at design point

S/No	Properties	GE Website	Turbomatch	Difference (%)
1	Efficiency (%)	40	39.7	0.3
2	Power output (MW)	43.3	43.3	0
3	Pressure ratio	29.1	29.1	0
4	Fuel flow (kg/s)	2.1	2.3	-0.2
5	Inlet mass Flow (Kg/s)	124.9	129	-4.1
6	TET (K)	-	1550	-
7	Comp turbine efficiency	-	0.9	-
8	Power turbine efficiency	-	0.9	-

GE Fuel flow

Heat rate = 8648kJ/kWh

Fuel flow = Heat rate*Power output/ (FHV)

= 8648*43.3/ (49*3600)

= 2.1Kg/s

GE Inlet Mass flow

Exhaust flow= 127kg/s

Inlet mass flow = Exhaust flow – fuel flow

= 127-2.1

= 124.9kg/s

At the design point the compressor map was drawn using the variation in mass flow, efficiency and pressure ratio along with constant rotational speed data obtained from Turbomatch simulation as shown in Figure 7-5 and Figure 7-6 below. A compressor running line is obtained when its rotational speed, pressure ratio and mass flow match with each other.

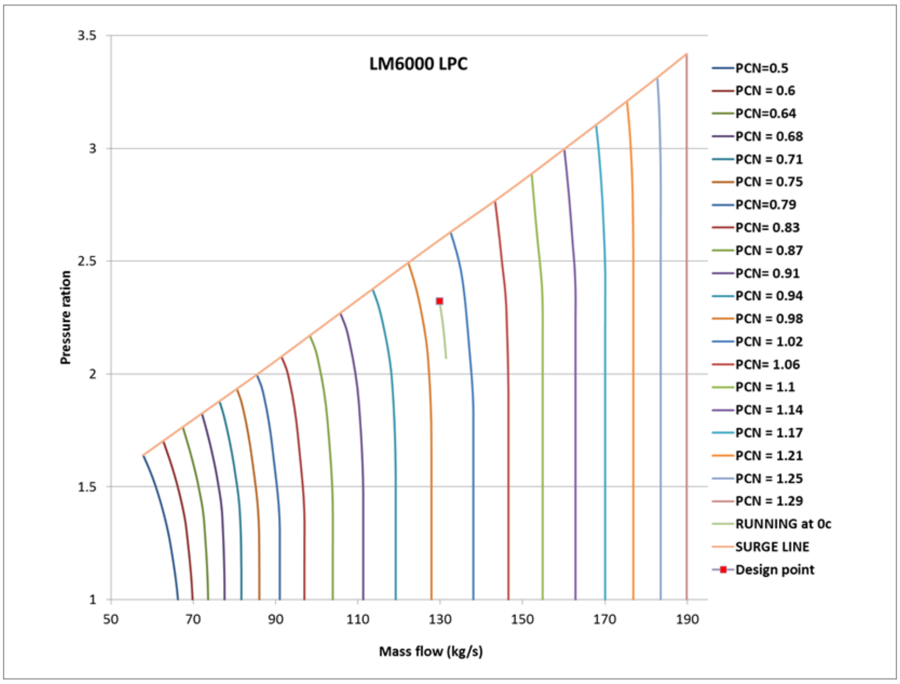

Figure 7-5 LM6000 Low-pressure compressor map

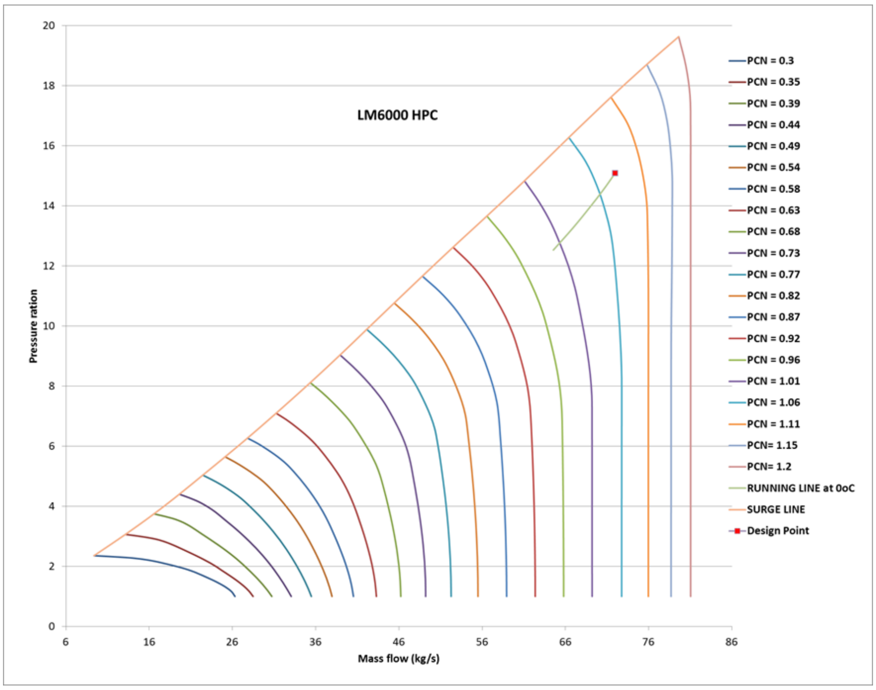

Figure 7-6 LM6000 High-pressure compressor map

II. LM 100

The LMS100 is an intercooled gas turbine system, developed from GE frame and aero-derivative gas turbine technologies, with simple cycle thermal efficiencies of up to 41%. The engine consists of a low-pressure compressor, high-pressure compressor, intercooler, a high-pressure turbine, intermediate pressure turbine and a power turbine. The intercooler provides significant benefit by reducing the compression work for the high-pressure compressor, which allows for higher pressure ratio and increasing the engine overall efficiency.

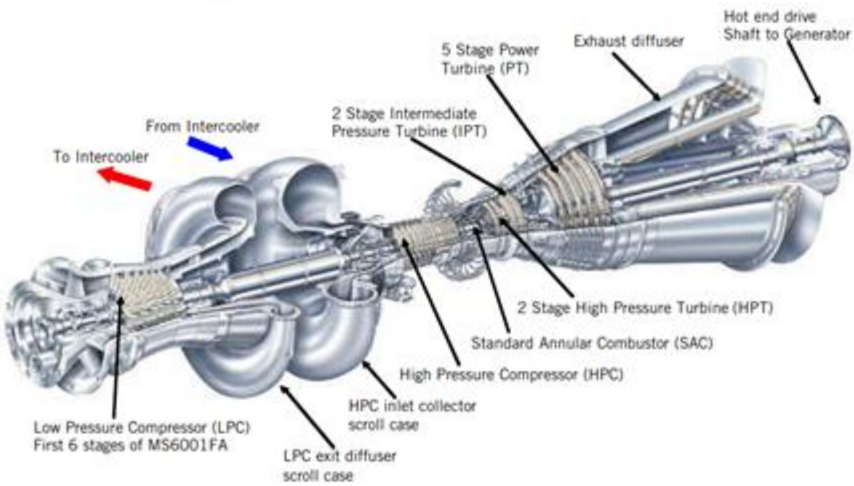

Figure 7-7 LMS100 Gas Turbine [101]

7.6.1 Optimisation Objective Function

The genetic algorithm optimization presented in this research is supposed to come up with a pipeline network which has a minimum capital and operating cost. The optimization objective function, constraint, and variable are explained below. The initial step in the implementation of the genetic algorithm is the creation of an objective function. The function to be optimized is regarded as the objective function. In genetic algorithm optimization to minimize a function a negative sign is attached to the function. In this research, the objective function is lifecycle cost of different gas turbines used on natural gas pipeline compression system. The objective function is expressed in Equation **(7-1)**

$$Objective\ func = GT_{CAPEX} + GT_{FUEL\ COST} + GT_{O\&M} + GC_{CPEX} + Pipe_{CAPEX} \quad \textbf{(7-1)}$$

As mentioned earlier, the variable used is the distance between compressor stations. From the Weymouth flow equation, the discharge pressure of each compressor station along the pipeline is related to the inlet pressure of the next compressor station. The longer the distance between compressor stations, the higher the pressure drop and more power is required to compress the gas and vice-versa. The distance parameter varies between lower and upper bounds with the intention of getting a gas turbine power that matches the gas turbines selected. The relationships between the distance and pipeline discharge pressure are shown in Equation 2.1

7.6.2 Optimization Constraint

The constraint for this optimization is the maximum allowable operating pressure (MAOP) of the pipeline. The MAOP is achieved at the exit of each of the compressor station while, the inlet pressure of each of the compressor stations should lower than the MAOP because of the pressure drop along the pipeline as a result of friction between the gas and inner walls of the pipeline, distance, elevation and surrounding temperature. The pressure ratio for the compressor station varies depending on the compressor station locations and the gas compressor power requirement. The MAOP is expressed in Equation **(7-2)** below.

$$MAOP = Pressure\ ratio * inlet\ pressure \quad \textbf{(7-2)}$$

7.6.3 Effect of Population Size

Population size is one of the important parameters in the application of genetic algorithms. Population size is the population solutions that permit the GA to run in any number of generations. In many cases, the choice of population size defines the quality of the solutions obtained. Usually, smaller population size could lead the algorithms to poor results while larger population size could make the algorithms expend more computation time in finding solutions and consequently provide a better result. Large population size requires a longer time to complete the generation iteration process.

The pictorial representation of the results in Figure 7-8 shows the maximum fitness value in terms of total cost against the number of generations for population sizes of 50 and generation of 25. For every generation there is corresponding mean fitness and best fitness. The capital cost, fuel cost and maintenance cost for the station presented as best fitness and mean fitness value. The fitness values relatively redefined from generation to generations as the simulation continued. The mean fitness value increases as the simulation continued until convergence is achieved since more power and fuel consumption is required to compress the gas to a long distance.

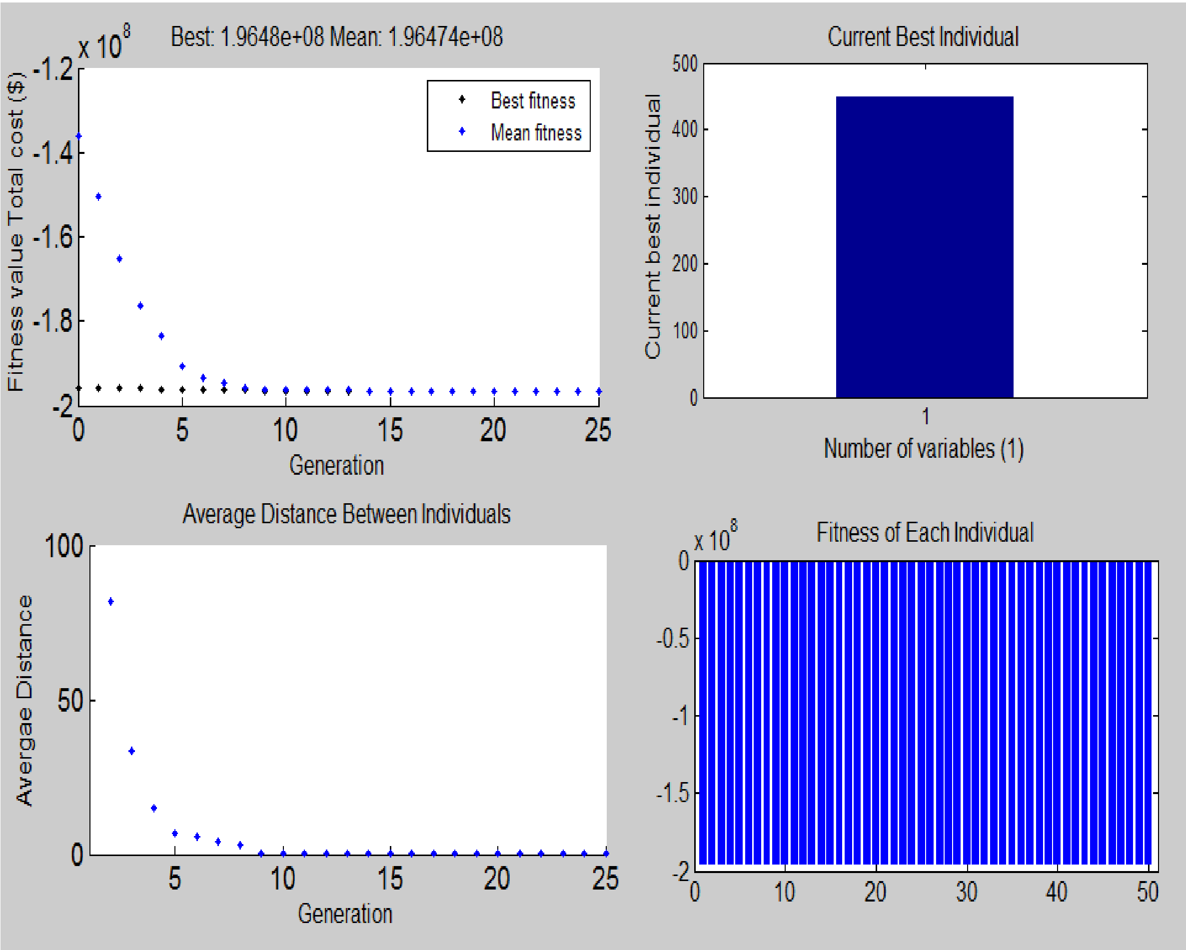

Figure 7-8 Fitness value against Generation for the population size of 50 for station 2 (100MW)

From the top left Fitness against Generation a good convergence was achieved from about Generation 7 and it became consistent up to the upper limit of Generation 25. This result is good since the convergence was achieved within 28% of the available generation of 25 in the design space. GA operator called elitism responsible for copying of the fitness individual into the next generation so as to ensure it is not lost as the generation progresses. The best faintness value which represents the total maximum cost is for station 2 including the capital cost and operating cost for one year is $196,480,000. The negative sign added to the fitness value represent maximization in MATLAB.

The bottom left shows the average distance between individuals as optimization runs continued. Here again, good convergence was achieved at the 9th generation.

The top right is the variable distance which is about 448km that is the maximum the pressure can travel within the pipeline using a 100MW gas turbine. The relationship between the distance and power is shown in Figure 7-9.

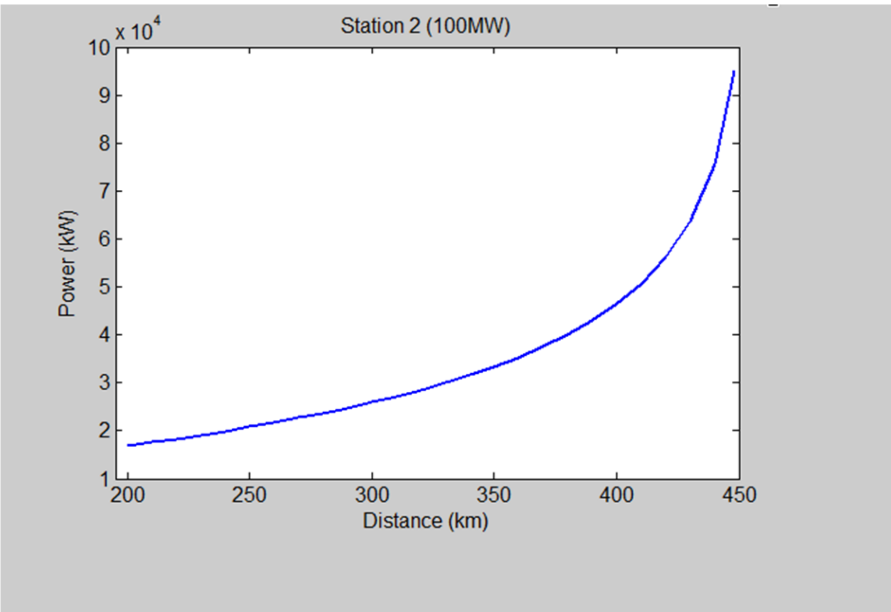

Figure 7-9 Distance and Power relationship for station 2

Applying the GA constraint of 100 bar, the 100MW gas turbine provided the power to compress the gas along the pipeline to its maximum distance of about

448km based on the operating conditions at station 2. At this distance, a compressor station is required to compress the gas to the next level.

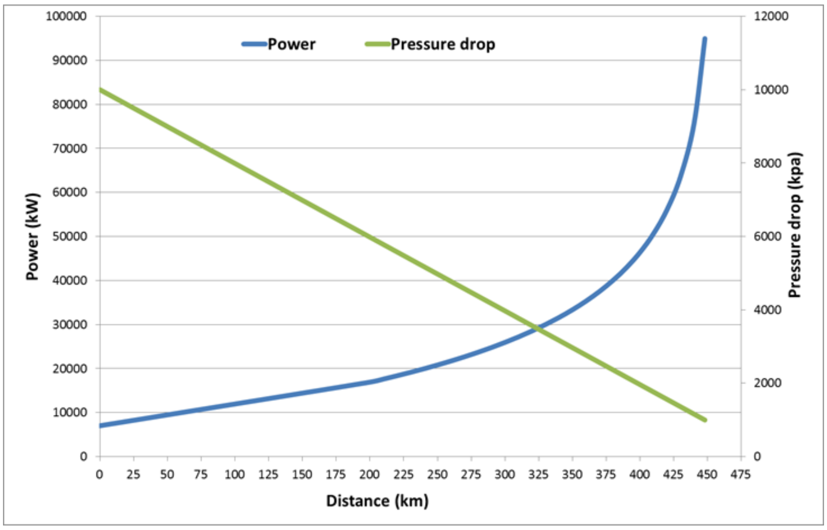

Figure 7-10 Power and Pressure drop against Distance for station 2

Figure 7-10 is compressor station 2 (100MW) capacities that shows the relationship between the drive power and pressure drop along the pipeline. The pressure at the exit of the gas compressor of 10000kpa required a drive power of 94.9MW to compress the gas through a pipeline distance of 448km. the pressure at the exit of this pipeline segment is 996kpa and beyond this distance, the drive power required will be bigger than the selected gas turbine.

The gas velocity depends upon the pressure and, hence, will vary along the pipeline even at constant pipe diameter. The highest velocity will be at the downstream end, where the pressure is the least [14]. The wider the compressor station separation, the steeper the flow resistance and more power requirement are required to compensate the gas pressure to the next compressor station [6].

Figure 7-11 shows the maximum fitness value in terms of total cost against the number of generations for population sizes of 50 and generation of 25 for station 2. In this case, two gas turbine of 43.3MW were used against the 100MW shown in Figure 7-8. The best and mean fitness values represented the capital cost, fuel cost, and maintenance cost. The values redefined from generation to generations as the simulation continued. The mean fitness value increases as the simulation continued until convergence is achieved since more power and fuel consumption is required to compress the gas to a long distance.

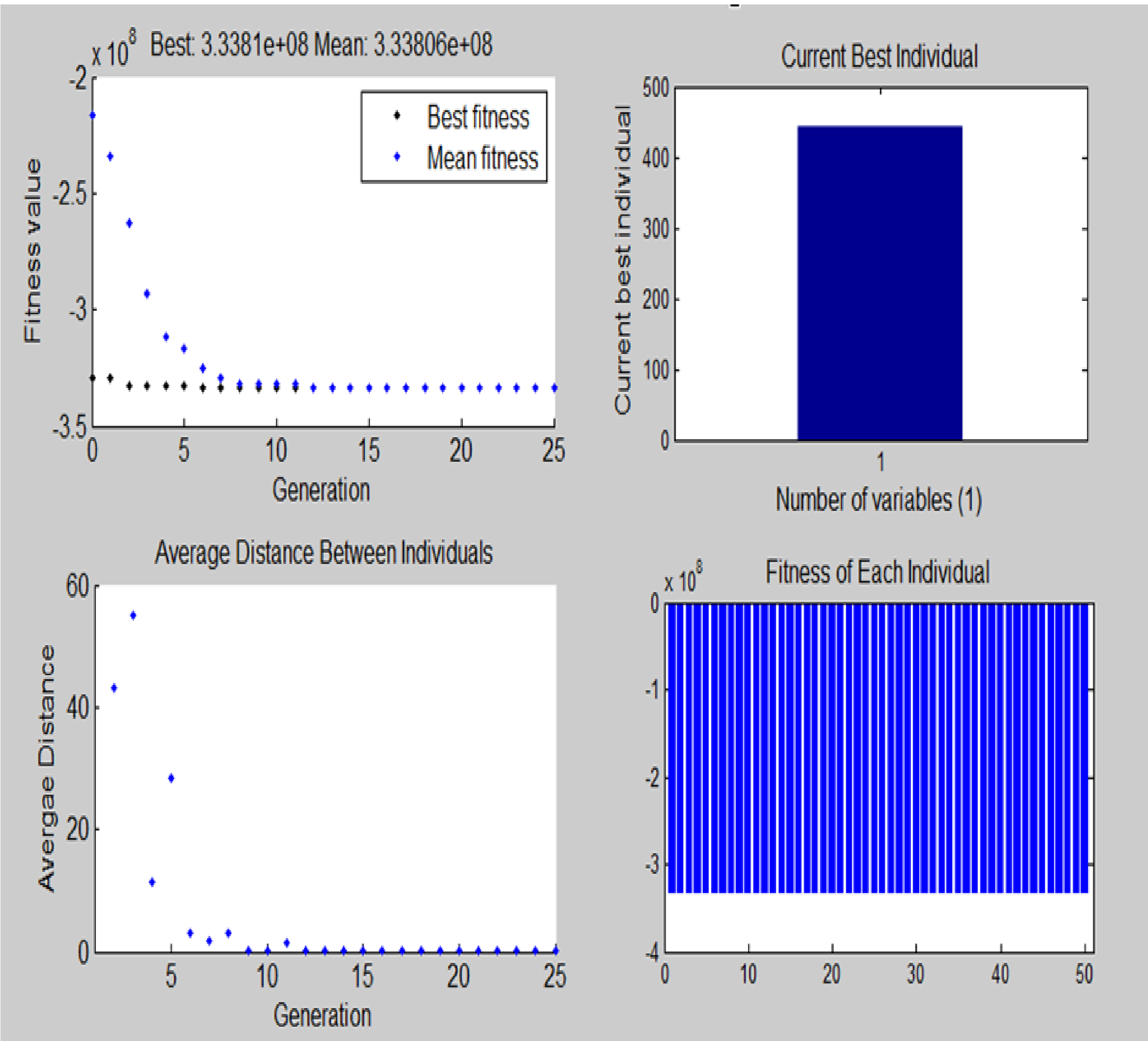

Figure 7-11 Fitness value against Generation for the Population size of 25 (43.3MWX2)

From the Fitness against Generation, a good convergence was achieved from about Generation of 8 and it became consistent until the upper limit of Generation 25. The result is good enough since the convergence was achieved within 32% of the available generation of 25 in the design space. GA operator called elitism was responsible for copying of the fitness individual into the next generation so as to ensure it is not lost as the generation progresses. The best fitness values which represent the total maximum cost for the two gas turbines in station 2 including the capital cost and operating cost for one year is $333,810,000.

For the average distance between individuals and generation, a good convergence was achieved at the 9th generation and it became consistent as simulation continued to the last upper limit of 25.

The top right is the variable distance which is about 443km that is the maximum the pressure can travel within the pipeline using an 81MW gas turbine.

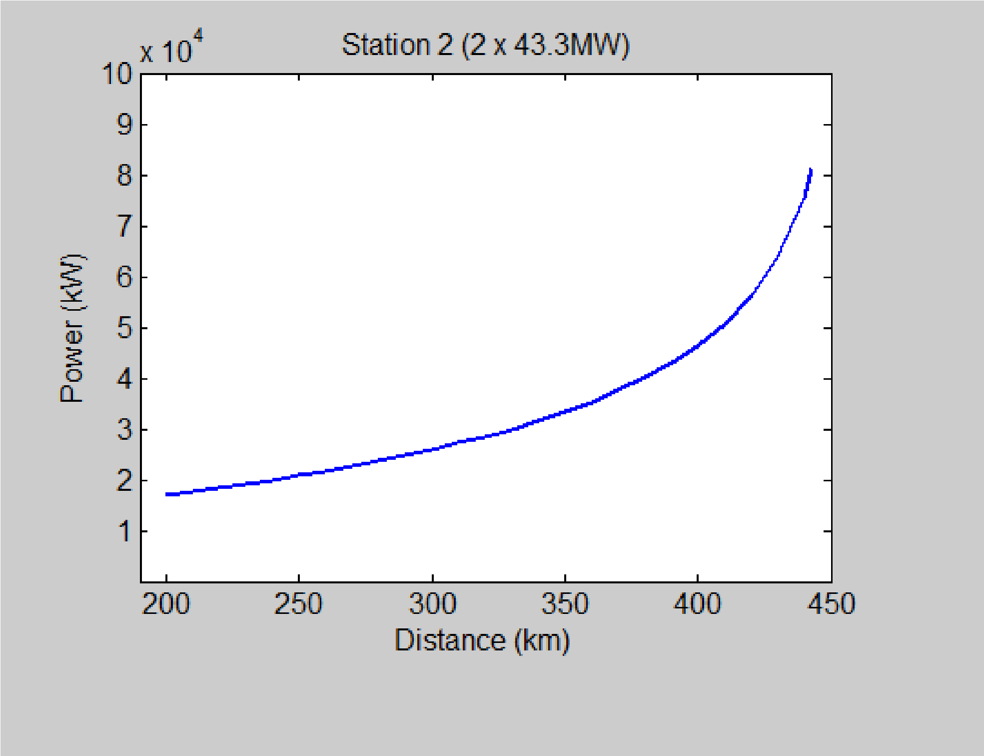

Figure 7-12 Distance and Power relationship

Figure 7-12 shows the relationship between distance and power requirement for station 2 using two 43.3MW gas turbines as obtained from the optimization. As mentioned earlier using GA constraint of 100 bar, the 86.6MW gas turbine provided the power to compress the gas along the pipeline to its maximum distance of about 443km based on the operating conditions at station 2.beyond this distance, a compressor station is required to compress the gas to the next level.

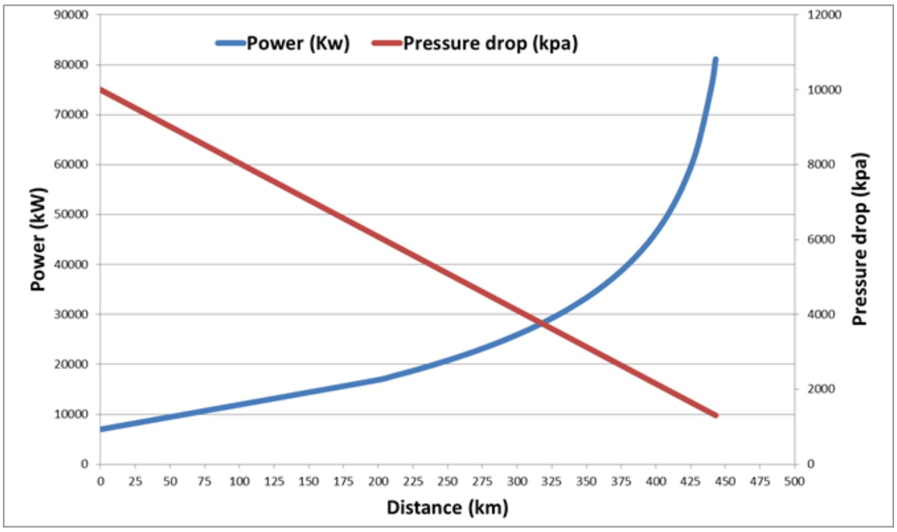

Figure 7-13 Power and Pressure drop against Distance

Figure 7-13 is a compressor station 2 for (2 x 43.3MW) capacities that shows a relationship between the drive power and pressure drop along the pipeline. The pressure at the exit of the gas compressor of 10000kpa required a drive power of 81MW to compress the gas to through a pipeline distance of 443km. the pressure at the exit of this pipeline segment is 1305kpa and beyond this distance, the drive power required will be bigger than the selected gas turbine. The combination of the pressure profile and the compressor station locations for the different power capacities is shown in Figure 7-14. The gas velocity depends upon the pressure and, hence, will vary along the pipeline even at constant pipe diameter. The highest velocity will be at the downstream end, where the pressure is the least [14]. The wider the compressor station separation, the steeper the flow resistance and more power requirement are required to compensate the gas pressure to the next compressor station [6]. See Appendix F for the other optimized compressor station locations.

In this research, I tried the optimization for the whole distance at once but it did not work for me and the others too. The GA simulation continues to fail despite using different scenarios. Hence, the optimization was done based on station by station. Although the optimization has shown an improvement with reference to the baseline, still there is a room for further improvement. The optimized cost based on the station by station is shown in Figure 7-15.

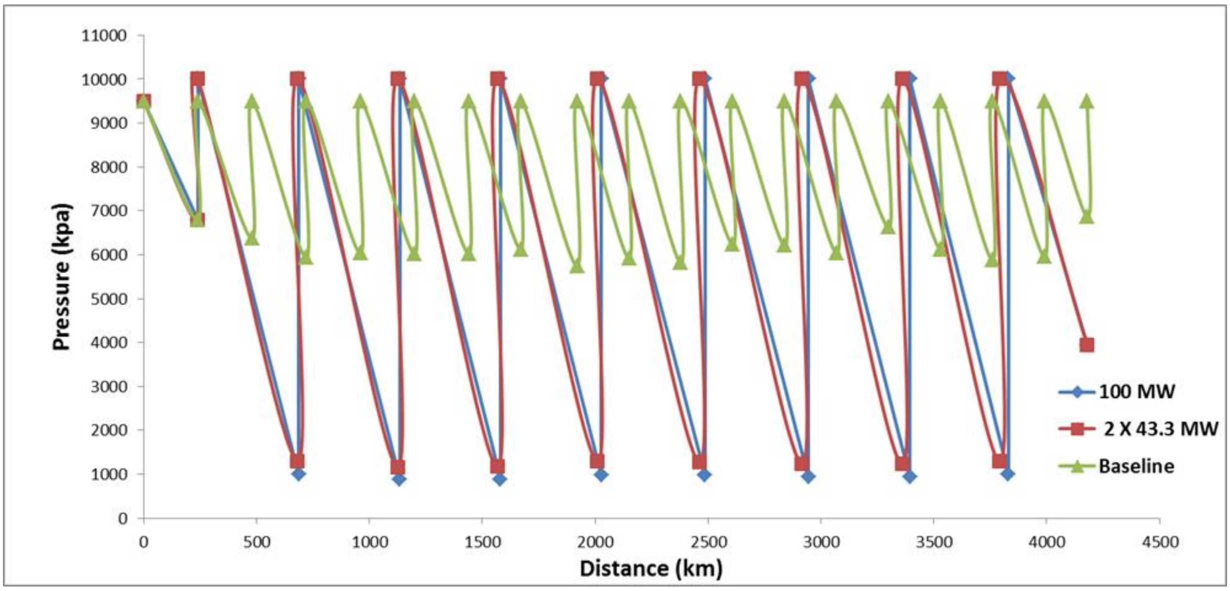

Figure 7-14 Pressure profile and compressor station locations for different power capacities

The base-line and optimized compressor station locations for the 4180 km gas pipeline of the same diameter and gas composition is shown Figure 7-14. The first compressor station is fixed as stated before and has four identical gas compressors arrange in parallel driven by four identical gas turbine of 9.3 MW power output. The discharge pressure from the station is 9500 kpa which is also the MAOP (inlet pressure of the pipeline). At a distance of 240 km, the pipeline pressure drops to 6786 kpa, hence, a second booster station is required at this location since the first gas compressor has achieved its maximum pressure ratio of 1.4.

The optimization considered two different cases as mentioned earlier; case 1 was done based on 43.3 MW gas turbine capacities while case 2 was done based on 100MW gas turbine capacity as explained below.

Case 1- applying the Weymouth equation flow equation, the flow pressure drop increases as the distance between the booster stations increases. At station 2, Two identical gas turbine of 43.3 MW power output arrange in parallel was installed to raise the pressure from 6786 kpa to 10000 kpa. This pressure travels through a pipeline until it reached a distance of 443km where it drops (1305 kpa). At this distance, it is the maximum the power drive can compress the gas. Therefore, another compressor station is needed. This process continued until the last compressor station was achieved.

Case 2- one unit of the 100MW gas turbine was installed. At station 2, the pipeline discharge pressure was raised from 6786 kpa to 10000 kpa. This pressure travels through a pipeline until it reached a distance of 448km where it drops to 996kpa. This is maximum the power derives can compress another compressor was installed. This process continued until last compressor station was achieved.

Figure 7-14 shows that the optimized case 1 (43.3MW) has nine booster stations plus the first booster station making a total of 10 compressor locations along the distance of 4180km. Optimized case 2 (100MW) also has nine stations plus the first station making a total of 10 compressor locations.

The economic assumptions used for the optimized cases are shown Table 13 while Figure 7-15 shows the project cost comparison.

Table 13 Economic assumptions for the optimized cases

Parameter	Value
Plant life (years)	30
Fuel cost ($/kg)	0.16
Discount rate (%)	15
Natural gas price ($/MMbtu)	4.04
Auxiliaries (%)	3.5
Material cost ($)	1150
Coating & wrapping ($/feet)	5
Installation cost ($/ mile)	846594.2312
Pipe thickness (inch)	0.875
Pipe grade	X80

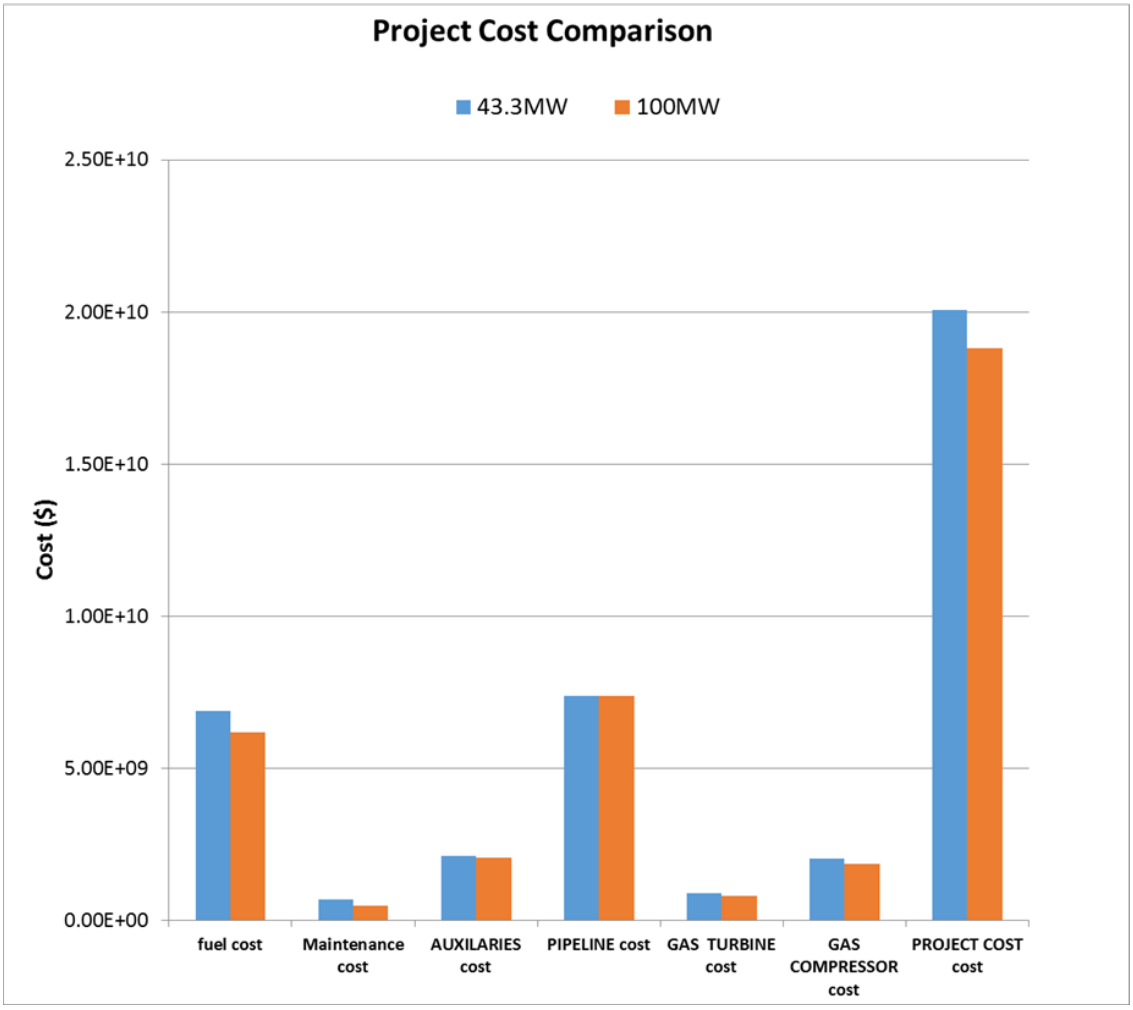

Figure 7-15 Project cost comparison

Figure 7-15 shows the project cost comparison. The project cost is made up of the addition of total fitness value of all the compressor stations plus pipeline and auxiliaries costs. The scenario has two 43.3MW and one 100MW for each compression station operating at the same ambient temperatures. The pipeline cost is the same since operating pressure is also the same. The fuel consumed over the project lifetime of 30 years is more in 43.3MW than the 100MW. This is because 100MW is an efficient engine with the intercooler system. The maintenance cost is also higher for 43.3MW because the maintenance cost decreases as the gas turbine capacity increases. Using the TERA approach, the optimization of gas turbine power at different gas temperature for the lowest lifecycle cost shows that, it is cheaper to used bigger gas turbines than using several smaller ones.

7.6.4 Net Present Value Approach

Net Present Value (NPV) techniques are defined as the actual cash flow from a project over a time. In evaluating NPV, many project economic parameters are considered. These include the capital cost, fuel cost, and maintenance cost. A Project with a positive NPV is regarded as financially viable while projects with negative NPV not viable and difficult to break-even. Among the several techniques used for projects appraisal, NPV techniques are regarded as excellent because they contain less assumptions and are easy to apply. Generally, projects with higher NPV are the viable ones. NPV involves the calculating of net annual cash flows divided by one plus the discount rate rose to a power corresponding to years of project duration [11]. This research adopts the NPV technique for the economic analysis and is expressed below:

$$NPV = \sum_{t=1}^{n} \frac{C_t}{(1+r)^t} - C_O \quad \textbf{(7-3)}$$

Where
C_t = net cash flow
n = project duration
r = discount rate
C_O = capital cost

7.6.4.1 Revenue

The revenue in this research is the natural gas sold. In order words, is the quantity of natural gas transported through the pipeline and sale to consuming market. The price of the gas per MMBtu is $4.51 as obtained from the European energy portal. The revenue is calculated in Excel using the below expression.

$$R = Gp * Dp * 8760 \quad \textbf{(7-4)}$$

Where

Gp = gas price ($/MMbtu)
Dp = Daily production

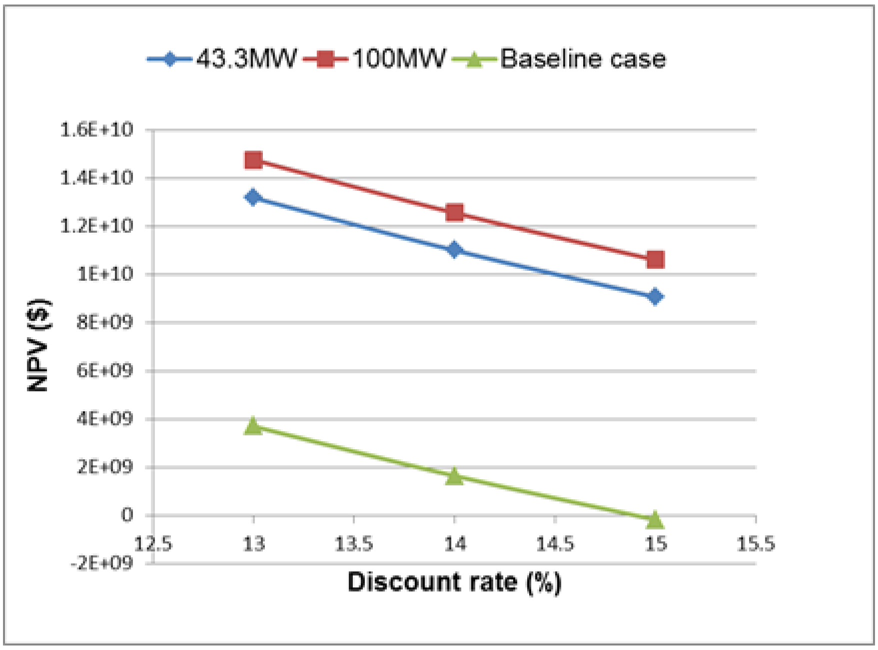

Figure 7-16 NPV against the discount rate

Figure 7-16 shows the influence of discount rate on the NPV for the 43.3MW, 100MW and baseline case. The lower the discount rate the better the NPV. At the 13% discount rate, both engines have the maximum NPV. The investment analyses also show that for the baseline case at the discount rate of 15% a negative NPV is obtained which means that the project will result in a net loss.

7.6.5 Isothermal Flow

Here it is assumed that the gas temperature is constant (isothermal flow) along the length of the pipeline. General flow equation is the basic equation used for relating pressure drop with a mass flow rate in an isothermal flow. The gas temperature of 22.2^{O}C is assumed to be constant. Therefore, the compressor power requirements for all the stations were calculated based on this gas temperature. The gas turbine of 43.3MW was selected to drive the gas compressors. This gas turbine was simulated with Turbomatch to ensure that it provided the power required by the gas compressor and also to get the corresponding fuel consumption.

In other to calculate the gas turbine fuel consumption for the isothermal flow case, the optimized 43.3MW gas turbine was used.

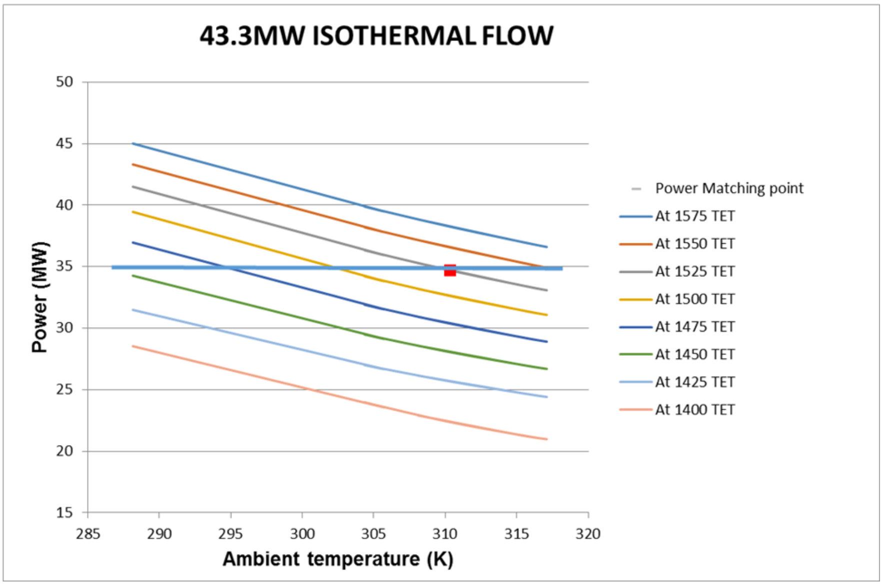

Figure 7-17 Gas turbine power output based on isothermal flow

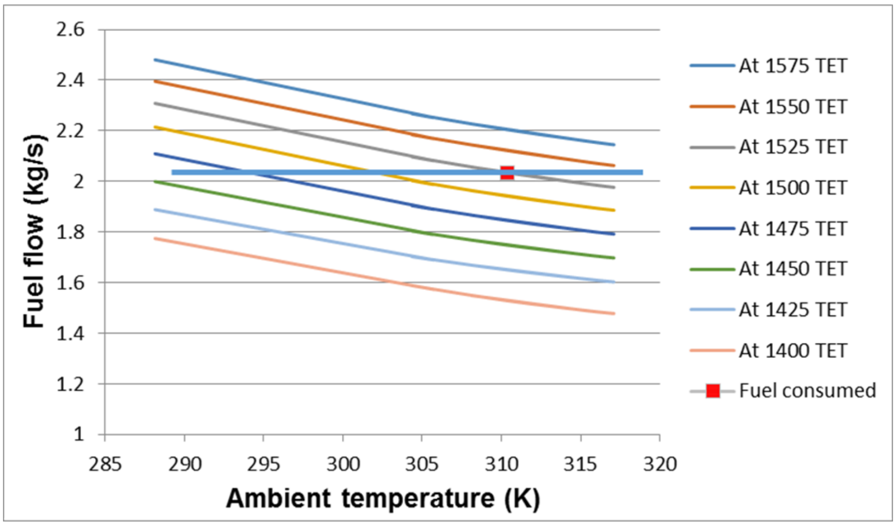

Figure 7-18 Fuel consumed based on isothermal flow

Figure 7-17and Figure 7-18 above is the result obtained from Turbomatch for gas turbine power output and its corresponding fuel consumption for station 2. The cost was calculated using the following equation.

$$Fuel\ cost = C_f * F_f * 8760 * 3600 \qquad \textbf{(7-5)}$$

Where

C_f = cost of fuel ($/Kg)
F_f = Gas turbine fuel flow

Using the procedure of optimized 43.3MW above with a total of ten compressor stations the total fuel cost for the isothermal flow is found to be USD 5.56E+09 for the project duration of 30years against the varying gas temperatures which is USD 6.90E+09.

7.7 Conclusion

For the optimized case, the studies considered two gas turbines of 43.3MW and 100MW capacities. For the first case, optimization study was done for two 43.3MW gas turbine driving two gas compressors while for case 2, one 100MW gas turbine was used to driving one gas compressor. The result shows 10 numbers of compressor stations along the pipeline. The optimized result also shows a reduction in the lifecycle cost from USD 20.1 billion in 43.3MW to USD 18.8 billion in 100MW. Furthermore, the fuel cost is higher for gas turbine driving gas compressors at varying gas temperatures than in isothermal flow. The NPV at 15% discount rate for both engines is seen to be positive.

8 Conclusion

Gas compressors used in oil and gas industry operate within a specified envelope which consists of many operating points. The variation in the operating point is as a result of changes in the process condition. The process condition considered in this thesis is the gas temperature. The research contribution to knowledge is the TERA application on gas compressor stations taking into account the ambient temperature, power matching, and equipment selection while optimizing for the lowest lifecycle cost. Also, the model and methodology developed to provide a useful decision-making guide for Nigerian government on investment of Trans –Saharan gas pipeline. In this research different gas turbine operations were investigated based on different gas temperatures and also for isothermal flow; the operating pressure, pipeline thickness and yield strength are considered. The booster station locations were identified and the gas turbines were simulated based on the location temperature at the different time of the day.

The result shows that for centrifugal compressors power increases with increase in gas temperatures while gas turbine power decreases with increase in ambient temperatures. For every 1% increase in gas temperature, there was 3.5% increase in power required to drive the gas compressor and 1% decrease in gas turbine output power. A very significant increase in ambient is reflected in the life cost of the gas turbine driven a centrifugal compressor in terms of fuel cost which translated to increase in the gas turbine TET to compensate for the variations in power. It was also confirmed that gas compressor with high-pressure ratio and inlet temperature require more polytropic head and power to transport natural gas from one location to another. The compressor pressure ratio has more effect on polytropic head and power than its inlet temperature. The compressor increases by 850Kw for increasing the gas temperature by 0.25^{o}C and pressure ratio by 0.04.

For constant pipe diameter, the result shows that the pipe segment distance has more effect on the gas pressure loss along the pipeline than the pipe elevation. Also, as the distance between compressor station location increases;

the gas compressor and gas turbine power requirements, also increase. This implies the use of bigger gas compressor and gas turbine and fewer stations along the pipeline transmission network. In this research, a baseline case and two other case studies were considered.

In this thesis 18 compressor stations along the total pipeline distance of 4180 km with a 56-inch diameter and diameter of the 0.812-inch diameter of API 5L X70 grades was considered as a baseline during the study. Each of the compressor stations consists of four gas compressor driven by four gas turbines with the maximum allowable operating pressure of 95 bar. From the result obtained the operating cost of the gas turbine is seen to be increasing with increase in gas temperature. The TERA model predicted the project lifecycle cost is USD 27.6 billion. The lifecycle cost consisted to be based on the prevailing assumptions utilized in research 33% fuel cost, 10% maintenance cost, 26% pipeline cost, 6% gas turbine cost, 12% gas compressor cost, and 13% order auxiliary cost. The project cost breakdown shows fuel cost having the larger percentage. The net present value of this case shows that NPV is increasing with the decreased in the discount rate. At the discount rate of 15%, the NPV becomes negative.

Case study 1 considered optimized gas turbine of 43.3MW capacity. The booster station locations were obtained using the pressure drop equation (Weymouth equation). Each of the booster stations has two gas compressors driven by two gas turbines with a maximum allowable operating pressure of 100 bar. Considering a pipeline of the 0.875-inch diameter of API 5L X80 grades with similar distance to baseline. The optimization was done using a genetic algorithm (Matlab). The lifecycle cost was selected as an objective function; the variable is the distance between compressor stations while the constrained is the maximum allowable operating pressure. Comparing with baseline, the optimization result shows a decrease in the number of compressor stations from 18 stations to 10 as a result of an increase in capacity of gas turbine and gas compressor. The optimized result also shows a reduction in the lifecycle cost from USD 27.6 billion to USD 20.1 billion. Unlike the baseline condition, the NPV at 15% discount rate seen to be positive.

Case study 2 considered optimized gas turbine of 100MW capacity. The booster locations were obtained Using similar pressure drop equation and pipeline parameters as that of case 1. Comparing with case 1, the optimization result shows 10 number of compressor stations but with a reduced number of a gas turbine for each station from 2 stations to 1 with the exception of station one as a result of an increase in capacity of gas turbine and gas compressor. The optimized result also shows a reduction in the lifecycle cost from USD 20.1 billion to USD 18.8 billion. The NPV at 15% discount rate is also seen to be positive.

The overarching research shows that using bigger and more efficient gas turbines reduced the number of booster stations and also more economically viable than using smaller gas turbines with many numbers of booster stations. The result also shows that the fuel cost is cheaper in isothermal flow than varying gas temperatures. The optimization result for the lifecycle cost shows a preference for the 100MW gas turbine capacity.

8.1 Recommendation

I. This model was developed based on the operation of clean gas turbines. Comprehensive TERA application on the degraded gas turbines should be looked into. The gas turbine power, the operating TET, the fuel and maintenance costs based on the ambient temperature and gas temperature variation should also be considered.

II. The model can be further improved with the inclusion of different gas composition. Also, more complex pipeline network with several injections and delivery points should be looked into.

III. Detail studies of gas compressors and booster stations equipment failures should be looked into. Also, there is a need also to developed risk model for the pipeline components and incorporating with the economic model.

IV. Comprehensive studies should be carry out on infrastructures changes as a result of a change in compressor station location due to distance variations.

V. The optimization done on this research was based on station by station. There is need for further improvement on the optimization based on entire pipeline distance at once.

REFERENCES

1. Cabalu H. Indicators of security of natural gas supply in Asia. Energy Policy. 2010; 38(1): 218–225. Available at: DOI:10.1016/j.enpol.2009.09.008

2. NNPC, Sonatrach, Penspen,. (NNPC Towers, Central Business District H., Macaulay Way, P.M.B. 190, Garki A. Trans-Saharan Gas 258 Pipeline Project: Final Feasibility Report (unpublished Feasibility Report), London. 2006.

3. Rajnauth J., Ayeni K., Barrufet M. Gas Transportation: present and future. Society of Petroleum Engineers - SPE Gas Technology Symposium. 2008; 2(June): 528–544. Available at: DOI:10.2118/114935-MS

4. Chaudry M., Jenkins N., Strbac G. Multi-time period combined gas and electricity network optimisation. Electric Power Systems Research. 2008; 78(7): 1265–1279. Available at: DOI:10.1016/j.epsr.2007.11.002

5. Ratio P., Inertia L., Compressor C. Single vs . Dual Recycle System Requirements in the Design of High Pressure Ratio , Low Inertia Centrifugal Compressor Stations. 2013; 60: 1–15.

6. Suleiman1 SM., Li YG. Steady State Performance Simulation of Natural Gas Pipeline Driven by Compressor Stations. Proceedings of ASME Turbo Expo. Seoul, South Korea; 2016. pp. 1–11.

7. Lubomirsky, M., Kurz, R., Klimov, P., and Mokhatab S. Configuration Imapacts Vailability, Fuel Consumption and Pipeline Capacity. Pipeline and Gas Journal. 2010; 237(1): 38–44.

8. Ogaji SOT., Pilidis P., Hales R. TERA- A Tool for Aero-engine Modelling and Management. Second Word Conference on Engineering Asset Management. 2009. pp. 11–14. Available at: http://hdl.handle.net/1826/3880

9. Khan RSR., Lagana MC., Ogaji SOT., Pilidis P., Bennett I. Risk Analysis of Gas Turbines for Natural Gas Liquefaction. Journal of Engineering for Gas Turbines and Power. 2011; 133(7): 071704. Available at: DOI:10.1115/1.4002673

10. Nasir A. Techno-Economic Study of Gas Turbine in Pipeline Applications (PhD thesis). Cranfield University; 2013.

11. El-Suleiman, A., P P. Gas Turbine Application to CO2 Pipeline: Techno-Economic and Environmental Risk Analysis (PhD thesis). Cranfield University; 2014.

12. Watanabe T., Inoue H., Horitsugi M., Oya S. Gas to Wire (GTW) System for Developing 'Small Gas Field' and Exploiting 'Associated Gas'. International Oil and Gas Conference and Exhibition in China 2006 - Sustainable Growth for oil and Gas. 2006; 1(2): 310–315.

13. Montoya-O, S., Jovel-T, W., Hernandez-R, J. and Gonzalez-R C. Genetic Algorithms Applied to the Optimum Design of Gas Transmission Networks. SPE International Petroleum Conference and Exhibition in Mexico,. 2000. pp. 1–7.

14. Shashi Menon E. Gas Pipeline Hydraulics. System. United State: CRC Press Taylor and Francis Group; 2005. 1-407 p. Available at: DOI:10.1201/9781420038224

15. Brennen CE. Fundamentals of Multiphase Flow. California.: Cambridge University Press; 2005. 1-410 p. Available at: DOI:10.1017/CBO9780511807169

16. Aziz, K. and Ouyang LB. Simplified Equation Predicts Gas Flow rate, Pressure Drop. Oil and Gas Journal. 1995; 93(19): 70–71.

17. Mokhatab, S., Poe, W. A., Poe, W., Speight, J. G. and Zatzman G.

Handbook of Natural Gas Transmission and Processing, Gulf Professional Publishing. 2nd Editio. Oxford: Gulf Publishing Company; 2006. 425-440 p.

18. Keulegan GH., Beij KH. Pressure losses for Fluid Flow in Curved Pipes. Journal of Research of the National Bureau of Standards. 1937; 18(1): 89. Available at: DOI:10.6028/jres.018.049

19. Folga S. Natural Gas Pipeline Technology Overview. 2007. Available at: http://corridoreis.anl.gov/documents/docs/technical/apt_61034_evs_tm_08_5.pdf

20. Woldeyohannes AD., Majid MAA. Simulation Model for Natural Gas Transmission Pipeline Network System. Simulation Modelling Practice and Theory. 2011; 19(1): 196–212. Available at: DOI:10.1016/j.simpat.2010.06.006

21. Tukur N. A Comparative Study of Liquefied Natural Gas and Pipelines as Means of Transporting Natural Gas in Nigeria. Coventry University, UK.; 2012.

22. U.S. Energy Information Administration. Natural Gas Compressor Stations on the Interstate Pipeline Network: Developments since 1996. Energy Information Administration, Office of Oil and Gas. 2007; (November): 1–12. Available at: http://www.eia.gov/pub/oil_gas/natural_gas/analysis_publications/ngcompressor/ngcompressor.pdf

23. Gallar L., Volpe V., Salussolia M., Pachidis V., Jackson A. Thermodynamic Gas Model Effect on Gas Turbine Performance Simulations. Journal of Propulsion and Power. 2012; 28(4): 719–727. Available at: DOI:10.2514/1.B34359

24. Mokhatab, S., Poe, A, W., Mark, Y J. Handbook of Natural Gas Transmission and Processing. Third Edit. Waltham, USA: Elsevier; 2015. 1-581 p.

25. Pereira S., Gas SP., Rio G. Series or Parallel – Tailor Made Design or a General Rule for a Compressor Station Arrangement ? 2000; : 1–10.

26. Kurz R., Lubomirsky M., Brun K. Gas Compressor Station Economic Optimization. International Journal of Rotating Machinery. 2012; 2012. Available at: DOI:10.1155/2012/715017

27. Ohanian S., Kurz R. Series or Parallel Arrangement in a Two-Unit Compressor Station. Journal of Engineering for Gas Turbines and Power. 2002; 124(4): 936. Available at: DOI:10.1115/1.1478074

28. Kurz, R., Mokhatab S. Consideration on Compressor Station Layout. Pipeline and Gas Journal. 2007; 234(9): 24–26.

29. Lubomirsky, M., Kurz, R., Klimov, P. and Mokhatab S. Configuration Impacts Availability, Fuel Consumption and Pipeline Capacity. Pipeline and Gas Journal. 2010; 237(1): 48–54.

30. Kurz R., Ohanian S., Brun K. Compressors in High Pressure Pipeline Applications. Proceedings of the ASME Turbo Expo. 2010; 5(June 2010): 631–640.

31. Royce, P. E., Brown N. Compressos: Selection and Sizing. Second edi. Houston,TX.: Gulf Publishing Company; 1997. 1-543 p.

32. Bahadori A. Natural Gas Processing Technology and Engineering Design. Waltham, USA: Elsevier; 2014. 1-881 p.

33. Sorokes JM. Selecting a Centrifugal Compressor. Chemical Engineering Progress. 2013; 109(6): 44–51.

34. Kolmetz K. KLM Technology Group COMPRESSOR SELECTION (Engineering Design Guideline) Scope Nomenclature Theory Application References Compressor Calculation Spreadsheet (Excel Format) KLM Technology Table 1 : Compressor Characteristics Table 2 : Performance

Param. 2011;

35. Wang Y., Xue C., Jia X., Peng X. Fault Diagnosis of Reciprocating Compressor Valve With the Method Integrating Acoustic Emission Signal and Simulated Valve Motion. Mechanical Systems and Signal Processing. 2015; 56-57: 197–212. Available at: DOI:10.1016/j.ymssp.2014.11.002

36. Ludtke K. Process Centrifugal Compressor: Basics, Function, Operation, Application. Springe Verlag; 2004.

37. Rasmussen PC., Kurz R. Table of Contents Centrifugal Compressor Applications — Upstream and Midstream by and. : 169–186.

38. Taylor RA and D-RC. Petroleum Engineering Handbook, Volume III: Facilities and Construction Engineering. In: Arnold KE (ed.) Society of Petroleum Engineers; 2006. pp. 261–262 – 263.

39. Al-busaidi WK. Techno-economic Assessment of Radial Turbomachinery in Process Gas Applications. (PhD thesis). Cranfield University; 2014..

40. Akhtar MS. Determining the Real Performance of Centrifugal Compressors Operating in oil & Gas Production Facilities. (2).

41. Boyce MP. Centrifugal compressors: A Basic Guide. 1st editio. Oklahoma: Penn Well; 2003.

42. Chu F., Wang F., Wang X., Zhang S. Performance Modeling of Centrifugal Compressor Using Kernel Partial Least Squares. Applied Thermal Engineering. Elsevier Ltd; 2012; 44: 90–99. Available at: DOI:10.1016/j.applthermaleng.2012.03.043

43. (AP1) API. Centrifugal Compressors for Petroleum, Chemical, and Gas Service Industries. Six Editio. USA: American Petroleum Institute; 1995. 1-98 p.

44. Brun, K. and MGN. Guideline for Field Testing of Gas Turbine and Centrifugal Compressor Performance. Gas Machinery Research Council/Southwest Research Institute. 2006; : 1–93.

45. Odom FM., Muster GL. Tutorial On Modeling of Gas Turbine Driven Centrifugal Compressors. 2009; Available at: DOI:PSIG-09A4

46. Fang X., Chen W., Zhou Z., Xu Y. ScienceDirect Empirical Models for Efficiency and Mass Flow Rate of Centrifugal Compressors `. 2014; 1. Available at: DOI:10.1016/j.ijrefrig.2014.03.005

47. White RC., Kurz R. Surge Avoidance for Compressor Systems. 35th Turbomachinery Symposium. 1988; : 123–134.

48. Kurz R., Fowler EJ., Cave MJ., Marechale RK., Ji M. Operation of Centrifugal Compressors in Choke Conditions. Turbomachinary. 2016.

49. Kurz, R., Ohanian, S. and Lubomirsky M. On Compressor Station Layout. Atlanta, Georgia, USA, ASME. 2003;

50. Hardy-Bishop. The Specification of Mechanical & Electrical Rotating Machines: Synchronous and Asynchronous Machines (unpublished Short Course). Cranfield, UK.; 2012.

51. Walsh, P. P. and Fletcher P. Gas turbine performance. 2nd ed. Oxford: Blackwell Science; 2004.

52. Smalley, A. J., Mauney, D. A., Ash, D. I., Clowney, S. L. and Pappas G., P. Evaluation and Application of Data Sources for Assessing Operating Costs for Mechanical Drive Gas Turbines in Pipeline Service. Journal of Engineering for Gas Turbines and Power. 2000; 122(3): 462–465.

53. Kurz R. The Physics of Centrifugal Compressor Performance. Pipeline

Simulation Interest Group. California.: Palm Springs, California.; 2004.

54. Horowitz FB. Compressor Control and Optimization. 2006; (1970): 1763–1793.

55. Pilidis, P., Palmer JR. Gas Turbine Theory and Performance. Cranfield: Cranfield University; 2013. 1-200 p.

56. Al-attab K A., Zainal Z A. Externally Fired Gas Turbine Technology: A Review. Applied Energy. 2015; 138: 474–487. Available at: DOI:10.1016/j.apenergy.2014.10.049

57. Diakunchak, I., Kiesow, H. J. and McQuiggan G. The History of the Siemens Gas Turbine. Proceedings of the ASME Turbo Expo. 2008; 4: 475–935.

58. Aschenbruck, E., Cagna, M., Langusch, V., Orth, U., Spiegel A., Wiedermann, A. and Wiers S. Man's New Gas Turbines for Mechanical Drive and Power Generation Applications. 2013; 5 B.

59. Ulizar, I. and Pilidis P. A Semiclosed-Cycle Gas Turbine with Carbon Dioxide-Argon as Working Fluid. Journal of Engineering for Gas Turbines and Power. 1997; 119(3): 612–616.

60. Saravanamuttoo, H. I. H., Rogers, G. F. C., Cohen H and S., P.V. Gas Turbine Theory. 6th ed. Harlow: Pearson Education Limited; 2009.

61. Eisaku, I., Ikuo, O., Kelm, T., Akimasa, M. and Junichiro M. Development of Key Technologies for the Next Generation Gas Turbine. Proceedings of the ASME Turbo Expo. 2010; 1: 847.

62. Razak AMY. Industrial Gas Turbines Performance and Operability. Cambridge, UK.; 2007. 1-601 p.

63. Soares C. Gas turbines. Butterworth-Heinemann, Amsterdan; Boston; 2008. 749 p.

64. Singh and Di Lorenzo G. GT Technology and Application: An Introductory Overview (unpublished MSc Lecture Notes). Cranfield, UK.; 2012.

65. Giampaolo T. The Gas Turbine Handbook: Principles and Practice. 3rd ed. Control. Lilburn, USA.: The Fairmont Press; 2003. 451 p. Available at: DOI:10.1017/CBO9781107415324.004

66. Lebedev, A. S. and Kostennikov S V. Trends in Increasing Gas-Turbine Units Efficiency. Thermal Engineering. 2008; 55(6): 461–468.

67. Kakaras E., Doukelis a., Prelipceanu a., Karellas S. Inlet Air Cooling Methods for Gas Turbine Based Power Plants. Journal of Engineering for Gas Turbines and Power. 2006; 128(2): 312. Available at: DOI:10.1115/1.2131888

68. Connors H. U.S. Patent No. 3,521,431.21 Jul.1970: Particle Separator for Engines Air Inlets. 1970.

69. Clara S. Effect of Engine Degradation on Fuel Burn Optimum Civil Aircraft Trajectories. Cranfield University; 2012.

70. Abdul Ghafir M. Performance Based Creep Life Estimation for Gas Turbines Application (PhD Thesis). Cranfield University; 2011.

71. Naeem M., Singh R., Probert D. Impacts of Aero-engine Deteriorations on Military Aircraft Mission's Effectiveness. Aeronautical Journal. 2001; 105(1054): 685–695.

72. Baioni CA. TERA for LNG - Risk Methodology for Gas Turbine Selection in LNG application. Cranfield University; 2009.

73. Pascovici, D., Colmenares, F., Ogaji, S. and Pilidis P. An Economic and Risk Analysis Model for Aircrafts and Engines. ASME Turbo Expo. 2007; 3: 103–116.

74. Gad-Briggs, A., Haslam, A., Laskaridis P. Effect of Change in Role of an Aircraft on Engine Life. The Aeronautical Journal. 117(1196): 1053–1070.

75. Nikolaidis, T., Pachidis V. Gas Turbine Performance Simulation. Ed. 1.21. Proppulsion Engineering Center, Cranfield University; 2016. 163 p.

76. Carroll L., Hudkins RW. Advanced Pipeline Design.

77. Cornot-gandolphe S., Agency IE., Chabrelie M., Rojey A., Français I. the Challenges of Further Cost Reductions for New Supply Options (Pipeline , Lng , Gtl). 2003; (June): 1–17.

78. GAMANNOSSI A and UI. Gas Turbine Engine Selection: Performance and Economic Investigation. Cranfield University; 2016.

79. Gamannossi N. Gas Turbine Engine Selection; Performance and Economic Investigation. 2016.

80. Isaiah T. A Techno-Economic and Environmental Evaluation of Gas Turbines Operating in a Load-following Mode. (PhD Thesis). Cranfield University; 2015.

81. Kurz, R. and Ohanian S. Modeling Turbomachinery in Pipeline Simulations. Proceedings PSIG. 3.

82. Lapina RP. Estimating Centrifugal Comperssor Performance, Process Compressor Technology. Volume 1, . Gulf Publishing Company, Houston, Texas.; 1982.

83. Savidge JL., Ishm T., Reid L., Recipient A., et al. Compressibility of Natural Gas Class 1040 Jeffrey L. Savidge, Ph.D. “. 2000; (1): 8–27.

84. Dharmesh M. Selection of Gas Turbine For Centrifugal Compressor Drive For Oil & Gas Industry (Based on Engine Performance). 2014; (February): 2013–2014.

85. Goodger, E. M. and Ogaji SOT. Fuel and Combustion in Heat Engines. First Edit. Cranfield: Cranfield University Press; 2011.

86. Rasmussen, P. C., & Kurz R. Centrifugal Compressor Applications-Upstream and Midstream. In Proceedings of the Thirty-Eight Turbomachinery Symposium, Houston, Texas,. 2009. pp. 169–186.

87. Berdanier, R. A., Smith, N. R., Fabian, J., & Key NL. Humidity Effects on Experimental Compressor Performance-Corrected Conditions for Real Gases. Journal of Turbomachinery. 2015; (3): 137.

88. K. Jordan, P. Walter, A. Emde and CC. The Respective Merits of Gas Turbine Vs Electric Drive for Pipeline Turbo-compressor. in Proc. International Pipeline Conf. Alberta, Canada; 2004. pp. 4–8.

89. Muhammed, A., Olivia, S., Arshad H. Development of User-Defined Extension for the Simulation of Membrane Process in ASPEN HYSYS. Sigma Engineering and Natural Science. 2017; 35(1): 35–45.

90. Arne G. Overpressure Protection of Oil and Gas Production Facilities. Billington Process Technology at AspenTech Optimize Conference. Washington, D.C.; 2011.

91. Hamid AK. HYSYS: An introduction to Chemical Engineering Simulation. Simulation. 2007; : 4–5. Available at: http://eprints.utm.my/3030/

92. Salamat R. Gas Path Diagnostics for Compressors. Cranfield University; 2012.

93. Haupt, R. L. and Haupt SE. Practical Genetic Algorithms. Second Edi. New Jersey, USA: John Wiley and Sons, Inc,; 2004. 1-251 p.

94. Stephanie F. Genetic Algorithms: Principles of Natural Selection Applied to Computation. Journal of Science. 1993; 261(5123): 872–878.

95. Khouja M., Michalewicz Z., Wilmot M. The Use of Genetic Algorithms to Solve the Economic lot Size Scheduling Problem. European Journal of Operational Research. 1998; 110(3): 509–524. Available at: DOI:10.1016/S0377-2217(97)00270-1

96. Zitzler E., Thiele L. Multiobjective Evolutionary Algorithms: a Comparative Case Study and the Strength Pareto Approach. IEEE Transactions on Evolutionary Computation. 1999; 3(4): 257–271. Available at: DOI:10.1109/4235.797969

97. Deb K., Pratap A., Agarwal S., Meyarivan T. A fast and elitist multiobjective genetic algorithm: NSGA-II. IEEE Transactions on Evolutionary Computation. 2002; 6(2): 182–197. Available at: DOI:10.1109/4235.996017

98. Renner G., Ekárt A. Genetic Algorithms in Computer Aided Design. Computer-Aided Design. 2003; 35(8): 709–726. Available at: DOI:10.1016/S0010-4485(03)00003-4

99. Beasley D., Bull DR., Martin RR. An Overview of Genetic Algorithms : Part 1, fundamentals. University Computing. 1993; 2(15): 1–16. Available at: DOI:10.1017/CBO9781107415324.004

100. Moon I., Silver EA., Choi S. Hybrid Genetic Algorithm for the Economic lot-scheduling Problem. International Journal of Production Research. 2002; 40(4): 809–824. Available at: DOI:10.1080/00207540110095222

101. Reale MJ. New high Efficiency Simple Cycle Gas Turbine - GE's

LMS100TM. USA: General Electric Company. 2004; : 20. Available at: www.ge.com

APPENDICES

Appendix A Ambient Temperatures for Station locations

Appendix A shows the ambient temperature for each of the compressor stations along the TSGP. The ambient temperatures were segmented based on 3 hourly differences in a day and three seasons in a year namely, winter, dry, and hot. The ambient temperatures are used to calculate the power requirement of the gas compressors and also for GT performance simulations.

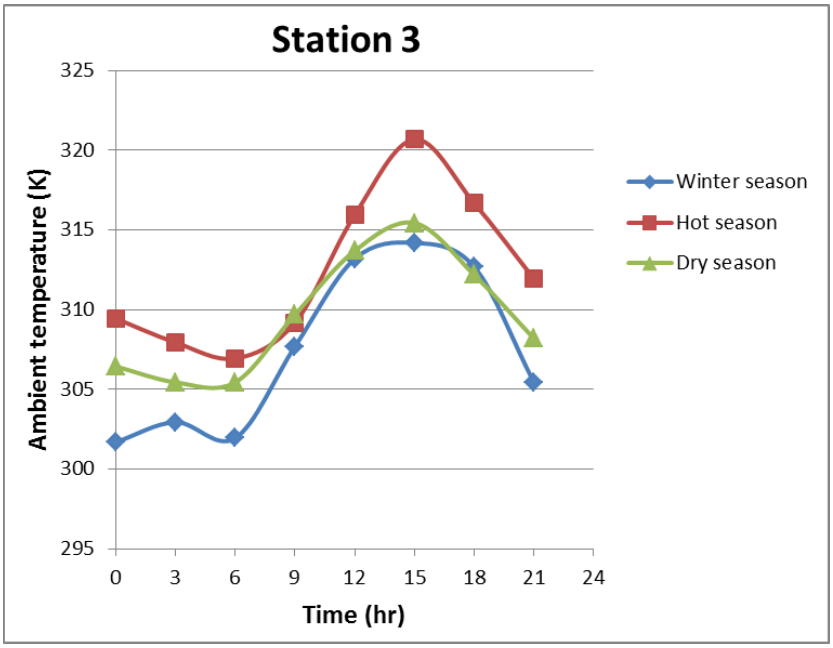

Figure A 1 Ambient temperature for booster station 3

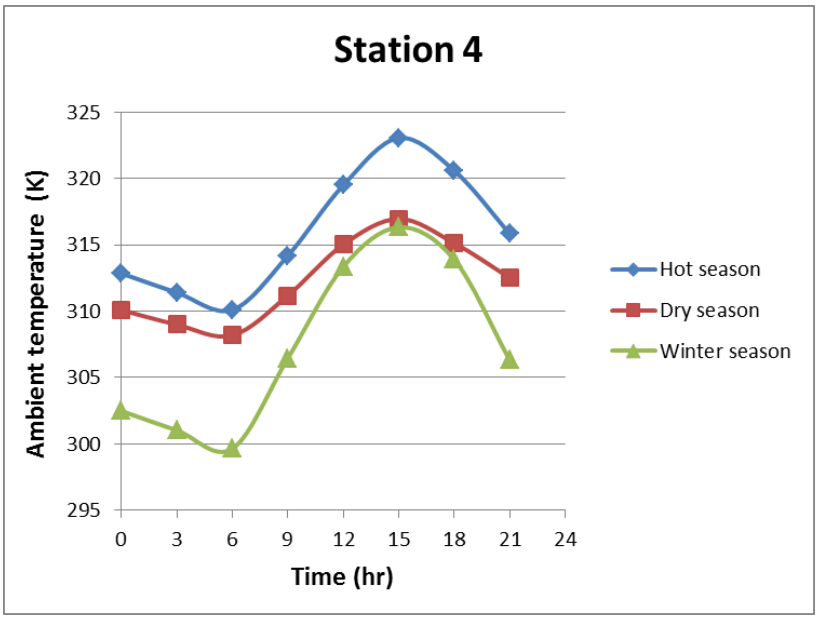

Figure A 2 Ambient temperature for booster station 4

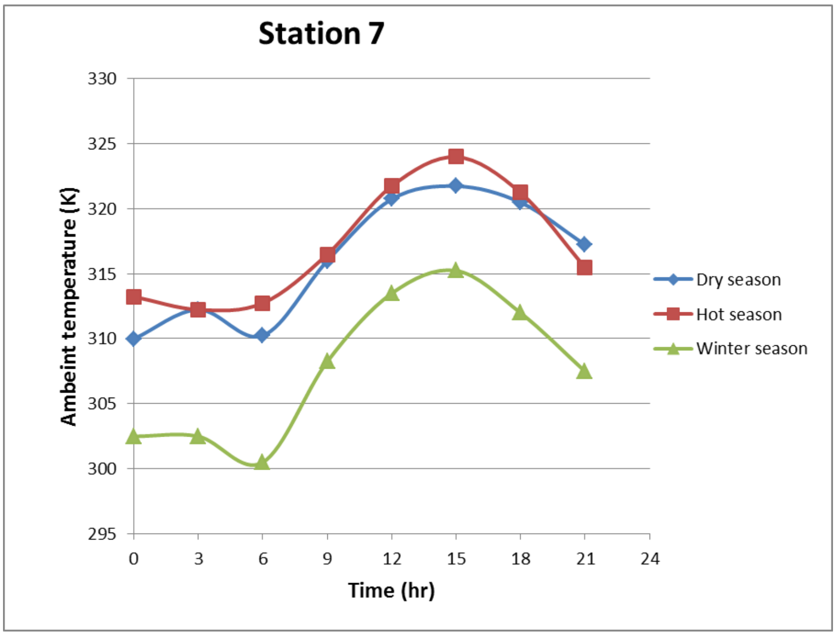

Figure A 3 Ambient temperature for booster station 7

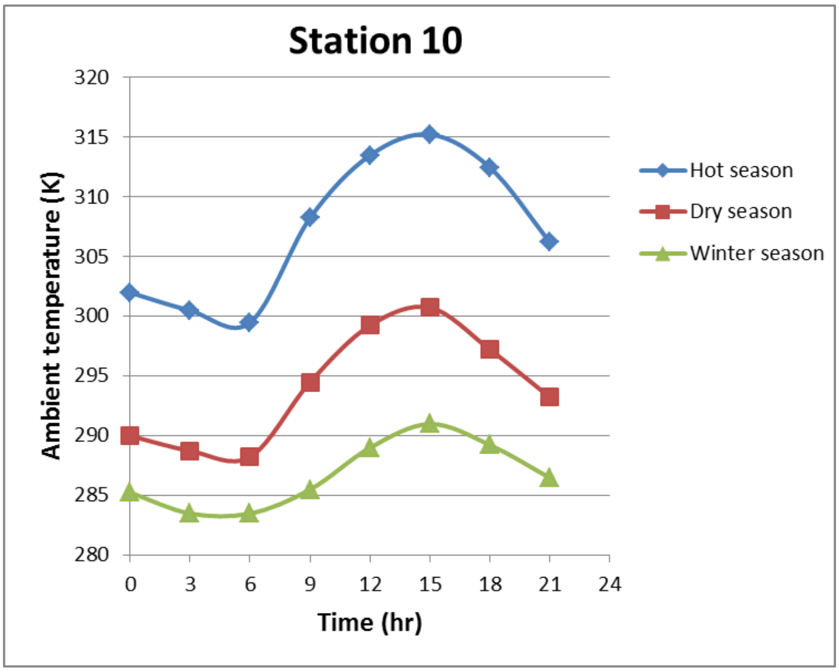

Figure A 4 Ambient Temperature for booster station 10

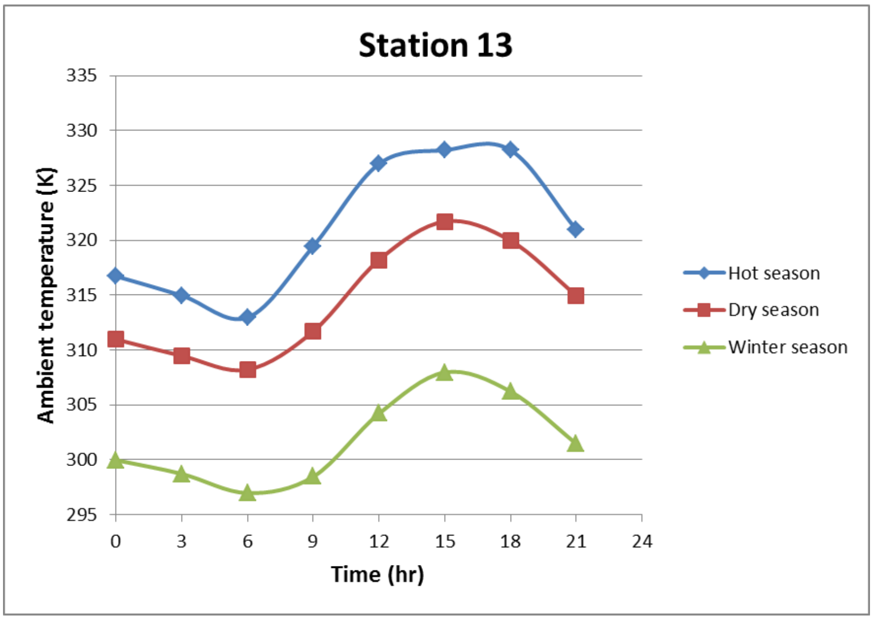

Figure A 5 Ambient temperature for booster station 13

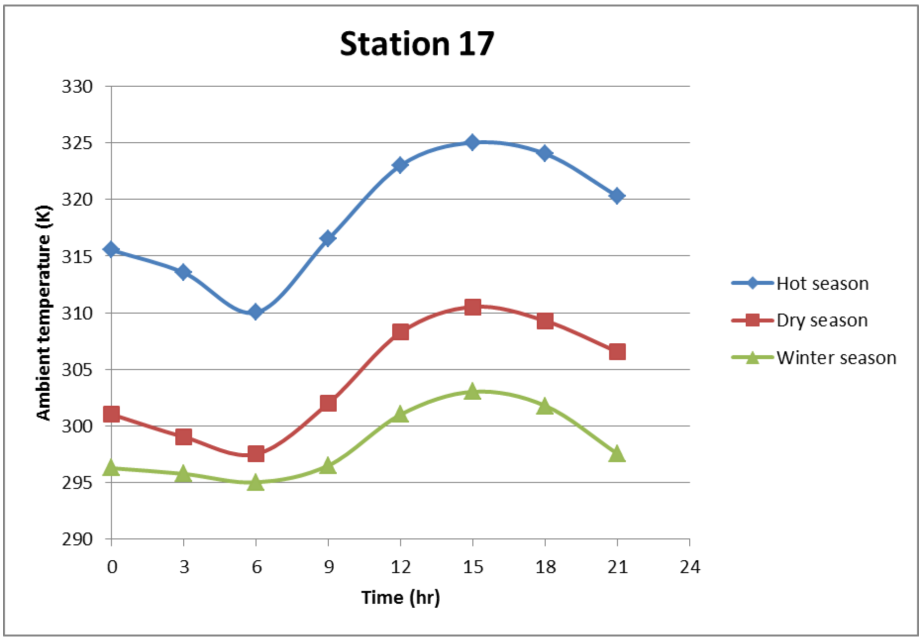

Figure A 6 Ambient temperature for booster station 17

Appendix B Turbomatch design point input files

Appendix B shows Turbomatch design point input files used for the performance of the gas turbine. The input file consists of bricks, bricks data, station vectors and engine vector results.

Table 1 Turbomatch input file for LM1600 gas turbine

```
Industrial Gas Turbine Performance simulation of LM1600
Inspired by GE LM1600
Author: Nasiru Tukur
_______________________________________________________
////
DP SI GM VA FP
-1
-1
INTAKE S1,2       D1-6        R200
COMPRE S2,3       D7-18       R205   V7   V8
COMPRE S3,4       D19-30      R205   V19  V20
PREMAS S4,25,5    D31-34
PREMAS S5,26,6    D35-38
BURNER S6,7       D39-46      R215
MIXEES S7,26,8
TURBIN S8,9       D47-61             V48
MIXEES S9,25,10
TURBIN S10,11     D62-76             V63
TURBIN S11,12     D77-91             V77 V78
NOZCON S12,13,1   D92,93      R220
PERFOR S1,0,0     D77,94-96,220,200,215,0,0,0,0,0,0
CODEND

DATA ITEMS ////
1 0.0        ! INTAKE: Altitude [m]
2 0.0        ! Deviation from ISA temperature [K]
3 0.0        ! Mach number
4 0.9954     ! Pressure recovery, according to USAF
5 0.0        ! Deviation from ISA pressure [atm]
6 60.0       ! Relative humidity [%]

7 -1.0       ! COMPRESSOR - FAN: Z = (R-R[choke])/(R[surge]-R[choke]) (if =-1.
the default value 0.85 is invoked)
8 -1.0       ! Relative rotational speed PCN
9 2.538      ! DP Pressure ratio
10 0.87      ! isentropic efficiency
11 0.0       ! Error selection
12 5.0       ! Compressor Map Number
13 1.0       ! Shaft number
14 1.0       ! Scaling factor of Pressure Ratio – Degradation factor
15 1.0       ! Scaling factor of Non-D Mass Flow – Degradation factor
16 1.0       ! Scaling factor of ETAc is (Compressor isentropic efficiency) –
Degradation factor
17 1.5       ! Effective component volume [m^3]
18 0.0       ! Stator angle (VSV) relative to DP

19 -1.0      ! COMPRESSOR HP: Z = (R-R[choke])/(R[surge]-R[choke]) (if =-1.
the default value 0.85 is invoked)
20 -1.0      ! Relative rotational speed PCN
21 8.786     ! DP Pressure ratio
```

```
22 0.87          ! isentropic efficiency
23 1.0           ! Error selection
24 5.0           ! Compressor Map Number
25 2.0           ! Shaft number
26 1.0           ! Scaling factor of Pressure Ratio – Degradation factor
27 1.0           ! Scaling factor of Non-D Mass Flow – Degradation factor
28 1.0           ! Scaling factor of ETAc is (Compressor isentropic efficiency) –
Degradation factor
29 -1.0          ! Effective component volume [m^3]
30 0.0           ! Stator angle (VSV) relative to DP

31 0.085          ! BYPASS:  (Wout/Win) BPR = 6.4 CRUISE!
32 0.0           ! DELTA W
33 1.0           ! LAMBDA P
34 0.0           ! DELTA P

35 0.0725      ! PREMAS: LAMDA W Cooling bypass (Wout/Win)
36 0.0           ! DELTA W
37 1.0           ! LAMBDA P
38 0.0           ! DELTA P

39 0.05          ! COMBUSTOR: Pressure loss (=Total pressure loss/Inlet total
pressure)
40 0.999         ! Combustion efficiency
41 -1.0          ! Fuel flow (If -1. is given the TET must be determined in the station
vector
42 0.0           ! (>0) Water flow [kg s-1 or lb s-1] or (<0) Water to air ratio
43 288.0         ! Temperature of water stream [K]
44 0.0           ! Phase of water (0=liquid, 1=vapour)
45 1.0           ! Scaling factor of ETAb (combustion efficiency) – Degradation factor
46 -1.0          ! Effective component volume [m^3]

47 0.0           ! COMPRESSOR TURBINE: Auxiliary or power output [W]
48 -1            ! Relative non-dimensional massflow W/Wmax (if = -1, value 0.8 is
invoked)
49 -1            ! Relative non-rimensional speed CN (if = -1, value 0.6 is invoked)
50 0.88          ! Design isentropic efficiency
51 -1.0          ! Relative non-dimensional speed PCN (= -1 for compressor turbine)
52 2.0           ! Shaft Number (for power turbine, the value "0." is used)
53 3.0           ! Turbine map umber
54 -1.0          ! Power law index "n" (POWER = PCN^n) If = -1, power is assumed
to be a constant
55 1.0           ! Scaling factor of TF (non-D inlet mass flow) – Degradation factor
56 1.0           ! Scaling factor of DH (enthalpy change) – Degradation factor
57 1.0           ! Scaling factor of ETAc is (Turbine isentropic efficiency) –
Degradation factor
58 200           ! Rotor rotational speed [RPS]
59 15.0          ! Rotor moment of inertia [kg.m^2]
60 -1.0          ! Effective component volume [m^3]
61 0.0           ! NGV angle, relative to D.P.
```

```
62 0.0          ! COMPRESSOR TURBINE: Auxiliary or power output [W]
63 0.8          ! Relative non-dimensional massflow W/Wmax (if = -1, value 0.8 is
invoked)
64 0.6          ! Relative non-rimensional speed CN (if = -1, value 0.6 is invoked)
65 0.89         ! Design isentropic efficiency
66 -1.0         ! Relative non-dimensional speed PCN (= -1 for compressor turbine)
67 1.0          ! Shaft Number (for power turbine, the value "0." is used)
68 3.0          ! Turbine map umber
69 -1.0         ! Power law index "n" (POWER = PCN^n) If = -1, power is assumed
to be a constant
70 1.0          ! Scaling factor of TF (non-D inlet mass flow) – Degradation factor
71 1.0          ! Scaling factor of DH (enthalpy change) – Degradation factor
72 1.0          ! Scaling factor of ETAc is (Turbine isentropic efficiency) –
Degradation factor
73 200          ! Rotor rotational speed [RPS]
74 15.0         ! Rotor moment of inertia [kg.m^2]
75 -1.0         ! Effective component volume [m^3]
76 0.0          ! NGV angle, relative to D.P.


77 15200000     ! POWER TURBINE: Auxiliary or power output [W]
78 -1           ! Relative non-dimensional massflow W/Wmax (if = -1, value 0.8 is
invoked)
79 -1           ! Relative non-rimensional speed CN (if = -1, value 0.6 is invoked)
80 0.8895       ! Design isentropic efficiency
81 1.0          ! Relative non-dimensional speed PCN (= -1 for compressor turbine)
82 0.0          ! Shaft Number (for power turbine, the value "0." is used)
83 3.0          ! Turbine map umber
84 -1.0         ! Power law index "n" (POWER = PCN^n) If = -1, power is assumed
to be a constant
85 1.0          ! Scaling factor of TF (non-D inlet mass flow) – Degradation factor
86 1.0          ! Scaling factor of DH (enthalpy change) – Degradation factor
87 1.0          ! Scaling factor of ETAc is (Turbine isentropic efficiency) –
Degradation factor
88 200          ! Rotor rotational speed [RPS]
89 20.0         ! Rotor moment of inertia [kg.m^2]
90 -1.0         ! Effective component volume [m^3]
91 0.0          ! NGV angle, relative to D.P.

92 -1.0         ! CONVERGENT NOZZLE: = "-1" exit area is fixed
93 1.0          ! Scaling factor

94 1.0          ! ENGINE RESULTS: Propeller efficiency (= -1 for turbojet/turbofan)
95 0.0          ! Scaling index ("1" = scalling needed, "0" = no scaling)
96 0.0          ! Required DP net thrust(Turbojet,turbofan) or shaft power
(Turboprop,turboshaft)
                ! = 0 if Scaling index = 0
-1
1 2 46.0        ! item 2 at station 1 = Mass flow(kg/s)
```

```
7 6 1550.0    ! item 6 at station 7 = Total temperature (K)
-1            ! End of DP data
-3
```

Table 2 Turbomatch input file for LM6000 gas turbine

```
Industrial Gas Turbine Performance simulation of LM6000
Inspired by GE LM6000
Author: Nasiru Tukur
_____________________________________________________________
////
DP SI GM VA FP
-1
-1
INTAKE  S1,2      D1-6          R200
COMPRE  S2,3      D7-18         R205     V7
COMPRE  S3,4      D19-30        R205     V19   V20
PREMAS  S4,25,5   D31-34
PREMAS  S5,26,6   D35-38
BURNER  S6,7      D39-46        R215
MIXEES  S7,26,8
TURBIN  S8,9      D47-61                 V48
MIXEES  S9,25,10
TURBIN  S10,11    D62-76                 V62   V63
NOZCON  S11,12,1  D77,78        R220
PERFOR  S1,0,0    D62,79-81,220,200,215,0,0,0,0,0,0
CODEND

DATA ITEMS ////
1 0.0          ! INTAKE:  Altitude [m]
2 0.0          ! Deviation from ISA temperature [K]
3 0.0          ! Mach number
4 0.9954       ! Pressure recovery, according to USAF
5 0.0          ! Deviation from ISA pressure [atm]
6 60.0         ! Relative humidity [%]

7 -1.0         ! COMPRESSOR - FAN: Z = (R-R[choke])/(R[surge]-R[choke]) (if =-1. the
default value 0.85 is invoked)
8 1.0          ! Relative rotational speed PCN
9 2.3225       ! DP Pressure ratio
10 0.85        ! isentropic efficiency
11 0.0         ! Error selection
12 3.0         ! Compressor Map Number
13 1.0         ! Shaft number
14 1.0         ! Scaling factor of Pressure Ratio – Degradation factor
15 1.0         ! Scaling factor of Non-D Mass Flow – Degradation factor
16 1.0         ! Scaling factor of ETAc is (Compressor isentropic efficiency) – Degradation
factor
17 0.02        ! Effective component volume [m^3]
18 -1.0        ! Stator angle (VSV) relative to DP

19 -1.0        ! COMPRESSOR HP: Z = (R-R[choke])/(R[surge]-R[choke]) (if =-1. the
default value 0.85 is invoked)
20 1.0         ! Relative rotational speed PCN
21 12.5286     ! DP Pressure ratio
22 0.85        ! isentropic efficiency
23 1.0         ! Error selection
24 4.0         ! Compressor Map Number
25 2.0         ! Shaft number
26 1.0         ! Scaling factor of Pressure Ratio – Degradation factor
27 1.0         ! Scaling factor of Non-D Mass Flow – Degradation factor
```

28 1.0 ! Scaling factor of ETAc is (Compressor isentropic efficiency) – Degradation factor
29 -1.0 ! Effective component volume [m^3]
30 0.0 ! Stator angle (VSV) relative to DP

31 0.05 ! BYPASS: (Wout/Win) BPR = 6.4 CRUISE!
32 0.0 ! DELTA W
33 1.0 ! LAMBDA P
34 0.0 ! DELTA P

35 0.05 ! PREMAS: LAMDA W Cooling bypass (Wout/Win)
36 0.0 ! DELTA W
37 1.0 ! LAMBDA P
38 0.0 ! DELTA P

39 0.05 ! COMBUSTOR: Pressure loss (=Total pressure loss/Inlet total pressure)
40 0.999 ! Combustion efficiency
41 -1.0 ! Fuel flow (If -1. is given the TET must be determined in the station vector
42 0.0 ! (>0) Water flow [kg s-1 or lb s-1] or (<0) Water to air ratio
43 288.0 ! Temperature of water stream [K]
44 0.0 ! Phase of water (0=liquid, 1=vapour)
45 1.0 ! Scaling factor of ETAb (combustion efficiency) – Degradation factor
46 -1.0 ! Effective component volume [m^3]

47 0.0 ! COMPRESSOR TURBINE: Auxiliary or power output [W]
48 -1 ! Relative non-dimensional massflow W/Wmax (if = -1, value 0.8 is invoked)
49 -1 ! Relative non-rimensional speed CN (if = -1, value 0.6 is invoked)
50 0.9 ! Design isentropic efficiency
51 -1.0 ! Relative non-dimensional speed PCN (= -1 for compressor turbine)
52 2.0 ! Shaft Number (for power turbine, the value "0." is used)
53 5.0 ! Turbine map umber
54 -1.0 ! Power law index "n" (POWER = PCN^n) If = -1, power is assumed to be a constant
55 1.0 ! Scaling factor of TF (non-D inlet mass flow) – Degradation factor
56 1.0 ! Scaling factor of DH (enthalpy change) – Degradation factor
57 1.0 ! Scaling factor of ETAc is (Turbine isentropic efficiency) – Degradation factor
58 200 ! Rotor rotational speed [RPS]
59 15.0 ! Rotor moment of inertia [kg.m^2]
60 -1.0 ! Effective component volume [m^3]
61 0.0 ! NGV angle, relative to D.P.

62 43300000.0 ! POWER TURBINE: Auxiliary or power output [W]
63 0.8 ! Relative non-dimensional massflow W/Wmax (if = -1, value 0.8 is invoked)
64 0.6 ! Relative non-rimensional speed CN (if = -1, value 0.6 is invoked)
65 0.9 ! Design isentropic efficiency
66 -1.0 ! Relative non-dimensional speed PCN (= -1 for compressor turbine)
67 1.0 ! Shaft Number (for power turbine, the value "0." is used)
68 5.0 ! Turbine map umber
69 -1.0 ! Power law index "n" (POWER = PCN^n) If = -1, power is assumed to be a constant
70 1.0 ! Scaling factor of TF (non-D inlet mass flow) – Degradation factor
71 1.0 ! Scaling factor of DH (enthalpy change) – Degradation factor
72 1.0 ! Scaling factor of ETAc is (Turbine isentropic efficiency) – Degradation factor
73 200 ! Rotor rotational speed [RPS]

```
74 20.0         ! Rotor moment of inertia [kg.m^2]
75 -1.0         ! Effective component volume [m^3]
76 0.0          ! NGV angle, relative to D.P.

77 -1.0         ! CONVERGENT NOZZLE: = "-1" exit area is fixed
78 1.0          ! Scaling factor

79 0.9          ! ENGINE RESULTS: Propeller efficiency (= -1 for turbojet/turbofan)
80 0.0          ! Scaling index ("1" = scalling needed, "0" = no scaling)
81 0.0          ! Required DP net thrust(Turbojet.turbofan) or shaft power
(Turboprop.turboshaft)
                ! = 0 if Scaling index = 0
-1
1 2 123.80      ! item 2 at station 1 = Mass flow(kg/s)
7 6 1550.0      ! item 6 at station 7 = Total temperature (K)
-1              ! End of DP data
-3
```

Table 3 Turbomatch input result for SGT-500 Industrial gas turbine

```
The study inspired by SGT-500 Industrial Gas Turbine
Author: Nasiru Tukur
________________________________________________________________
////
DP SI GM VA FP
-1
-1
INTAKE  S1,2      D1-6        R200
COMPRE  S2,3      D7-18       R205    V7   V8
COMPRE  S3,4      D19-30      R205    V19  V20
PREMAS  S4,25,5   D31-34
PREMAS  S5,26,6   D35-38
BURNER  S6,7      D39-46      R215
MIXEES  S7,26,8
TURBIN  S8,9      D47-61              V48
MIXEES  S9,25,10
TURBIN  S10,11    D62-76              V63
TURBIN  S11,12    D77-91              V77 V78
NOZCON  S12,13,1  D92,93      R220
PERFOR  S1,0,0    D77,94-96,220,200,215,0,0,0,0,0,0
CODEND

DATA ITEMS ////
1 0.0         ! INTAKE:  Altitude [m]
2 0.0         ! Deviation from ISA temperature [K]
3 0.0         ! Mach number
4 0.9954      ! Pressure recovery, according to USAF
5 0.0         ! Deviation from ISA pressure [atm]
6 60.0        ! Relative humidity [%]

7 -1.0        ! COMPRESSOR - FAN: Z = (R-R[choke])/(R[surge]-R[choke]) (if =-1. the
default value 0.85 is invoked)
8 -1.0        ! Relative rotational speed PCN
9 2.167       ! DP Pressure ratio
10 0.80       ! isentropic efficiency
11 0.0        ! Error selection
12 5.0        ! Compressor Map Number
13 1.0        ! Shaft number
14 1.0        ! Scaling factor of Pressure Ratio – Degradation factor
15 1.0        ! Scaling factor of Non-D Mass Flow – Degradation factor
16 1.0        ! Scaling factor of ETAc is (Compressor isentropic efficiency) – Degradation
factor
17 1.5        ! Effective component volume [m^3]
18 0.0        ! Stator angle (VSV) relative to DP

19 -1.0       ! COMPRESSOR HP: Z = (R-R[choke])/(R[surge]-R[choke]) (if =-1. the
default value 0.85 is invoked)
20 -1.0       ! Relative rotational speed PCN
21 6.0        ! DP Pressure ratio
22 0.80       ! isentropic efficiency
23 1.0        ! Error selection
24 5.0        ! Compressor Map Number
25 2.0        ! Shaft number
26 1.0        ! Scaling factor of Pressure Ratio – Degradation factor
27 1.0        ! Scaling factor of Non-D Mass Flow – Degradation factor
```

28 1.0 ! Scaling factor of ETAc is (Compressor isentropic efficiency) – Degradation factor
29 -1.0 ! Effective component volume [m^3]
30 0.0 ! Stator angle (VSV) relative to DP

31 0.05 ! BYPASS: (Wout/Win) BPR = 6.4 CRUISE!
32 0.0 ! DELTA W
33 1.0 ! LAMBDA P
34 0.0 ! DELTA P

35 0.05 ! PREMAS: LAMDA W Cooling bypass (Wout/Win)
36 0.0 ! DELTA W
37 1.0 ! LAMBDA P
38 0.0 ! DELTA P

39 0.05 ! COMBUSTOR: Pressure loss (=Total pressure loss/Inlet total pressure)
40 0.999 ! Combustion efficiency
41 -1.0 ! Fuel flow (If -1. is given the TET must be determined in the station vector
42 0.0 ! (>0) Water flow [kg s-1 or lb s-1] or (<0) Water to air ratio
43 288.0 ! Temperature of water stream [K]
44 0.0 ! Phase of water (0=liquid, 1=vapour)
45 1.0 ! Scaling factor of ETAb (combustion efficiency) – Degradation factor
46 -1.0 ! Effective component volume [m^3]

47 0.0 ! COMPRESSOR TURBINE: Auxiliary or power output [W]
48 -1 ! Relative non-dimensional massflow W/Wmax (if = -1, value 0.8 is invoked)
49 -1 ! Relative non-rimensional speed CN (if = -1, value 0.6 is invoked)
50 0.88 ! Design isentropic efficiency
51 -1.0 ! Relative non-dimensional speed PCN (= -1 for compressor turbine)
52 2.0 ! Shaft Number (for power turbine, the value "0." is used)
53 3.0 ! Turbine map umber
54 -1.0 ! Power law index "n" (POWER = PCN^n) If = -1, power is assumed to be a constant
55 1.0 ! Scaling factor of TF (non-D inlet mass flow) – Degradation factor
56 1.0 ! Scaling factor of DH (enthalpy change) – Degradation factor
57 1.0 ! Scaling factor of ETAc is (Turbine isentropic efficiency) – Degradation factor
58 200 ! Rotor rotational speed [RPS]
59 15.0 ! Rotor moment of inertia [kg.m^2]
60 -1.0 ! Effective component volume [m^3]
61 0.0 ! NGV angle, relative to D.P.

62 0.0 ! COMPRESSOR TURBINE: Auxiliary or power output [W]
63 -1 ! Relative non-dimensional massflow W/Wmax (if = -1, value 0.8 is invoked)
64 -1 ! Relative non-rimensional speed CN (if = -1, value 0.6 is invoked)
65 0.88 ! Design isentropic efficiency
66 -1.0 ! Relative non-dimensional speed PCN (= -1 for compressor turbine)
67 1.0 ! Shaft Number (for power turbine, the value "0." is used)
68 3.0 ! Turbine map umber
69 -1.0 ! Power law index "n" (POWER = PCN^n) If = -1, power is assumed to be a constant
70 1.0 ! Scaling factor of TF (non-D inlet mass flow) – Degradation factor
71 1.0 ! Scaling factor of DH (enthalpy change) – Degradation factor
72 1.0 ! Scaling factor of ETAc is (Turbine isentropic efficiency) – Degradation factor
73 200 ! Rotor rotational speed [RPS]
74 15.0 ! Rotor moment of inertia [kg.m^2]

75 -1.0 ! Effective component volume [m^3]
76 0.0 ! NGV angle, relative to D.P.

77 19300000.0 ! POWER TURBINE: Auxiliary or power output [W]
78 -1 ! Relative non-dimensional massflow W/Wmax (if = -1, value 0.8 is invoked)
79 -1 ! Relative non-rimensional speed CN (if = -1, value 0.6 is invoked)
80 0.88 ! Design isentropic efficiency
81 1.0 ! Relative non-dimensional speed PCN (= -1 for compressor turbine)
82 0.0 ! Shaft Number (for power turbine, the value “0.” is used)
83 3.0 ! Turbine map umber
84 -1.0 ! Power law index "n" (POWER = PCN^n) If = -1, power is assumed to be a constant
85 1.0 ! Scaling factor of TF (non-D inlet mass flow) – Degradation factor
86 1.0 ! Scaling factor of DH (enthalpy change) – Degradation factor
87 1.0 ! Scaling factor of ETAc is (Turbine isentropic efficiency) – Degradation factor
88 200 ! Rotor rotational speed [RPS]
89 20.0 ! Rotor moment of inertia [kg.m^2]
90 -1.0 ! Effective component volume [m^3]
91 0.0 ! NGV angle, relative to D.P.

92 -1.0 ! CONVERGENT NOZZLE: = "-1" exit area is fixed
93 1.0 ! Scaling factor

94 1.0 ! ENGINE RESULTS: Propeller efficiency (= -1 for turbojet/turbofan)
95 0.0 ! Scaling index ("1" = scalling needed, "0" = no scaling)
96 0.0 ! Required DP net thrust(Turbojet,turbofan) or shaft power (Turboprop,turboshaft)
! = 0 if Scaling index = 0
-1
1 2 96.75 ! item 2 at station 1 = Mass flow(kg/s)
7 6 1300.0 ! item 6 at station 7 = Total temperature (K)
-1 ! End of DP data
-3

Appendix C Gas Turbine Power Off-design results for Compressor stations

The Appendix C results show the trend in the variation of a gas turbine with changes in ambient temperature at constant TET. The inlet air temperature is a strong function for efficiency and power output of the gas turbine. As the ambient air temperature increases, the density of inlet air decreases. Therefore, at constant volume flow rate, the mass flow rate into the gas turbine decreases and this has an equivalent influence on its performance. The reduction in the inlet air density means a decrease of mass flow into the turbine. As the inlet air temperature raises the work done per unit mass of compression increases because more work is required to compress hot air but the expansion work done by the turbine remains the same. Hence, the useful work reduces as a result but the thermal efficiency and fuel flow decrease. As the turbine entry temperature increases the power output increase and the power output decreases with increase in ambient condition.

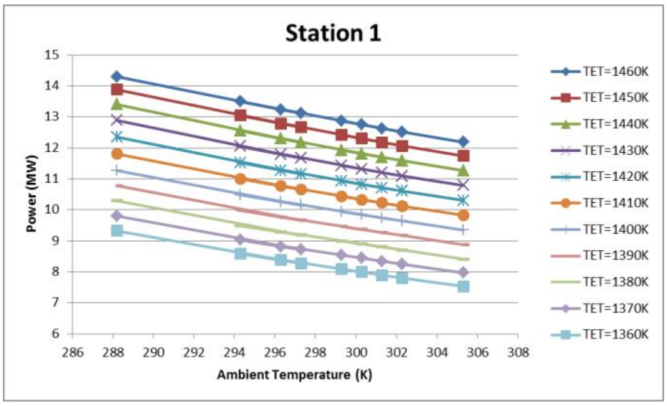

C 1 Effect of ambient temperature on power at constant TET

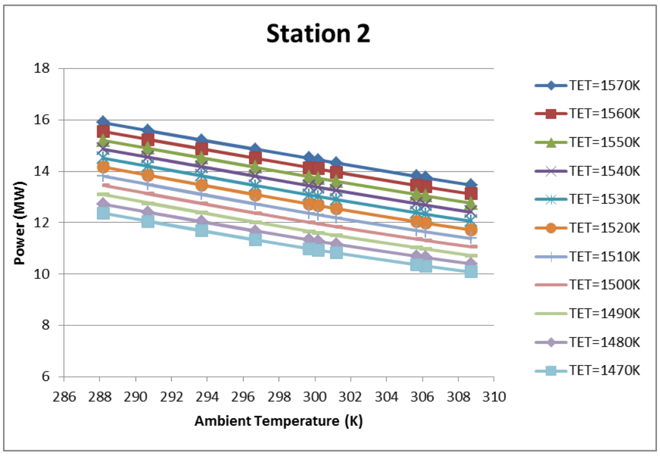

C 2 Effect of ambient temperature on power at constant TET

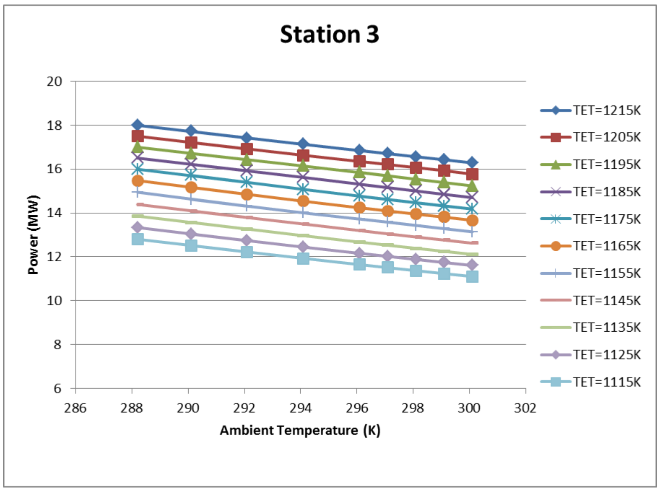

C 3 Effect of ambient temperature on power at constant TET

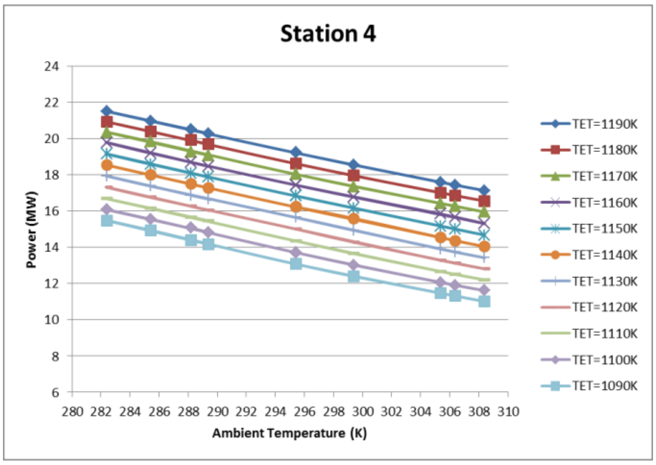

C 4 Effect of ambient temperature on power at constant TET

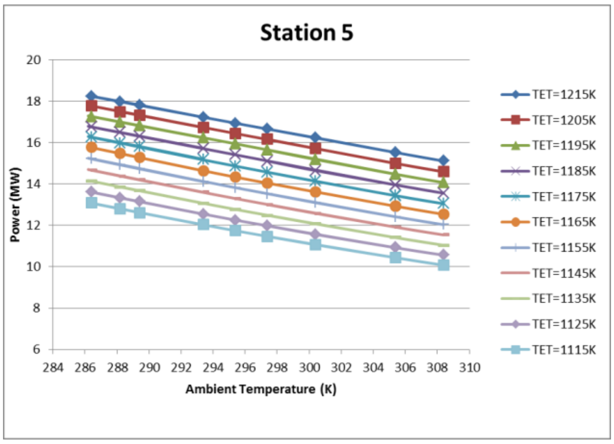

C 5 Effect of ambient temperature on power at constant TET

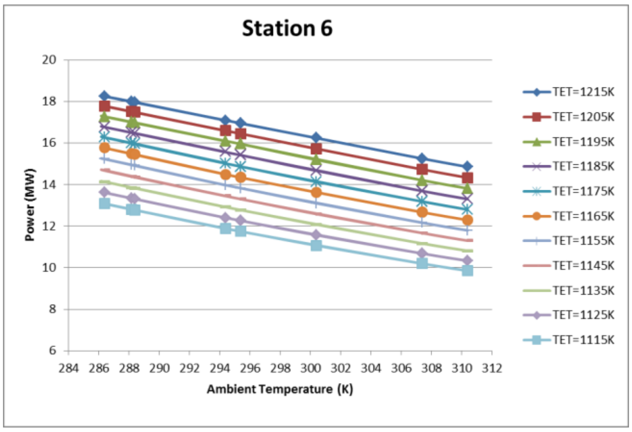

C 6 Effect of ambient temperature on power at constant TET

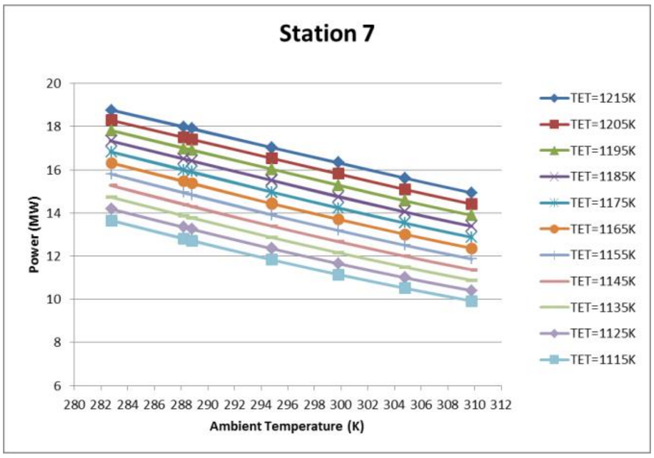

C 7 Effect of ambient temperature on power at constant TET

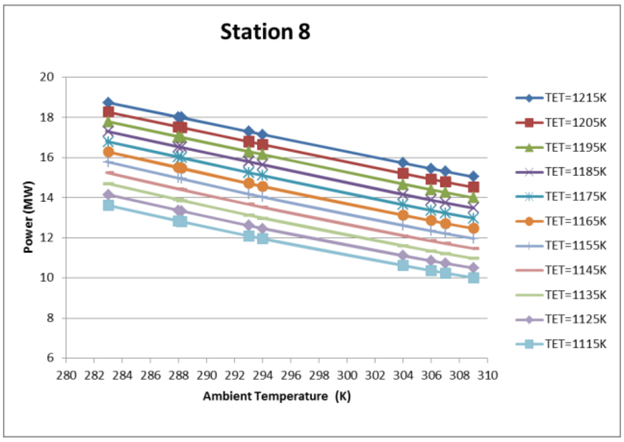

C 8 Effect of ambient temperature on power at constant TET

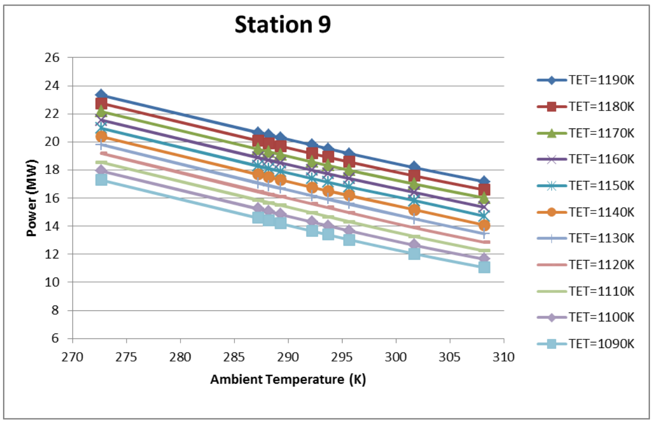

C 9 Effect of ambient temperature on power at constant TET

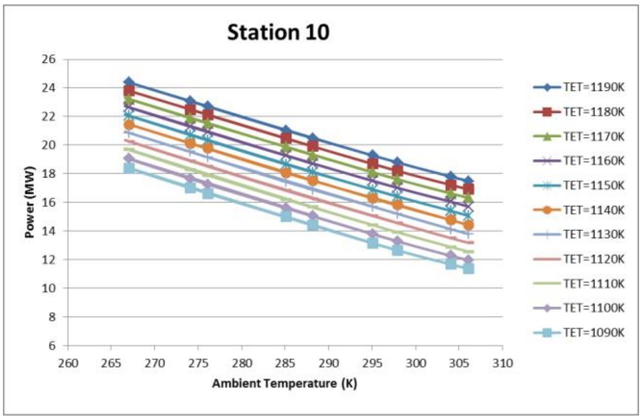

C 10 Effect of ambient temperature on power at constant TET

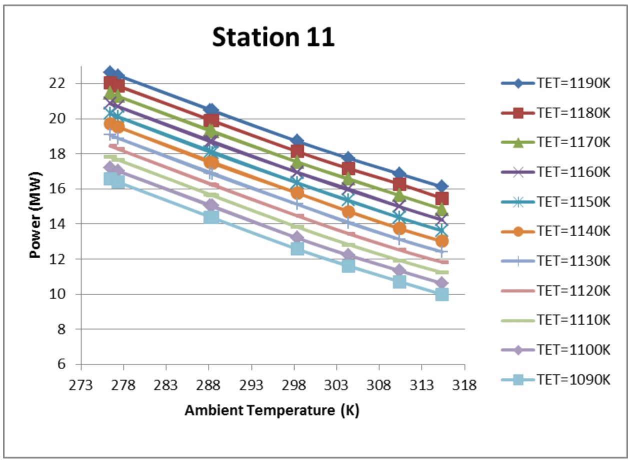

C 1 1 Effect of ambient temperature on power at constant TET

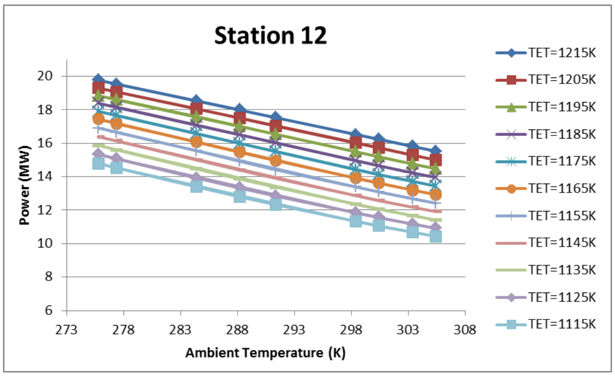

C 1 2 Effect of ambient temperature on power at constant TET

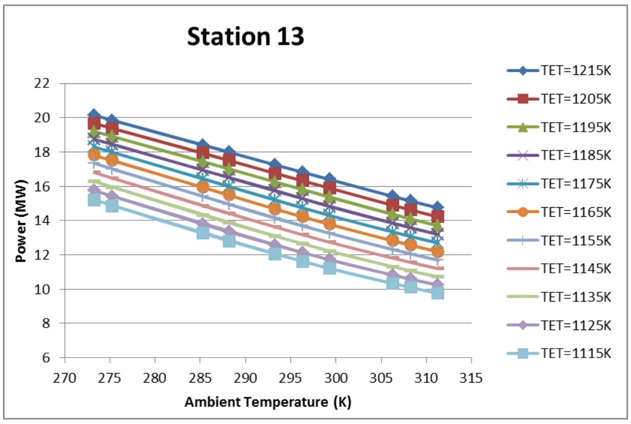

C 1 3 Effect of ambient temperature on power at constant TET

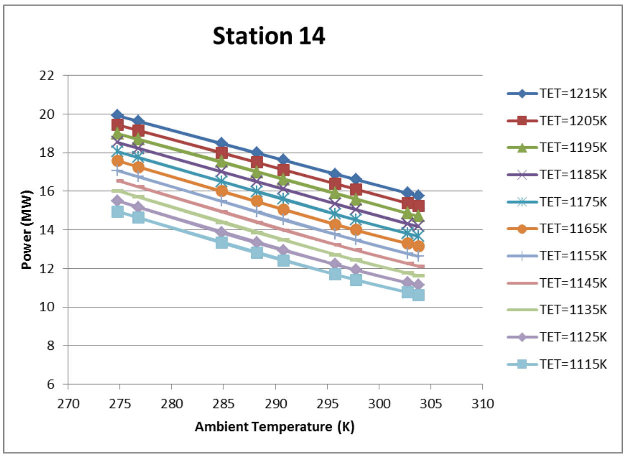

C 1 4 Effect of ambient temperature on power at constant TET

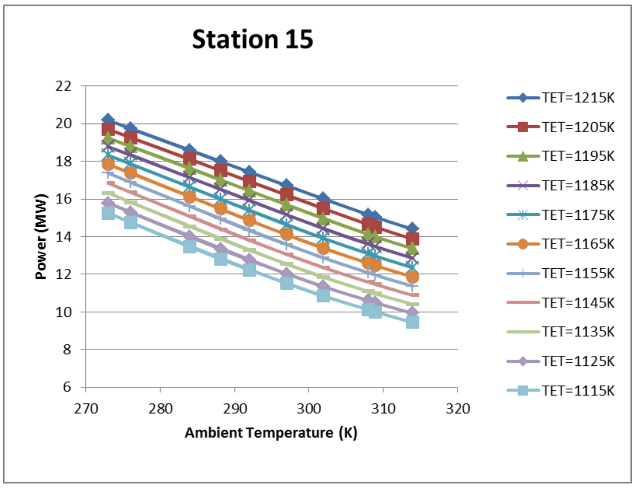

C 1 5 Effect of ambient temperature on power at constant TET

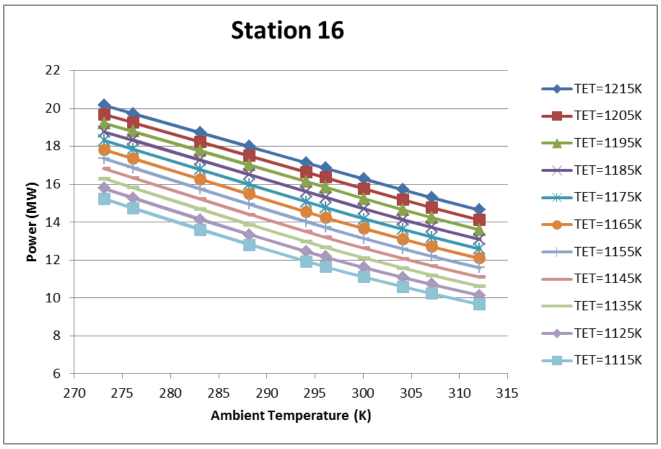

C 1 6 Effect of ambient temperature on power at constant TET

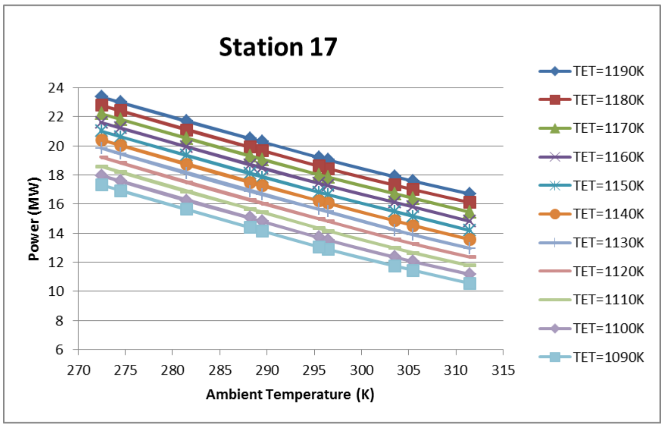

C 1 7 Effect of ambient temperature on power at constant TET

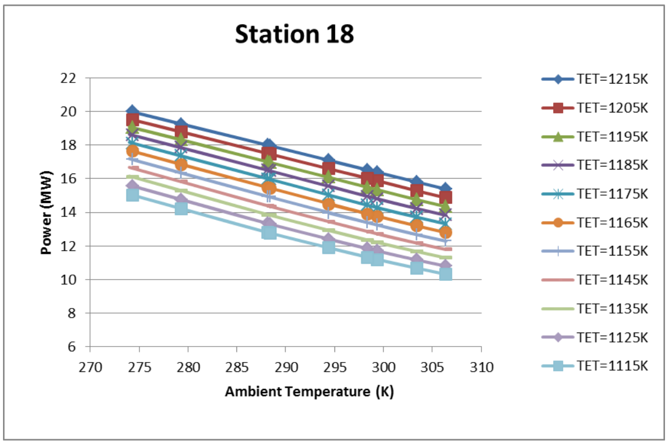

C 1 8 Effect of ambient temperature on power at constant TET

Appendix D Compressor curves from OEM

The original equipment manufacturers (OME) gas compressor data was supplied for the analysis of this research. The OEM performance curves for various rotational speeds together with the associated inlet gas properties and compressor inlet conditions are shown in Appendix D. The OEM gas compressor data are used to scale the proposed TSGP gas compressors. The new scaled TSGP gas compressors have a fairly accurate representation of the expected gas compressor performance curves.

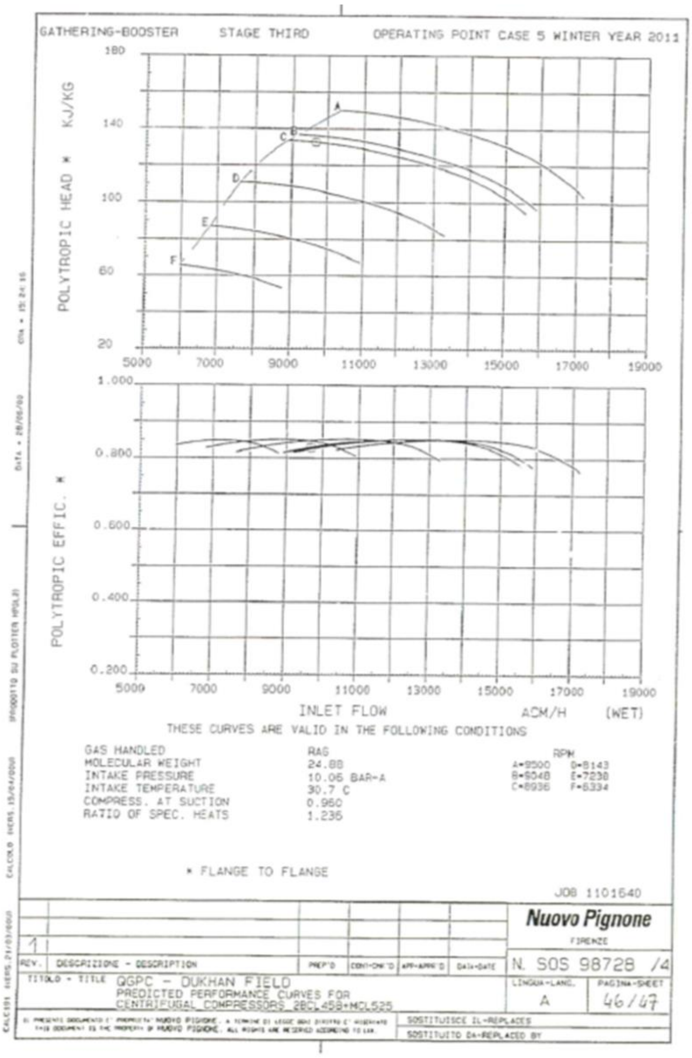

Figure D 1 Polytropic head and polytropic efficiency from OEM

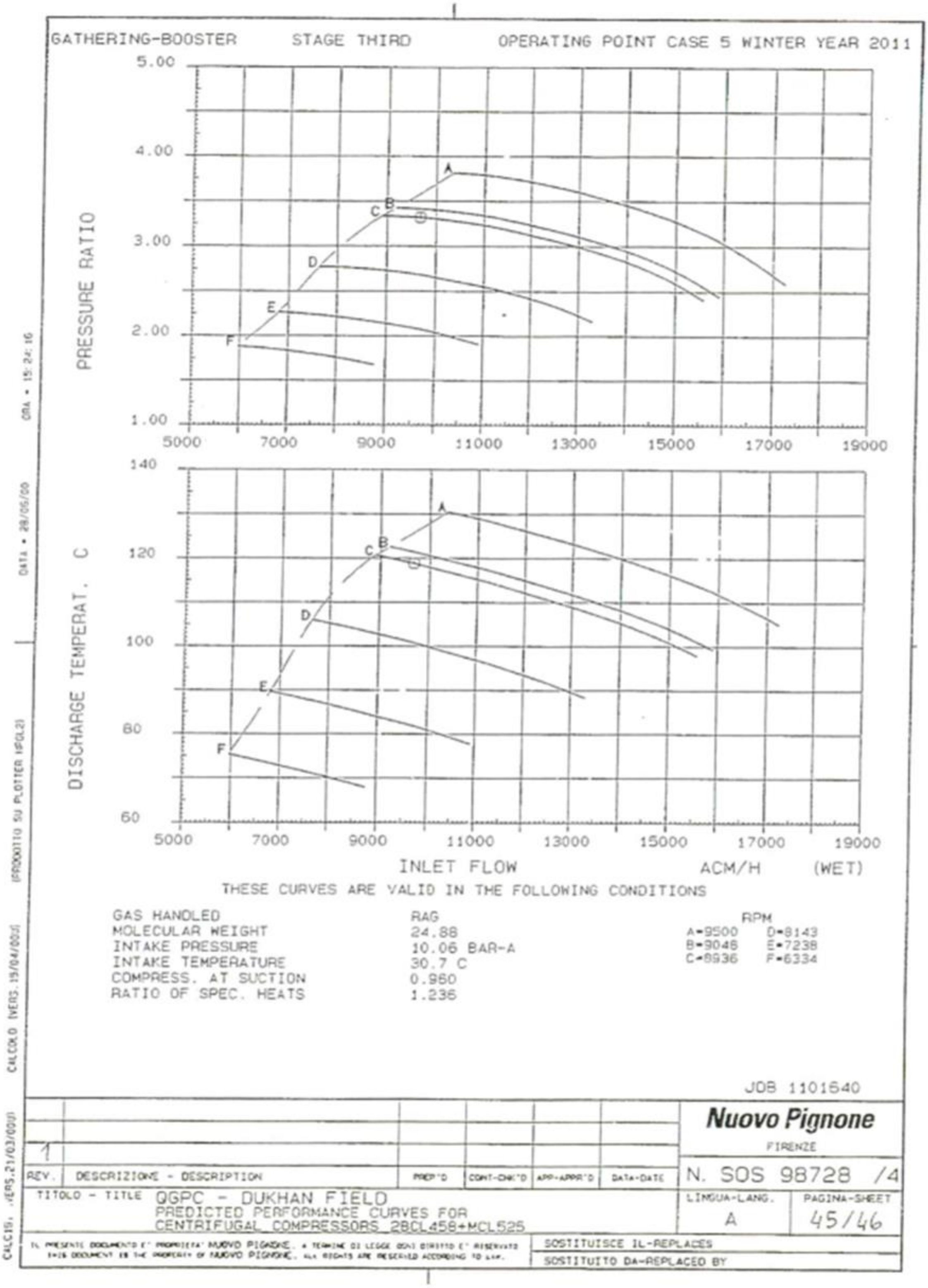

Figure D 2 Pressure ratio and discharge temperature from OEM

Appendix E Gas compressor and gas turbine power matching

Results in Appendix E shows the power matching for gas compressor and gas turbine at different TET, as the ambient temperature fluctuates daily in winter, dry and hot seasons across Trans-Sahara pipeline stations. An increase in ambient condition from ISO increases the polytropic head of the centrifugal compressor, and as such increases, the gas compressor power demand, whereas the same effect on the gas turbine resulting in a decrease in gas turbine output power for the three seasons. The GT performance was done in Turbomatch code to ensure that the GT provides the power required by the gas compressor at every time.

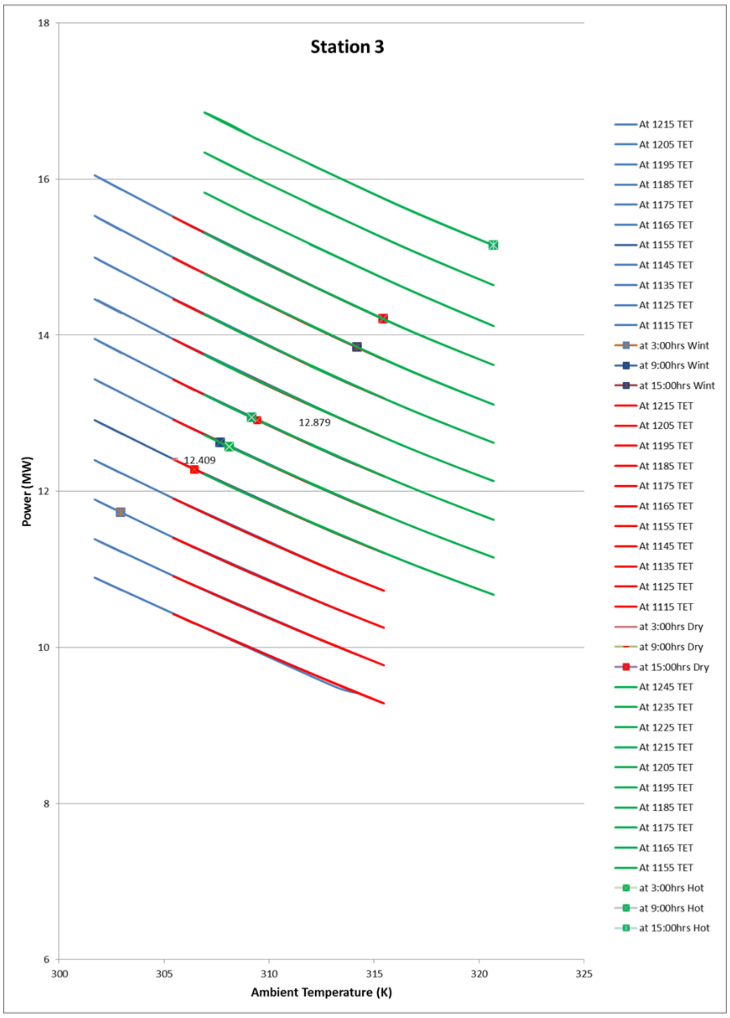

Figure E 1 Gas compressor and gas turbine power matching for station 3

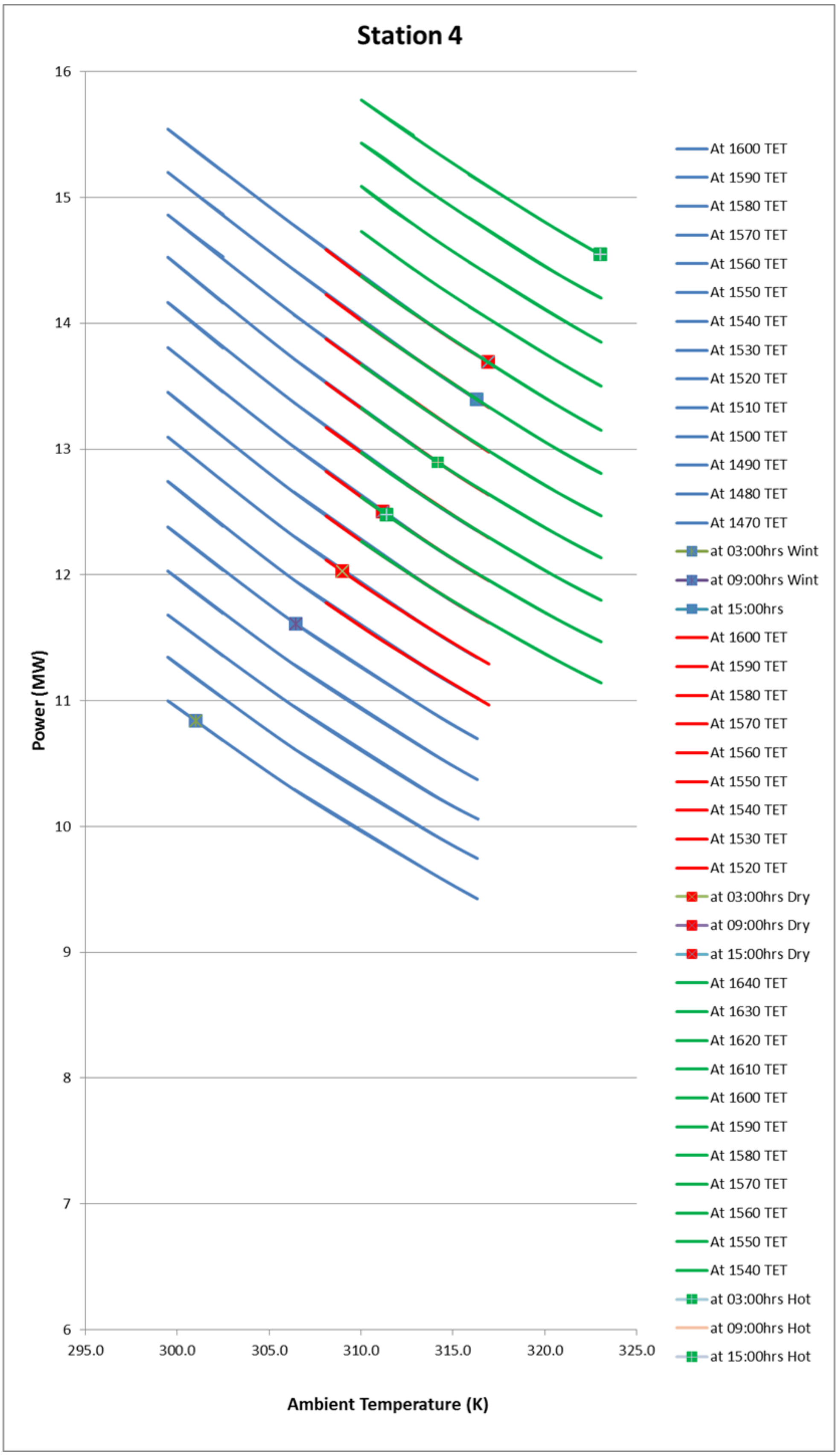

Figure E 2 Gas compressor and gas turbine power matching for station 4

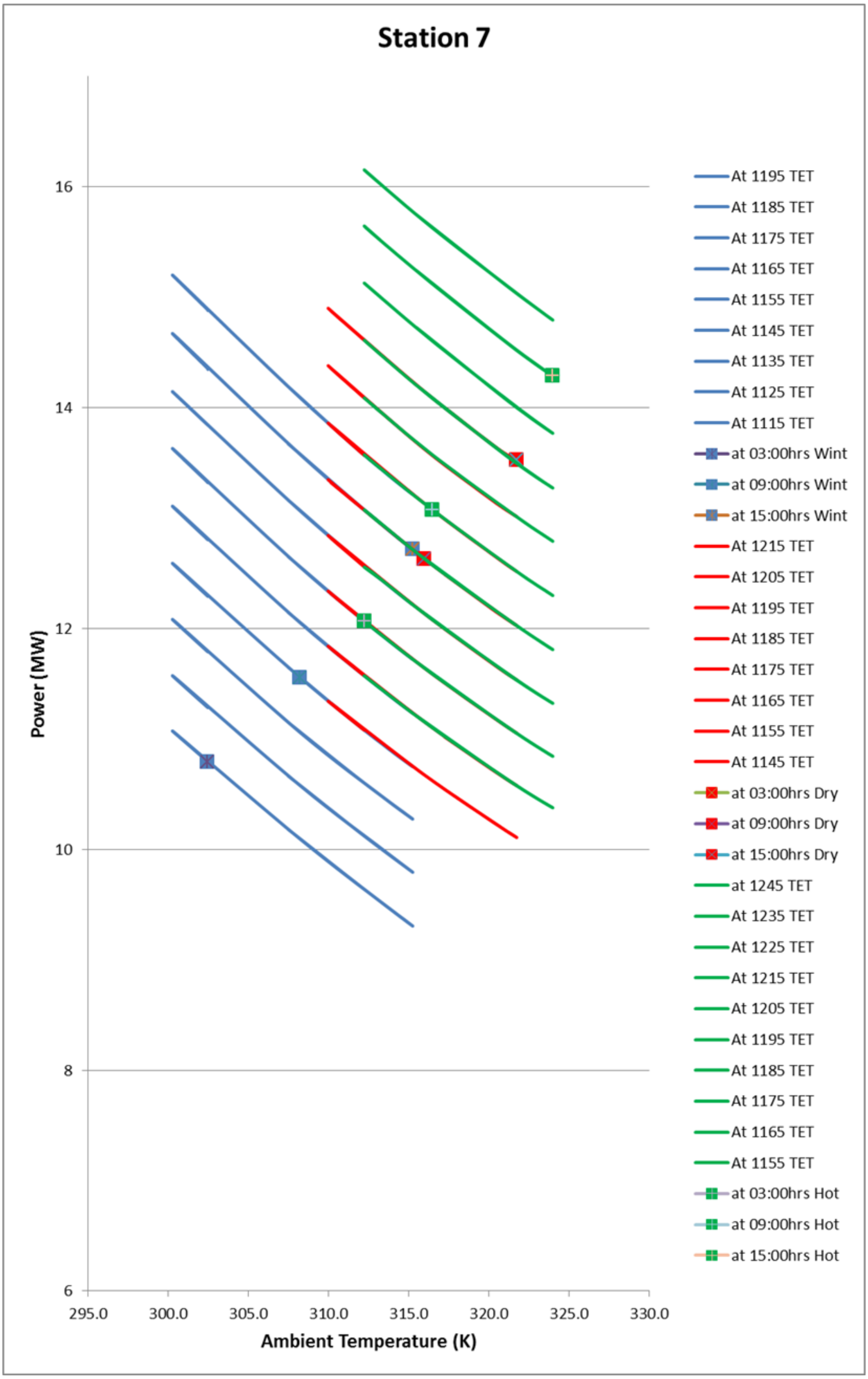

Figure E 3 Gas compressor and gas turbine power matching for station 7

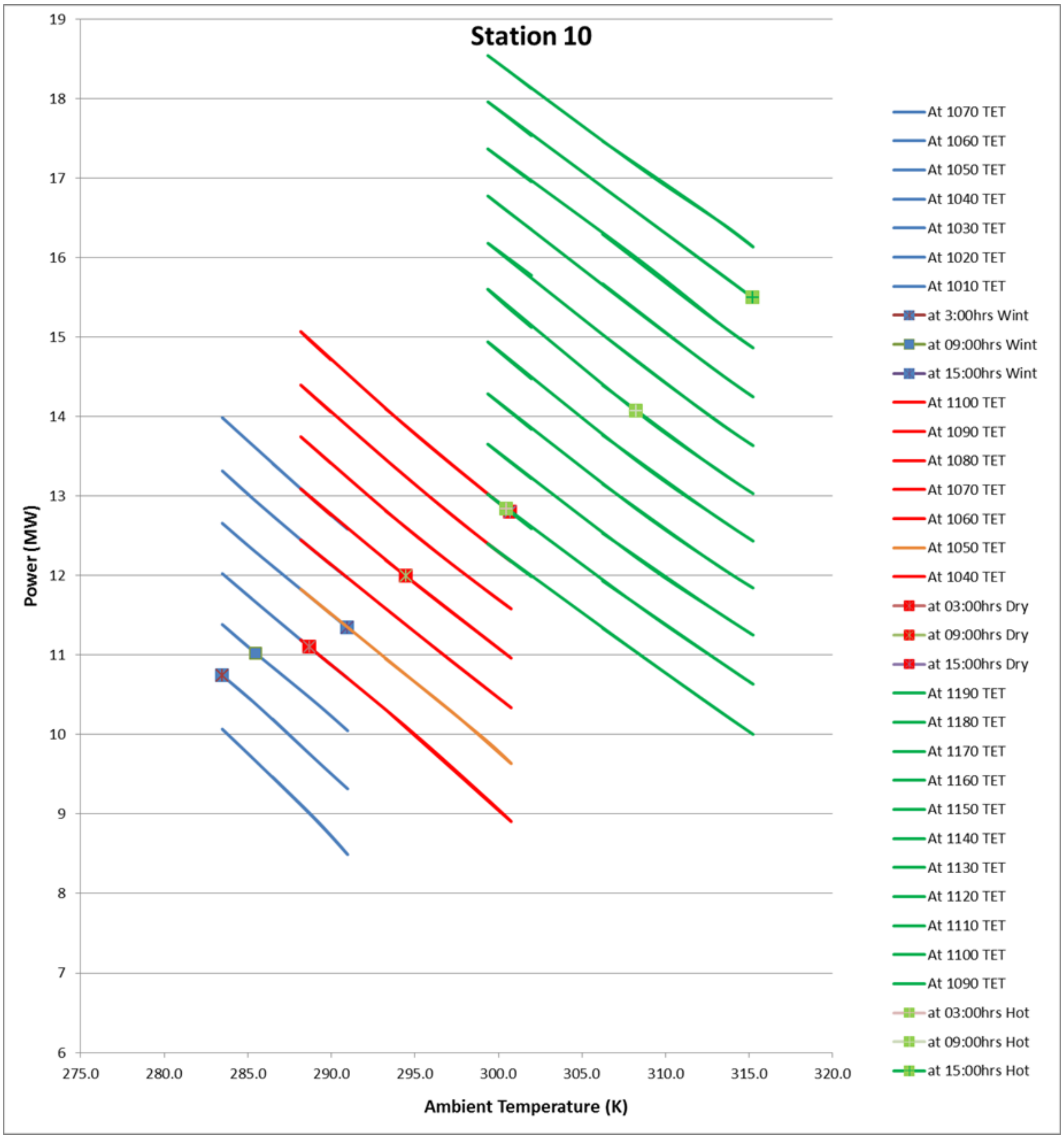

Figure E 4 Gas compressor and gas turbine power matching for station 10

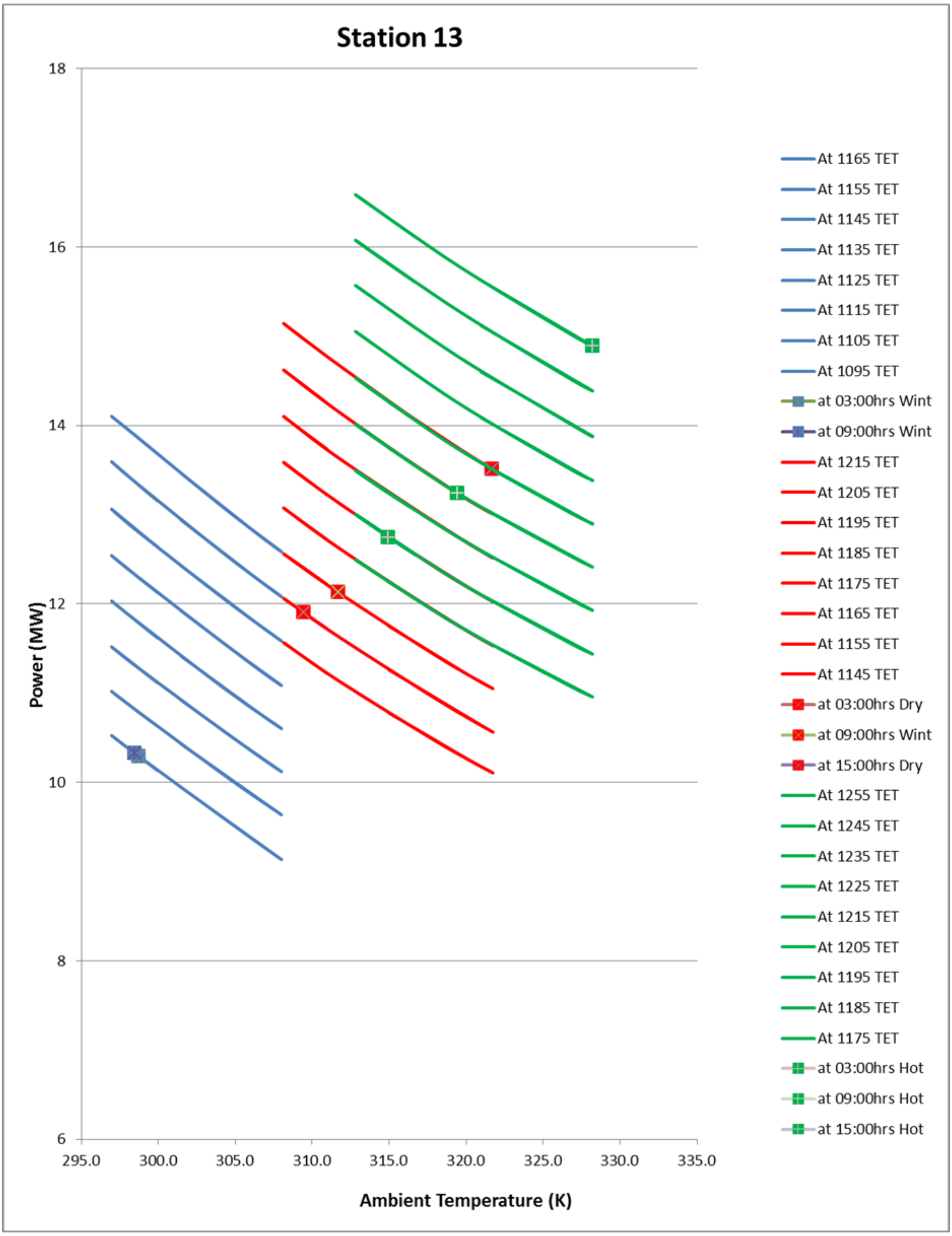

Figure E 5 Gas compressor and gas turbine power matching for 13

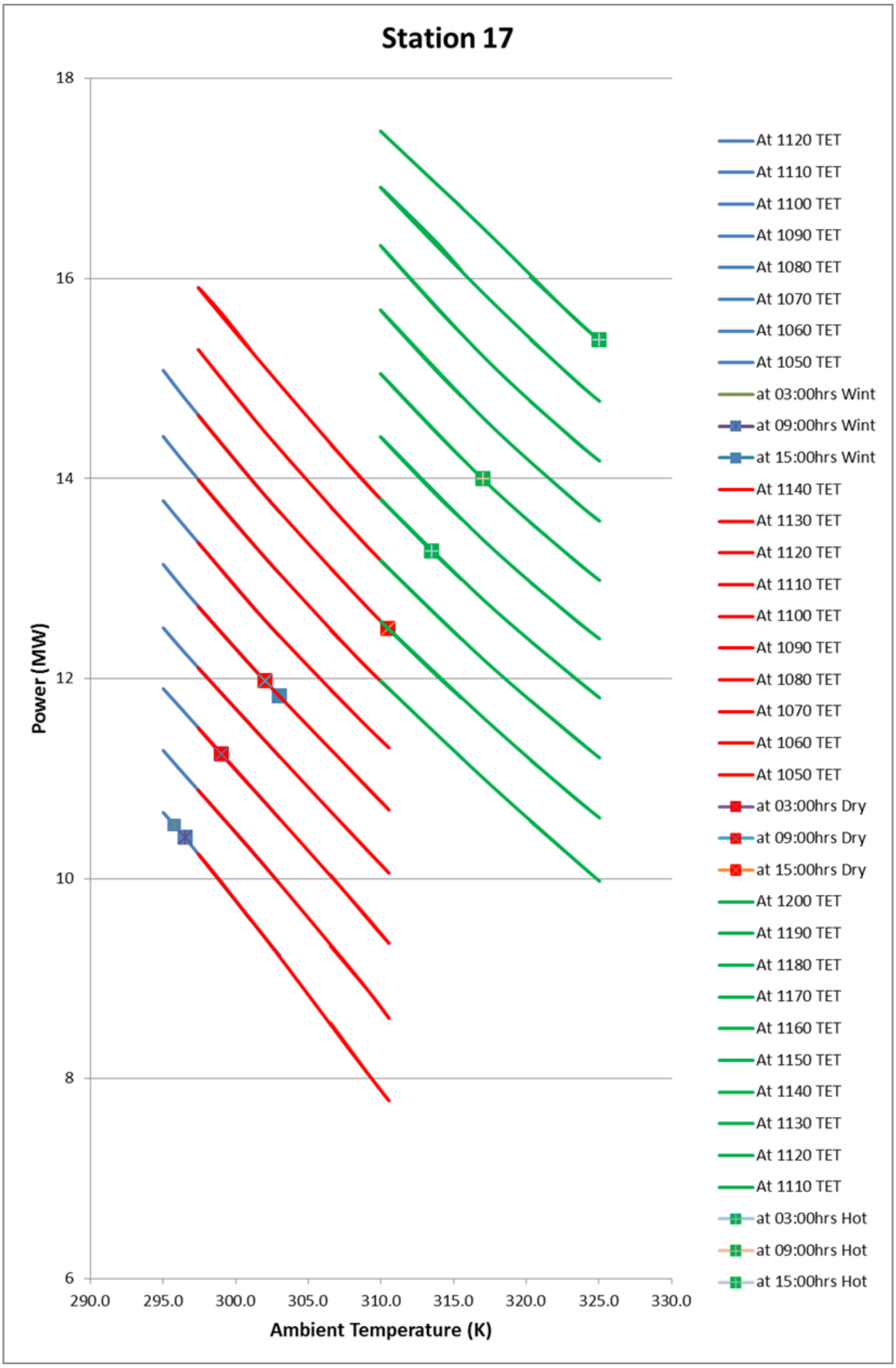

Figure E 6 Gas compressor and gas turbine power matching for station 17

Appendix F Optimized Compressor Station Locations

The pictorial representation of the results in Appendix F1 shows the maximum fitness value in terms of total cost against the number of generations for population sizes of 50 and generation of 25 for station 3 for the 100MW capacities. For every generation, there is corresponding mean fitness and best fitness. Appendix F2 shows the distance and power relationship for station 3 for 100MW capacities.

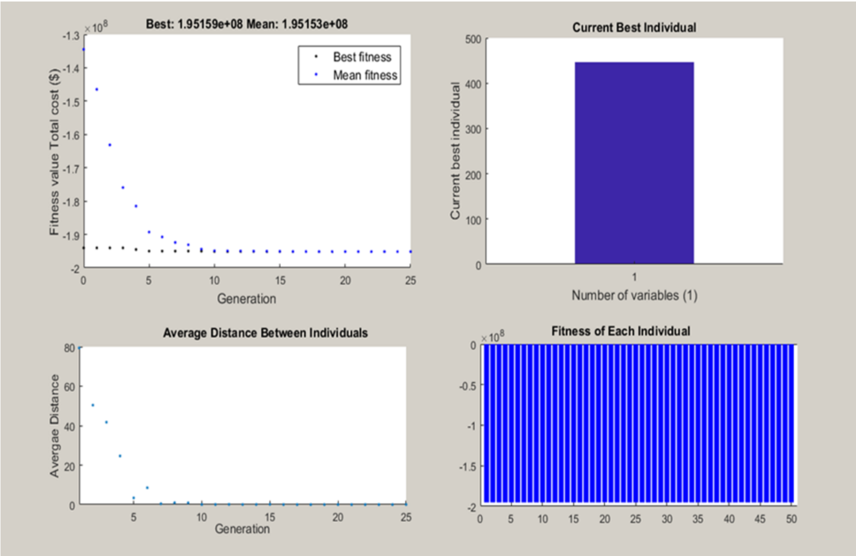

F 1 Fitness Value against Generation for the population size of 50 for station 3 (100MW)

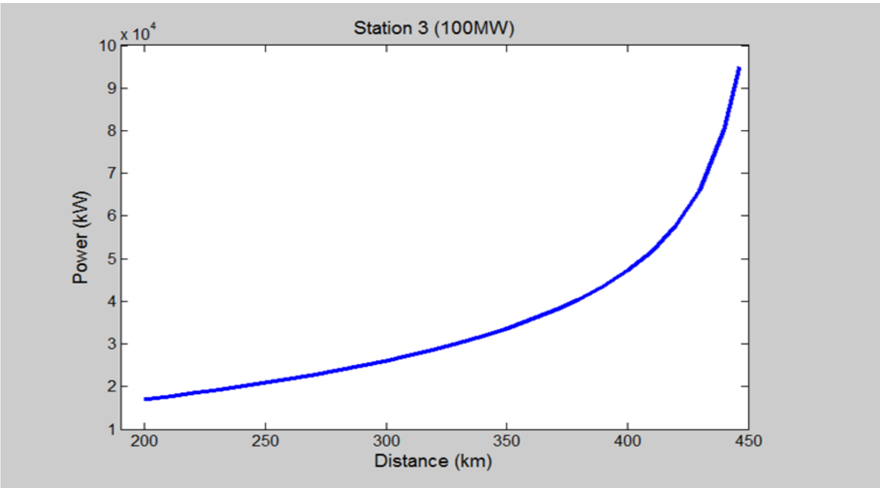

F 2 Distance and Power relationship for station 3 (100MW)

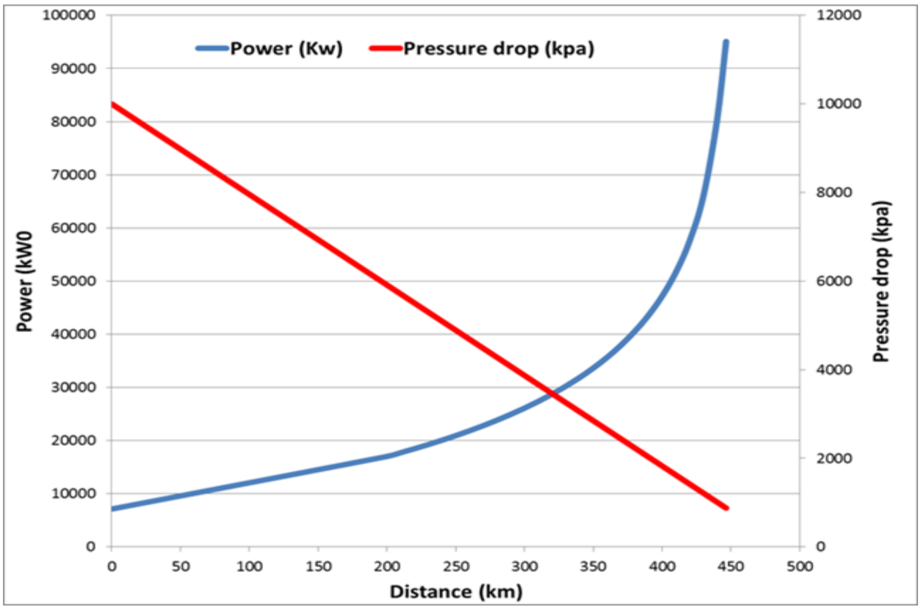

F 3 Power and Pressure drop against distance for station 3 (100MW)

The pictorial representation of the results in Appendix F4 shows the maximum fitness value in terms of total cost against the number of generations for population sizes of 50 and generation of 25 for station 3 for the 2 x 43.3MW capacities. For every generation there is corresponding mean fitness and best fitness. Appendix F5 shows the distance and power relationship for station 3 for 2 x 43.3MW capacities.

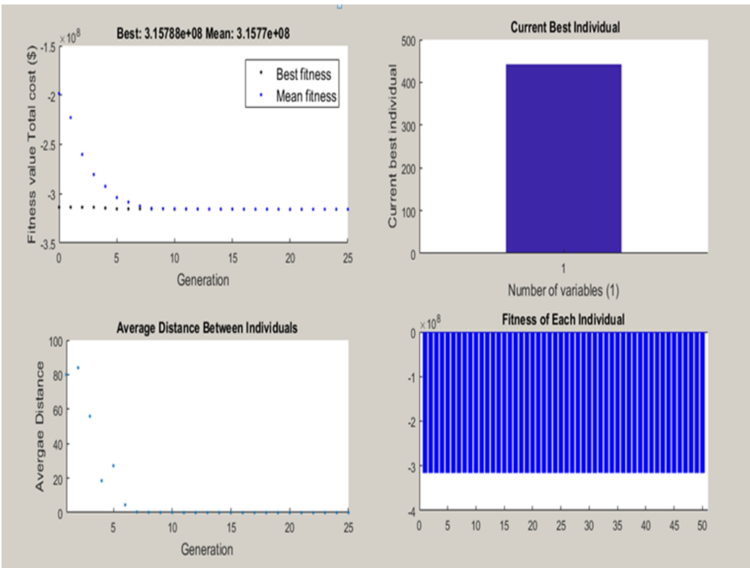

F 4 Fitness against Generation for the population size of 50 for station 3 (2 x 43.3MW)

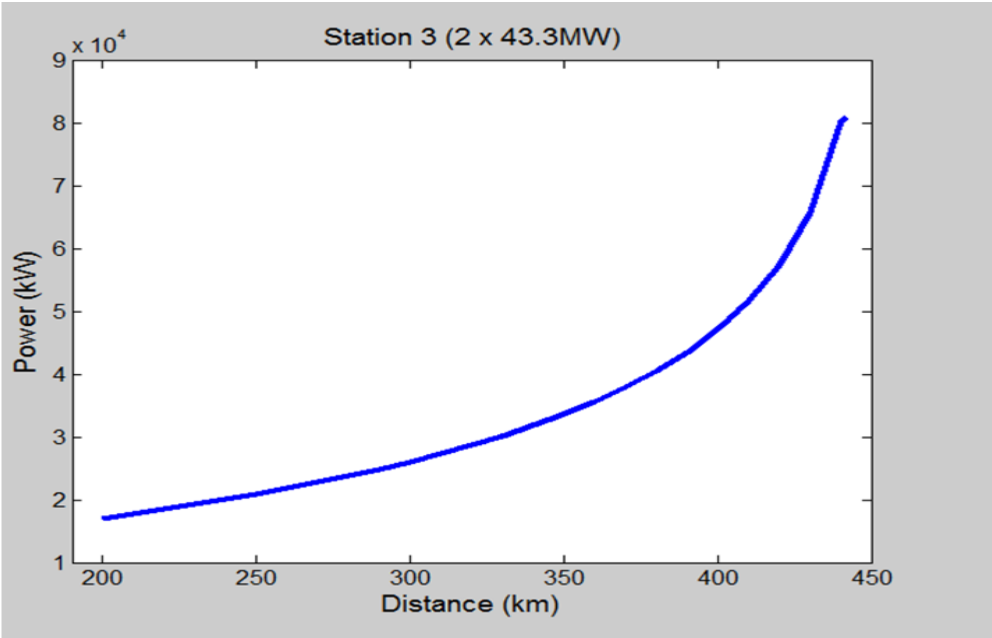

F 5 Distance and Power relationship for station 3 (2 x 43.3MW)

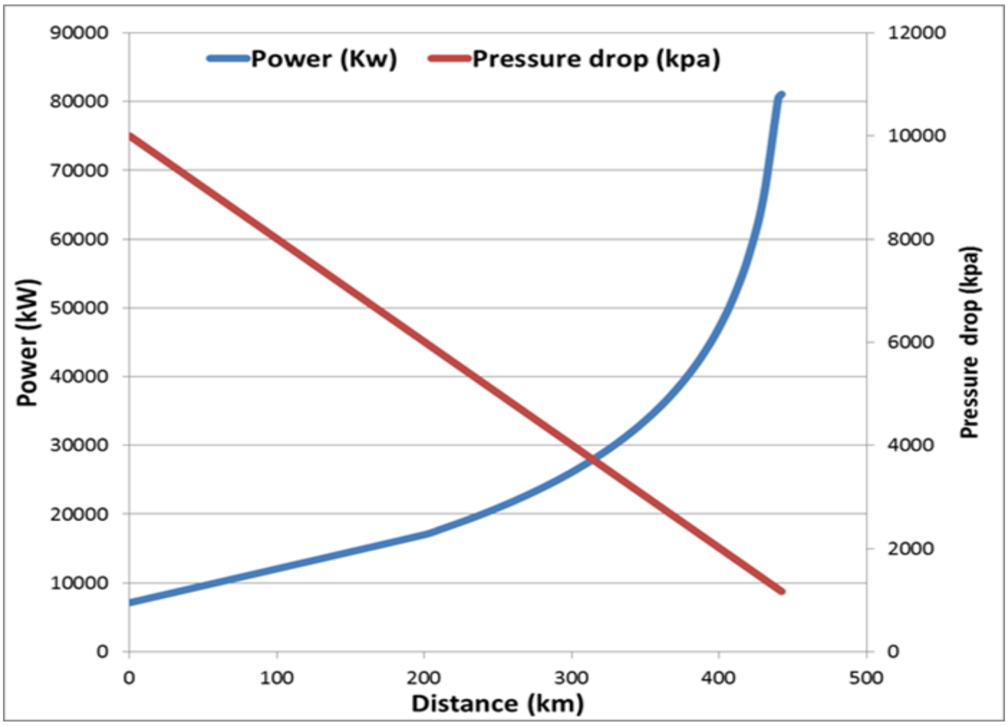

F 6 Power and Pressure drop against distance for station 3 (2 x 43.3MW)

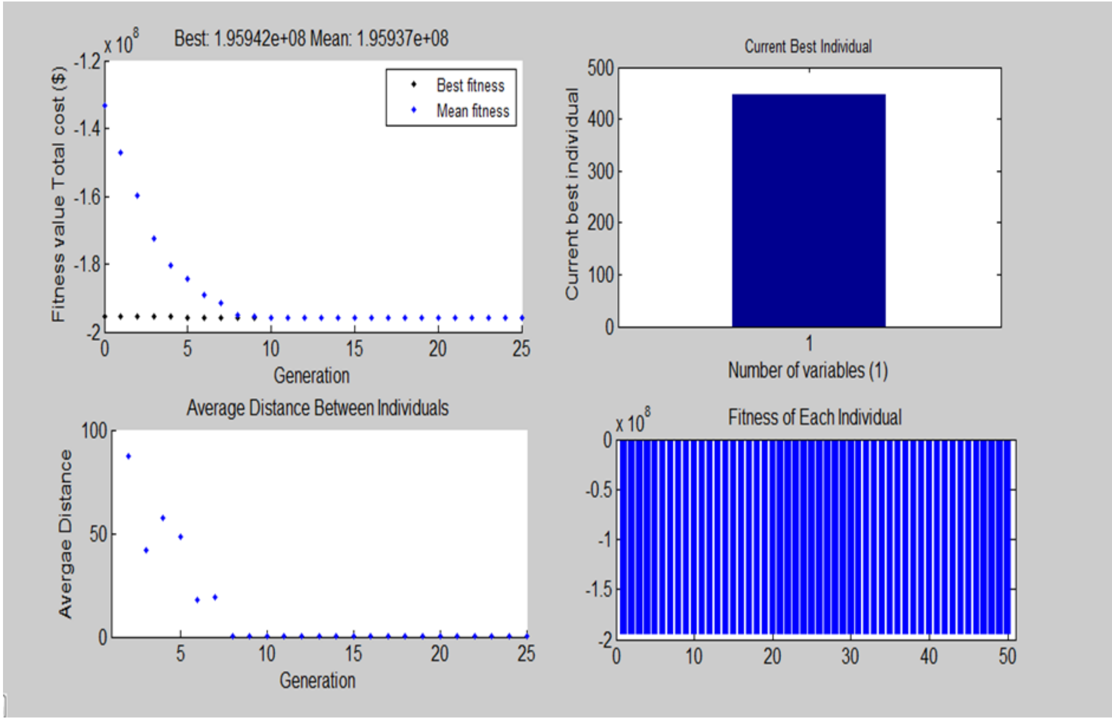

F 7 Fitness value against Generation for the population size of 50 for station 4 (100MW)

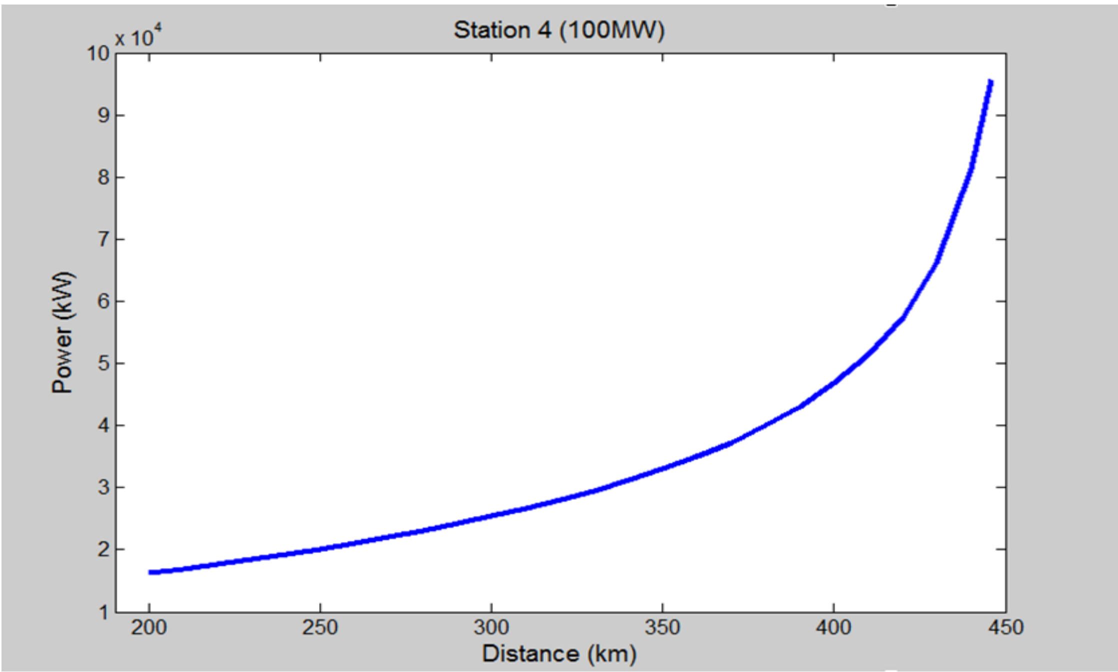

F 8 Distance and Power relationship for station 4 (100MW)

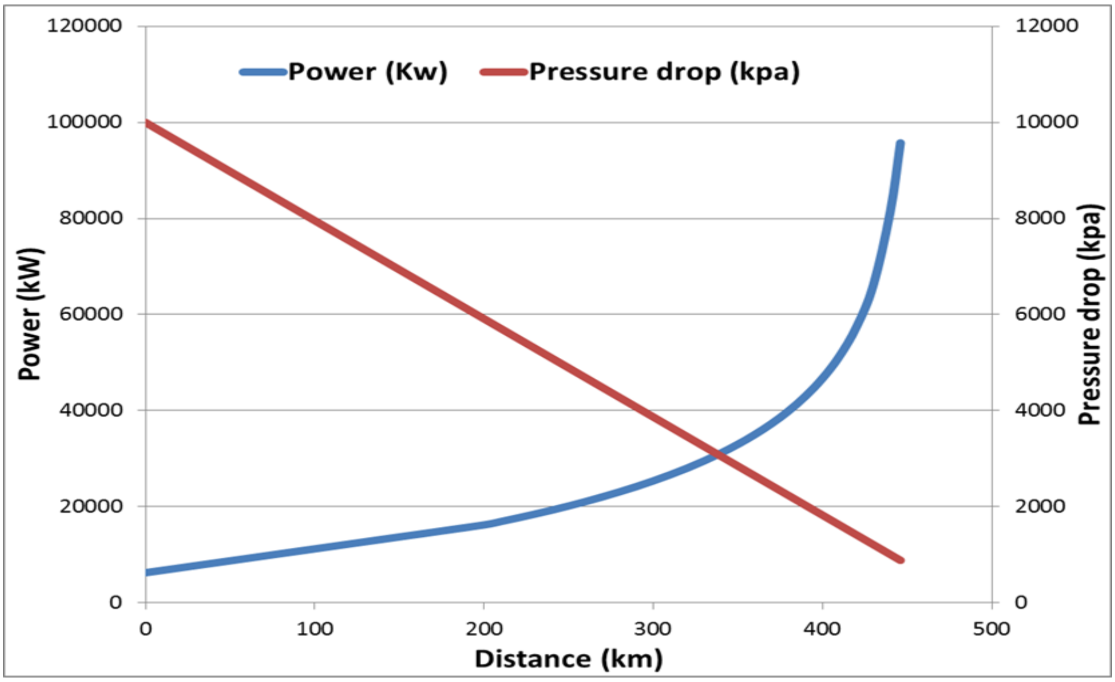

F 9 Power and Pressure drop against Distance for station 4 (100MW)

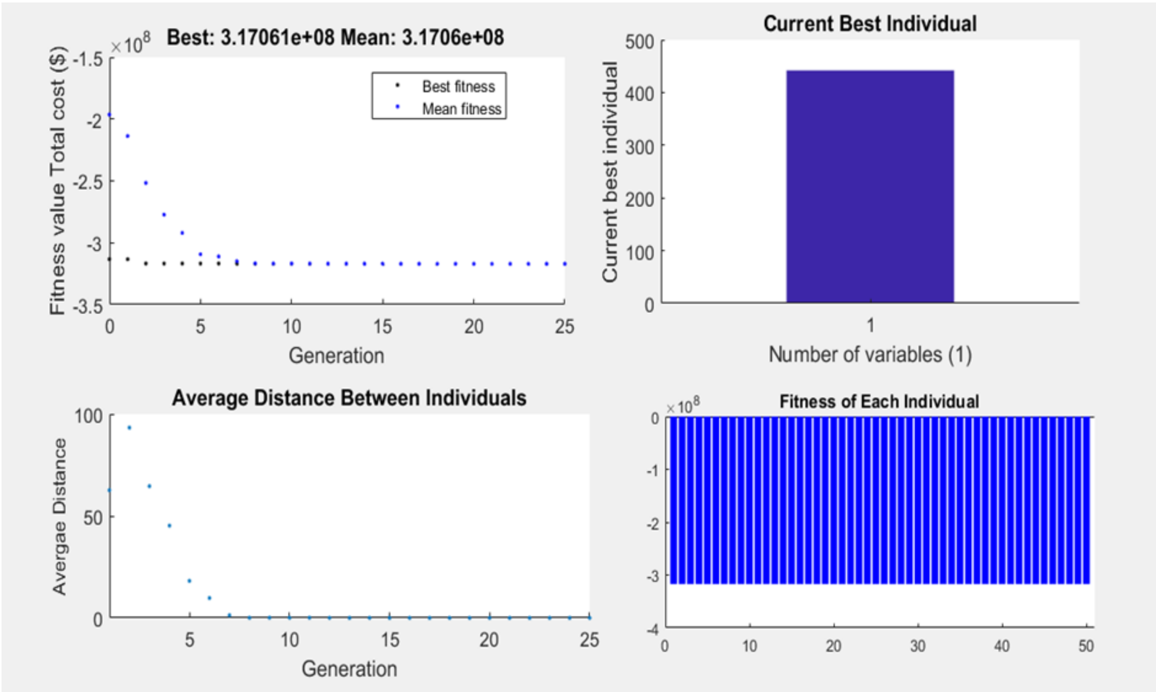

F 10 Fitness value against Generation for the population size of 50 for station 4 (2x 43.3MW)

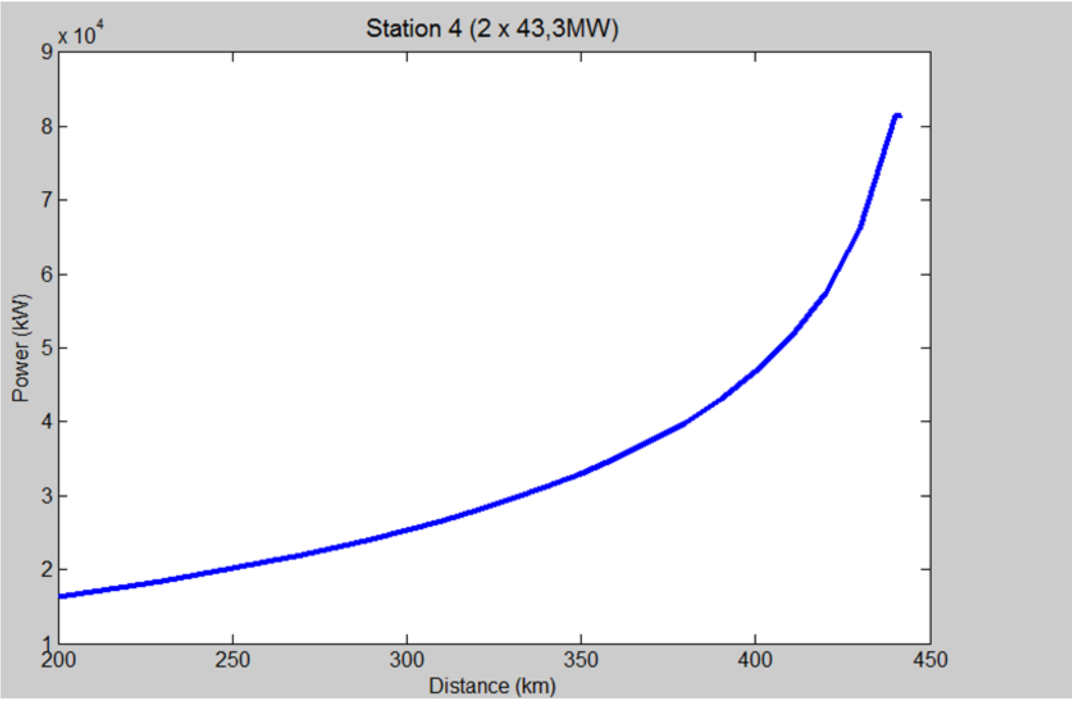

F 11 Distance and Power relationship for station 4 (2x 43.3MW)

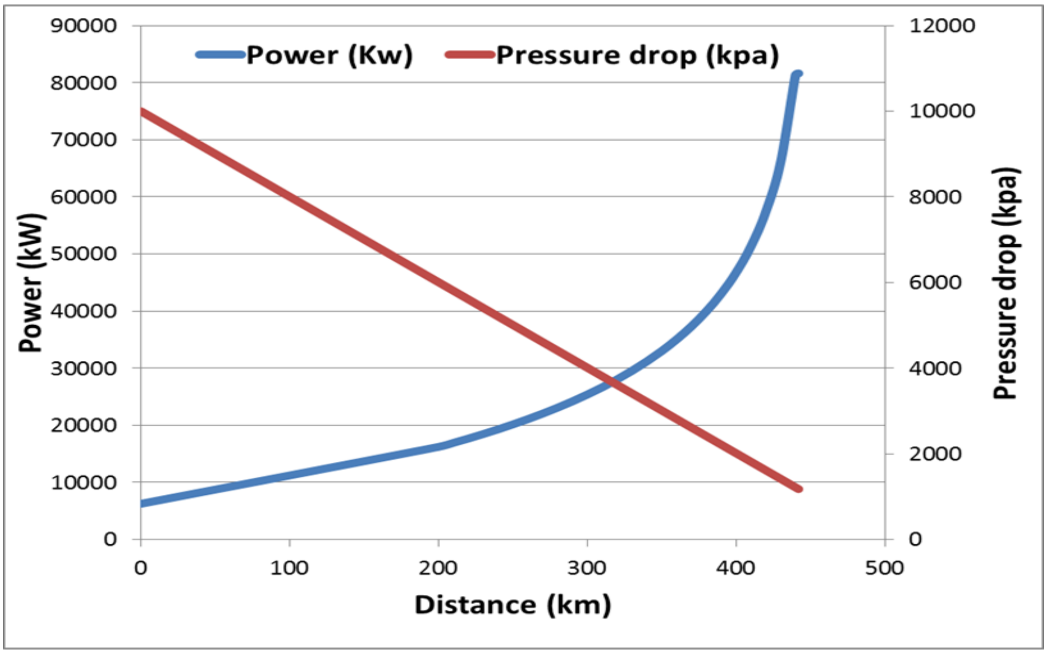

F 12 Power and Pressure drop against Distance for station 4 (2 x 43.3MW)

Appendix G Genetic Algorithm optimization code

The genetic algorithm optimization code developed for this research is shown in Appendix G. The algorithm came up with a pipeline network optimum capital and operating costs. The optimization objective function, constraint, and variable are also encoded. The optimization can also carry-out interpolations were necessary. The initial step in the implementation of the genetic algorithm is the creation of an objective function.

```
function GC_CAPEX = projectoptimum(L)

% Copy Engine data from file
filename = 'NEWMODEL.csv';
NEWMODEL = csvread(filename);

% define constants
Q = (82*10^6)^2;
G = 0.6048;
C2 = (3.7435*0.001)^2;
E = (0.918)^2;
Tb = (288.15)^2;
Pb = (101)^2;
D = (1381.2^2.667)^2;
P1 = (9500)^2;
C = 3600;
GTN = 4;
GCN = 4;

% Station Parameter Calculation

for i=1:25(NEWMODEL)
   NEWMODEL_L(i)= NEWMODEL(i,9);
   NEWMODEL_P2(i)=NEWMODEL(i,6);
   NEWMODEL_P1(i)=NEWMODEL(i,5);
   NEWMODEL_Hp(i)=NEWMODEL(i,20);
   NEWMODEL_Power(i)=NEWMODEL(i,21);
   NEWMODEL_rp(i)=NEWMODEL(i,8);
   NEWMODEL_GCC(i)=NEWMODEL(i,25)
end

 % Carryout Interpolation

P2 = interp1(NEWMODEL_L,NEWMODEL_P2,L,'spline');
Hp = interp1(NEWMODEL_L,NEWMODEL_Hp,L,'spline');
```

```
Power = interp1(NEWMODEL_L,NEWMODEL_Power,L,'spline');
rp= interp1(NEWMODEL_L,NEWMODEL_rp,L,'spline');
GCC = interp1(NEWMODEL_L,NEWMODEL_GCC,L,'spline');

Dia = 56;
Thickness = 0.875;
C_mile = 1150;
Mile_converssion = 5280;
Cost_feet = 5;
Installation_mile = 1362457.96;
GT_Cost = 81070465.3;
GT_Fuel = 19174079.35;
GT_Mtaince = 100000*12.89;

Pipe_Material = (10.68*(Dia -
Thickness)*Thickness*L*C_mile*Mile_converssion)/(2000);
Coating_Rapping = Cost_feet*L*Mile_converssion;
Installation_Cost = Installation_mile*L;
Pipeline_Cost = Pipe_Material + Coating_Rapping + Installation_Cost

GC_CAPEX = (GCC + GT_Cost + GT_Fuel + GT_Mtaince)
end
```

```
close all
clear all
clc
%GC_CAPEX = @(var) fitnessfun(var);
GC_CAPEX = @ projectoptimum;
lb = 200;ub = 405;
opts =
gaoptimset('populationSize',25,'Generations',25,'PlotFcns',{@gaplotbestf,@gap
lotbestindiv,@gaplotscores,@gaplotrange,@gaplotselection,@gaplotdistance},'Di
splay','iter');
% an optimization structure settinginitpop as the initial population
[varga fga flga oga population scores] =
ga(GC_CAPEX,1,[],[],[],[],lb,ub,[],opts)
% calls ga@gaplotscorediversity,@gaplotgenealogy,@gaplotstopping
opts
```

Appendix H Power, pressure relationship for station 2

Stations	Z	T1	Tf	P1	P2	E_S	rp	L	W	EFF	S	R	K	N	n	MW	Q	A	Hp	Power
2	0.9566	308.4717	305.51	10000	6028.072	1.24185	1.658905	200	12620	0.7769	50.01	8.314	1.207	4.53004	0.220749	17.54	139.8705	0.535518	74.90323	16902.43
	0.9566	308.4717	305.51	10000	5908.672	1.24185	1.692428	210	12620	0.7769	50.01	8.314	1.207	4.53004	0.220749	17.54	139.8705	0.557939	78.03923	17610.09
	0.9566	308.4717	305.51	10000	5786.808	1.24185	1.728068	220	12620	0.7769	50.01	8.314	1.207	4.53004	0.220749	17.54	139.8705	0.5814	81.32072	18350.58
	0.9566	308.4717	305.51	10000	5662.322	1.24185	1.76606	230	12620	0.7769	50.01	8.314	1.207	4.53004	0.220749	17.54	139.8705	0.605997	84.76109	19126.92
	0.9566	308.4717	305.51	10000	5535.037	1.24185	1.806673	240	12620	0.7769	50.01	8.314	1.207	4.53004	0.220749	17.54	139.8705	0.631839	88.37563	19942.57
	0.9566	308.4717	305.51	10000	5404.755	1.24185	1.850223	250	12620	0.7769	50.01	8.314	1.207	4.53004	0.220749	17.54	139.8705	0.659052	92.1819	20801.48
	0.9566	308.4717	305.51	10000	5271.254	1.24185	1.897082	260	12620	0.7769	50.01	8.314	1.207	4.53004	0.220749	17.54	139.8705	0.687781	96.2002	21708.24
	0.9566	308.4717	305.51	10000	5134.284	1.24185	1.947691	270	12620	0.7769	50.01	8.314	1.207	4.53004	0.220749	17.54	139.8705	0.718194	100.4542	22668.17
	0.9566	308.4717	305.51	10000	4993.557	1.24185	2.002581	280	12620	0.7769	50.01	8.314	1.207	4.53004	0.220749	17.54	139.8705	0.750491	104.9716	23687.55
	0.9566	308.4717	305.51	10000	4848.748	1.24185	2.062388	290	12620	0.7769	50.01	8.314	1.207	4.53004	0.220749	17.54	139.8705	0.784906	109.7852	24773.78
	0.9566	308.4717	305.51	10000	4699.479	1.24185	2.127896	300	12620	0.7769	50.01	8.314	1.207	4.53004	0.220749	17.54	139.8705	0.82172	114.9343	25935.73
	0.9566	308.4717	305.51	10000	4545.31	1.24185	2.20007	310	12620	0.7769	50.01	8.314	1.207	4.53004	0.220749	17.54	139.8705	0.861271	120.4664	27184.08
	0.9566	308.4717	305.51	10000	4385.726	1.24185	2.280124	320	12620	0.7769	50.01	8.314	1.207	4.53004	0.220749	17.54	139.8705	0.903976	126.4395	28531.95
	0.9566	308.4717	305.51	10000	4220.111	1.24185	2.369606	330	12620	0.7769	50.01	8.314	1.207	4.53004	0.220749	17.54	139.8705	0.950348	132.9256	29995.57
	0.9566	308.4717	305.51	10000	4047.725	1.24185	2.470524	340	12620	0.7769	50.01	8.314	1.207	4.53004	0.220749	17.54	139.8705	1.001036	140.0155	31595.45
	0.9566	308.4717	305.51	10000	3867.664	1.24185	2.58554	350	12620	0.7769	50.01	8.314	1.207	4.53004	0.220749	17.54	139.8705	1.056876	147.8258	33357.91
	0.9566	308.4717	305.51	10000	3678.8	1.24185	2.718278	360	12620	0.7769	50.01	8.314	1.207	4.53004	0.220749	17.54	139.8705	1.118963	156.5099	35317.53
	0.9566	308.4717	305.51	10000	3479.7	1.24185	2.873811	370	12620	0.7769	50.01	8.314	1.207	4.53004	0.220749	17.54	139.8705	1.188775	166.2745	37520.99
	0.9566	308.4717	305.51	10000	3268.494	1.24185	3.059513	380	12620	0.7769	50.01	8.314	1.207	4.53004	0.220749	17.54	139.8705	1.268372	177.4079	40033.3
	0.9566	308.4717	305.51	10000	3042.663	1.24185	3.286595	390	12620	0.7769	50.01	8.314	1.207	4.53004	0.220749	17.54	139.8705	1.360743	190.3278	42948.77
	0.9566	308.4717	305.51	10000	2798.668	1.24185	3.573128	400	12620	0.7769	50.01	8.314	1.207	4.53004	0.220749	17.54	139.8705	1.47045	205.6726	46411.44
	0.9566	308.4717	305.51	10000	1305.352	1.24185	7.66077	443	12620	0.7769	50.01	8.314	1.207	4.53004	0.220749	17.54	139.8705	2.570705	359.5658	81138.5